University of Southampton

Faculty of Environmental and Life Sciences

School of Biological Sciences

Functional Analysis of Potential Therapeutic Target(s) in PTEN-inactive Triple Negative Breast Cancer

Volume 1 of 1

by

Ayse Ertay

Thesis for the degree of Doctor of Philosophy

August 2021

University of Southampton

Abstract

Faculty of Environmental and Life Sciences

School of Biological Sciences

Thesis for the degree of Doctor of Philosophy

Functional Analysis of Potential Therapeutic Target(s)

in PTEN-inactive Triple Negative Breast Cancer

by

Ayse Ertay

Triple negative breast cancer (TNBC) is the most aggressive type of breast cancer that lacks the oestrogen receptor, progesterone receptor and human epidermal growth factor receptor 2, making it difficult to target therapeutically. Targeting synthetic lethality is an alternative approach for cancer treatment. TNBC shows frequent loss of phosphatase and tensin homolog (PTEN) expression, which is associated with poor prognosis and treatment response. PTEN is a tumour suppressor gene and has a role in inhibiting oncogenic AKT signalling pathway by dephosphorylating phosphatidylinositol 3,4,5-triphosphate (PIP_3) into phosphatidylinositol 4,5-bisphosphate (PIP_2).

To identify PTEN synthetic lethal interactions, TCGA analysis coupled with a whole-genome siRNA screen in isogenic *PTEN*-negative and -positive cells was performed. Among the candidate genes essential for the survival of PTEN-inactive TNBC cells, *WD repeat and high mobility group [HMG]-box DNA binding protein 1* (*WDHD1*) expression was increased in the low *vs.* high *PTEN* TNBC samples. It was also the top hit in the siRNA screen. Knockdown of *WDHD1* significantly inhibited cell viability in *PTEN*-negative cells, which was further validated in 2D and 3D cultures. We also showed that PTEN status affects the expression of WDHD1 in TNBC cells via AKT signalling. The importance of WDHD1 in TNBC was confirmed in patient samples obtained from the TCGA and tissue microarrays with clinicopathological information. Mechanistically, WDHD1 is important for cell cycle progression as well as mediating a high demand of protein translation in PTEN-inactive TNBC via directly interacting with the components of translation machinery.

Taken together, this study demonstrated that WDHD1 expression is regulated by the PTEN/AKT signalling pathway and it has an impact on cell cycle and protein translation in TNBC. Thus, as an essential gene for the survival of PTEN-inactive TNBC cells, *WDHD1* could be a potential therapeutic target for TNBC.

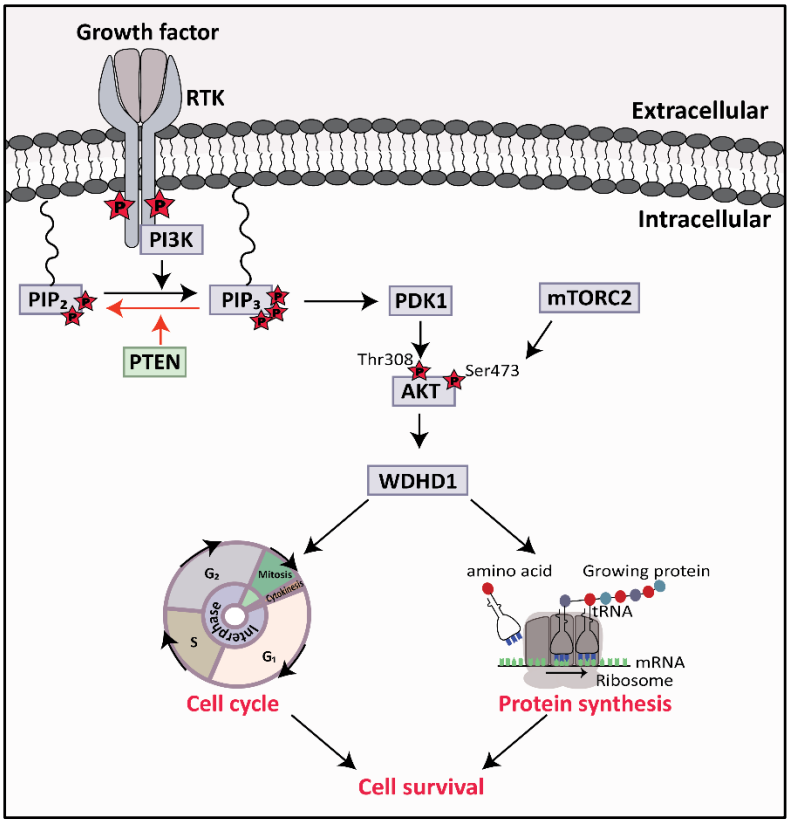

Figure 1 Graphical Abstract: The signalling axis and the role of WDHD1 in PTEN-inactive TNBC. PTEN expression is frequently lost in TNBC and leads to the activation of oncogenic AKT signalling pathway. We have showed that *WDHD1* is a synthetic essential gene for the survival of PTEN-inactive TNBC and its expression is regulated by the PTEN/AKT signalling pathway. We further identified that WDHD1 has important roles in cell cycle as well as in protein translation by directly interacting with translation machinery components in PTEN-inactive TNBC. P in red star indicates phosphorylation. Arrows indicate induction. PTEN: phosphatase and tensin homolog; RTK: receptor tyrosine kinase; PI3K: phosphoinositide 3-kinase; PIP_2: phosphatidylinositol 4,5-bisphosphate; PIP_3: phosphatidylinositol 3,4,5-triphosphate; PDK1: phosphoinositide-dependent kinase 1; mTORC2: mammalian target of rapamycin complex 2; WDHD1: WD repeat and high mobility group [HMG]-box DNA binding protein 1.

Table of Contents

Table of Contents ..... **iii**

Table of Tables ..... **xi**

Table of Figures ..... **xiii**

Research Thesis: Declaration of Authorship ..... **xvii**

Acknowledgements ..... **xix**

Definitions and Abbreviations ..... **xxi**

Chapter 1 Introduction **1**

1.1 Overview of cancer 1

1.1.1 Oncogenes and tumour suppressor genes 1

1.1.2 Hallmarks of cancer 1

1.2 Breast cancer 3

1.2.1 Incidence rate of breast cancer 3

1.2.2 Mortality and survival rate of breast cancer 3

1.2.3 Risk factors for breast cancer 4

1.2.3.1 Age 4

1.2.3.2 Inherited genes and family history 5

1.2.3.3 Reproductive factors 5

1.2.3.4 Environmental and lifestyle factors 5

1.2.4 Types of breast cancer 6

1.2.4.1 Histological types and development of breast cancer 6

1.2.4.2 Grading system 8

1.2.4.3 Tumour staging 9

1.2.4.4 Molecular classification of breast cancer 9

1.2.4.4.1 Luminal A 10

1.2.4.4.2 Luminal B 10

1.2.4.4.3 HER2+ 10

1.2.4.4.4 Triple negative breast cancer (TNBC) 11

1.2.5 Treatment of breast cancer 12

1.2.5.1 Treatment options for luminal subtypes of breast cancer 12
1.2.5.2 Treatment options for HER2+ breast cancer 14
1.2.5.3 Treatment options for TNBC 16
1.3 Phosphatase and tensin homolog (PTEN) 18
1.3.1 *PTEN* as a tumour suppressor gene 18
1.3.2 Structure of PTEN 19
1.3.3 PTEN as a dual lipid and protein phosphatase 20
1.3.4 PTEN and PI3K/AKT signalling pathway 20
1.3.5 Regulations of *PTEN* 22
1.3.5.1 Genetic alterations of *PTEN* 22
1.3.5.2 Epigenetic silencing of *PTEN* 23
1.3.5.3 Transcriptional regulation of *PTEN* 23
1.3.5.4 Post-transcriptional regulation of *PTEN* 24
1.3.5.5 Post-translational modification of PTEN 25
1.3.5.6 Protein-protein interactions of PTEN 26
1.3.6 Subcellular localisation of PTEN 28
1.3.7 Mechanisms of cytoplasmic and nuclear shuttling of PTEN 28
1.3.8 Cellular functions of PTEN 31
1.3.8.1 PTEN and cell metabolism 31
1.3.8.2 PTEN and cell motility/polarity 32
1.3.8.3 PTEN and tumour microenvironment 32
1.3.8.4 PTEN and angiogenesis 33
1.3.8.5 Nuclear PTEN 33
1.4 PTEN in breast cancer 36
1.4.1 Treatment challenges in PTEN-inactive breast cancer 36
1.4.2 Inactive PTEN in TNBC 37
1.4.3 Treatment for PTEN-inactive TNBC 38
1.5 Alternative approach for cancer treatment; synthetic lethality 42
1.5.1 Synthetic lethality in PTEN-inactive cancer 42
1.6 Project background 45
1.7 Hypothesis 45

1.8 Project Aims 45

1.8.1 Bioinformatic analysis to reveal the candidate gene(s) that are essential for the survival of PTEN-inactive TNBC cells 45

1.8.2 Validation of bioinformatic analysis findings with *in vitro* work and patients' samples in PTEN-inactive TNBC 46

1.8.3 Functional characterisation of WDHD1 in PTEN-inactive TNBC 46

Chapter 2 Materials and Methods 49

2.1 Bioinformatic analysis 49

2.1.1 The Cancer Genome Atlas (TCGA) data mining of PTEN 49

2.1.2 TCGA breast invasive carcinoma (Protein, RPPA) analysis 50

2.1.3 TCGA breast invasive carcinoma (mRNA, IlluminaHiSeq) analysis 51

2.1.4 A whole genome siRNA high-throughput screening and data analysis 51

2.1.5 Identification of top hit genes 52

2.1.6 TCGA data mining with the identified top hit gene, *WDHD1* 52

2.2 Cell culture 53

2.2.1 Storage and thawing of cell lines 53

2.2.2 Passaging cells 53

2.3 Generation of a whole genome siRNA high-throughput screening 54

2.4 Drug treatments 55

2.4.1 Doxycycline (DOX) treatment 55

2.4.2 Small interfering RNA (siRNA) knockdown 56

2.4.3 AKT inhibition 56

2.4.4 Puromycin treatment 56

2.5 Western blot 58

2.5.1 Buffers for western blot 58

2.5.2 Cell lysis with Urea buffer 59

2.5.3 Cell lysis with pNAS buffer 59

2.5.4 Quantification of total protein 59

2.5.5 Sodium dodecyl sulfate-polyacrylamide gel electrophoresis (SDS-PAGE) 60

2.5.6 Sample preparation 61

2.5.7 Electrophoresis 61
2.5.8 Electrotransfer 61
2.5.9 Blocking, antibody incubation and visualisation 62
2.6 QuantiNova™ SYBR green real time-polymerase chain reaction (RT-PCR) 64
2.6.1 RNA extraction 64
2.6.2 RT-PCR analysis 64
2.7 Immunofluorescence microscopy 66
2.7.1 Plating cells 66
2.7.2 Fixing and staining cells 66
2.8 Cell viability assay by CellTiter-Glo® in 2D culture 67
2.9 Colony formation assay with crystal violet 67
2.10 Mammosphere formation assay 68
2.10.1 Plating 3D cell culture 68
2.10.2 Mammosphere formation efficiency (MFE) and mammosphere volume analysis 68
2.10.3 Cell viability assay by CellTiter-Glo® in 3D culture 68
2.11 Immunohistochemical and haemotoxylin/eosin (H/E) staining and scoring 69
2.12 Flow cytometry 69
2.12.1 Plating cells 69
2.12.2 Fixing cells 69
2.12.3 Propidium iodide (PI) staining and cell analysis 70
2.13 Immunoprecipitation-mass spectrometry (IP-MS) 70
2.13.1 Immunoprecipitation 70
2.13.2 Sample preparations for mass spectrometry 70
2.13.3 Mass spectrometry and database search 71
2.13.4 Immunoprecipitation-mass spectrometry (IP-MS) analysis 71
2.14 Puromycin incorporation assay 72
2.14.1 Puromycin incorporation assay optimisation 72
2.14.2 *WDHD1* siRNA with puromycin incorporation assay 72
2.15 Pathway analysis 73

2.16 Subcellular localisation....73
2.17 Statistical analysis....73

Chapter 3 Bioinformatic analysis to reveal the candidate gene(s) that are essential for the survival of PTEN-inactive TNBC cells 75

3.1 Introduction....75
3.1.1 The Cancer Genome Atlas (TCGA)....75
3.1.2 RNA interference (RNAi) whole-genome screening....76
3.1.3 Summary of the chapter 77
3.2 Results 78
3.2.1 *PTEN* mutation associates with low PTEN expression 78
3.2.2 The link between PTEN, *PIK3CA* and the AKT activity....80
3.2.3 TCGA analysis confirms PTEN expression is decreased in TNBC....83
3.2.4 TCGA analysis confirms the correlation between the loss of PTEN expression and clinical stages....84
3.2.5 Negative correlation between PTEN expression levels and AKT activity in TNBC....87
3.2.6 Candidate gene(s) essential for the survival of PTEN-inactive TNBC cells are identified by the TCGA analysis and a whole-genome siRNA screen 89
3.3 Discussion....98

Chapter 4 Validation of bioinformatic analysis findings with *in vitro* work and patients' samples in PTEN-inactive TNBC 101

4.1 Introduction....101
4.1.1 *WD repeat and high mobility group [HMG]-box DNA binding protein 1* (*WDHD1*) 101
4.1.2 Structure of WDHD1....101
4.1.3 Function of WDHD1....102
4.1.3.1 Cell cycle 102
4.1.3.2 DNA replication 104
4.1.3.3 WDHD1 maintains genomic integrity....107
4.1.4 WDHD1 in cancer 109

4.1.5 Summary of the chapter 111
4.2 Results 112
4.2.1 WDHD1 expression is affected by PTEN status in TNBC cell lines 112
4.2.2 WDHD1 expression is affected by PTEN status in TNBC cells via AKT signalling pathway 117
4.2.3 WDHD1 is required for the survival of PTEN null TNBC cells cultured in 2D and 3D 121
4.2.4 WDHD1 levels are increased in TNBC compared to normal breast tissues, and associated with tumour size and proliferation 126
4.3 Discussion 130
Chapter 5 Functional characterisation of WDHD1 in PTEN-inactive TNBC 133
5.1 Introduction 133
5.1.1 Target proteins of WDHD1 in cancer 133
5.1.2 WDHD1 and PTEN/AKT signalling in TNBC 134
5.1.3 Summary of the chapter 134
5.2 Results 135
5.2.1 Essential role of WDHD1 in cell cycle in PTEN null TNBC cell lines 135
5.2.2 IP-MS analysis reveals the role of WDHD1 in protein translation in PTEN-inactive TNBC cell lines 141
5.2.3 WDHD1 depletion reduced the protein translation in PTEN-inactive TNBC cell lines 145
5.2.4 RPS6 and eIF3β are the target proteins of WDHD1 in PTEN null TNBC cell lines 150
5.3 Discussion 152
Chapter 6 Overall Discussion 157
6.1 Future studies 160
List of References 163
Appendix A Materials and Methods 207
A.1 R scripts 207

A.1.1 Alignment of TNBC samples (TCGA, Provisional) with Protein (RPPA) and mRNA (IlluminaHiSeq) data from UCSC Cancer Genome Browser 207
A.1.2 Alignment of clinical data of TNBC samples (TCGA, Provisional) with PTEN, protein (RPPA) from UCSC Cancer Genome Browser 208
A.1.3 Identifying significantly different mRNAs between the *PTEN* high and low TNBC samples in TCGA (IlluminaHiSeq) data 209
A.1.4 Identifying genes that have significant decrease in cell viability between *PTEN*-positive and *PTEN*-negative TNBC cells obtained from the whole genome siRNA screen.....212
A.1.5 Identifying top hit candidate genes between TCGA and whole genome siRNA screen 213
A.1.6 TCGA data mining with WDHD1.....214
A.1.7 Proteomics analysis.....216

Appendix B Bioinformatic analysis to reveal the candidate gene(s) that are essential for the survival of PTEN-inactive TNBC cells 219
Appendix C Validation of bioinformatic analysis findings with *in vitro* work and patients' samples in PTEN-inactive TNBC 227
Appendix D Functional characterisation of WDHD1 in PTEN-inactive TNBC.....231
Appendix E List of publications during the PhD 239

Table of Contents

Table of Tables

Table 1.1. Breast cancer classification based on site of occurrence..... 7

Table 1.2 Molecular subtypes of invasive breast carcinoma. 11

Table 1.3 Features and targeted therapies of TNBC subtypes..... 17

Table 1.4 Clinical Trials of targeted therapies in PTEN-inactive TNBC population. 40

Table 1.5 Identified synthetic lethality genes in PTEN-inactive cancer types. 43

Table 2.1 siRNA oligo sequences used to knockdown *WDHD1*. 56

Table 2.2 Buffer compositions for western blot. 58

Table 2.3 Resolving gels recipe for western blot. 60

Table 2.4 5% Stacking gel recipe for western blot. 61

Table 2.5 Primary and secondary antibodies for western blot. 63

Table 2.6 Reaction mixture set up for RT-PCR. 65

Table 2.7 Real-time cycler conditions. 65

Table 3.1 The relationship between TNBC patients' clinicopathological characteristics and PTEN, protein expression in TCGA data. 86

Table 3.2 Expressions of 47 candidate mRNAs essential for the survival of PTEN-inactive TNBC cells in the TCGA samples with the high *vs.* low *PTEN* expression..... 96

Table 3.3 Forty-seven candidate genes essential for the survival of PTEN-inactive TNBC cells are identified by a whole genome siRNA screen. 97

Table 4.1 The expression of WDHD1 in different cancer tissue or cell lines. 109

Table 4.2 The relationship between TNBC patients' clinicopathological characteristics and *WDHD1* expression in TCGA data. 127

Table 4.3 The relationship between TNBC patients' clinicopathological characteristics and WDHD1 expression in tissue microarray. 128

Table 5.1 Functional enrichment (ToppGene) of WDHD1 binding partners identified via IP-MS. 143

Table of Figures

Figure 1.1 Hallmarks of cancer. 2

Figure 1.2. Diagram demonstrating the progression of breast cancer from normal breast to metastatic breast carcinoma. 8

Figure 1.3 PTEN protein domain structure. 19

Figure 1.4 Diagram showing PTEN/PI3K/AKT signalling pathway. 21

Figure 1.5 Regulation of PTEN. 27

Figure 1.6 Shuttling of PTEN between cytoplasm and nucleus. 30

Figure 1.7 Nuclear functions of PTEN. 35

Figure 1.8 The principle of synthetic lethality. 42

Figure 2.1 Diagram showing Tet-on system. 54

Figure 3.1 PTEN, protein and mRNA expression in *PTEN* WT and mutant breast invasive carcinoma samples (TCGA, Provisional) from cBioPortal. 79

Figure 3.2 Correlation between PTEN, protein expression and phosphorylated forms of AKT (pAKT_308 and pAKT_473) in breast invasive carcinoma samples (TCGA, Provisional) from cBioPortal. 80

Figure 3.3 Mutation frequency of different PI3K isoforms in breast invasive carcinoma samples (TCGA, Provisional) from cBioPortal. 81

Figure 3.4 PTEN and pAKT_308, protein expression levels in *PIK3CA* WT and mutant breast invasive carcinoma samples (TCGA, Provisional) from cBioPortal. 81

Figure 3.5 Correlation between PTEN, protein expression and pAKT_308, protein expression in *PIK3CA* WT and *PIK3CA* mutant breast invasive carcinoma samples (TCGA, Provisional) from cBioPortal. 82

Figure 3.6 PTEN expression levels in different molecular subtypes of breast invasive carcinoma samples (TCGA, PanCancer) from cBioPortal. 83

Figure 3.7 Venn chart for the combination of TCGA breast invasive carcinoma samples from different websites to identify common TNBC samples. 84

Figure 3.8 Correlation between PTEN, protein expression and *PTEN*, mRNA expression in TNBC samples (TCGA, Provisional) from cBioPortal. 85

Figure 3.9 The association between PTEN, protein expression (RPPA) and clinicopathological features of TNBC samples in TCGA data from UCSC Cancer browser. 86

Figure 3.10 pAKT_308, protein levels in different molecular subtypes of breast invasive carcinoma samples (TCGA, PanCancer) from cBioPortal. 87

Figure 3.11 Correlation between PTEN, protein expression and pAKT_308, protein expression in TNBC samples (TCGA, Provisional) from cBioPortal. 88

Figure 3.12 Workflow of TCGA and whole genome siRNA high-throughput screening analysis to identify candidate gene(s) essential for the survival of PTEN-inactive TNBC cells. 89

Figure 3.13 Identifying significantly different mRNAs between the high and low *PTEN* groups in TCGA (IlluminaHiSeq) TNBC samples. 90

Figure 3.14 Workflow showing the whole genome siRNA screen in isogenic *PTEN*-positive or -negative TNBC cells. 92

Figure 3.15 Candidate genes essential for the survival of PTEN-inactive TNBC cells are identified by a whole genome siRNA screen. 94

Figure 3.16 Candidate genes essential for the survival of PTEN-inactive TNBC cells are identified by the TCGA analysis and a whole-genome siRNA screen. 95

Figure 3.17 *WDHD1* as a synthetic essential gene in PTEN-inactive TNBC cells. 98

Figure 4.1 WDHD1 protein domain structure. 102

Figure 4.2 Diagram illustrating the process of DNA replication. 106

Figure 4.3 WDHD1 is highly expressed in PTEN-inactive TNBC cells. 113

Figure 4.4 Optimising the concentration of DOX for MDA-MB-468-TR-PTEN cell line to induce PTEN expression. 114

Figure 4.5 The effect of PTEN on the AKT signalling pathway in TNBC cells. 115

Figure 4.6 WDHD1 levels are reduced upon PTEN expression in MDA-MB-468 cells. 116

Figure 4.7 WDHD1 levels are reduced upon AKT inhibition in PTEN null TNBC cells. 118

Figure 4.8 pAKT (Thr308) levels are reduced upon *WDHD1* knockdown in PTEN null TNBC cell lines. 119

Figure 4.9 Correlation between pAKT_308, protein expression and *WDHD1*, mRNA level in TNBC samples (TCGA, Provisional) from cBioPortal. 120

Figure 4.10 WDHD1 is required for the survival of PTEN null TNBC cells. 122

Figure 4.11 *WDHD1* knockdown reduces the proliferation of PTEN null TNBC cells cultured in 2D. 123

Figure 4.12 WDHD1 is required for the survival of PTEN null TNBC cells cultured in 3D. 125

Figure 4.13 *WDHD1*, mRNA expression in normal breast and TNBC samples in TCGA (PanCancer) data from cBioPortal. 126

Figure 4.14 The association between *WDHD1* and clinicopathological features for TNBC samples in TCGA (IlluminaHiSeq) data from UCSC Cancer browser. 127

Figure 4.15 WDHD1 is associated with TNBC proliferation. 129

Figure 4.16 WDHD1 is essential for the survival of PTEN-inactive TNBC via the AKT signalling pathway. 130

Figure 5.1 TCGA analysis suggests an important role of *WDHD1* in cell cycle regulation. 136

Figure 5.2 Overlay genes between identified top hit genes and genes that were positively correlated with *WDHD1*. 137

Figure 5.3 Essential roles of WDHD1 in cell cycle in PTEN null TNBC cell lines. 140

Figure 5.4 Workflow to identify WDHD1 binding partners in PTEN-inactive TNBC cell line. .141

Figure 5.5 WDHD1 is immunoprecipitated in MDA-MB-468, a PTEN null type TNBC cell line.142

Figure 5.6 WDHD1 plays an important role in translation in MDA-MB-468, a PTEN null type TNBC cell line. 144

Figure 5.7 Optimisation of puromycin incorporation assay. 146

Figure 5.8 Essential roles of WDHD1 in protein translation in *PTEN*-negative TNBC cells. 148

Figure 5.9 *WDHD1* knockdown reduces global protein translation in PTEN null type TNBC cell line. 149

Figure 5.10 WDHD1 interacts with RPS6 and eIF3β in MDA-MB-468 PTEN null TNBC cell line.150

Figure 5.11 RPS6 and eIF3β levels are reduced upon *WDHD1* knockdown in PTEN null TNBC cell lines. 151

Figure 5.12 Function of WDHD1 in cell cycle and protein translation in PTEN-inactive TNBC cells. 152

Figure 6.1 Potential novel signalling pathway of WDHD1 in PTEN-inactive TNBC cells. 159

Research Thesis: Declaration of Authorship

Print name: Ayse Ertay

Title of thesis: Functional analysis of potential therapeutic target(s) in PTEN-inactive triple negative breast cancer

I declare that this thesis and the work presented in it are my own and has been generated by me as the result of my own original research.

I confirm that:

1. This work was done wholly or mainly while in candidature for a research degree at this University;
2. Where any part of this thesis has previously been submitted for a degree or any other qualification at this University or any other institution, this has been clearly stated;
3. Where I have consulted the published work of others, this is always clearly attributed;
4. Where I have quoted from the work of others, the source is always given. With the exception of such quotations, this thesis is entirely my own work;
5. I have acknowledged all main sources of help;
6. Where the thesis is based on work done by myself jointly with others, I have made clear exactly what was done by others and what I have contributed myself;
7. Parts of this work have been published as:

Ertay, A. *et al.* (2020) 'WDHD1 is essential for the survival of PTEN-inactive triple-negative breast cancer', *Cell Death and Disease*, 11(11):1001. doi: 10.1038/s41419-020-03210-5.

Signature:  Date: 13.08.2021

Acknowledgements

I would like to thank my supervisor Dr. Yihua Wang, who has always been supportive throughout my project and helped me to take the project forward. I appreciate that he gave me the opportunity to work with him and guided me to achieve my goals. I thank to my co-supervisor Dr. Rob M. Ewing for his advice throughout the project, helping me to learn bioinformatic analysis. I thank to Prof. Julian Downwards who supported this project and provided all the triple negative breast cancer cell lines. I would also like to thank my funder, Wessex Medical Research for providing me the opportunity to do my PhD. I thank Academy of Medical Sciences/the Wellcome Trust Springboard Award [SBF002\1038] and Medical Research Council [MR/S025480/1] for supporting the project.

I appreciate the help of Prof. Paul Skipp who performed mass-spectrometry experiment and analysis for me. I thank Dr. Huiquan Liu who performed IHC for the fourth chapter and Co-IP experiment for the fifth chapter of my thesis. I thank Dr. Mark Coldwell and Dr. Marcin Przewloka who advised me to do some experiments. Thanks to the people who trained me; Dr. Noor Shamki for the flow cytometry, Mr. Fuad M. M. Alzahrani for the puromycin incorporation assay and Mr. Matt Sherwood for the 3D mammosphere assay. I thank Yilu Zhou for the help he provided for the bioinformatic analysis when I needed.

Thanks to all of the members in Dr. Yihua Wang group; Juanjuan Li, Dr. Charlotte Hill, Liudi Yao, Yilu Zhou, Hualong Zhao and Zijian Zu, and Ahoud Abdulaziz Aleidan from Dr. Rob M. Ewing group. You have always been very supportive and great friend to me to enjoy working in the lab. Special thanks to Dr. Charlotte Hill who helped me a lot for my writing skills, I will never forget your help!

I would like to thank my mother Zuhal Ertay, father Ahmet Ertay and brothers Huseyin Ertay and Mehmet Ertay. I couldn't achieve my goals without your endless love, support and understanding. You always trust me in every aspect and made me who I am now. Despite being we were far away physically, you always made me feel we were together. Thanks to my grandparents Ayse and Mehmet Cakir and family relative Zekiye Goc who also trusted and supported me throughout my education. I also thank my family relative Aysan Kaya who was very supportive when she heard I was going to do a PhD. I will never forget what you have told me when we met last time and you will never be forgotten!

Very big thanks to my fiancée, Dr. Osman Dadas for being patient with me when I was anxious. I wouldn't be able to deal with all the stress that I had without you. You have always been by my side to support, help and encourage me to achieve more.

Definitions and Abbreviations

ADH	Atypical ductal hyperplasia
AJCC	American Joint Committee for Cancer
AND-1	Acidic and nucleoplasmic DNA binding protein 1
ANXA2	Annexin 2
APC/C	Anaphase-promoting complex/cyclosome
aPKC	Atypical protein kinase C
APS	Ammonium persulfate
AURKs	Aurora kinases
Bad	BCL-2 antagonist of cell death
BCL-2	B cell lymphoma 2
BL1	Basal-like 1
BL2	Basal-like 2
BMI	Body mass index
Bmi-1	B lymphoma Mo-MLV insertion region 1 homolog
BSA	Bovine serum albumin
CBF1	C-repeat binding factor 1
CBP	CREB-binding protein
Cdc45	Cell division cycle protein 45
Cdc6	Cell division cycle 6
Cdc7	Cell division cycle 7
CDK2	Cyclin dependent kinase 2
CDKs	Cyclin dependent protein kinases
Cdt1	Cdc10-dependent transcript 1
Cdt2	Cdc10-dependent transcript 2

CENP-C	Centromere protein-C
CHD1	Chromatin helicase DNA binding protein 1
CHK1	Checkpoint kinase 1
CK2	Casein kinase 2
CKI	CDK inhibitors
CMG	Cdc45-Mcm2-7-GINS
CRK 5/6	Cytokeratin 5/6
CST	CTC1-STN1-TEN1
Ctf4	Chromosome transmission fidelity 4
Cul4	Cullin 4
DAPI	4'6-diamidino-2-pheylindole
Dbf4	Dumbbell former 4
DCIS	Ductal carcinoma *in situ*
DDB1	DNA damage-binding protein 1
DDK	DBf4-Cdc7 kinase
DM1	Myotenic dystrophy type 1
DMEM	Dulbecco's Modified Eagle's Medium
DMSO	Dimethyl sulfoxide
DOX	Doxycycline
dsRNA	Double-stranded RNA
DTT	Dithiothreitol
EGFR	Epidermal growth factor receptor
EGR1	Early growth regulated transcription factor 1
eIF3β	Eukaryotic translation initiation factor 3 subunit beta
EMT	Epithelial mesenchymal transition
ER	Oestrogen receptor

ETS2	Ets eryhtoblastosis virus E26 oncogene homolog 2
FACS	Fluorescence-activated cell sorting
FAK	Focal adhesion kinase
FBS	Fetal bovine serum
FDA	Food and Drug Administration
FDR	False discovery rate
FOXO1	Forkhead box O1
GBM	Glioblastoma multiforme
GCN5	General control non-derepressible 5
GFP	Green fluorescent protein
GINS	Go ichi ni san complex
GLUT1	Glucose transporter 1
GLUT4	Glucose transporter 4
GSK3β	Glycogen synthase kinase 3 beta
H/E	Haemotoxylin/eosin
HCD	Higher-energy collisional dissociation
HER2	Human epidermal growth factor receptor 2
HIF1-α	Hypoxia induced factor 1-alpha
HPV	Human papillomavirus
HR+	Hormonal receptor positive
HRT	Hormone replacement therapy
IAA	Iodoacetamide
Id-1	Inhibitor of differentiation-1
IGF-2	Insulin-like growth factor 2
IgG	Immunoglobulin G
IHC	Immunohistochemistry

IM	Immunomodulatory
IP-MS	Immunoprecipitation-mass spectrometry
LAR	Luminal androgen receptor
LCIS	Lobular carcinoma *in situ*
M	Mesenchymal
MAGI2	Membrane-associated guanylate kinase inverted 2
MAN2C1	Mannosidase 2C1
MAPK	Mitogen activated protein kinases
MAPRE2	Microtubule-associated protein RP/EB family member 2
MAST	Microtubule-associated protein
Mcl1	Mini-chromosome loss 1
Mcm2-7	Mini chromosome maintenance 2-7
MDM2	Mouse double minute 2 homolog
MFE	Mammosphere formation efficiency
MKK4	Mitogen-activated protein kinase kinase 4
MMAC1	Mutated in multiple advanced cancers 1
MMR	Mismatch repair
MSL	Mesenchymal stem-like
mTORC1	Mammalian target of rapamycin complex 1
mTORC2	Mammalian target of rapamycin complex 2
MVP	Major vault protein
Myt1	Myelin transcription factor 1
NFκB	Nuclear factor kappa B
NGS	Next-generation sequencing
NHERF	NA+/H+ exchanger regulatory factor
NLS	Nuclear localisation signal

Nts	Nucleotides
NUAK1	NUAK family kinase 1
ORC	Origin recognition complex
PAR6	Partitioning defective 6
PARK7	Parkinson protein 7
PARP	Poly (ADP ribose) polymerase
PBD	Phosphatidylinositol 4,5-bisphosphate (PIP_2)-binding domain
PBS	Phosphate buffered saline
PCAF	P300/CBP-associated factor
PCNA	Proliferating cell nuclear antigen
PDGFR	Platelet derived growth factor receptor
PDK1	Phosphoinositide-dependent kinase 1
PD-L1	Programmed death-ligand 1
PFA	Paraformaldehyde
PFS	Progression-free survival
PGC1α	PPAR gamma-coactivator 1 alpha
PHTS	PTEN hamartoma tumour syndromes
PI	Propidium Iodide
PI3K	Phosphoinositide 3-kinase
PIP_2	Phosphatidylinositol 4,5-bisphosphate
PIP_3	Phosphatidylinositol 3,4,5-triphosphate
PKC	Protein kinase C
PLK1	Polo-like kinase 1
PNKP	Polynucleotide kinase-phosphatase
Pol α	Polymerase alpha
Pol δ	Polymerase delta

Pol ϵ	Polymerase epsilon
PPARγ	Peroxisome proliferator-activated receptor gamma
PR	Progesterone receptor
PRAS40	Proline-rich AKT substrate of 40 kDa
Pre-RC	Pre-replicative complex
PREX2a	PIP_3-dependent RAC exchanger factor 2a
PTEN	Phosphatase and tensin homolog
PTEN-	PTEN-negative
PTEN+	PTEN-positive
PTENP1	PTEN pseudogene 1
PTGS	Post-transcriptional gene silencing
RecQL4	RecQ protein like 4
RISC	RNA-induced silencing complex
RNAi	RNA interference
RNA-Seq	RNA-sequencing
ROCK	RHOA-associated protein kinase
ROS	Reactive oxygen species
RPC	Replisome progression complex
RPMI	Roswell Park Memorial Institute
RPPA	Reverse-phase protein assay
RPS6	Ribosomal protein S6
RTK	Receptor tyrosine kinase
RT-PCR	Real time-polymerase chain reaction
rtTA	Reverse Tet transactivators
SALL4	Sal-like protein 4
SDS	Sodium dodecyl sulfate

SDS-PAGE	SDS-polyacrylamide gel electrophoresis
shRNA	Short hairpin RNA
SIPL1	Shank-interacting protein-like 1
siRNA	Small interfering RNA
SREBP1C	Sterol-regulatory element-binding protein 1C
STAT3	Signal transducers and activators of transcription 3
TARGET	Tamoxifen or Arimidex Randomised Group Efficacy and Tolerability
TBST	Tris-buffered saline and Tween 20
TCGA	The Cancer Genome Atlas
TEP1	Tensin-like phosphatase 1
TET	Tetracycline
TFGβ	Transforming growth factor beta
TNBC	Triple negative breast cancer
TNM	Primary tumour, regional lymph node status and metastasis status
TRE	Tet-responsive element
TSC1/TSC2	Tuberous sclerosis 1/2
UK	United Kingdom
VEGFs	Vascular endothelial growth factors
WDHD1	WD repeat and high mobility group [HMG]-box DNA binding protein 1
WT	Wild-type

Chapter 1 Introduction

1.1 Overview of cancer

Cancer is the first or second leading cause of death worldwide and can be considered as a major public health problem (Sung *et al.*, 2021). The incidence and mortality rate of cancer are rapidly increasing around the world. The increasing cancer rates might be due to population growth and an ageing population in the world (Bray *et al.*, 2018). The report from GLOBOCAN 2021 stated an estimated 19.3 million new cancer cases and almost 10.0 million cancer deaths around the world in 2020 (Sung *et al.*, 2021).

Cancer can occur from the uncontrollable growth of any type of cells that leads to the formation of different types of cancer (Pelengaris and Khan, 2013). Cancer cells can keep growing as the cells dividing to form abnormal cells (Trichopoulos, Li and Hunter, 1996). Some cancer cells have ability to spread to the other parts of the body via lymph vessels and blood circulation (Fidler, 2003).

1.1.1 Oncogenes and tumour suppressor genes

The combination of genetic and non-genetic alterations caused by environmental factors can lead to abnormal activation or inactivation of specific genes which can cause cancer development (Wu *et al.*, 2018).

During the 1970s, two important families of genes (oncogenes and tumour suppressor genes) were discovered and scientists clarified how genes could be damaged by mutations which may cause cancer (Vogelstein *et al.*, 2003; Javier and Butel, 2008). Proto-oncogenes and tumour suppressor genes are normal genes. Proto-oncogenes control cell division, cell differentiation and programmed cell death (apoptosis) (Anderson *et al.*, 1992). Tumour suppressor genes control DNA repair, cell division and apoptosis (Hinds and Weinberg, 1994). Genetic mutations can activate oncogenes (mutated form of proto-oncogenes) and inactivate tumour suppressor genes, which can lead to the abnormal growth of cells and cause cancer (Wu *et al.*, 2018).

1.1.2 Hallmarks of cancer

Tumorigenesis is a multistep process and requires some biological capabilities to enable the survival of cancer cells and these are known as the hallmarks of cancer (Hanahan and Weinberg, 2000,

2011). In 2000, six hallmarks of cancer were identified which included: sustaining proliferative signalling, inducing angiogenesis, resisting cell death, enabling replicative immortality, evading growth suppressors and activating invasion and metastasis (Fig. 1.1) (Hanahan and Weinberg, 2000). Following advances explaining the mechanisms of cancer, two more hallmarks: reprogramming of energy metabolism and evading immune destruction were also discovered in 2011 (Fig. 1.1) (Hanahan and Weinberg, 2011). Tumours are complex which lead to difficulties in understanding the biology of tumours. Therefore, studying the cell types within the tumour or the tumour microenvironment that are involved in multistep tumorigenesis can help to understand the biology of tumours (Hanahan and Weinberg, 2011).

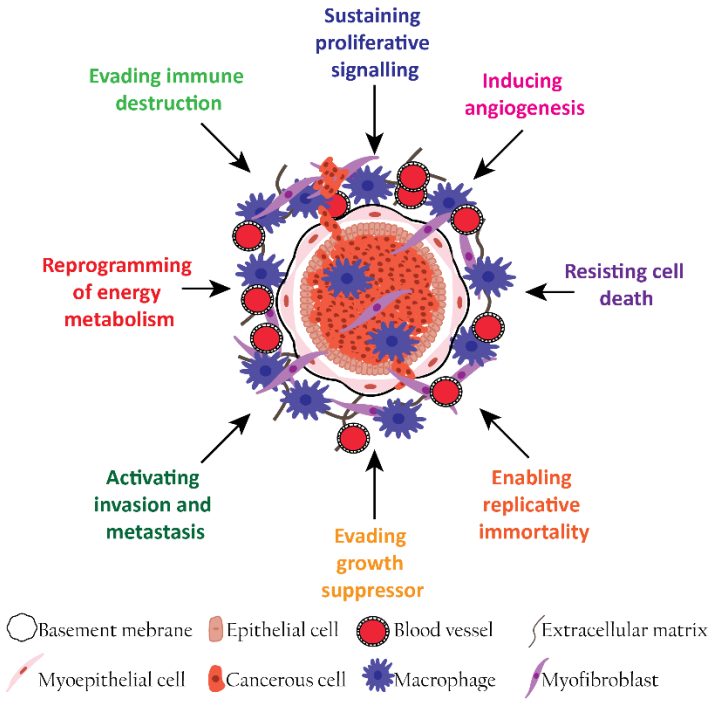

Figure 1.1 Hallmarks of cancer.
The hallmarks of cancer shows the features of cancer cells during tumorigenesis. Sustaining proliferative signalling, inducing angiogenesis, resisting cell death, enabling replicative immortality, evading growth suppressor and activating invasion and metastasis were the first identified features of cancer cells in 2000. In 2011, two more cancer cell features were discovered: reprogramming of energy metabolism and evading immune destruction. [Information collected from (Hanahan and Weinberg, 2011)].

1.2 Breast cancer

Breast cancer is mostly diagnosed in women and is the leading cause of death in women (Bray *et al.*, 2018; Sung *et al.*, 2021). There are various genetic and non-genetic risk factors that cause breast cancer (Sharma *et al.*, 2010). Improvements in public awareness and screening programs led to early diagnosis of breast cancer (Maddams, Utley and Møller, 2012). The diagnosis of breast cancer can help to identify the stages or molecular subtypes of breast cancer such as luminal A, luminal B, human epidermal growth factor receptor-positive (HER2+) and triple negative breast cancer (TNBC), which provides important information both for the prognosis of the disease and the treatment plan for the patients (Velloso *et al.*, 2017).

1.2.1 Incidence rate of breast cancer

Breast cancer is the most common cancer type in females, which includes an estimated 2.3 million new cases (11.7%) among all cancer types in 2020 and has the highest incidence rate in 159 of 185 countries (Sung *et al.*, 2021). Incidence rate of breast cancer varies in each region of the world; developing and developed countries have higher incidence rate compared to undeveloped countries (Coccia, 2013). The study from GLOBOCAN 2020 showed that developed countries have an 88% higher incidence rate than the developing countries (Sung *et al.*, 2021).

The United Kingdom (UK) is one of the countries that has the highest incidence rate of breast cancer (Bray *et al.*, 2018). Around 55,200 new breast cancer cases were recorded in the UK in each year from 2015 to 2017 and approximately 54,700 new breast cancer cases were seen in women (*Breast Cancer Statistics*, 2017). Breast cancer incidence rate is correlated with age and the highest incidence rates are seen in elderly people. 24% of new breast cancer cases were observed in patients aged 75 or above in the UK between 2015 and 2017 (*Breast Cancer Statistics*, 2017). Breast cancer incidence rate is expected to be 2% higher by 2035 compared to 2014 (*Breast Cancer Statistics*, 2017) due to improvements in public awareness of the early symptoms as well as screening programs (Maddams, Utley and Møller, 2012).

1.2.2 Mortality and survival rate of breast cancer

Breast cancer is the fifth leading cause of cancer death and the mortality rate of breast cancer was low (685,000 deaths) compared to the incidence rate (an estimated 2.3 million) of breast cancer worldwide in 2020 (Sung *et al.*, 2021). Among females, 1 in 6 cancer deaths are due to the breast

cancer, which leads to the highest mortality rate in 110 of 185 countries (Sung *et al.*, 2021). Globally, the mortality rates of breast cancer in men were not in the top 15 most common causes of cancer death (Bray *et al.*, 2018; Sung *et al.*, 2021).

Breast cancer was the second most common cause of female cancer death in the UK in 2017 (*Breast Cancer Statistics*, 2017). The highest mortality rate for breast cancer was in patients aged 90 and above in the UK between 2015 and 2017 (*Breast Cancer Statistics*, 2017). Overall breast cancer mortality rate is expected to decrease by 26% between 2014 to 2035 in the UK (Smittenaar *et al.*, 2016).

Around 85% of women who had breast cancer in the UK survived for five years or more (*Breast Cancer Statistics*, 2017). Women diagnosed with breast cancer at the age of 60-69 showed longest survival rate in the UK, which could be due to the improvements in screening programmes and less favourable tumour features in younger women (*Breast Cancer Statistics*, 2017).

1.2.3 Risk factors for breast cancer

There are various factors such as age, inherited genes and family history, reproductive factors and exposure to risk factors (environmental and lifestyle factors) which can increase the risk of breast cancer.

1.2.3.1 Age

Age is one of the most significant risk factors for breast cancer (Thakur *et al.*, 2017). 69.1% of total cases were diagnosed above the age of 50 years (postmenopausal) based on global statistics (Heer *et al.*, 2020). The risk of breast cancer increases with age (Kim, Yoo and Goodman, 2015; Heer *et al.*, 2020) and this could be due to abnormal changes such as genetic mutations (Feng *et al.*, 2018), and mammary gland epithelium changes (increase in adipose tissue and stromal cell production of enzyme, called aromatase or accumulation of combined more dense collagenous breast stroma with fatty tissues) (Benz, 2008).

1.2.3.2 Inherited genes and family history

There are different genetic factors that increase the risk of breast cancer. Germline mutations in *BRCA1* and *BRCA2* represents around 40% of hereditary breast cancer cases (Cobain, Milliron and Merajver, 2016). 55% - 65% of *BRCA1* and 45% of *BRCA2* mutation carriers develop breast cancer by age 70 (Antoniou *et al.*, 2003; Chen and Parmigiani, 2007). Apart from *BRCA1* and *BRCA2*, there are other genes including *TP53*, *CDH1*, *PTEN*, *STK11*, *ATM*, *BRIP1*, *CHEK2* and *PALB2* that cause 5% of hereditary breast cancers due to being mutated (Melchor and Benítez, 2013). *TP53*, *CDH1*, *PTEN and STK11* can cause familial syndromes, which then contributes to breast cancer. *ATM*, *BRIP1*, *CHEK2* and *PALB2* are known as moderate susceptibility genes (Melchor and Benítez, 2013).

Family history is a well-known risk factor of breast cancer and patients with first degree relative with breast cancer represents 5-7% of all breast cancer cases (Melchor and Benítez, 2013). A cohort study in the UK showed women who have a first-degree relative affected by breast cancer, have almost a two times higher risk of developing breast cancer than women who have no first-degree relative affected by breast cancer (Brewer *et al.*, 2017; Al Ajmi *et al.*, 2020). A woman without *BRCA* mutations has a four-fold increased risk of developing breast cancer if they had ≥ 2 breast cancer cases before 50 years old, or ≥ 3 cases in their family history at any age (Metcalfe *et al.*, 2009).

1.2.3.3 Reproductive factors

Late onset of menopause, early age of menarche and nulliparity are some of the factors that can increase the risk of breast cancer development due to the modulation of high menstrual cycles which lead to prolonged or increased exposure to oestrogen (Martin and Weber, 2000; Key *et al.*, 2002). The risk of breast cancer increases by 3% with each one year delay in menopause (Beral *et al.*, 1997). The risk of breast cancer decreases by 25% with late age of menarche and higher parity (Hunter *et al.*, 1997). A case-control study also showed that late menopause and early age of menarche increase the risk of breast cancer by more than two fold (Thakur *et al.*, 2017) and a recent study also supported these findings (Rahmati *et al.*, 2020).

1.2.3.4 Environmental and lifestyle factors

Many studies identified that increasing oestrogen levels contribute to the development of breast cancer (Klassen and Smith, 2011) due to the differentiation of epithelial tissue, which could then transform into malignant breast cancer (Travis and Key, 2003). Although body mass index (BMI) is

not a very strong risk factor for breast cancer, BMI is known as hormonal risk factor for breast cancer development. Post-menopause women with high BMI have higher risk of breast cancer compared to women who have low BMI (Singletary, 2003). High BMI can increase the risk of breast cancer as adipose tissue is an extragonadal source of bioavailable oestrogen and production of oestrogen in adipose tissue is associated with breast cancer initiation and promotion (Clemons and Gross, 2001). Moreover, high BMI causes abdominal fat due to the excess levels of insulin and increases the breast cancer incidence (Verkasalo *et al.*, 2001). Hormone replacement therapy (HRT) is known as one of the major sources of exogenous oestrogen and is used for post-menopausal females to prevent osteoporosis and control the symptoms of menopause (Sun *et al.*, 2017). However, women who use HRT have a higher risk of developing breast cancer (adjusted relative risk 1.66 [95% CI 1.58-1.75], $P < 0.0001$) compared to women who do not use HRT (Banks *et al.*, 2003).

Non-hormonal risk factors can lead to the formation of breast cancer, however some non-hormonal risk factors modulate oestrogen indirectly as a hormonal risk factor (Martin and Weber, 2000). It has been stated that ionising radiation significantly increases the risk of breast cancer and this could be because of somatic mutation that ionising radiation causes (Goss and Sierra, 1998). Alcohol consumption as a non-hormonal factor also increases the risk of breast cancer (Thakur *et al.*, 2017) due to: 1) the changes in the level of the hormone estradiol, which is an oestrogen (Nagata *et al.*, 1997), 2) the effects on some biological pathways for example one carbon metabolism pathway inhibition (Varela-Rey *et al.*, 2013) and 3) ethanol metabolism (Boffetta and Hashibe, 2006).

1.2.4 Types of breast cancer

Breast cancer can develop by various mechanisms including imbalanced activity of pathways, which cause changes in the breast duct morphology and pattern (Velloso *et al.*, 2017). The development of breast cancer causes different morphological features, histopathological subtypes and immunohistochemical profiles (Makki, 2015). Therefore, different methods for the classification of breast cancer are utilised based on their invasive characteristics, histological grade, tumour size, lymph node involvement and histology or molecular profiling (IHC profiles) (Velloso *et al.*, 2017).

1.2.4.1 Histological types and development of breast cancer

Breast cancer can be classified into two main groups: *in situ* carcinoma (non-invasive) and infiltrating (invasive) carcinoma, which are then divided into different subtypes (Table 1.1)

(Malhotra *et al.*, 2010). In *in situ* carcinoma, cells are located in the ducts or lobules and do not invade the enclosing connective and fatty tissues. However, in infiltrating carcinoma, cells penetrate the duct and lobular wall and invade the surrounding tissues, which then spread to other parts of the body (Sharma *et al.*, 2010).

In situ carcinoma is divided into ductal carcinoma *in situ* (DCIS) or lobular carcinoma *in situ* (LCIS), as mentioned in table 1.1 (Velloso *et al.*, 2017). The types of invasive carcinoma include invasive ductal carcinoma, invasive lobular carcinoma, invasive medullary carcinoma, invasive mucinous carcinoma and invasive tubular carcinoma (Table 1.1) (Velloso *et al.*, 2017). Ductal carcinoma occurs in the ducts of the breast and in lobular carcinoma, the number of cells in the lobules (milk glands) of the breast increase dramatically (Sharma *et al.*, 2010). Ductal and lobular carcinoma could be a non-invasive or invasive carcinoma (Sharma *et al.*, 2010). In invasive medullary carcinoma, there is a distinct boundary between normal tissue and tumour tissue (Sharma *et al.*, 2010). Invasive mucinous carcinoma and invasive tubular carcinoma arise from mucus-producing cancer cells and invasive ductal carcinoma subtype, respectively (Sharma *et al.*, 2010).

Table 1.1. Breast cancer classification based on site of occurrence.

Types	***Location/Arise from***
***In situ* Carcinoma (Non-invasive)**	
Ductal carcinoma *in situ*	Ducts of the breast
Lobular carcinoma *in situ*	Lobules
Infiltrating Carcinoma (Invasive)	
Invasive ductal carcinoma	Ducts of the breast
Invasive lobular carcinoma	Lobules
Invasive medullary carcinoma	Invasive epithelial cells
Invasive mucinous carcinoma	Mucus-producing cancer cells
Invasive tubular carcinoma	Invasive ductal carcinoma

Normal breast ducts consist of the basement membrane surrounding a layer of myoepithelial cells, which surround luminal epithelial cells (Place, Jin Huh and Polyak, 2011). Additionally, stromal cells comprise of endothelial cells, leukocytes, fibroblasts and myofibroblasts in normal breast gland (Bissel and Radisky, 2001; Elenbaas and Weinberg, 2001). Epigenetic and genetic changes can lead to the progression of breast cancer from benign epithelial atypical ductal hyperplasia (ADH), to *in situ* carcinoma (Fig. 1.2) (Burstein *et al.*, 2004; Allred *et al.*, 2008). The basement membrane is

degraded and contributes to the loss of myoepithelial cells and increase of lymphocytes, endothelial cells, myofibroblasts and stromal fibroblasts (Fig. 1.2) (Polyak, 2007). Subsequently, degradation of basement membrane and depletion of myoepithelial cells cause invasive carcinoma. Progression of invasive carcinoma requires two main mechanisms: intravasation and extravasation (Fig. 1.2). Cancer cells enter into the blood, where they can circulate to distant sites of the body and this is known as intravasation (Kang and Pantel, 2014). The cells then invade through the vascular basement membrane and extracellular matrix into a distant tissue, which is the extravasation process (Lambert, Pattabiraman and Weinberg, 2017). As the final stage, invasive carcinoma can progress into metastatic carcinoma and causes the proliferation of circulated cells at distant organs (Fig. 1.2) (Burstein *et al.*, 2004).

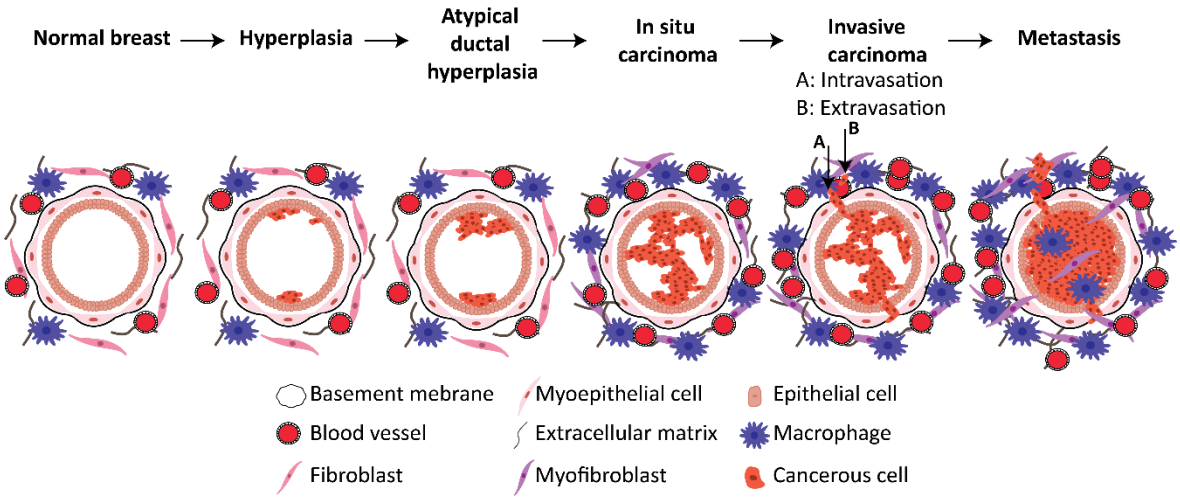

Figure 1.2. Diagram demonstrating the progression of breast cancer from normal breast to metastatic breast carcinoma.

Normal breast ducts consist of basement membrane, myoepithelial and epithelial cells. Stroma cells include blood vessel, extracellular matrix, macrophages and fibroblasts. In *in situ* carcinoma, epigenetic and genetic changes cause the abnormal proliferation of luminal epithelial cells and increase the number of stromal cells. Invasive carcinoma progresses by degradation of myoepithelial cells and basement membrane, which include intravasation (A) and extravasation (B). In metastatic breast carcinoma, migration of cancerous cells to distant organ occurs [Information collected from (Myal, Leygue and Blanchard, 2010; Santi, Kugeratski and Zanivan, 2018)].

1.2.4.2 Grading system

The grading system is one of the aspects of breast cancer classification. The Nottingham grading system also known as Elston-Ellis is the most common grading system and is used for the patient's prognosis determination and treatment strategy (Elston and Ellis, 1991). Nottingham grading system was a modified version of the Scarff-Bloom & Richardson grading system (Bloom and

Richardson, 1957; Elston and Ellis, 1991). The grading system provides information on the morphology of cancer cells compared to the normal breast tissue under the microscope. The tumour grading is based on the formation of tubule, nuclear grade and mitotic count; the score is given from 1 to 3 points in each category (Bloom and Richardson, 1957; Elston and Ellis, 1991). The points from each category are added together to have the total tumour grade, ranging from 3 to 9 points. The grading system classifies cancer cells as low-grade (grade 1, well differentiated, 3-5 points), intermediate-grade (grade 2, moderately differentiated, 6-7 points) and high-grade (grade 3-4, poorly differentiated-undifferentiated, 8-9 points) (Elston and Ellis, 1991). Some studies showed that the majority of the breast cancer cases at diagnosis were high-grade followed by intermediate and low-grade tumours (Krishnamurthy and Kumar, 2016; Sejben *et al.*, 2020). Other studies have suggested that the majority of the cases were intermediate-grade (Rakha *et al.*, 2010; Oluogun *et al.*, 2019). High-grade breast cancer cases have significantly shorter survival rates compared to the low and intermediate-grade breast cancer cases (Rakha *et al.*, 2008).

1.2.4.3 Tumour staging

Tumour staging determines the severity of cancer and provides important information both for the prognosis of the disease and the treatment plan for the patients. Primary tumour, regional lymph node status and metastasis status (TNM) staging is a frequently used staging system which has been used since the 1940s-1950s, which was clarified by the American Joint Committee for Cancer (AJCC) (Amin, Edge, *et al.*, 2017; Amin, Greene, *et al.*, 2017). The T stage indicates the size and the loco-regional invasion degree of primary tumour, which can be staged as T1, T2, T3 or T4 (Koh and Kim, 2019). The N stage indicates whether the cancer cells have spread to the lymph nodes and can be graded as N1, N2 or N3 (Koh and Kim, 2019). The M stage shows the presence of distant metastasis in the body, which can be staged as M0 or M1 (Koh and Kim, 2019). According to the TNM staging system by grouping them into overall stages, breast cancer could be staged as: stage 0, stage I (IA, IB), stage II (IIA-IIB), stage III (IIIA, IIIB, IIIC) and stage IV with stage 0 being DCIS and stage IV being the most advanced (Amin, Edge, *et al.*, 2017; Koh and Kim, 2019). Advanced breast cancer cases have the highest mortality rate (Li *et al.*, 2020).

1.2.4.4 Molecular classification of breast cancer

One well-known breast cancer classification method uses molecular biomarkers, which shows prognosis and the response to treatment of cancer (Carey *et al.*, 2006). The majority of breast

cancers are derived from luminal cells, which express oestrogen receptor (ER), progesterone receptor (PR), and/or human epidermal growth factor receptor 2 (HER2 or c-erbB2) (Velloso *et al.*, 2017). Immunohistochemistry (IHC) is used to determine the expression levels of ER and PR. HER2 expression level is measured by IHC or *in situ* hybridisation (ISH) (Kittaneh, Montero and Glück, 2013). Ki67 is a proliferation marker and is also used for the molecular classification of breast cancer (Ragab *et al.*, 2018). Breast cancer has been divided into four main groups based on the receptor expression; luminal A, luminal B, HER2+ and TNBC (Howlader *et al.*, 2014). The incidence rate of breast cancer subtypes are varied; luminal subtypes are 66%-73%, HER2+ are 4%-11% and TNBC are 10%-20% (Table 1.2) (Carey *et al.*, 2006; Kulkarni *et al.*, 2019).

1.2.4.4.1 Luminal A

Biomarker status of luminal A is ER+/PR+/HER2-/Ki67low (Table 1.2) (Prat, Ellis and Perou, 2011). Luminal A is slow growing, and the least aggressive subtype compared to other molecular subtypes of breast cancer. This subtype includes a variety of low-grade variants such as tubular carcinoma, lobular carcinoma, low-grade invasive ductal carcinoma, and expresses high levels of hormone receptors and associated genes (Carey *et al.*, 2006; Tamimi *et al.*, 2008; Al-Tamimi *et al.*, 2009). Luminal A also has a good prognosis compared to the other subtypes (Blows *et al.*, 2010).

1.2.4.4.2 Luminal B

Biomarker status of luminal B is ER+/PR+/HER2±/Ki67high (Table 1.2) (Prat, Ellis and Perou, 2011). Luminal B includes grade 2 invasive ductal carcinoma and has moderate-to-weak hormone receptors or associated genes expression (Carey *et al.*, 2006; Tamimi *et al.*, 2008; Al-Tamimi *et al.*, 2009). Luminal B has worse prognosis than luminal A (Carey *et al.*, 2006; Fan *et al.*, 2006).

1.2.4.4.3 HER2+

Biomarker status of HER2+ is ER-/PR-/HER2+ (Table 1.2) (Prat, Ellis and Perou, 2011). This subtype of breast cancer has a greater likelihood of being high grade and increased risk of metastasis to the lymph nodes (Carey *et al.*, 2006; Tamimi *et al.*, 2008; Al-Tamimi *et al.*, 2009). Transmembrane glycoprotein HER2 regulates cell proliferation, growth, differentiation, survival and angiogenesis (Iqbal and Iqbal, 2014). Thus, upon activation, HER2 can initiate various signalling pathways

involving transcription factors such as: mitogen activated protein kinases (MAPK), phosphoinositide 3-kinase (PI3K) and protein kinase C (PKC) (Iqbal and Iqbal, 2014). HER2+ subtype has a poor prognosis (Fan *et al.*, 2006) and is sensitive to HER2 directed targeted (trastuzumab (Herceptin)) therapy (Table 1.2), as mentioned in section 1.2.5.2 (Schnitt, 2010).

1.2.4.4.4 Triple negative breast cancer (TNBC)

TNBC (basal-like subtype) lacks ER, PR and HER2 (Table 1.2) (Prat, Ellis and Perou, 2011). TNBC is cytokeratin 5/6 (CK5/6) and/or epidermal growth factor receptor (EGFR) positive, has high expression of Ki67 and frequent *TP53* mutation (Carey *et al.*, 2006; Tamimi *et al.*, 2008; Al-Tamimi *et al.*, 2009). High-grade invasive cancers are included in TNBC (Carey *et al.*, 2006). TNBC has the poorest short term prognosis, higher risk of relapse and metastatic phenotype (Bianchini *et al.*, 2016; Reyes *et al.*, 2017). As TNBC lacks all three receptors, it does not respond to endocrine treatment or trastuzumab, and chemotherapy is used as a systemic treatment (Table 1.2) (Schnitt, 2010).

Table 1.2 Molecular subtypes of invasive breast carcinoma.

Molecular subtypes	***Molecular markers***	***Incidence***	***Treatment***
Luminal	ER/PR positive HER2 positive (Some Luminal B) Ki67low (Luminal A) Ki67high (Luminal B)	66%-73%	Endocrine therapy Chemotherapy Trastuzumab (Herceptin) for HER2 positive Luminal B
HER2+	ER/PR negative HER2 positive	4%-11%	Trastuzumab (Herceptin)
TNBC	ER/PR/HER2 negative Ki67high	10%-20%	Limited targeted therapy Chemotherapy

1.2.5 Treatment of breast cancer

Surgery, radiotherapy, chemotherapy and targeted therapy (endocrine therapy, HER2 therapy and targeting molecular pathways) are the four main treatment options for breast cancer (Dhankhar *et al.*, 2010).

The aim of non-metastatic breast cancer treatment is to prevent metastatic recurrence by removing the tumour completely from the breast and regional lymph nodes. Local treatment for non-metastatic breast cancer includes surgical resection or removal of axillary lymph nodes, with adjuvant radiotherapy. Systemic treatment includes neo-adjuvant or adjuvant treatments; endocrine therapy (plus chemotherapy if it is required) for luminal A and luminal B, HER2-directed therapy with chemotherapy for HER2+ patients and chemotherapy alone for TNBC (Waks and Winer, 2019). Therapies (radiotherapy, chemotherapy or endocrine therapy) before the surgery (neo-adjuvant) or after the surgery (adjuvant) could be performed to shrink the bulk of tumour or to fully treat the disease, respectively (Dhankhar *et al.*, 2010).

On the other hand, the aim of the metastatic breast cancer treatment is to improve the survival rate of patients and decrease the symptoms of the disease. There is still no cure for metastatic breast cancer but similar systemic treatment and local treatment options with non-metastatic breast cancer can be used in metastatic breast cancer to reduce the symptoms of the disease and prolong life (Waks and Winer, 2019).

1.2.5.1 Treatment options for luminal subtypes of breast cancer

Patients with luminal subtypes breast cancer shows poor response to chemotherapy but well response to hormonal therapy (Brenton *et al.*, 2005). The response rate between luminal A and luminal B can be different (Brenton *et al.*, 2005). Based on the study of recurrence score, it was shown that luminal A tumours have low recurrence score while luminal B tumours have high recurrence score (Paik *et al.*, 2004). Therefore, endocrine therapy could be used for luminal A tumours and combination of endocrine and chemotherapy can be used for luminal B tumours (Brenton *et al.*, 2005; Dai *et al.*, 2015).

According to the hormone receptor expression, endocrine therapy is used to balance the hormones or inhibit the hormonal activities (Freedman *et al.*, 2015). There are four main current hormonal treatment regimens for breast cancer which are tamoxifen, aromatase inhibitors (letrozole, anastrozole and exemestane), luteinizing hormone-releasing hormone analogs (goserelin and leuprolide) and fulvestrant (Tong *et al.*, 2018). Endocrine therapies are the most commonly used

options for the patients who have ER+ and PR+ status with asymptomatic visceral and limited metastases, or soft tissue metastases (Rugo *et al.*, 2016).

Tamoxifen is an antagonist of ER and binds to ER to inhibit its activity (Anjum, Razvi and Masood, 2017). Therefore, patients who have ER+ molecular status could be treated with tamoxifen. It has been shown that the disease free survival rate of pre-menopausal and post-menopausal women with breast cancer has improved with tamoxifen since the 1970s (Robert, 1997; Meisel *et al.*, 2018).

In post-menopausal females, aromatase inhibitors (exemestane, letrozole, and anastrozole), are usually used, which is the alternative treatment option for the patients who have ER+ breast cancer (Nounou *et al.*, 2015). Aromatase is a critical enzyme involved in oestrogen synthesis as it is a member of the cytochrome P450 (CYP) family enzymes that converts androstenedione to oestrogen and testosterone to estradiol (Dutta and Pant, 2008). Therefore, aromatase inhibitors block aromatase activity by inhibiting oestrogen synthesis. There are two types of aromatase inhibitors: steroidals (exemestane) and non-steroidals (letrozole and anastrozole). Steroidals aromatase inhibitors bind aromatase enzyme competitively; bind covalently to the site of aromatase where substrate binds and inactive the enzyme irreversibly (Van Asten *et al.*, 2014; Greenwalt *et al.*, 2020). Non-steroidal aromatase inhibitors bind to the heme moiety of the enzyme and aromatase enzyme is reversibly inhibited (Van Asten *et al.*, 2014; Anjum, Razvi and Masood, 2017).

Letrozole showed more successful results (9.4 months for time to progression) than tamoxifen alone (6.0 months for time to progression) in post-menopausal women who have advanced breast cancer (Mouridsen *et al.*, 2003). Luteinizing hormone-releasing hormone analogs inhibit the release of hormone from the ovary and fulvestrant is a selective ER degrader (Tong *et al.*, 2018).

Tamoxifen or Arimidex Randomised Group Efficacy and Tolerability (TARGET) trial (Bonneterre *et al.*, 2000) and the North American trial (Nabholtz *et al.*, 2000) have been the two largest randomised phase III trials which compared the efficacy of tamoxifen and aromatase inhibitor in reducing cancer recurrence. The median time to disease progression and clinical benefit (complete response and partial response) rates were similar between the patients who were treated with anastrozole 1 mg/d orally or tamoxifen 20 mg/d orally in the TARGET trial (Bonneterre *et al.*, 2000; Greenwalt *et al.*, 2020). Thus, TARGET trial highlighted that anastrozole was at least as effective as tamoxifen in terms of time to disease progression and clinical benefits. In the North American trial, anastrozole showed median time to disease progression of 11.1 months whereas, tamoxifen showed 5.6 months (Nabholtz *et al.*, 2000). Then, the follow-up study combined the analysis of TARGET and the North American trials which showed that anastrozole (10.7 months) was significantly associated with longer median time to disease progression than tamoxifen (6.4 months) (Bonneterre *et al.*, 2001).

The main challenge of the endocrine therapies is the resistance mechanism due to the link between growth factor receptor signalling pathways and ER (Roop and Ma, 2012). The amplification of cyclin D1 and cyclin-dependent kinase 4 (CDK4) was observed in almost 29% and 14% of hormonal receptor positive (HR+)/HER2- breast cancer patients, respectively (Koboldt *et al.*, 2012). When the cells are resistant to hormonal treatment, the proliferation of cancer cells relies on CDK4/6-cyclin D1 (Musgrove and Sutherland, 2009). Therefore, CDK4/6 inhibitors (palbocilib, ribociclib, and abemaciclib) are one of the targeted therapies that could be used to treat HR+/HER2- breast cancer patients (Cristofanilli *et al.*, 2016; Finn *et al.*, 2016; Hortobagyi *et al.*, 2016; Sledge *et al.*, 2017). Studies showed that the combination of palbociclib with aromatase inhibitor and ribociclib with aromatase inhibor could be used as first-line treatment for HR+/HER2- advanced breast cancer patients (Finn *et al.*, 2016; Hortobagyi *et al.*, 2016). The combination treatment of palbociclib-letrozole improved median PFS by approximately 10 months (Finn *et al.*, 2016) and ribociclib-letrozole improved PFS rate by approximately 20% (Hortobagyi *et al.*, 2016) compared to the group with placebo-letrozole in HR+/HER2- metastatic breast cancer. Abemaciclib-fulvestrant combination therapy was approved for HR+/HER2- metastatic breast cancer patients who had resistance to aromatase inhibitor in the MONARCH-2 trial (Sledge *et al.*, 2017). The PFS rate of patients who have aromatase inhibitor sensitive advanced breast cancer was significantly improved with abemaciclib-non-steroidal aromatase inhibitor combination (Goetz *et al.*, 2017). The abnormal activation of the PI3K-AKT-mTOR signalling pathway can also cause resistance to endocrine treatment (Miller *et al.*, 2010). This resistance mechanism could be reversed with the combination of hormonal receptor treatment with PI3K/AKT/mTOR treatment (Miller *et al.*, 2010). PI3K inhibitor plus aromatase inhibitor are used as a second-line treatment for HR+/HER2-advanced breast cancer. A pan-class I PI3K inhibitor (buparlisib) plus fulvestrant showed significant improvements in PFS in the patients with *PIK3CA* mutation but had higher toxicities (Baselga *et al.*, 2017). However, α-specific PI3K inhibitors (alpelisib and taselisib) plus fulvestrant showed less toxicities and more selectivity in HR+ patients with *PIK3CA* mutation (Bosch *et al.*, 2016; Dickler *et al.*, 2018). mTOR inhibitor (everolimus) is one of the treatment options for PI3K/AKT/mTOR signalling pathway (Baselga, Campone, *et al.*, 2012). Everolimus is an FDA approved drug with the combination of exemestane for HR+ advanced breast cancer cases which were resistant to letrozole or anastrozole (Baselga, Campone, *et al.*, 2012).

1.2.5.2 Treatment options for HER2+ breast cancer

The Food and Drug Administration (FDA) has approved several drugs to treat metastatic HER2+ breast cancer including trastuzumab, lapatinib, trastuzumab emtansine (antibody-cytotoxic agent

conjugate) and pertuzumab (Mohamed *et al.*, 2013). Trastuzumab is a monoclonal antibody which was approved in 1998, and was the first FDA approved drug to treat HER2+ breast cancer patients (Slamon *et al.*, 2001). Trastuzumab inhibits the extracellular domain of HER2 receptor and is known as a targeted therapy for HER2+ breast cancer (Meisel *et al.*, 2018). Lapatinib is a dual tyrosine kinase inhibitor and interrupts both HER2 and EGFR pathways (Tong *et al.*, 2018). Trastuzumab emtansine is an antibody-cytotoxic agent conjugate where the trastuzumab is linked with a small-molecule microtubule inhibitor (emtansine) (Tong *et al.*, 2018). Trastuzumab emtansine inhibits HER2 signalling by trastuzumab and prevents microtubule function by cytotoxic activity of myotenic dystrophy type 1 (DM1) (Verma *et al.*, 2012). Pertuzumab also acts on HER2 by inhibiting heterodimerisation domain of HER2-HER3 (Capelan *et al.*, 2013).

HER2 directed therapies could be combined with each other or chemotherapy to improve the response to treatment (Waks and Winer, 2019). In HER2+ metastatic breast cancer, the first-line treatment includes taxane chemotherapeutic agents with trastuzumab and pertuzumab (Baselga, Cortés, *et al.*, 2012), and the second line treatment includes trastuzumab emtansine (Verma *et al.*, 2012). The study with HER2+ early breast cancer patients who had residual invasive disease after completion of neo-adjuvant treatment with taxane and trastuzumab demonstrated that the risk of recurrence or death of patients who were treated with trastuzumab emtansine have 50% lower risk than the patients who were treated with trastuzumab alone (Von Minckwitz *et al.*, 2019).

HER2 directed therapies can be combined with chemotherapy or endocrine therapy in HR+ breast cancer patients if resistance develops (Waks and Winer, 2019). The combination therapy of trastuzumab and chemotherapy significantly improved the overall response from 32% to 50%, duration of response from 6.1 months to 9.1 months and treatment failure time from 4.5 months to 6.9 months compared to the treatment with chemotherapy alone (Slamon *et al.*, 2001). It has been shown that the combination of trastuzumab, docetaxel and pertuzumab improved the progression-free survival (PFS) from 12.4 months to 18.7 months and overall survival from 40.8 months to 56.5 months compared to the group without pertuzumab (Swain *et al.*, 2015).

The resistance mechanism of HER2+ patients is also the major challenge of the disease. Therefore, HER2-directed therapy was improved with the combination treatment strategy. For HR-/HER2+ advanced breast cancer, when pan-class I PI3K inhibitors (buparlisib and pilaralisib) were combined with lapatinib (tyrosine kinase inhibitor) (Guerin *et al.*, 2017) and trastuzumab (Saura *et al.*, 2014) or trastuzumab and paclitaxel (Tolaney *et al.*, 2015), median PFS was improved compared to trastuzumab and paclitaxel alone. Trastuzumab (Hudis *et al.*, 2013) or trastuzumab and paclitaxel (Chien *et al.*, 2016) treatment followed by AKT inhibitor (MK-2206) showed promising anti-tumour activities in HER2+ metastatic breast cancer. mTOR inhibitor (everolimus) was also combined with

trastuzumab and vinorelbine (chemotherapeutic drug) or trastuzumab and paclitaxel to treat the patients with trastuzumab resistance in HR-/HER2+ advanced breast cancer (André *et al.*, 2014; Hurvitz *et al.*, 2015). However, these treatment strategies were highly toxic (André *et al.*, 2014; Hurvitz *et al.*, 2015). Additionally, the combination of mTOR inhibitors (ridaforolimus and sirolimus) with trastuzumab showed anti-tumour activity and may overcome the trastuzumab resistance in HER2+ patients (Acevedo-Gadea *et al.*, 2015; Seiler *et al.*, 2015).

1.2.5.3 Treatment options for TNBC

TNBC lacks all three receptors; ER, PR and HER2, thus endocrine or HER2-directed treatments are not successful for this disease. Therefore, chemotherapy has been used as a systemic treatment for TNBC (Schnitt, 2010). However, the efficacy of the adjuvant chemotherapy is poor (Yin *et al.*, 2020) and tumour could be recurrent due to the residual metastatic lesions (Chaudhary, Wilkinson and Kong, 2018). The combination of bevacizumab and chemotherapeutic drugs was used for TNBC, but the survival time of patients was not significantly increased (Cameron *et al.*, 2013). Thus, developing new treatment strategies and targeted therapies was crucial for TNBC.

As TNBC lacks ER, PR and HER2 and is molecularly heterogeneous (Lehmann *et al.*, 2011), discovering a new biomarker or targeted therapy for TNBC is challenging. Therefore, this paves the way for studies into identification of different gene expression signatures in TNBC (Lehmann *et al.*, 2011; Criscitiello *et al.*, 2012). Lehmann *et al.,* 2011 identified six different TNBC subtypes; basal-like 1 (BL1), basal-like 2 (BL2), immunomodulatory (IM), mesenchymal (M), mesenchymal stem-like (MSL) and luminal androgen receptor (LAR) (Lehmann *et al.*, 2011). The main features of each TNBC subtype are described in Table 1.3. However, Bareche *et al.,* 2018 discovered five stable TNBC subtypes; BL1, IM, M, MSL and LAR (Bareche *et al.*, 2018). According to the improved molecular characterisation of TNBC, different therapeutic targets have been revealed; poly (ADP-ribose) polymerase (PARP) inhibitors, receptor tyrosine kinase (RTK) inhibitors (EGFR, FGFR, VEGFR, MET), non-RTK inhibitors (PI3K/AKT/mTOR, Src, MEK), epigenetic targets, androgen receptor inhibitors and immunotherapies, Table 1.3 (Lee and Djamgoz, 2018). PARP inhibitors (olaparib, talazoparib, veliparib, niraparib and rucaprib) or the DNA-targeting platinum drug (carboplatin) showed promising outcomes in *BRCA1/2* deficient TNBC which could be used as a monotherapy or combined therapy (Konecny and Kristeleit, 2016; Castrellon *et al.*, 2017). The drug with the furthest clinical development is olaparib which showed 2.8 months improvement in median PFS and 42% reduction in the risk of disease progression/death compared to systemic chemotherapy (Robson *et al.*, 2017).

Table 1.3 Features and targeted therapies of TNBC subtypes.

Subtypes	Gene ontology terms	Targeted therapy
BL1	Cell cycle DNA damage repair	PARP inhibitors CDK inhibitors Cisplatin
BL2	Growth factor signalling Growth factor receptor Glycolysis and Gluconeogenesis	mTOR inhibitors Growth factor inhibitors
IM	Immune cell processes Angiogenesis	Immune checkpoint inhibitors
M	Cell motility ECM receptor interaction Cell differentiation pathways	Drugs to target EMT Abl/Src inhibitor
MSL	Angiogenesis Immune signalling Growth factor pathways	PI3K/mTOR inhibitor Abl/Src inhibitor
LAR	Hormonally regulated pathways	Androgen inhibitors Hsp90 inhibitors

Atezolizumab (TECENTRIQ®), an anti-programmed death-ligand 1 (PD-L1) monoclonal antibody (checkpoint inhibitor), was the first FDA approved breast cancer immunotherapy to be combined with chemotherapy (Abraxane; nab®-Paclitaxel) for PD-L1 positive TNBC cases (Cyprian *et al.*, 2019). FDA recently approved sacituzumab govitecan for TNBC patients who have received two or more prior systemic therapies. Sacituzumab govetecan is an antibody-drug conjugate where the antibody targets trophoblast cell-surface antigen 2 (Trop-2) that is highly expressed in majority of breast cancer and linked to topoisomerase I inhibitor via proprietary hydrolysable linker (Bardia *et al.*, 2021). Additionally, pembrolizumab, an anti–programmed death 1 (PD-1) monoclonal antibody combined with neoadjuvant chemotherapy and as adjuvant therapy was also recently FDA approved for locally recurrent unresectable or metastatic TNBC whose tumours express PD-L1 (Schmid, Cortes, Pusztai, *et al.*, 2020).

1.3 Phosphatase and tensin homolog (PTEN)

PTEN is a tumour suppressor gene, which dephosphorylates phosphatidylinositol 3,4,5-triphosphate (PIP_3) into phosphatidylinositol 4,5-bisphosphate (PIP_2) (Leevers, Vanhaesebroeck and Waterfield, 1999) and inhibits oncogenic phosphatidylinositol-3-kinase (PI3K)/AKT signalling pathway and thereby inhibits cell proliferation and growth (details are included in section 1.3.4) (Myers *et al.*, 1997; Cantley and Neel, 1999).

There are different mechanisms that regulate the PTEN activity and expression including genetic changes, epigenetic silencing, transcriptional regulation, post-transcriptional regulation, post-translational mechanisms and protein-protein interactions (details are in section 1.3.5) (Salmena, Carracedo and Pandolfi, 2008; Song, Salmena and Pandolfi, 2012). It has also been shown that PTEN can shuttle between cytoplasm and nucleus and apart from its cytoplasmic role, it has functions within the nucleus (details are in sections 1.3.7 and 1.3.8) (Planchon, Waite and Eng, 2008).

1.3.1 *PTEN* as a tumour suppressor gene

PTEN deleted on chromosome 10 was identified as a tumour suppressor gene, which is located on 10q23 chromosome band (Song, Salmena and Pandolfi, 2012). *PTEN*, also known as tensin-like phosphatase 1 (*TEP1*) or mutated in multiple advanced cancers 1 (*MMAC1*) was first identified as a lost or mutated phosphatase in various cancer types such as brain, breast, kidney and prostate in 1997 (Li and Sun, 1997; Li *et al.*, 1997; Steck *et al.*, 1997). *PTEN* is the second most mutated or deleted gene after *TP53* in different cancer types (Kechagioglou *et al.*, 2014).

At the end of 1990s and beginning of 2000s, both *in vitro* and *in vivo* studies showed that loss of *PTEN* expression contributes to oncogenesis, reduced apoptosis, increased proliferation and migration of cells (Di Cristofano *et al.*, 1998; Stambolic *et al.*, 1998; Suzuki *et al.*, 1998; Podsypanina *et al.*, 1999; Sun *et al.*, 1999; Liliental *et al.*, 2000; Stambolic, Tsao and Macpherson, 2000; Backman *et al.*, 2001). *In vivo* studies showed that PTEN plays a role during embryonic development as loss of *PTEN* contributes to severe hyperproliferation and the failure to elicit apoptosis, causing early embryonic mortality (Di Cristofano *et al.*, 1998; Suzuki *et al.*, 1998; Podsypanina *et al.*, 1999). Moreover, heterogeneous deletion of *PTEN* causes carcinogenesis that identified *PTEN* as a haplo-insufficient tumour suppressor gene (Hollander, Blumenthal and Dennis, 2011; Song, Salmena and Pandolfi, 2012). Wild-type (WT) PTEN promotes apoptosis and inhibits cell migration and cell cycle progression (Gu, Tamura and Yamada, 1998; Li and Sun, 1998; Tamura *et al.*, 1998). Additionally,

PTEN plays a role in activating DNA damage checkpoints to prevent genetic instability (Puc *et al.*, 2005).

1.3.2 Structure of PTEN

PTEN contains two main active domains; one at the N-terminus and one at the C-terminus (Fig. 1.3) (Lee *et al.*, 1999). The N-terminal domain has lipid phosphatase activity, which is the main domain for the tumour suppressor role of PTEN (Cantley and Neel, 1999; Yin and Shen, 2008). The N-terminal domain contains PIP_2 binding domain (PBD) and phosphatase domain which has an enzymatic activity and phosphatase activity role (Campbell, Liu and Ross, 2003; Walker *et al.*, 2004). The C-terminal domain consists of the C2 domain and C-tail region with PDZ motif which are involved in PTEN stability (Georgescu *et al.*, 1999) and protein-protein interaction (Fanning and Anderson, 1999). The C2 domain of PTEN modulates its stability (Georgescu *et al.*, 1999) and its recruitment to the phospholipid membranes (Das, Dixon and Cho, 2003). Crystal structure analysis of the C2 domain demonstrated a β-sandwich structure which forms loop and is involved in DNA and other protein interaction (Lee *et al.*, 1999). Additionally, the C2 domain of PTEN is also involved in the interaction with the centromere (Shen *et al.*, 2007).

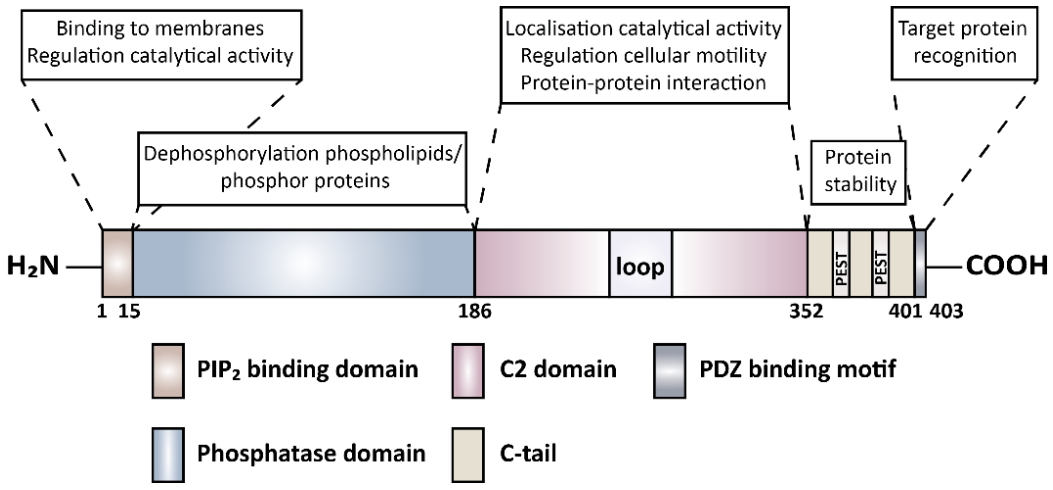

Figure 1.3 PTEN protein domain structure.
PTEN has 403 amino acids and contains five domains; N-terminal PIP_2 binding domain (residues 6-15), N-terminal phosphatase domain (15-186), C2 domain (186-352), the C-tail (352-403) and PDZ binding motif. "Loop" represents conserved but flexible region, from residues 286 to 309 in C2 domain. The C-tail contains two PEST (proline, glutamic acid, serine, threonine) sequences. PIP_2 binding domain has a role to mediate membrane binding and regulate catalytical activity, phosphatase domain regulates enzymatic activity, C2 domain is responsible for cellular localisation and protein-protein interaction, C-tail is responsible for protein stability and PDZ binding motif functions for the recognition of target protein. [Information collected from (Wang and Jiang, 2008; Jerde, 2015)].

1.3.3 PTEN as a dual lipid and protein phosphatase

PTEN is a dual-specificity phosphatase (Myers *et al.*, 1997, 1998; Cantley and Neel, 1999). PTEN protein phosphatase activity dephosphorylates phosphorylated tyrosine, serine and threonine residues in peptide substrates (Myers *et al.*, 1997). PTEN also has lipid phosphatase function as it dephosphorylates PIP_3 into PIP_2 and inhibits several PIP_3 dependent kinases such as PI3K/AKT/mTOR signalling pathway (Myers *et al.*, 1998; Cantley and Neel, 1999), which is the primary physiological target of PTEN (Sulis and Parsons, 2003; Leslie and Downes, 2004; Sansal and Sellers, 2004).

1.3.4 PTEN and PI3K/AKT signalling pathway

PI3Ks are a family of intracellular lipid kinases which phosphorylates the 3 position hydroxyl group of the inositol ring of phosphatidylinositol (Maehama and Dixon, 1998). PIP_3 is the primary substrate of PTEN and the catalytic product of PI3Ks (Maehama and Dixon, 1998).

In the absence or loss of *PTEN*, proteins which contain pleckstrin homology domains such as AKT family members and phosphoinositide-dependent kinase 1 (PDK1), are recruited to and activated on the cell membrane by excessive PIP_3 (Klippel *et al.*, 1997; Ziemba *et al.*, 2013). AKT isoforms have two residues which are Thr308 and Ser473 and are phosphorylated by PDK1 and mammalian target of rapamycin complex 2 (mTORC2), respectively (Manning and Cantley, 2007). AKT is activated by the phosphorylation of Thr308 and Ser473 residues of AKT (Manning and Cantley, 2007). AKT1, AKT2 and AKT3 which are active AKT isoforms can regulate cell survival, protein synthesis, angiogenesis, epithelial mesenchymal transition (EMT), metastasis, cell proliferation and glucose metabolism by phosphorylating downstream signalling proteins (Fig. 1.4) (Manning and Cantley, 2007). Active AKT can regulate cell survival by inhibiting forkhead box O1 (FOXO1) (Nakamura *et al.*, 2000), B cell lymphoma 2 (BCL-2) antagonist of cell death (Bad) (Datta *et al.*, 1997) and activating mouse double minute 2 homolog (MDM2) (Mayo and Donner, 2001). Protein synthesis is also regulated by active AKT with the inhibition of tuberous sclerosis 1/2 (TSC1/TSC2) (Inoki *et al.*, 2002), and proline-rich AKT substrate of 40 kDa (PRAS40) (Haar *et al.*, 2007) and activating mammalian target of rapamycin complex 1 (mTORC1) (Sekulić *et al.*, 2000). Moreover, activated mTORC1 and reactive oxygen species (ROS) drive up-regulation of hypoxia induced factor 1-alpha (HIF1-α) and vascular endothelial growth factors (VEGFs) transcriptional activation to regulate angiogenesis (Dodd *et al.*, 2015). Active AKT regulates EMT/metastasis by phosphorylation of nuclear factor kappa B (NFκB) (Luo *et al.*, 2007; Sheng, Qiao and Pardee, 2009) and regulates cell proliferation by phosphorylation of cyclin dependent kinase 2 (CDK2) and inhibition of Wee1, myelin transcription

factor 1 (Myt1), $p27^{Kip1}$, $p21^{Waf1/cip1}$(Hollander, Blumenthal and Dennis, 2011) and glycogen synthase kinase 3 beta (GSK3β) (Diehl *et al.*, 1998). Additionally, inhibition of GSK3β can also regulate glucose metabolism (Chalhoub and Baker, 2008; Song, Salmena and Pandolfi, 2012).

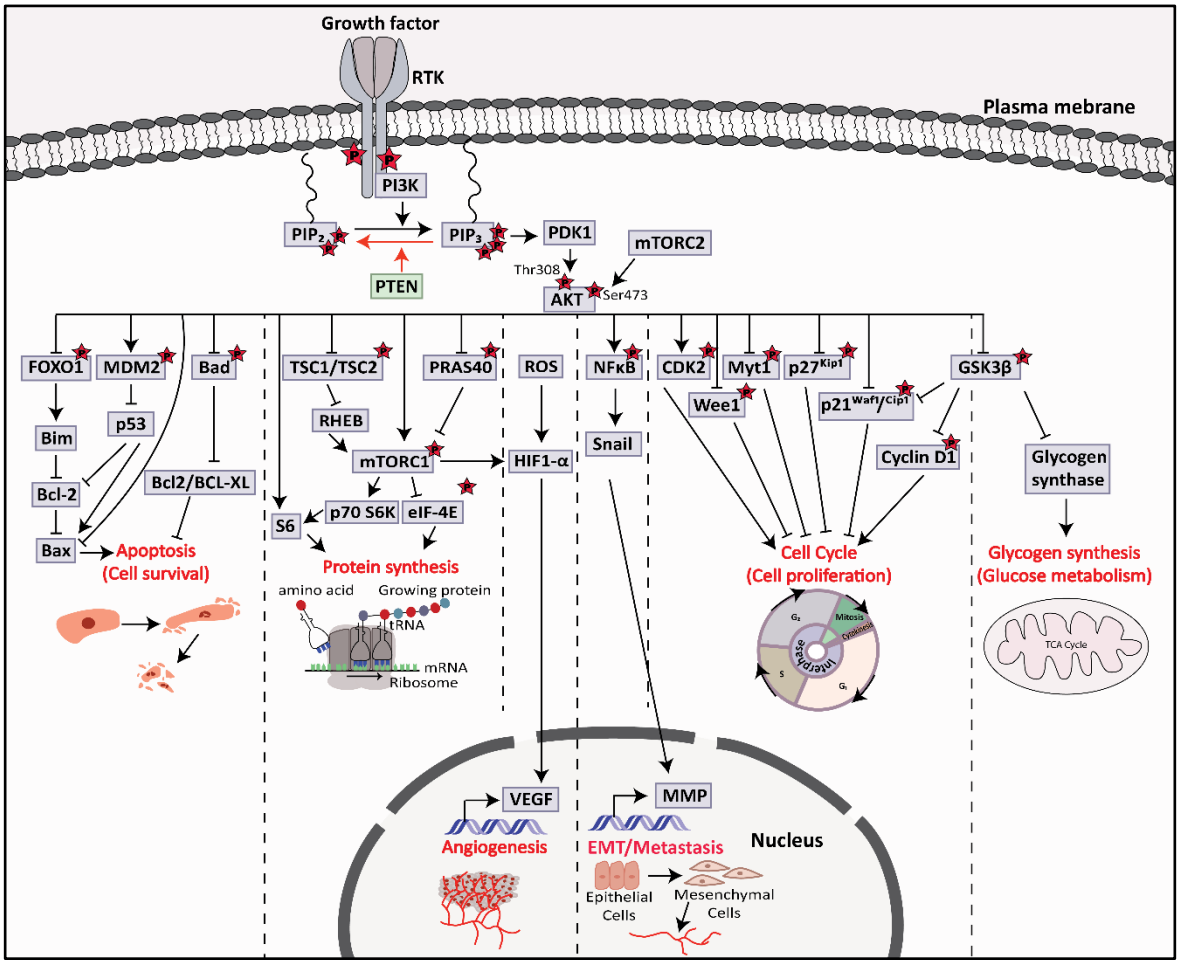

Figure 1.4 Diagram showing PTEN/PI3K/AKT signalling pathway.

Upstream of PI3K/AKT pathway includes RTKs. PTEN suppresses the function of PI3K by dephosphorylating PIP_3 into PIP_2 and causes inactivation of AKT through PDK1. However, loss of *PTEN* activates AKT, which has an influence on its downstream pathways such as inhibition of FOXO1 and Bad and activation of MDM2 to supress apoptosis. Activation of AKT due to the loss of *PTEN* inhibits TSC1/TSC2 and PRAS40 and activates mTORC1 which leads to protein synthesis. Active AKT also activates NFκB and contributes to EMT; activates CDK2, inhibits Wee1, Myt1, $p27^{Kip1}$, $p21^{Waf1/Cip1}$ and GSK3β which leads to cell proliferation. Active AKT also inhibits GSK3β to increase glucose metabolism. PTEN: phosphatase and tensin homolog; PI3K: phosphoinositide 3-kinase; RTK: receptor tyrosine kinase; PIP_2: phosphatidylinositol 4,5-bisphosphate; PIP_3: phosphatidylinositol 3,4,5-triphosphate; PDK1: phosphoinositide-dependent kinase 1; FOXO1: forkhead box O1; MDM2: mouse double minute 2 homolog; Bad: B cell lymphoma 2 (BCL-2) antagonist of cell death; TSC1/TSC2: tuberous sclerosis 1/2; PRAS40: proline-rich AKT substrate of 40 kDa; mTORC1: mammalian target of rapamycin complex 2; NFκB: nuclear factor kappa B; EMT: epithelial mesenchymal transition; CDK2: cyclin dependent kinase 2; Myt1: Myelin transcription factor 1; GSK3β: Glycogen synthase kinase 3 beta. [Information collected from (Hennessy *et al.*, 2005)].

1.3.5 Regulations of *PTEN*

Various molecular mechanisms that regulate PTEN have an influence on the functional PTEN levels in sporadic cancers, inherited syndromes and other diseases. Genetic mutations such as a heterozygous loss (50%) or a homozygous loss (100%) negatively affect the function of PTEN (Salmena, Carracedo and Pandolfi, 2008; Song, Salmena and Pandolfi, 2012). Moreover, PTEN is also regulated or altered by different mechanisms such as epigenetic silencing, transcriptional, post-transcriptional regulation, post-translational modifications and interaction with different proteins, which could initiate and progress breast cancer (Salmena, Carracedo and Pandolfi, 2008; Song, Salmena and Pandolfi, 2012). Therefore, decrease in PTEN expression causes aggressive tumour phenotype and tumorigenesis in different cancer types, as mentioned in section 1.3.4.

1.3.5.1 Genetic alterations of *PTEN*

Germline and somatic mutations of *PTEN*; large deletions, intragenic deletions and insertions, missense, nonsense and splice site variants can be found in the promoter and all exons of PTEN (Fig. 1.5A) (Lee, Chen and Pandolfi, 2018). Truncated PTEN mutations can be produced by nonsense mutation and lack C-terminal tail and PDZ-binding motif, which play important role in PTEN protein stability and recruitment to the membrane (Agrawal, Pilarski and Eng, 2005).

PTEN hamartoma tumour syndromes (PHTS): Cowden syndrome, PTEN-related Proteus syndrome, Bannayan-Riley-Ruvalcaba syndrome and Proteus-like syndrome are inherited cancer syndromes, which develop due to the *PTEN* germline mutation (Marsh *et al.*, 1999; Zhou *et al.*, 2001). Approximately 80% of PHTS patients have *PTEN* germline mutations (Marsh *et al.*, 1998). People with PHTS are more prone to develop cancers, such as breast cancer, who has hamartomatous excessive growth in breast tissue (Marsh *et al.*, 1998) because the function of PTEN is exerted in the initiation and the progression of cancer (Molinari and Frattini, 2014). Almost 70% of PTEN mutations are observed in exon 5, exon 7 and exon 8 in Cowden syndrome and 40% of these mutations are found in exon 5 that encodes the phosphatase core motif (Marsh *et al.*, 1998). Similar results were also observed in another study which showed that 32% of PTEN mutation in Cowden syndrome were observed in exon 5, 13% in exon 7 and 16% in exon 8 (Tan *et al.*, 2011). As exon 5 encodes phosphatase domain, mutation in exon 5 abrogates the tumour suppressor role of *PTEN* (Liaw *et al.*, 1997; Chow and Baker, 2006). Moreover, sporadic PTEN mutations are observed in different cancer types such as GBM (19-32%), endometrial (21%), prostate (17-21%), malignant melanoma (14-16%) and breast (4-11%) (Bazzichetto *et al.*, 2019). However, tumours with PTEN mutations can still have partial or full catalytic function of PTEN which hypothesised different

mechanisms can inactivate PTEN such as mutation at lysine (Lys,K)289 that change PTEN protein localisation (mentioned in sections 1.3.5.5 and 1.3.7) (Trotman *et al.*, 2007).

1.3.5.2 Epigenetic silencing of *PTEN*

In different cancer types, abnormal gene promoter methylation or abnormal modification of histones causes epigenetic silencing of *PTEN* expression (Fig. 1.5B). When CpG islands in the *PTEN* promoter are hypermethylated, it can silence the transcription of *PTEN* in breast cancer and melanoma (García *et al.*, 2004; Mirmohammadsadegh *et al.*, 2006). Sal-like protein 4 (SALL4) which is a zinc-finger transcription factor recruits an epigenetic repressor complex (Mi-2/NuRD) that contains ATP-dependent nucleosome remodelling activity and a histone deacetylase to the *PTEN* locus and leads to condensed heterochromatin and represses *PTEN* expression (Lu *et al.*, 2009). Despite the *PTEN* mutation frequency being low in breast cancer as mentioned in section 1.3.5.1, the frequency of *PTEN* promoter methylation is 50% in breast cancer cases (Zhang *et al.*, 2013). Thus, epigenetic silencing of PTEN inactivates this tumour suppressor gene and lead to activation of oncogenic AKT signalling (Mirmohammadsadegh *et al.*, 2006) .

1.3.5.3 Transcriptional regulation of *PTEN*

There are different transcription factors that have binding sites at the *PTEN* promoter and are known as positive or negative regulators of *PTEN* transcription (Fig. 1.5C).

There is a p53 binding site at the upstream of the *PTEN* and it was shown that p53 induction in primary and tumour cell lines with WT p53 upregulates *PTEN* mRNA levels compared to mutant p53 cells (Stambolic *et al.*, 2001). Early growth regulated transcription factor 1 (EGR1), peroxisome proliferator-activated receptor gamma (PPARγ) and C-repeat binding factor 1 (CBF1) also upregulate the expression of *PTEN*. It has been shown that EGR1 binds to the *PTEN* promoter and due to the stimulation of insulin-like growth factor 2 (IGF-2) by a negative-feedback loop (Moorehead *et al.*, 2003), *PTEN* expression is upregulated. Activated PPARγ can also bind to the *PTEN* promoter and this leads to the up-regulation of *PTEN* in both normal and cancerous cells such as macrophages, colorectal cancer cells and breast cancer cells (Patel *et al.*, 2001). For example, PTEN expression increases with rosiglitazone (PPARγ selective ligand to activate PPARγ) and this decreases hepatocarcinoma cell line (BEL-7404) migration (Zhang *et al.*, 2006). Moreover, it has been shown that transcriptional levels of *PTEN* are regulated by the Notch-1 signalling pathway via

the CBF-1 transcription factor which binds to the minimal *PTEN* promoter (Whelan, Forbes and Bertrand, 2007).

On the other hand, mitogen-activated protein kinase kinase 4 (MKK4) is a negative regulator of *PTEN* transcription via activating NFκB that binds to *PTEN* promoter region (Xia *et al.*, 2007). It has also been shown that transforming growth factor beta (TFGβ) inhibits *PTEN* transcription in mesangial (Mahimainathan *et al.*, 2006) and pancreatic cancer cells (Chow *et al.*, 2007). Additionally, c-Jun which is a transcription factor also decreases *PTEN* expression via the binding to the *PTEN* promoter at the variant AP-1 site (PF-1) and the negative correlation between c-Jun and PTEN levels were observed in different human cancer cell lines (Hettinger *et al.*, 2007). Inhibitor of differentiation-1 (Id-1) (Lee *et al.*, 2009), B lymphoma Mo-MLV insertion region 1 homolog (Bmi-1) (Song *et al.*, 2009) and SNAIL (Escrivà *et al.*, 2008) can also bind to *PTEN* promoter and inhibit its transcription.

These studies indicated that transcriptional control of PTEN plays an important role at the intersection of pathways to regulate PTEN expression and has an influence on tumour suppression and tumour promotion.

1.3.5.4 Post-transcriptional regulation of *PTEN*

miRNAs are small non-coding RNA molecules which have 20-25 nucleotides (nts) and regulate gene expression in many cancer types (Fig. 1.5D). Different studies showed that various miRNAs downregulate the expression of *PTEN* and this can lead to carcinogenesis and metabolic disorders (Tay, Song and Pandolfi, 2013). miR-21 is one of the oncogenic miRNAs that downregulates the expression of *PTEN* in ovarian, hepatocellular and lung cancers (Meng *et al.*, 2007; Zhang *et al.*, 2010). Additionally, miR-25 crosslinks the MEK/ERK and PTEN/PI3K/AKT/mTOR signalling pathways because activated ERK increases the expression of miR-25 which then inhibits PTEN protein level and lead to activation of AKT signalling (Poliseno, Salmena, Riccardi, *et al.*, 2010; Ciuffreda, Ludovica Sanza *et al.*, 2012). PTEN expression is also downregulated by *MYC* oncogene via increased expression of miR-19 (Mu *et al.*, 2009). PTEN pseudogene 1 (*PTENP1*) and *PTEN* mRNA have significant sequence identity and it has been found that *PTENP1* miR target sites regulate the expression of PTEN via sequestration of PTEN-targeting miR which leads to an increase of *PTEN* mRNA half-life and PTEN protein levels (Poliseno, Salmena, Zhang, *et al.*, 2010).

1.3.5.5 Post-translational modification of PTEN

The role of PTEN is also regulated by post-translational modifications such as phosphorylation, ubiquitination, oxidation and acetylation (Fig. 1.5E).

Phosphorylation of PTEN has an impact on PTEN stability, activity and cellular localisation. Phosphorylation of PTEN on Ser370, Ser380, Thr382, Thr383 and Ser385 is mediated with a protein kinase that is called casein kinase 2 (CK2). The phosphorylation by CK2 leads to stabilisation of PTEN and closed PTEN conformation that reduces the interaction between the binding partners and decreases its plasma membrane localisation, thus reducing its phosphatase activity (Torres and Pulido, 2001; Miller *et al.*, 2002). As the phosphorylation in the C-terminal tail stabilises PTEN conformation, this leads to the reduction of interaction with membrane phospholipids or PDZ domain containing proteins; membrane-associated guanylate kinase inverted 2 (MAGI2), and therefore inhibits its PIP_3 phosphatase activity (Vazquez *et al.*, 2001). The inactivation of PTEN can also be seen when PTEN is phosphorylated on Ser385 by LKB1 (Mehenni *et al.*, 2005). The phosphatase activity of PTEN is also reduced with the phosphorylation of PTEN by GSK3β at Thr366 (Al-Khouri *et al.*, 2005). Additionally, the C2 domain of PTEN is phosphorylated by tyrosine protein kinase RAK at Tyr336 (Yim *et al.*, 2009) and RHOA-associated protein kinase (ROCK) at Ser299 and Thr321 (Li *et al.*, 2005).

Ubiquitination also regulates PTEN subcellular localisation, vesicle trafficking and activation. Lys13 and Lys289 are PTEN ubiquitination and monoubiquitination sites and have a role in PTEN cytoplasmic-nuclear shuttling (mentioned in section 1.3.7) (Trotman *et al.*, 2007). Ubiquitin/proteasome pathway can regulate the function of PTEN (Trotman *et al.*, 2007). NEDD4-1 is an E3 ubiquitin-protein ligase which can polyubiquitinate PTEN at Lys13 and Lys289 leading to its degradation or it can also monoubiquitinate PTEN at Lys13 and Lys289 regulating its cytoplasmic-nuclear shuttling (Wang *et al.*, 2007). In non-small-cell lung cancer, PTEN is downregulated due to the ubiquitin-mediated degradation by NEDD4-1 and this leads to PTEN activity lost (Amodio *et al.*, 2010).

Acetylation is another mechanism to regulate PTEN function. The catalytic activity of PTEN is reduced by acetylation at Lys125 and Lys128 by acetyltransferase P300/CREB-binding protein (CBP)-associated factor (PCAF) and at Lys402 by CBP (Okumura *et al.*, 2006). ROS are also responsible for regulating PTEN catalytic activity by the oxidative-stress-induced formation of disulphide bond between active Cys71 and Cys124 (Lee *et al.*, 2002).

1.3.5.6 Protein-protein interactions of PTEN

Many different studies demonstrated that protein-protein interactions also play an important role in PTEN activity due to the effect on its stability, conformation, lipid membrane-binding potential and subcellular localisation (Fig. 1.5F).

NA^+/H^+ exchanger regulatory factor (NHERF) interacts and recruits PTEN to platelet derived growth factor receptor (PDGFR) and prevents the activation of PI3K/AKT signalling pathway (Takahashi *et al.*, 2006). In the downstream of ROCK, MAGI2 and β-arrestins interact with PTEN and increase its lipid phosphatase activity (X. Wu *et al.*, 2000; Lima-Fernandes *et al.*, 2011). PTEN also directly interacts with motor protein myosin V that leads to the movement of PTEN to the membrane and PTEN can dephosphorylate PIP_3 into PIP_2 (Diepen *et al.*, 2009).

There are different proteins that interact with PTEN and negatively affect its tumour suppressor activity. MSP58 that is an oncoprotein interacts with PTEN at the C-terminus region leading to cellular transformation (Okumura *et al.*, 2005). Parkinson protein 7 (PARK7 also known as DJ1) directly binds to PTEN in oxidative conditions, inhibits PTEN activity and increases AKT activity, leading to cell proliferation and transformation (Kim *et al.*, 2009). PIP_3-dependent RAC exchanger factor 2a (PREX2a) (Fine *et al.*, 2005), shank-interacting protein-like 1 (SIPL1) (He *et al.*, 2010) and α-mannosidase 2C1 (MAN2C1) (He *et al.*, 2011) can also interact with PTEN and directly inhibit its lipid phosphatase activity to convert PIP_3 into PIP_2 .

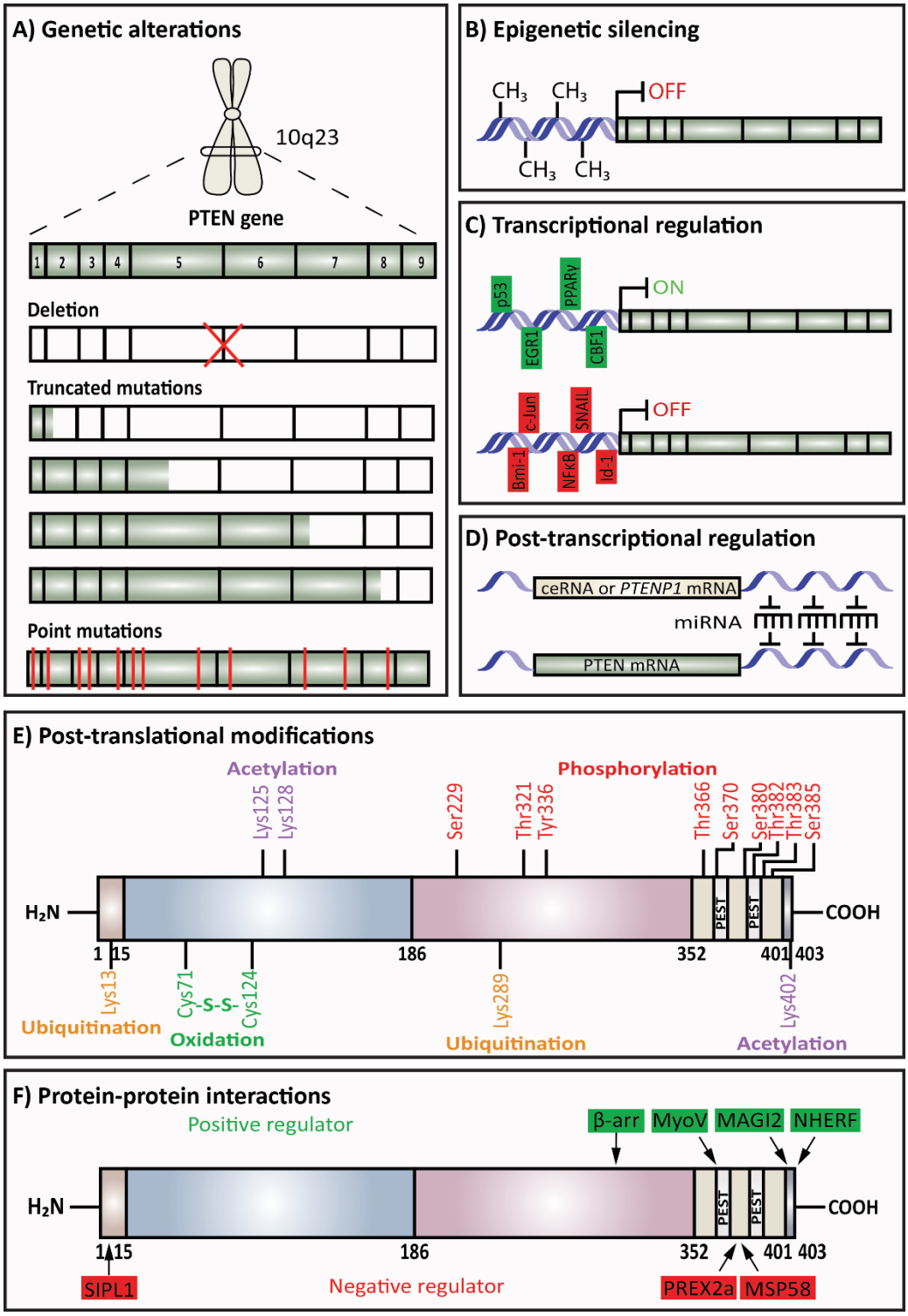

Figure 1.5 Regulation of PTEN.

A) Genetic alteration; deletion and mutations of *PTEN* can regulate PTEN expression. **B)** Epigenetic silencing; *PTEN* expression can be silenced by abnormal gene promoter methylation or abnormal modification of histones. **C)** Transcriptional regulation; transcription factors which can bind to *PTEN* promoter are positive or negative regulators of *PTEN* transcription. **D)** Post-transcriptional regulation; miRNAs can regulate *PTEN* expression. **E)** Post-translational modifications; phosphorylation, ubiquitination, oxidation and acetylation can regulate PTEN. **F)** Protein-protein interactions; interaction of PTEN with proteins can affect PTEN activity. [Information collected from (Song, Salmena and Pandolfi, 2012)].

1.3.6 Subcellular localisation of PTEN

Apart from the tumour suppressive role of PTEN in the cytoplasm (Leevers, Vanhaesebroeck and Waterfield, 1999), the role of PTEN as a tumour suppressor gene was also detected in the nucleus (Planchon, Waite and Eng, 2008). Initially, it was reported that PTEN was entering the nucleus and its expression levels were associated with cell cycle phases (Ginn-pease and Eng, 2003). It was shown that while higher nuclear PTEN expression associated with G_o-G_1 phase, lower PTEN expression was associated with S phase (Ginn-pease and Eng, 2003). In addition to the catalytic activity of PTEN, studies showed that PTEN was actively localised to the nucleus and played its tumour suppressive role by performing DNA damage response, controlling cell cycle progression and metabolism (Shen *et al.*, 2007; Song *et al.*, 2011; Garcia-cao *et al.*, 2012).

1.3.7 Mechanisms of cytoplasmic and nuclear shuttling of PTEN

PTEN is a well-known cytoplasmic protein as it is recruited to the membrane and dephosphorylates PIP_3 into PIP_2 and inhibits PI3K/AKT signalling, as mentioned in sections 1.3.3 and 1.3.4, (Leevers, Vanhaesebroeck and Waterfield, 1999). PTEN might be recruited to the membrane due to the interaction with different membrane-anchored proteins such as MAGIs (X. Wu *et al.*, 2000; Y. Wu *et al.*, 2000; Kotelevets *et al.*, 2005; Subauste *et al.*, 2005), microtubule-associated protein (MAST) (Valiente *et al.*, 2005), SAST (Valiente *et al.*, 2005), NEP (Sumitomo *et al.*, 2004) and NHERF (Takahashi *et al.*, 2006) (Fig. 1.6A).

Different mechanisms are involved to redirect the nuclear protein into nucleus. One of the mechanisms to redirect PTEN to nucleus involves nuclear localisation signal (NLS) (Hodel, Corbett and Hodel, 2001). Although, PTEN does not have NLS, Chung *et al.,* 2005 identified four redundant NLS-like sequences in PTEN (NLS1, NLS2, NLS3 and NLS4) in the MCF-7 breast cancer cell line (Chung, Ginn-Pease and Eng, 2005). It has been shown that a single mutation on the NLS-like sequences in PTEN cannot affect the localisation of PTEN. However, the combination of two mutations out of four NLS-like sequences prevents nuclear PTEN localisation and also interaction between PTEN and major vault protein (MVP) (Chung, Ginn-Pease and Eng, 2005). MVP is a protein which is postulated to be a general carrier molecule for the translocation between nucleus and cytoplasm and is another potential mechanism of PTEN import as PTEN binds to MVP (Chung, Ginn-Pease and Eng, 2005). The interaction between PTEN and MVP was seen in HeLa and 293T cells and the binding sites are localised at the C2 domain of PTEN and a calcium-binding motif, EF-hand pair, of MVP (Chung, Ginn-Pease and Eng, 2005) (Fig. 1.6B).

The study on the U87-MG human glioblastoma cell line demonstrated that PTEN nuclear shuttling was due to the RAN-GTPase which is a protein that is associated with importin-β and is essential for importin-related nuclear transport (Fig. 1.6C) (Gil *et al.*, 2006).

Simple diffusion has been identified as one of the mechanisms that PTEN can enter to the nucleus (Fig. 1.6D). This is because PTEN has 50-55,000 Da size and proteins which have less than 60,000 Da size can pass through the nuclear pores (Liu *et al.*, 2005). Liu *et al.,* 2005 showed that green fluorescent protein (GFP) tagged PTEN construct which had less than 60,000 Da size entered the nucleus in the HeLa cells (Liu *et al.*, 2005). Moreover, it has been found that larger GFP tagged PTEN fusion proteins or selectively mutated forms of PTEN; PTENK13 and PTENK14 nuclear PTEN, could not translocate to nucleus and cytoplasmic sequestration was induced (Liu *et al.*, 2005).

Posttranslational modification is another potential mechanism for PTEN nuclear localisation as mentioned in section 1.3.5.5. The regulation of PTEN enzymatic activity is connected to acetylation, phosphorylation and oxidation (Leslie and Foti, 2011) but the subcellular localisation of PTEN is linked to ubiquitination and SUMOylation (Trotman *et al.*, 2007; Wang *et al.*, 2007; Bassi *et al.*, 2013). The polyubiquitination of proteins contributes to protein degradation via proteasome. Therefore, when PTEN is recruited to the plasma membrane, it can be degraded due to the polyubiquitination (Fig. 1.6E) (Wang *et al.*, 2007). On the other hand, monoubiquitination of PTEN is important for its nuclear shuttling (Fig. 1.6F) (Trotman *et al.*, 2007). PTEN contains different Lys which are targeted by E3-ligases (Lee *et al.*, 2013). WWP and RFP are the two E3-ligases for PTEN which have a role in PTEN membrane recruitment and polyubiquitination (Lee *et al.*, 2013). However, another E3-ligase NEDD4-1, is responsible for regulating both monoubiquitination and polyubiquitination (Trotman *et al.*, 2007; Wang *et al.*, 2007). Trotman *et al.,* 2007 discovered lys289 (PTENK289) as one of the major targets for E3-ligases (Trotman *et al.*, 2007). Mutation in PTENK289 to Glutamic acid (E), PTENK289E, particularly identified in Cowden syndrome (CS) patients showed reduced PTEN nuclear localisation (Trotman *et al.*, 2007). Another study also showed that there is a SUMOylation site in the PTEN C-terminal region (Fig. 1.6G). Mutation of Lys254 to Arginine (R) in PTEN (PTENK254R) prevents SUMOylation of PTEN and its nuclear shuttling (Bassi *et al.*, 2013).

There are different mechanisms for PTEN nuclear shuttling and localisation which are situation and cell specific. These mechanisms may play an important role in PTEN protein stability/degradation and subcellular localisation.

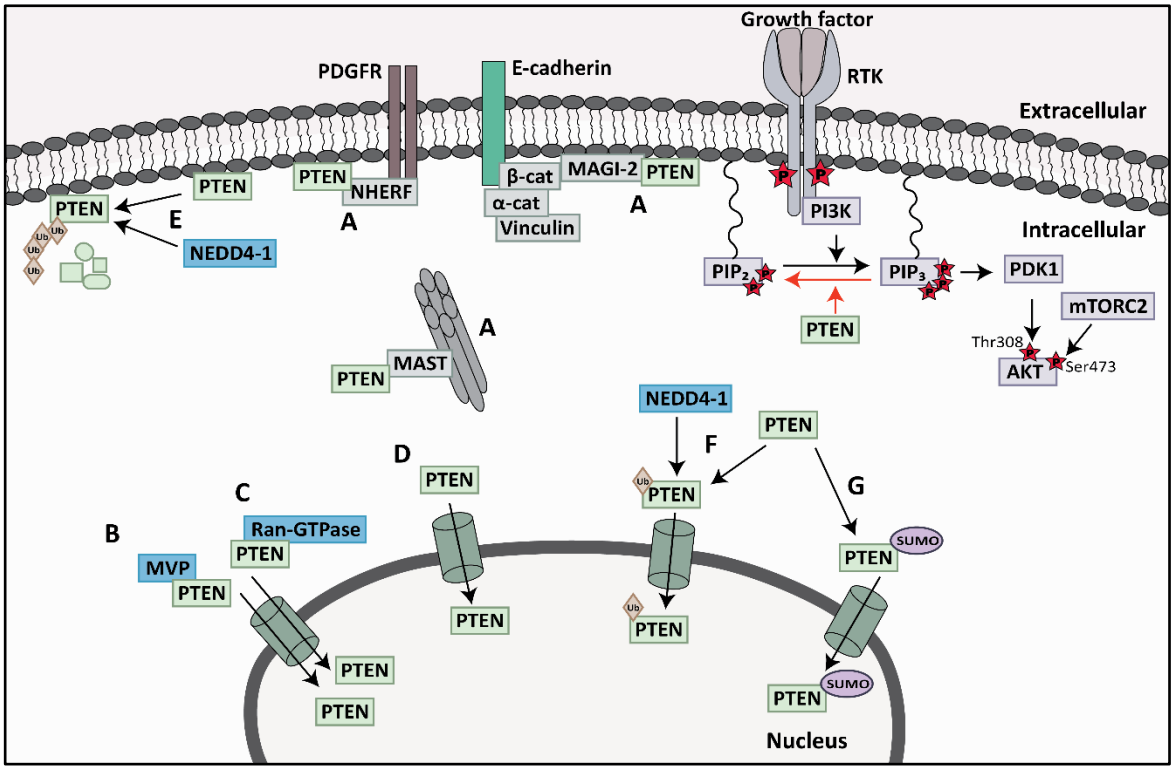

Figure 1.6 Shuttling of PTEN between cytoplasm and nucleus.
PTEN dephosphorylates PIP_3 into PIP_2 at the plasma membrane and activates the AKT signalling pathway. (**A**) PTEN can interact with membrane-anchored proteins such as MAGI2, MAST and NHERF and can be recruited to the membrane. PTEN can shuttle to the nucleus by (**B**) MVP or (**C**) Ran-GTPase which are carrier proteins on the nuclear membrane or by (**D**) passive diffusion. (**E**) Polyubiquitinated PTEN is degraded in the cytoplasm. (**F**) Monoubiquitination of PTEN by NEDD4 and (**G**) SUMOylation of PTEN also lead to PTEN nuclear localisation. P in red star indicates phosphorylation. Ub in brown rhombus indicates ubiquitination. SUMO in purple ellipse indicates SUMOylation. Arrows indicate induction or transport. PTEN: phosphatase and tensin homolog; PIP_3: phosphatidylinositol 3,4,5-triphosphate; PIP_2: phosphatidylinositol 4,5-bisphosphate; MAGI2: membrane-associated guanylate kinase inverted 2; MAST: microtubule-associated protein; NHERF: NA^+/H^+ exchanger regulatory factor; MVP: major vault protein; β-cat: beta-catenin; α-cat: alpha-catenin. [Information collected from (Tamguney and Stokoe, 2007; Papa and Pandolfi, 2016)].

1.3.8 Cellular functions of PTEN

PTEN regulates PI3K/AKT signalling with its phosphatase-dependent activity. However, PTEN also has phosphatase-independent functions (Song, Salmena and Pandolfi, 2012). As PTEN can shuttle between cytoplasm and nucleus, it is a tumour suppressor gene both in cytoplasm and nucleus (Leevers, Vanhaesebroeck and Waterfield, 1999; Planchon, Waite and Eng, 2008).

1.3.8.1 PTEN and cell metabolism

Metabolic reprogramming leads to rapid cell proliferation. Cancer cells or rapidly proliferating cells convert glucose into lactate via aerobic glycolysis, regardless of the presence of oxygen and this is known as the Warburg effect (Warburg, 1956). Cellular mediators of signal transduction and gene expression; PTEN/PI3K/AKT/mTOR pathway, HIF1-α and MYC can affect the metabolic pathways during cell proliferation and carcinogenesis (Heiden, Cantley and Thompson, 2009). PI3K/AKT regulates glucose uptake, HIF1-α and MYC regulate genes that are involved to regulate glucose and glutamine metabolism (Heiden, Cantley and Thompson, 2009).

It has been shown that overexpressing *PTEN* in transgenic mice decreased body size due to the reduction of cell number, increased energy expenditure and decreased accumulation of body fat (Garcia-cao *et al.*, 2012). Additionally, the reduction in the glucose and glutamine uptake, increased mitochondrial oxidative phosphorylation and resistance to oncogenic transformation were observed in transgenic mice cells with *PTEN* overexpression (Garcia-cao *et al.*, 2012). Another study showed that additional genomic copies of *PTEN* in transgenic mice prevents metabolic pathologies and cancer (Ortega-Molina *et al.*, 2012).

PTEN/PI3K/AKT/mTOR pathway has an important role in regulating glucose metabolism. As PTEN modulates insulin signalling, it has a role in regulating glucose uptake (Vellai *et al.*, 2006; Wong *et al.*, 2007). It has been discovered that overexpression of PTEN in adipocytes reduced the uptake of glucose due to the inhibition of insulin-stimulated, PI3K activation-dependent 2-deoxyglucose uptake and glucose transporter 4 (GLUT4) translocation which is known as key event in insulin signalling (Nakashima *et al.*, 2000). Another study showed that GLUT4 translocation and insulin metabolic function cannot be modulated by PTEN in normal physiological conditions (Mosser, Li and Quon, 2001). However, it was found that PTEN regulates GLUT1 expression and thus glucose uptake in transformed cells such as thyroid cancer cells (Morani *et al.*, 2014). PTEN regulates FOXO, PPAR gamma-coactivator 1 alpha (PGC1α) and inhibits gluconeogenesis (Ortega-Molina *et al.*, 2012). Moreover, PI3K/AKT signalling inhibits GSK3, which activates lipogenic transcription factor

sterol-regulatory element-binding protein 1C (SREBP1C), thus loss of *PTEN* induces adipogenic-like transformation and genes involved in lipogenesis and β-oxidation via PPARγ and SREBP1C (Horie *et al.*, 2004).

1.3.8.2 PTEN and cell motility/polarity

PTEN/PI3K signalling pathway has been shown to have a role in migration both in development and cancer cells. Genetic deletion of *PTEN* in mouse fibroblast lines induced cell motility via overexpression of key downstream effectors of the PI3K pathway: RAC1 and CDC42, which promote cell migration (Liliental *et al.*, 2000). The migration of glioma cells can be inhibited by the C2 domain of PTEN showing its lipid phosphatase-independent activity (Raftopoulou *et al.*, 2004), which may indicate the influence of the PI3K pathway-independent effect of PTEN (Tamura *et al.*, 1998). It has also been shown that glioblastoma cell migration was enhanced with the knockdown of *PTEN* via focal adhesion kinase (FAK). FAK is a cytoplasmic phosphoprotein and is activated by integrins which can be dephosphorylated by PTEN, inhibiting migration of cells (Park *et al.*, 2002). Moreover, SHC is also dephosphorylated by PTEN and this inhibits downstream MAPK that have a role in cell motility (Gu *et al.*, 1999).

To establish the polarity of the cell, when PTEN is found on apical cell membrane during epithelial morphogenesis, PTEN and PIP_2 recruit annexin 2 (ANXA2), CDC42 and partitioning defective 6 (PAR6)-atypical protein kinase C (aPKC) to the apical plasma membrane (Martin-Belmonte *et al.*, 2007). Therefore, the normal development of the apical surface and lumen might be blocked with the loss of *PTEN* and could lead to changing of cells from epithelial to mesenchymal properties and increase the cell motility and invasion which is known as EMT (Song *et al.*, 2009).

1.3.8.3 PTEN and tumour microenvironment

The role of PTEN was also identified in regulating the tumour microenvironment. Tumour microenvironment consists of immune and stromal cells (Aquila *et al.*, 2020). Loss of PTEN activity does not only affect the cancer cell behaviour but also affects the tumour microenvironment and immune-infiltrate composition. Studies showed that loss of *PTEN* function leads to tumour microenvironment remodelling and formation of immunosuppressive tumour microenvironment with properties such as reduced frequency of cytotoxic T cells, helper T cells and natural killer (NK) cell, increased levels of pro-oncogenic inflammatory cytokines and increased frequency of immunosuppressive cells (Yang *et al.*, 2018; Vidotto *et al.*, 2019; Lin *et al.*, 2021).

Genetic and epigenetic changes in *TP53* and *PTEN* were observed in stromal fibroblasts from the tumour microenvironment of human breast cancer samples (Kurose *et al.*, 2002). Stromal fibroblasts are the major important cell types which have ability to shape the microenvironment architecture leading to tumour growth and progression (Kalluri and Zeisberg, 2006). Trimboli *et al.,* 2009 showed that the deletion of PTEN in fibroblasts of mouse mammary gland tumours forms a tumour-permissive stroma including remodelling of extracellular matrix and increased collagen deposition, innate immune cell infiltration and angiogenesis. These features increase the tumour initiation, progression and malignant transformation of mammary epithelial tumours (Trimboli *et al.*, 2009). Mechanistically, down-regulation of miR-320 upregulates v-ets eryhtoblastosis virus E26 oncogene homolog 2 (ETS2) in *PTEN*-deleted mammary stromal fibroblasts which activates an oncogenic secretome that reprogrammes the tumour microenvironment and promotes angiogenesis and tumour cell invasion (Bronisz *et al.*, 2012). Thus, PTEN regulates the communication between various cellular compartments in the tumour microenvironment, which can influence the cancer phenotype.

1.3.8.4 PTEN and angiogenesis

PTEN/PI3K/AKT signalling is also important for angiogenesis via mechanisms such as HIF1-α and transcriptional activation of VEGF (Skinner *et al.*, 2004). For example it has been shown that PTEN negatively regulates transcription factor HIF1-α that is activated by hypoxic stress and VEGF, which promotes angiogenesis and produce tumour stroma in ovarian cancer and inhibits tumour angiogenesis (Shen *et al.*, 2017). Moreover, overexpressing *PTEN* in a *PTEN*-deficient glioma model significantly reduced tumour growth *in vivo* and increased mice survival which was due to the induction of a negative regulator of angiogenesis, thrombospondin-1 which led to decreased blood vessel formation in the tumour (Wen *et al.*, 2001).

1.3.8.5 Nuclear PTEN

It has been shown that PTEN can shuttle from cytoplasm to nucleus and has a functional role in nucleus as mentioned in sections 1.3.6 and 1.3.7. Thus, *PTEN* is also a tumour suppressor gene in nucleus and nuclear loss of *PTEN* contributes to more aggressive cancers and can be used as a prognostic marker (Perren *et al.*, 1999; Gimm *et al.*, 2000).

Puc *et al.,* 2005 discovered that loss of *PTEN* promotes genomic instability in tumours via checkpoint kinase 1 (CHK1), which is involved in cell cycle progression and this reflects one of the PTEN

functions in nucleus (Puc and Parsons, 2005; Puc *et al.*, 2005). Mechanistically, when *PTEN* is deficient, cytoplasmic AKT signalling pathway is activated and contributes to CHK1 degradation by phosphorylation and subsequent ubiquitination in cytoplasm and entry of CHK1 to nucleus is prevented (Fig. 1.7A) (Puc *et al.*, 2005). Both *in vitro* (in embryonic stem cells) (Puc and Parsons, 2005) and *in vivo* (primary breast carcinoma) (Puc *et al.*, 2005) studies demonstrated that *PTEN* deficiency leads to the accumulation of unrepaired double strand breaks due to the lack of CHK1, in G2 checkpoint and stimulates tumour development. Apart from PTEN/AKT/CHK1 mechanism, nuclear PTEN has other two mechanisms related to its tumour suppressive role to maintain the chromosomal stability (Shen *et al.*, 2007; Song, Salmena and Pandolfi, 2012). First, PTEN interacts with centromeres by physical association with integral kinetochore component centromere protein-C (CENP-C) (Fig. 1.7B). The physical interaction between PTEN and CENP-C does not require PTEN phosphatase activity as PTEN with PTENC124S mutation was able to interact with CENP-C (Shen *et al.*, 2007). However, a specific nonsense mutation, R189X, of PTEN which lacks the entire C-terminus but has the intact N-terminal phosphatase domain showed a disruption of the interaction and led to centromere breakage and chromosomal translocations (Shen *et al.*, 2007). Secondly, PTEN could be essential for DNA repair as PTEN null type cells showed DNA double strand breaks. It has been shown that PTEN interacts with E2F-1 transcription factor to regulate the key component for homologous recombination repair of DNA double-strand breaks (Rad51) but *PTEN* deficiency prevents this interaction (Fig. 1.7C) (Shen *et al.*, 2007). Similar to the first mechanism described above, Rad51 regulation was PTEN phosphatase activity independent because PTENC124S mutant, lacking catalytical activity did not change Rad51 expression (Shen *et al.*, 2007).

The phosphatase-independent activity of PTEN increases E3-ligase activity of anaphase-promoting complex/cyclosome (APC/C) via the association of APC/C with its activator CDC20 and CDH1 (Fig. 1.7D) (Song *et al.*, 2011). APC/C-CDH1 complex has tumour suppressive activity which causes the degradation of oncoproteins such as Aurora kinases (AURKs) and polo-like kinase 1 (PLK1) (Liu *et al.*, 2011; Song *et al.*, 2011). This indicates the phosphatase-independent tumour suppressive activity of nuclear PTEN due to the activation of APC/C-CDH1 (Song *et al.*, 2011).

It has also been reported that the role of nuclear PTEN might be regulated by physical interaction of PTEN with other nuclear target proteins such as p53 (Freeman *et al.*, 2003). The crosstalk between PTEN and p53 was discovered in mice which showed loss of *PTEN* causes p53-driven carcinogenesis due to the phosphatase-dependent and phosphatase-independent activities of PTEN (Freeman *et al.*, 2003). Loss of *PTEN* activates AKT signalling, phosphorylates MDM2 and translocates MDM2 to the nucleus, which then leads to p53 degradation (Fig. 1.7E), as mentioned in 1.3.4, (Mayo and Donner, 2001; Ogawara *et al.*, 2002). Thus, PTEN is involved in the stabilisation

and transcriptional activity of p53, which has an important function in tumorigenesis (Freeman *et al.*, 2003).

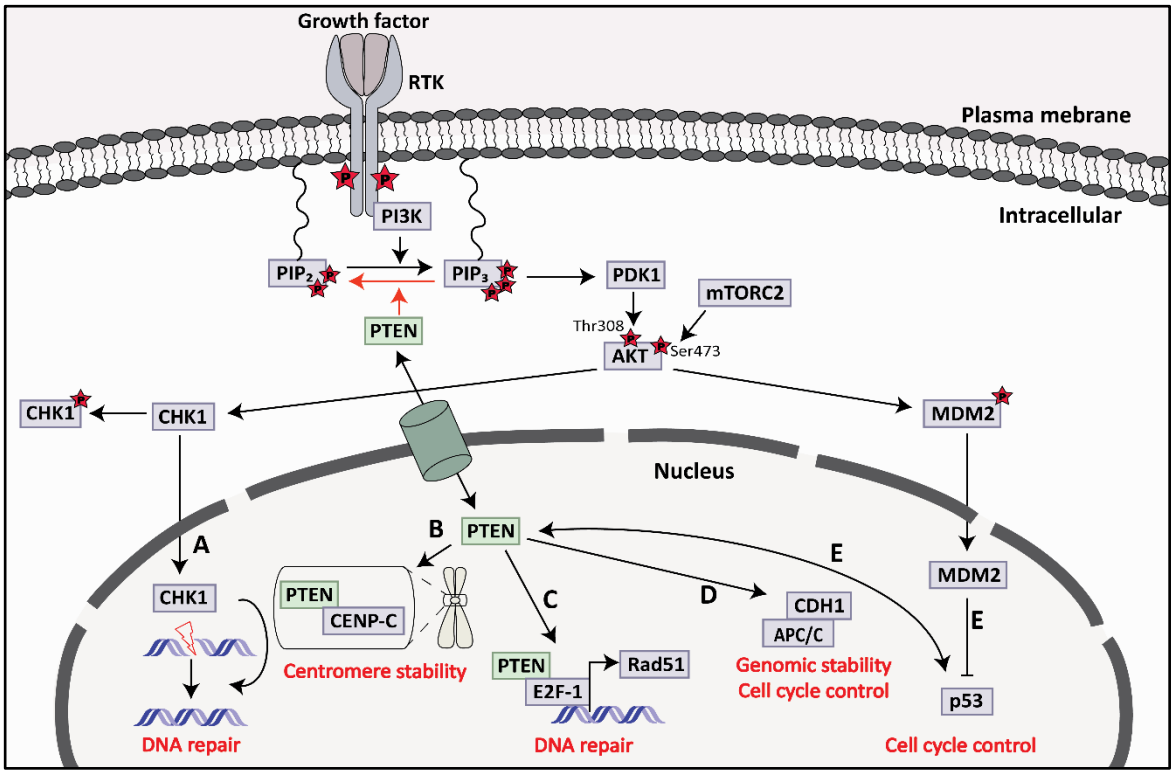

Figure 1.7 Nuclear functions of PTEN.

PTEN has functions both in cytoplasm and nucleus. **A)** Cytoplasmic PTEN dephosphorylates PIP_3 into PIP_2 and inhibits AKT activity and CHK1 phosphorylation, leading CHK1 translocation into the nucleus for DNA repair. **B)** In nucleus, PTEN can bind to CENP-C and maintain centromere stability. **C)** PTEN interacts with E2F-1 and leads to transcriptional regulation of Rad51 to control DNA repair in the nucleus. **D)** Nuclear PTEN enhances the interaction between APC/C and CDH1 to maintain genomic stability and control the cell cycle. **E)** Nuclear PTEN interacts with p53 to control the cell cycle due to the phosphatase-dependent and phosphatase-independent activities of PTEN. PTEN: phosphatase and tensin homolog; PIP_2: phosphatidylinositol 4,5-bisphosphate; PIP_3: phosphatidylinositol 3,4,5- triphosphate; CHK1: checkpoint kinase 1; CENP-C: centromere protein-C; APC/C: anaphase-promoting complex/cyclosome; CDH1: CDC20 homologue 1. [Information collected from (Song, Salmena and Pandolfi, 2012)].

1.4 PTEN in breast cancer

PTEN is one of the tumour suppressor genes that shows frequent loss of activity in human cancer (Salmena, Carracedo and Pandolfi, 2008; Kechagioglou *et al.*, 2014). As mentioned in 1.3.5, the loss of PTEN function could be due to genetic changes, epigenetic silencing, transcriptional regulation, post-transcriptional regulation, post-translational regulation and protein-protein interactions (Song, Salmena and Pandolfi, 2012).

Loss of heterozygosity at *PTEN* locus in breast cancer tumours is more common (40%-50%) (Bose *et al.*, 1998; Freihoff *et al.*, 1999) than loss of PTEN function due to the *PTEN* mutations observed in breast cancer cases (4-11%) (Bazzichetto *et al.*, 2019). Moreover, *PTEN* promoter methylation and loss of expression are observed in 50% and approximately 40% of breast cancers, respectively (Pérez-Tenorio *et al.*, 2007; Zhang *et al.*, 2013).

One of the studies showed that breast cancer can be developed and progressed in the PTEN-hypermorphic mouse model which expresses 80% of normal PTEN level with slightly reduced PTEN expression (Alimonti *et al.*, 2010). Recently, it was found that *PTEN*, mRNA level is downregulated in breast cancer cell lines compared to normal breast cell lines (Pappas *et al.*, 2021). Loss of PTEN expression both at the genomic or proteomic level in breast tumours increases the risk of aggressiveness of the disease and worse outcomes and more frequently observed in TNBCs, which is difficult to treat (S. Li *et al.*, 2017). Therefore, PTEN plays an important role in the development, prognosis and treatment of breast cancer (Kechagioglou *et al.*, 2014).

1.4.1 Treatment challenges in PTEN-inactive breast cancer

Luminal A and luminal B breast cancer cells have ER+ status, however, luminal A/B breast cancer cells were not sensitive to anti-oestrogen tamoxifen and fulvestrant (treatment for HR+ patients) when *PTEN* was knocked-down (Miller *et al.*, 2009). Knockdown of *PTEN* engages ErbB3 and IGF-IR signalling, thus, co-targeting oestrogen and tyrosine kinase pathways can be a promising treatment for PTEN-deficient ER+ breast cancers (Miller *et al.*, 2009). Moreover, PI3Kα-selective inhibitor alpelisib was recently approved to be used as a second line treatment for ER+ breast cancer patients with *PIK3CA* mutation (André *et al.*, 2019). However, it was previously shown that loss of *PTEN* leads to resistance to alpelisib (Juric *et al.*, 2015). As mentioned in sections 1.2.5.1 and 1.2.5.3, CDK4/6 inhibitors can be used as first line or second line treatment for ER+ breast cancer patients which are resistant to endocrine therapy. However, the cross-resistance mechanisms in these tumours were observed due to the loss of *PTEN* expression and *PIK3CA* mutation (Costa *et al.*, 2020).

Mechanistically, AKT is activated due to the loss of *PTEN*, which then inhibits p27 expression in the nucleus and activates CDK4 and CDK2 that leads to resistance to CDK4/6 inhibitors (Costa *et al.*, 2020).

HER2+ breast cancer patients with loss of PTEN expression also showed resistance to trastuzumab due to PI3K/AKT/mTOR pathway activation (Nagata *et al.*, 2004; Berns *et al.*, 2007). These trastuzumab resistant tumours can also induce EMT and transform to TNBC (Burnett *et al.*, 2015; Sun *et al.*, 2016). Although PI3K inhibitor inhibits the activation of AKT, it can activate MAPK signalling in HER2+ breast cancers (Serra *et al.*, 2011). Moreover, AKT inhibition promotes FOXO-dependent transcription and RTKs activation (Chandarlapaty *et al.*, 2011). This suggested that combination of trastuzumab with PI3K-targeting might overcome the resistance mechanism (Nagata *et al.*, 2004). *In vitro* and *in vivo* studies showed that combination of p110α-specific inhibitor BYL719 (PI3Kα inhibitor) and HER2 antibody decreased tumour growth in HER2+ *PTEN*-deficient breast cancer (Zhang, Xu and Liu, 2016).

In Phase I/II studies, *PTEN*-deficient metastatic breast cancer patients who were treated with trastuzumab and everolimus (mTORC1 inhibitor) showed significantly lower overall survival rate compared to the patients who had normal *PTEN* status in tumour cells (Morrow *et al.*, 2011). Weigelt *et al.,* 2011 discovered that breast cancer cell lines, which have *PIK3CA* mutation were sensitive to everolimus and to the active-site mTORC1/mTORC2 kinase inhibitor, PP242 (Weigelt, Warne and Downward, 2011). However, cell lines with PTEN null type were resistant to everolimus and PP242 due to the feedback loop on S6K/PI3K/RAS that might activate MAPK signalling (Weigelt, Warne and Downward, 2011). These studies highlighted the importance of PTEN expression loss in luminal A, luminal B and HER2+ breast cancer types.

As mentioned in section 1.4, PTEN expression loss is more frequent in TNBC and chemotherapy has been the only treatment option for TNBC. However, the main problem of these patients is that the disease is recurrent. Therefore, this paves the way for studies to focus on targeted therapy in PTEN-inactive TNBC.

1.4.2 Inactive PTEN in TNBC

López-Knowles *et al.,* 2010 reported that low PTEN expression, activation of AKT or PI3K mutation were observed in >70% of TNBC patients that showed poor prognosis (López-Knowles *et al.*, 2010). Another study also stated that low PTEN protein level was detected in 77% of TNBC cases by IHC and fluorescence *in situ* hybridisation, which was significantly linked with high grade, large tumour size and tumour recurrence (Beg *et al.*, 2015). Meta-analysis identified that PTEN expression loss is

more frequently seen in breast cancer patients than normal matched tissue (S. Li *et al.*, 2017). In addition to this, loss of PTEN expression was seen in the aggressive type of breast cancer which has large tumour size, lymph node metastasis, poor differentiation and late stage TNM classification (S. Li *et al.*, 2017), consistent with the study mentioned above (Beg *et al.*, 2015). Also, molecular subtypes of breast cancer were analysed for PTEN expression loss and there was significant association between TNBC subtype and loss of PTEN expression (S. Li *et al.*, 2017; Khan *et al.*, 2018). Thus, these studies highlighted the importance of PTEN expression in in TNBC.

1.4.3 Treatment for PTEN-inactive TNBC

Various studies showed that TNBC patients who have inactive PTEN have been shown to develop resistance mechanisms against treatments similar to other subtypes of breast cancer as mentioned in section 1.4.1.

It has been found that altered PTEN in TNBC which activates AKT is associated with resistance to chemotherapy and this suggested that treating patients with PI3K, AKT or mTOR inhibitors might overcome the resistance mechanism (Balko *et al.*, 2014). However, PI3K, AKT and mTOR therapeutic inhibition can trigger a feedback loop in the signalling pathway which might reduce the efficacy of these agents and also lead to resistance to RTK inhibition with single agent (Chan, Tan and Dent, 2019). While the TNBC cell lines with PTEN WT status are sensitive to statin treatment via PI3K pathway, TNBC cell lines with the loss of PTEN expression are resistant to statin and this could be due to the activation of PI3K/AKT signalling pathway (Park *et al.*, 2013). Inhibition of mTOR can also activate the upstream RTKs which contributes to the rebound activation of AKT in PTEN null TNBC cell lines (Haruta *et al.*, 2000; O'Reilly *et al.*, 2006). Moreover, it has been found that PTEN loss and EGFR overexpression genomic alterations are observed in 74% and 75% of TNBC cases, respectively (Martin *et al.*, 2012). Therefore, EGFR inhibitors were used to treat PTEN-inactive TNBC but a drug resistance developed due to the increased in phosphorylation of AKT and activation of Wnt-beta-catenin and NF-κB activity (Kappler *et al.*, 2014). Due to this resistance mechanism of PTEN-inactive TNBC, EGFR (gefitinib) and mTOR (everolimus) inhibitors were combined but they did not induce synergistic growth inhibition in PTEN null TNBC cell lines (El Guerrab *et al.*, 2020).

There are also promising findings which showed potential targeted therapy in *in vitro* and *in vivo* work. It has been shown that knockdown of *INPP4B*, which converts PIP_2 into PIP_3 reduced pAKT level and cell growth in PTEN null TNBC cell lines, which also sensitised the cells to PI3Kα and PI3Kβ inhibitors (Reed and Shokat, 2017). The combination of CDC25 with PI3K inhibitors also showed synergistic effect that suppressed the growth of PTEN-inactive TNBC cells (Liu *et al.*, 2018).

Additionally, recent study which combined the treatment of G-protein-coupled receptor (PAR1), EGFR signalling and PI3Kβ inhibitor (Zecchin *et al.*, 2020) and another study which combined PI3Kβ inhibitor with paclitaxel (chemotherapeutic agent) and anti-PD1 (Owusu-Brackett *et al.*, 2020) suggested that these combinations could be new potential therapeutic strategies for PTEN-inactive TNBC.

There are also various clinical trials that include combination therapies for PTEN-inactive TNBC. LOTUS trial included combination therapy of paclitaxel with ipatasertib or placebo for metastatic TNBC patients who had low PTEN or PIK3CA/AKT1/PTEN genomic alterations (Kim *et al.*, 2017). In PTEN low population, median PFS was higher in paclitaxel with ipatasertib (6.2 months) than paclitaxel with placebo group (3.7 months) but no significant difference was observed (Kim *et al.*, 2017). However, significant difference in PFS was observed in PIK3CA/AKT1/PTEN altered population, 9.0 months with ipatasertib versus 4.9 months with placebo (Kim *et al.*, 2017). The recent findings of the LOTUS trial showed the median overall survival in paclitaxel with ipatasertib arm versus paclitaxel with placebo arm is 23.1 *vs* 15.8 months in PTEN low population and 25.8 *vs* 22.1 months in PIK3CA/AKT1/PTEN altered population (Dent *et al.*, 2020). NCT04177108 and NCT03337724 trials mentioned in table 1.4 are the ongoing phase III trials for LOTUS tiral. Consistent with LOTUS trial, FARLAINE trial also showed that pathological complete response (pCR) of paclitaxel with ipatasertib arm vs paclitaxel with placebo arm rates is 16% *vs* 13% in PTEN low and 18% *vs* 12% in PIK3CA/AKT/PTEN altered population (Oliveira *et al.*, 2019). The list of other clinical trials for PTEN-inactive TNBC population are in table 1.4.

Table 1.4 Clinical Trials of targeted therapies in PTEN-inactive TNBC population.

Title	ClinicalTrials.gov identifier	Trial phase (Recruitment Status)	Drug-*target*	Treatment
AZD8186 First Time In Patient Ascending Dose Study.				
	NCT01884285	Phase I (Completed)	AZD8186-*PI3Kβ/δ* AZD2014-*mTORC1/2*	Combination
Safety, Pharmacokinetics (PK) of AKT and MEK Combination.				
	NCT01138085	Phase I (Completed)	GSK1120212-*MEK* GSK2141795-*AKT*	Combination
A Study Assessing the Safety and Efficacy of Adding Ipatasertib to Paclitaxel Treatment in Participants With Breast Cancer That Has Spread Beyond the Initial Site, and the Cancer Does Not Have Certain Hormonal Receptors (Kim *et al.*, 2017).				
	NCT02162719 LOTUS	Phase II (Completed)	Ipatasertib-*AKT* Placebo	Combination with paclitaxel (chemotherapy)
A Study of Ipatasertib (GDC-0068) in Combination With Paclitaxel as Neoadjuvant Treatment for Participants With Early Stage Triple Negative Breast Cancer (Oliveira *et al.*, 2019).				
	NCT02301988 FAIRLANE	Phase II (Completed)	Ipatasertib-*AKT* Placebo	Combination with paclitaxel (chemotherapy)
PI3Kbeta Inhibitor AZD8186 and Docetaxel in Treating Patients Advanced Solid Tumors With PTEN or PIK3CB Mutations That Are Metastatic or Cannot Be Removed by Surgery.				
	NCT03218826	Phase I (Recruiting)	AZD8186-*PI3Kβ*	Combination with doxetaxel (chemotherapy)
Leflunomide in Previously Treated Metastatic Triple Negative Cancers.				
	NCT03709446	Phase I/II (Recruiting)	Leflunomise-*dihydroorotate dehydrogenase*	Monotherapy
Testing the Addition of Copanlisib to Eribulin for the Treatment of Advanced-Stage Triple Negative Breast Cancer.				
	NCT04345913	Phase I/II (Recruiting)	Copanlisib-*Pan-specific (PI3Kα/δ)*	Combination with eribulin (chemotherapy)
Phase II Trial of Talazoparib in BRCA1/2 Wild-type HER2-negative Breast Cancer and Other Solid Tumors.				
	NCT02401347	Phase II (Recruiting)	Talazoparib (PARP)	Monotherapy

Continued on next page

Table 1.4 Continued from previous page

Title	ClinicalTrials.gov identifier	Trial phase (Recruitment Status)	Drug-*target*	Treatment
Nab-paclitaxel and Alpelisib for the Treatment of Anthracycline Refractory Triple Negative Breast Cancer With PIK3CA or PTEN Alterations.				
	NCT04216472	Phase II (Recruiting)	Alpelisib-*α-specific class 1 protein kinase inhibitor*	Combination with Nab-paclitaxel (chemotherapy)
AZD5363 in Combination With Paclitaxel in Triple-Negative Advanced or Metastatic Breast Cancer (Schmid, Abraham, *et al.*, 2020).				
	NCT02423603 PAKT	Phase II (Active, Not recruiting)	AZD5363-AKT Placebo	Combination with paclitaxel (chemotherapy)
A Study of Ipatasertib in Combination With Paclitaxel as a Treatment for Participants With PIK3CA/AKT1/PTEN-Altered, Locally Advanced or Metastatic, Triple-Negative Breast Cancer or Hormone Receptor-Positive, HER2-Negative Breast Cancer.				
	NCT03337724 IPATunity130	Phase II/III (Active, Not recruiting)	Ipatasertib-*AKT* Placebo	Combination with paclitaxel (chemotherapy)
Capivasertib+Paclitaxel as First Line Treatment for Patients With Locally Advanced or Metastatic TNBC (Schmid, Cortes, Robson, *et al.*, 2020).				
	NCT03997123 CAPItello-290	Phase III (Recruiting)	Capivasertib-*AKT* Placebo	Combination with paclitaxel (chemotherapy)
Study Assessing the Efficacy and Safety of Alpelisib + Nab-paclitaxel in Subjects With Advanced TNBC Who Carry Either a PIK3CA Mutation or Have PTEN Loss Without PIK3CA Mutation.				
	NCT04251533 EPIK-B3	Phase III (Recruiting)	Alpelisib-*α-specific class 1 protein kinase inhibitor* Placebo	Combination with Nab-paclitaxel (chemotherapy)
A Study Of Ipatasertib in Combination With Atezolizumab and Paclitaxel as a Treatment for Participants With Locally Advanced or Metastatic Triple-Negative Breast Cancer.				
	NCT04177108	Phase III (Active, Not recruiting)	Ipatasertib-*AKT* Atezolizumab-*PD-L1* Placebo	Combination with paclitaxel (chemotherapy)

1.5 Alternative approach for cancer treatment; synthetic lethality

Synthetic lethality is a phenomenon between two genes when the alteration (a mutation, RNAi knockdown or inhibition) of one gene is viable but the alteration of both genes simultaneously leads to loss of viability (Fig. 1.8) (O'Neil, Bailey and Hieter, 2017). Synthetic lethality has a major effect on cancer research as it can be used to target cancers with inactive tumour suppressor genes (Topatana *et al.*, 2020).

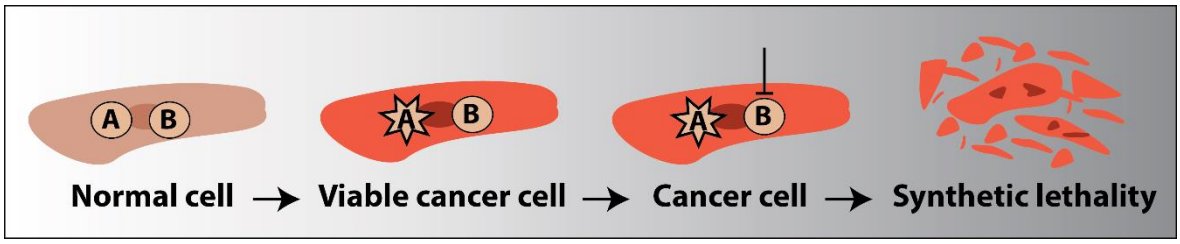

Figure 1.8 The principle of synthetic lethality.
The survival of cancer cells with inactive tumour suppressor gene A (loss of function) depends on the expression of gene B. Inhibition of gene B leads to synthetic lethality (cell death). The star represents the inactive gene. [Information collected from (Fece de la Cruz, Gapp and Nijman, 2014)].

Targeting synthetic lethality provides an alternative approach for cancer treatment (Doye and Hurt, 1995; Fece de la Cruz, Gapp and Nijman, 2014). To identify novel targeted therapies, synthetic lethality screens can be performed, including RNA interference (RNAi) screens (Brummelkamp and Bernards, 2003; Brunen and Bernards, 2017), mentioned in Chapter 3, section 3.1.2. One of the well-known examples of synthetic lethality interaction is between *BRCA1/2* and PARP1. *BRCA1/2* are tumour suppressor genes that have a role in homologous-recombination-mediated DNA repair and PARP1 is involved in base excision repair. Tumours with *BRCA1/2* deficiency depend on PARP1 for DNA repair. Thus, inhibition of PARP1 kills *BRCA1/2* deficient tumours (Bryant *et al.*, 2005; Farmer *et al.*, 2005).

1.5.1 Synthetic lethality in PTEN-inactive cancer

Loss-of-function mutations in tumour suppressor genes, such as *PTEN*, are major genetic alterations leading to more challenges to identify targeted drugs since it is difficult to restore their functions (Hartwell *et al.*, 1997). Therefore, studies have been focusing to target downstream signalling pathways that are altered by inactivation of tumour suppressor genes (Hartwell *et al.*, 1997; Brunen

and Bernards, 2017). As PTEN is the second most mutated gene following *TP53* in different cancer types (Kechagioglou *et al.*, 2014), various studies have been performed to identify PTEN synthetic lethal interactions in a variety of cancer types (Table 1.5). *PARP*, *MPS1, monoPolar spindle 1* (*TTK*), *Nemo-like kinase* (*NLK*), *ataxia telangiectasia mutated* (*ATM*), *chromatin helicase DNA binding protein 1* (*CHD1*)*, NUAK family kinase 1* (*NUAK1*) and *ataxia telangiectasia-mutated- and Rad3-related kinase* (*ATR*) were identified as synthetic essential genes in PTEN-inactive breast cancer (Table 1.5). Discovering PTEN synthetic lethal interactions in TNBC may provide potential targeted therapies for TNBC which does not have successful treatment options.

Table 1.5 Identified synthetic lethality genes in PTEN-inactive cancer types.

Synthetic lethality gene partner	Function	Tumour cell line	Reference
Poly-ADP ribose polymerase (*PARP*)	DNA repair mechanism	Colorectal Endometroid Breast Glioma Bladder Melanoma	(Mendes-Pereira *et al.*, 2009)
MPS1, MonoPolar Spindle 1 (*TTK*)	Regulates cell division	Breast	(Brough *et al.*, 2011)
Nemo-Like Kinase (*NLK)*	Regulates transcriptional molecules such as AKT-independent phosphorylation of FOXO1	Colorectal Endometrial Ovary Bladder Melanoma Lung Breast	(Mendes-Pereira, Lord and Ashworth, 2012)
Polynucleotide kinase-phosphatase (*PNKP)*	DNA repair mechanism	Lung Colon Prostate	(Mereniuk *et al.*, 2013)

Continued on next page

Table 1.5 Continued from previous page

Synthetic lethality gene partner	**Function**	**Tumour cell line**	**Reference**
Apurinic/apyrimidinic endonuclease 1 (*APE1*)	DNA base excision repair (BER)	Melanoma	(Abbotts *et al.*, 2014)
Ataxia telangiectasia mutated (*ATM)*	DNA repair	Colorectal Prostate Breast	(McCabe *et al.*, 2015; Li *et al.*, 2018)
Integrin a5 (*ITGA5)*	Cell adhesion	Prostate	(Ren, Joshi and Mathew, 2016)
Death domain associated protein (*DAXX*)	Histone chaperone	Glioblastoma	(Benitez *et al.*, 2017)
Chromatin helicase DNA binding protein 1 (*CHD1*)	Activate gene transcription	Prostate Breast	(Zhao *et al.*, 2017)
NUAK family kinase 1 (*NUAK1)*	Cell proliferation, cell cycle, DNA repair	Breast	(Tang *et al.*, 2018)
Ataxia telangiectasia-mutated- and Rad3-related kinase (*ATR*)	DNA repair	Breast	(Al-Subhi *et al.*, 2018)
Pyruvate dehydrogenase kinase1 (*PDHK1*)	Regulates energy metabolism	Lung	(Chatterjee *et al.*, 2019)
Yes-associated protein 1 (*YAP1*)	Coactivates transcription, regulates LOX and recruits macrophages and myeloid-derived suppressor cells	Glioblastoma	(Chen *et al.*, 2019)

1.6 Project background

TNBC is the most aggressive form of breast cancer and chemotherapy has been the only systemic treatment option. Due to low response rate and recurrent nature of TNBC, it is crucial to identify different gene signatures to discover a novel targeted therapy for the disease.

PTEN is frequently lost in TNBC and this is associated with poor prognosis which indicates that PTEN loss might drive TNBC progression. Targeting synthetic lethality is an alternative approach for cancer treatment. To identify novel targeted therapies, synthetic lethality screens can be performed, including RNAi screens. Discovering *PTEN* synthetic lethal interactions in TNBC may provide potential targeted therapies for this breast cancer type.

1.7 Hypothesis

The candidate gene to be identified is highly expressed in PTEN-inactive TNBC and is crucial for the survival of PTEN-inactive TNBC cells.

1.8 Project Aims

The aim of this project is to identify a candidate gene, which could be used as targeted therapy for PTEN-inactive TNBC. Briefly, the aim was to analyse TCGA breast invasive carcinoma data which was coupled with whole genome siRNA screening data to identify top hit candidate gene(s) that might be required for the survival of PTEN-inactive TNBC (details are mentioned in section 1.8.1). Then, the aim was to validate the findings of bioinformatic analysis with *in vitro* work and patients' samples in PTEN-inactive TNBC (details are mentioned in section 1.8.2). The final aim was then to functionally characterise the candidate gene in PTEN-inactive TNBC (details are mentioned in section 1.8.3).

1.8.1 Bioinformatic analysis to reveal the candidate gene(s) that are essential for the survival of PTEN-inactive TNBC cells

- To validate PTEN/PI3K/AKT signalling axis in different patient cohort of breast invasive carcinoma (TCGA, Provisional).

- To identify the expression of PTEN in different molecular subtypes of breast cancer in breast invasive carcinoma (TCGA, Provisional) data and to discover the association between PTEN expression and TNBC patients' clinical features.

- To identify the significantly different genes between high and low *PTEN* expressing TNBC patient samples in TCGA breast invasive carcinoma data.

- To identify the genes that show significant killing effect between *PTEN*- and *PTEN*+ TNBC cell lines in whole genome siRNA screening data.

- To find the top hit genes that might be required for the survival of PTEN-inactive TNBC by merging the genes that are highly expressed in low PTEN expressing TNBC group in TCGA data with the genes that show significant killing effect in PTEN- TNBC cells in whole genome siRNA screening data.

1.8.2 Validation of bioinformatic analysis findings with *in vitro* work and patients' samples in PTEN-inactive TNBC

- To identify the expression of candidate gene (*WDHD1*) both in non-isogenic and isogenic PTEN WT and PTEN null type TNBC cell lines.

- To identify whether AKT is involved in the regulation of WDHD1 expression in TNBC cell lines.

- To validate the findings of bioinformatic analysis in 2D and 3D cell line models.

- To identify WDHD1 expression in TNBC tissue samples and its association with clinic and pathological features in TCGA and tissue microarray data.

1.8.3 Functional characterisation of WDHD1 in PTEN-inactive TNBC

- To analyse TCGA breast invasive carcinoma (IlluminaHiSeq) data for further understanding of the role of WDHD1 and validate the findings with *in vitro* work.

- To perform immunoprecipitation (IP) and run mass-spectrometry (MS) to identify the functional enrichment of WDHD1 binding partners in PTEN null type TNBC cell lines.

- To validate the identified potential role of WDHD1 in TNBC cell lines.

Chapter 2 Materials and Methods

2.1 Bioinformatic analysis

2.1.1 The Cancer Genome Atlas (TCGA) data mining of PTEN

PTEN, protein expression Z-score (RPPA), *PTEN*, mRNA expression Z-score and *PTEN* mutation status of breast invasive carcinoma (TCGA, Provisional) were obtained from the cBioPortal for Cancer Genomics (https://www.cbioportal.org/). *PTEN* mutation status data was separated into WT and mutant status. PTEN, protein and mRNA levels within *PTEN* WT and mutant groups were analysed by unpaired *t-test* in GraphPad Prism 8. Pearson's correlation analysis was also performed between PTEN, protein expression and *PTEN*, mRNA expression in GraphPad Prism 8.

The phosphorylated forms of AKT (pAKT_308 and pAKT_473), protein expression Z-score (RPPA) levels of breast invasive carcinoma (TCGA, Provisional) were obtained from the cBioPortal for Cancer Genomics (https://www.cbioportal.org/). The correlations between the phosphorylated forms of AKT (pAKT_308 and pAKT_473), protein expression (RPPA) and PTEN, protein expression (RPPA) were analysed by Pearson's correlation analysis in GraphPad Prism 8.

Mutation frequency and status of PI3K isoforms of breast invasive carcinoma (TCGA, Provisional) were also obtained from the cBioPortal for Cancer Genomics (https://www.cbioportal.org/). Mutation status of *PIK3CA* isoform of PI3K was separated into WT and mutant status. PTEN and pAKT_308, protein expression levels between *PIK3CA* WT and mutant groups were analysed by unpaired *t-test* in GraphPad Prism 8. Then, association between PTEN, protein expression and pAKT_308, protein expression was observed both in *PIK3CA* WT and mutant samples by Pearson's correlation analysis in GraphPad Prism 8.

Clinical data for molecular subtype of breast invasive carcinoma, PTEN, protein expression Z-score (RPPA) and *PTEN*, mRNA expression Z-score and *PTEN* mutation status of breast invasive carcinoma (TCGA, PanCancer) were obtained from the cBioPortal for Cancer Genomics (https://www.cbioportal.org/). PTEN, protein expression and *PTEN*, mRNA expression levels were analysed in each breast cancer molecular subtype along with normal breast samples by ordinary one-way ANOVA in GraphPad Prism 8.

Clinical data for molecular subtypes of breast invasive carcinoma (TCGA, Provisional) were obtained from cBioPortal for Cancer Genomics (https://www.cbioportal.org/). Molecular subtypes of breast samples were separated based on ER, PR and HER2 status in the clinical data.

Two different data sets TCGA_BRCA_RPPA-2015-02-24 for protein expression (RPPA) and TCGA_BRCA_exp_HiSeqV2-2015-02-24 for mRNA expression (IlluminaHiSeq), were extracted from the UCSC Cancer Genome Browser (https://genome-cancer.ucsc.edu/) for the analysis of TNBC samples. TNBC samples in clinical data from the cBioPortal for Cancer Genomics (TCGA, Provisional) website were aligned with the samples in the TCGA data for both protein and mRNA expression that were extracted from the UCSC Cancer Genome Browser in RStudio (version 3.4.4). Codes are available in Appendix A.1.1.

Identified TNBC samples in protein (RPPA) were aligned with the identified TNBC samples in mRNA (IlluminaHiSeq) data in RStudio (version 3.4.4). Codes are available in Appendix A.1.1. The correlation between PTEN, protein expression in the TCGA protein data (RPPA) and *PTEN*, mRNA expression in the TCGA data (IlluminaHiSeq) was analysed by Pearson's correlation analysis in TNBC samples that were subcategorised from breast invasive carcinoma (TCGA, Provisional) in GraphPad Prism 8.

2.1.2 TCGA breast invasive carcinoma (Protein, RPPA) analysis

Protein (RPPA) TCGA breast invasive carcinoma data that included 410 breast invasive carcinoma samples and 142 proteins was obtained from the UCSC Cancer Genome Browser (https://genome-cancer.ucsc.edu/). Breast invasive carcinoma samples from the Cancer Genome Browser were aligned with TNBC samples, which were categorised in breast invasive carcinoma (TCGA, Provisional) data in RStudio (version 3.4.4) (mentioned in section 2.1.1). Codes are available in Appendix A.1.1. There were 43 common TNBC samples between these two data sets. Frequency of PTEN, protein expression distribution was analysed in RStudio (version 3.4.4). Codes are available in Appendix A.1.2. PTEN, protein expression across the TNBC samples was narrowly distributed. Samples were grouped as high and low PTEN expressing TNBC samples according to approximately the top 40% and bottom 40% of samples, respectively. The clinical features: patients' age, tumour location, tumour stage, tumour size, lymph node spread and distant metastasis were analysed by Chi-Square (X^2) test between the high and low PTEN expressing TNBC samples in GraphPad Prism 8.

pAKT_308, protein expression was analysed in each breast cancer molecular subtype along with normal breast samples by ordinary one-way ANOVA in GraphPad Prism 8. The correlation between PTEN and pAKT_308 protein expressions (TCGA, RPPA) in TNBC samples that were subcategorised from breast invasive carcinoma (TCGA, Provisional) was analysed by Pearson's correlation analysis in GraphPad Prism 8.

2.1.3 TCGA breast invasive carcinoma (mRNA, IlluminaHiSeq) analysis

mRNA (IlluminaHiSeq) TCGA breast invasive carcinoma data that included 1,215 breast invasive carcinoma samples and 20,530 mRNAs was obtained from the UCSC Cancer Genome Browser (https://genome-cancer.ucsc.edu/). Breast invasive carcinoma samples from the Cancer Genome Browser were aligned with TNBC samples, which were categorised in breast invasive carcinoma (TCGA, Provisional) data in RStudio (version 3.4.4) (mentioned in section 2.1.1). Codes are available in Appendix A.1.1. There were 92 common TNBC samples between these two data sets. Frequency of *PTEN*, mRNA expression distribution was analysed in RStudio (version 3.4.4). Codes are available in Appendix A.1.3. *PTEN*, mRNA expression across the samples was widely distributed. The TNBC samples were grouped into high and low *PTEN* expression based on approximately the top 10% and bottom 10% of samples, respectively. Then, analysis was performed to find the significantly different mRNAs by unpaired *t-test* ($P < 0.05$) between the high and low *PTEN* groups in RStudio (version 3.4.4). Codes are available in Appendix A.1.3.

2.1.4 A whole genome siRNA high-throughput screening and data analysis

The whole genome siRNA high-throughput screening was previously generated by Dr. Yihua Wang. The details for the generation of whole genome siRNA screening data, which included MDA-MB-468-TR-PTEN/CherryFP (*PTEN*-positive, *PTEN*+) or MDA-MB-468-TR-EV/GFP (*PTEN*-negative, *PTEN*-) cell lines are mentioned in section 2.3.

Triplicate data points from CherryFP channel (*PTEN*+) and GFP channel (*PTEN*-) screens underwent plate and position normalisation and Z-score calculation using cellHTS software (Boutros, Brás and Huber, 2006; Steckel *et al.*, 2012). Differential Z-score (ΔZ score) between the two channels were subsequently used to create a gene hit list. Reproducibility of the replicates was analysed by performing Pearson correlation analysis in GraphPad Prism 8. P value < 0.05 was considered significant.

The whole genome siRNA screen data contained siRNAs targeting 21,121 genes in two cell lines expressing GFP fluorescence (*PTEN*-) or red fluorescence (*PTEN*+), respectively. Then, analysis was performed to find the genes that have significant response on cell viability by paired *t-test* ($P < 0.05$) in *PTEN*- *vs PTEN*+ cells in RStudio (version 3.4.4). Codes are available in Appendix A.1.4.

2.1.5 Identification of top hit genes

The statistically different mRNAs in TCGA (IlluminaHiseq) data set that were highly expressed in low *PTEN* TNBC samples were merged with statistically different genes in whole genome siRNA screening data set, which showed a decrease in cell viability in *PTEN*- TNBC cell line group by using RStudio (version 3.4.4) to identify the top hit candidate gene(s). Codes are available in Appendix A.1.5.

2.1.6 TCGA data mining with the identified top hit gene, *WDHD1*

WDHD1, mRNA expression of subcategorised-TNBC samples using clinical data (TCGA, Provisional) was extracted from the TCGA breast invasive carcinoma (IlluminaHiSeq) data set as mentioned in section 2.1.3. Frequency of *WDHD1*, mRNA expression distribution was analysed in RStudio (version 3.4.4). Codes are available in Appendix A.1.6. *WDHD1*, mRNA expression across the samples was widely distributed. Approximately the top 10% and bottom 10% of TNBC samples were chosen for the high and low *WDHD1*, mRNA expression in IlluminaHiSeq data, respectively. Then, significantly different mRNAs were identified between the high *vs.* low *WDHD1* groups in RStudio (version 3.4.4), by unpaired *t-test* ($P < 0.05$). Codes are available in Appendix A.1.6.

WDHD1, mRNA expression Z-score of breast invasive carcinoma (TCGA, PanCancer) were obtained from the cBioPortal for Cancer Genomics (https://www.cbioportal.org/). *WDHD1*, mRNA expression was analysed between the normal breast and TNBC samples by unpaired *t-test* in GraphPad Prism 8. Patients' age, tumour location, tumour stage, tumour size, lymph node spread and distant metastasis of TNBC samples from the clinical data (TCGA, Provisional) were extracted and analysed between the low and high *WDHD1*, mRNA expression by Chi-Square (X^2) test in GraphPad Prism 8.

To discover the positively and negatively correlated mRNAs with *WDHD1* in TNBC samples, Pearson correlation analysis was run in RStudio (version 3.4.4). *P* value < 0.05 was considered significant. Positively and negatively correlated mRNAs with *WDHD1* were identified. Top 50 positively and negatively correlated mRNAs with *WDHD1* were plotted on heatmap. Codes are provided in Appendix A.1.6.

The identified 47 top hit genes between TCGA and WGS were aligned with the positively correlated mRNAs with *WDHD1*. Codes are provided in Appendix A.1.6.

2.2 Cell culture

2.2.1 Storage and thawing of cell lines

To store the cells, growth media from the cells was removed. Cells were washed with 1X phosphate buffered saline (PBS), (Gibco® by life technology, UK). Then, 0.05% Trypsin-EDTA (1X), (Gibco® by life technology, UK) was added to the cells and cells were incubated at 37°C, 5% CO_2 incubator until the cells were detached. Trypsinisation was stopped with the addition of 1:1 ratio trypsin:media to the cells and cells were transferred into a 15 ml falcon tube, (Corning, UK). Cells were centrifuged at 500 x g for 5 minutes. The media was removed and cell pellets were re-suspended in a freezing media (a solution of 90% fetal bovine serum (FBS), (Thermo Fisher Scientific, UK) and 10% Dimethyl sulfoxide (DMSO), (Sigma-Aldrich, UK). Cells were transferred to the cryogenic tubes and placed in Mr. Frosty freezing container, (Merck, UK) and stored at -80°C.

To thaw cells, cells were thawed at 37°C water bath. Cells were transferred into a 15 ml falcon tube and an appropriate media with 1:1 ratio was added to the falcon tube. Cells were mixed with the media and centrifuged at 500 x g for 5 minutes. The media was removed and cells were re-suspended in fresh growth media with 10% FBS and 1% Penicillin/Streptomycin (10,000 U/ml), (Gibco® by life technology, UK). Cells were plated into an appropriate cell culture plate or flask, (Corning, UK) and cultured in normoxic conditions at 37°C, 5% CO_2. The media was changed with the fresh media next day.

2.2.2 Passaging cells

HCC1806, BT20, MDA-MB-157, MDA-MB-231, MDA-MB-468, HCC1395, HCC1937, HCC38 and previously generated MDA-MB-468-TR-PTEN/CherryFP cell lines belong to TNBC cells. The cell lines were gifts from Prof. Julian Downward, The Francis Crick Institute, London, UK.

Growth media, 1X PBS and trypsin were warmed to 37°C before applying to the cells to avoid cell stress. HCC1806, HCC1395, HCC1937 and HCC38 cells were maintained in Roswell Park Memorial Institute (RPMI) 1640 medium, (Gibco® by life technology, UK) with 10% FBS and 1% Penicillin/Streptomycin in normoxic conditions at 37°C, 5% CO_2. BT20, MDA-MB-157, MDA-MB-231, MDA-MB-468 and MDA-MB-468-TR-PTEN/CherryFP cell lines were maintained in Dulbecco's Modified Eagle's Medium (DMEM), (Gibco® by life technology, UK) with 10% FBS and 1% Penicillin/Streptomycin in normoxic conditions at 37°C, 5% CO_2.

When the cells reached 80-90% confluency, cells were passaged by removing the media from the cells. Cells were washed with 1X PBS and trypsinised with 0.05% Trypsin-EDTA (1X) at 37°C, 5% CO_2 incubator until the cells were detached. Trypsinisation was stopped with the addition of 1:1 ratio trypsin:media to the cells and cells were transferred into a 15 ml falcon tube. Cells were centrifuged at 500 x g for 5 minutes. The media was removed and cell pellets were re-suspended in fresh media and plated into the cell culture plate or flask.

2.3 Generation of a whole genome siRNA high-throughput screening

For PTEN-inducible cells, MDA-MB-468 cells were stably transfected with a tetracycline (Tet)-inducible PTEN vector and named MDA-MB-468-TR-PTEN, in which addition of doxycycline (DOX) acutely induces PTEN expression by Tet-on system (Fig. 2.1). MDA-MB-468 cells were also stably transfected with a Tet-inducible parent vector and used as vector-only controls (MDA-MB-468-TR-EV). For fluorescent labelling, MDA-MB-468-TR-PTEN and MDA-MB-468-TR-EV cells were stably transfected with pCherryFP-N1 and p-EGFP-N1, respectively. Single clones were picked and sorted by fluorescence-activated cell sorting (FACS) and named as MDA-MB-468-TR-PTEN/CherryFP or MDA-MB-468-TR-EV/GFP. This work was previously performed by Dr. Yihua Wang in Prof. Julian Downward's lab.

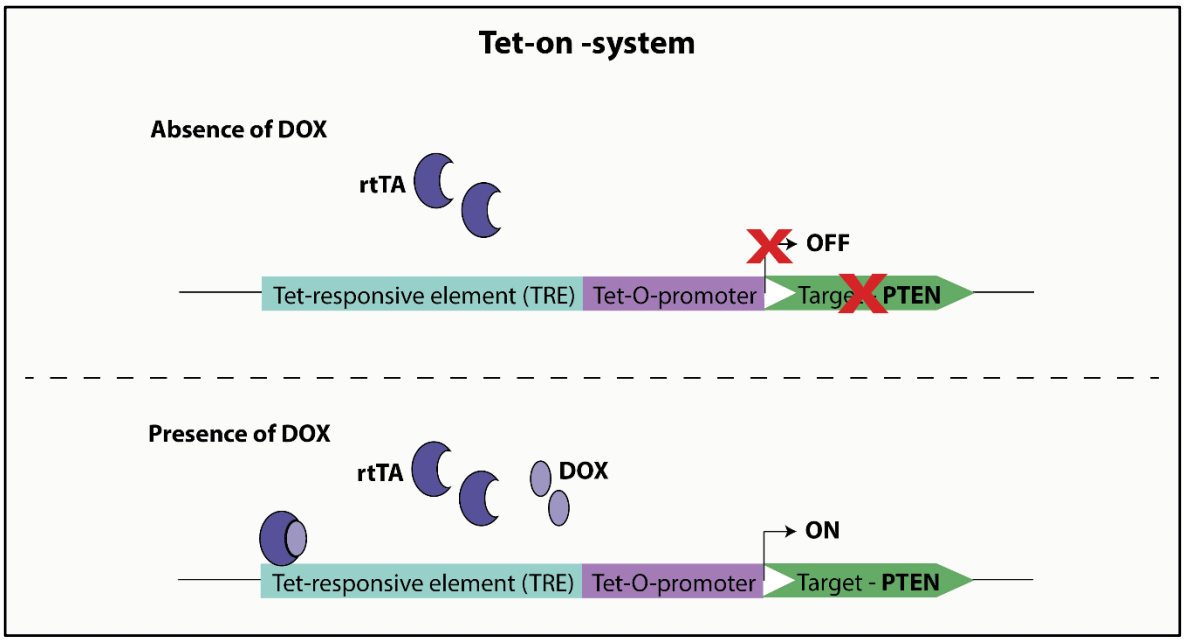

Figure 2.1 Diagram showing Tet-on system.
In the absence of DOX, rtTA cannot bind to TRE and target gene (*PTEN*) transcription is repressed. In contrast, rtTA can bind to TRE in the presence of DOX, which induces the expression of *PTEN*. DOX: doxycycline; Tet: tetracycline; rtTA: reverse tet transactivators; TRE: tet-responsive element; PTEN: phosphatase and tension homolog. [Information collected from (Evans and Mizrahi, 2015)].

Dr. Yihua Wang performed the human siGENOME siRNA library—Genome (G-005005) that was obtained from Dharmacon. siRNA transfection experiments were performed in 96-well format in antibiotic-free medium, using a reverse transfection employing 25 nM siRNA and 0.15 µl DharmaFECT 2 (Dharmacon), (Life Sciences, UK) per well together with a starting cell density optimised to produce an 80% confluent monolayer in mock-treated cells at the conclusion of the experiment. DOX-treated MDA-MB-468-TR-PTEN/CherryFP (*PTEN*+) or MDA-MB-468-TR-EV/GFP (*PTEN*-) cells were mixed and transfected at a 1:1 ratio in 96-well plates. Cells were fixed with 4% paraformaldehyde (PFA) at 96 hours post transfection. Fluorescence was read on an EnVision 2102 Plate-reader (Perkin-Elmer, UK) to evaluate cell numbers in *PTEN*+ or *PTEN*- cells, respectively.

2.4 Drug treatments

2.4.1 Doxycycline (DOX) treatment

DOX inducible system was used to express PTEN in MDA-MB-468-TR-PTEN cells, which were previously generated by Dr. Yihua Wang in Julian Downwards' lab, London as mentioned in section 2.1.4 and 2.3.

To optimise the concentration of DOX, MDA-MB-468-TR-PTEN/CherryFP (*PTEN*+) and MDA-MB-468-TR-EV/GFP (*PTEN*-) cell lines were treated with different concentrations of DOX to induce PTEN expression by Dr. Yihua Wang. MCF10A was also used to check endogenous PTEN expression, which is a non-tumorigenic triple negative breast cell line.

To re-optimise DOX concentration on MDA-MB-468-TR-PTEN/CherryFP (*PTEN*+) cell line for the follow up studies, cells were plated into four 20 cm^2 plate with 30% confluency in 3 ml of DMEM media. Different concentrations of DOX (0 ng/ml, 25 ng/ml, 50 ng/ml and 100 ng/ml), (Sigma-Aldrich, UK) were used to treat the cells. After 6 hours of treatment with different DOX concentrations, cell lysis was performed to run western blot as described in section 2.5.

To adapt the PTEN expression in MDA-MB-468-TR-PTEN cell line, cells were treated with optimum concentration of DOX (100 ng/ml) for two weeks. Cells were plated at 30% confluency into two 60 cm^2 plates in 10 ml of DMEM media. One plate was cultured in the absence of DOX and the other plate was cultured in the presence of 100 ng/ml DOX. Cells were split when they reached 90% confluency with the same treatment strategy up to two weeks. After two weeks, cell lysis for western blot and RNA extraction for qPCR were performed as described in section 2.5 and 2.6, respectively.

2.4.2 Small interfering RNA (siRNA) knockdown

siRNA oligos against *WDHD1* were purchased from Dharmacon. Sequences of the oligos are shown in table 2.1. siGENOME RISC-Free siRNA (Dharmacon) was used as a negative control. The total volume in each well of 6-well plate and 96-well plate was 2000 µl and 100 µl, respectively. Cells were washed with 1X PBS, trypsinised and centrifuged at 500 x g for 5 minutes. Then, cells were re-suspended in fresh media. Cells were plated with 30-35% confluency into each well of 6-well plate and 8000 cells per well of 96-well plate were plated. Cells were transfected with the indicated siRNA oligos at a final concentration of 35 nM using 4 µl and 0.2 µl DharmaFECT 2 reagent (Dharmacon) for 6-well and 96-well plate, respectively. Then, transfection was performed according to the manufacturer's protocols. Western blot (section 2.5) and cell viability assays (section 2.8) were performed 96 hours post transfection of *WDHD1* siRNA. Flow cytometry for cell cycle was performed 48 hours post transfection of *WDHD1* siRNA (section 2.12).

Table 2.1 siRNA oligo sequences used to knockdown *WDHD1*.

Name	***Sequence (5'→3')***
WDHD1 (D-019780-02)	*GGUAAUACGUGGACUCCUA*
WDHD1 (D-019780-03)	*GCUGUGAAUUUAGCCAUUA*

2.4.3 AKT inhibition

PTEN null type TNBC cells: MDA-MB-468, HCC1395, HCC1937 and HCC38 were plated into each well of 6-well plate at 65%-70% confluency. Cells were treated with 10 µM AKT VIII inhibitor, (Sigma-Aldrich, UK) 24 hours post plating. DMSO was used as a negative control. Cells were lysed 24 hours after AKT VIII inhibitor treatment to run western blot (Section 2.5).

2.4.4 Puromycin treatment

To optimise puromycin concentration and incubation time, MDA-MB-468-TR-PTEN cells in the absence or presence of DOX were treated with puromycin, (Sigma-Aldrich, UK) at a final concentration of 0 µM, 2.5 µM, 5 µM, 10 µM, 20 µM and 50 µM puromycin and incubated for 5, 10 and 15 minutes at 37°C and 5% CO_2 (details are mentioned in section 2.14.1).

After optimisation of puromycin treatment, MDA-MB-468-TR-PTEN, BT20, MDA-MB-231, MDA-MB-468 and HCC1937 cells were treated with optimised puromycin concentration for optimised incubation time as mentioned in section 2.14.2. Cells were lysed post treatment to run western blot (Section 2.5).

2.5 Western blot

2.5.1 Buffers for western blot

Table 2.2 shows the lysis buffers, reagents to make Sodium dodecyl sulfate (SDS) gels and buffers that were used during western blot.

Table 2.2 Buffer compositions for western blot.

Buffer	*Buffer Compositions*	*Total Volume*
Urea buffer	8 M Urea, (Sigma-Aldrich, UK) 1 M Thiourea, (Sigma-Aldrich, UK) 0.5% CHAPS, (Thermo Fisher Scientific, UK) 50 mM Dithiothreitol (DTT), (Sigma-Aldrich, UK) 24 mM Spermine, (Sigma-Aldrich, UK)	
pNAS buffer	50 mM Tris.HCl [pH 7.5], 120 mM Sodium chloride, (Thermo Fisher Scientific, UK) 1 M EDTA 0.1% Nonidet P-40	
1.5 M Tris.HCl (pH 8.8)	181.65 g Tris-base, (Thermo Fisher Scientific, UK) 800 ml distilled water Adjust the pH to 8.8 with concentrated hydrochloric acid, (Thermo Fisher Scientific, UK) Appropriate volume of distilled water	**1000 ml**
1.0 M Tris.HCl (pH 6.8)	121.14 g Tris-base 800 ml distilled water Adjust the pH to 6.8 with concentrated hydrochloric acid Appropriate volume of distilled water	**1000 ml**
10% ammonium persulfate (APS)	0.5 g APS salt, (Sigma-Aldrich, UK) 5 ml distilled water	**5 ml**
10X Tris-glycine running buffer	30 g Tris-base 144 g Glycine, (Thermo Fisher Scientific, UK) 10 g SDS, (Thermo Fisher Scientific, UK) Appropriate volume of distilled water	**1000 ml**
1X Tris-glycine running buffer	900 ml distilled water 100 ml 10X Tris-glycine running buffer	**1000 ml**
10X transfer buffer	30 g Tris-base 144 g Glycine Appropriate volume of distilled water	**1000 ml**

Continued on next page

Table 2.2 Continued from previous page

Buffer	*Buffer Compositions*	*Total Volume*
1X transfer buffer	700 ml distilled water 200 ml methanol, (Thermo Fisher Scientific, UK) 100 ml 10X transfer buffer	**1000 ml**
10X Tris-buffered saline and Tween 20 (TBST)	87.66 g sodium chloride 100 ml 1 M Tris.HCl (pH7.5-8) 10 ml Tween 20, (Thermo Fisher Scientific, UK) Appropriate volume of distilled water	**1000 ml**
1X TBST	900 ml distilled water 100 ml 1X TBST	**1000 ml**

2.5.2 Cell lysis with Urea buffer

Media was removed from the cells and cells were washed twice with an appropriate volume of 1X PBS. Depending on the confluency of cells, appropriate volume of 8 M Urea buffer (Table 2.2) was added to the cells. This was then followed by scraping cells and incubation on ice for 30 minutes. Lysates were transferred into 1.5 ml Eppendorf tubes and centrifuged at maximum speed for 10 minutes at 4°C, (Sorvall™ Legend™ Micro 21R Microcentrifuge, Thermo Fisher Scientific, UK). Lysates were kept at -20°C until they were required for further analysis.

2.5.3 Cell lysis with pNAS buffer

For immunoprecipitations, the cells were washed with 1X PBS and lysed for 30 minutes on ice in appropriate volume of pNAS buffer (Table 2.2) with protease inhibitors, (Roche, UK). After centrifuging the lysates, as previously mentioned in section 2.5.2, supernatant was transferred into new 1.5 ml Eppendorf tube. Lysates were kept at -20°C until they were required for further analysis.

2.5.4 Quantification of total protein

Protein quantification was performed by Bradford assay, (Biorad, UK). The samples were centrifuged at maximum speed for 10 minutes at 4°C before quantifying the protein concentration. Bovine serum albumin (BSA) standard curve was created with 4 µg, 2 µg, 1 µg, 0.5 µg and 0 µg of BSA, (Themo Fisher Scientific, UK) in triplicates and 1 µl of samples was added in triplicates in 96 well plate. The required volume of Bradford dye was diluted in distilled water with 1 in 5 ratio. Then,

200 µl of dye reagent (the mixture with Bradford dye and distilled water) was added into each well and protein was quantified by using PolarStar Omega, (BMG Labtech, UK) and Mars-data analysis software, (BMG Labtech, UK).

2.5.5 Sodium dodecyl sulfate-polyacrylamide gel electrophoresis (SDS-PAGE)

The rack with small and big glass (1.5 mm) plates were assembled for gel solidification. 1.5 mm comb was put between the glass plates and approximately 1 cm below the bottom of the comb were marked. Then, comb was removed.

10% or 8% SDS gels were prepared throughout the project. The resolving gels were prepared as shown in table 2.3 and added until the mark that was 1 cm below of the comb. A layer of isopropanol was added on top of the resolving gels to remove any bubbles. Once the resolving gels were solidified after 30 minutes, isopropanol was discarded, gels were washed with distilled water and the excess water was dried off. Then, stacking gel was prepared as shown in table 2.4 and transferred on top of the resolving gel. The comb was slowly inserted into the gel and the stacking gel was left for 15 minutes to solidify. Then, the comb was slowly removed from the gels.

Table 2.3 Resolving gels recipe for western blot.

Reagents	***10% Resolving gel (ml)***	***8% Resolving gel (ml)***
Autoclaved distilled water	4.0	4.6
30% acrylamide mix, (Severn Bioscience, UK)	3.3	2.7
1.5 M Tris.HCl (pH 8.8)	2.5	2.5
10% SDS	0.1	0.1
10% APS	0.1	0.1
TEMED, (Thermo Fisher Scientific, UK)	0.004	0.006
Total Volume	**10**	**10**

Table 2.4 5% Stacking gel recipe for western blot.

Reagents	*Stacking gel (ml)*
Autoclaved distilled water	3.4
30% acrylamide mix	0.83
1.0 M Tris.HCl (pH 6.8)	0.63
10% SDS	0.05
10% APS	0.05
TEMED	0.005
Total Volume	**5**

2.5.6 Sample preparation

Required amount of protein (indicated in the figure legends) was transferred into 1.5 ml Eppendorf tubes and 6 µl of sample loading buffer (100 µl NUPAGE® LDS Sample Buffer (4X), (Invitrogen, UK) and 5 µl β-mercaptoethanol, (Thermo Fisher Scientific, UK)) was added to the lysates. For immunoprecipitation, 40 µl of sample loading buffer (100 µl NUPAGE® LDS Sample Buffer (4X), 100 µl distilled water and 5 µl β-mercaptoethanol) was added. Lysates were then denatured at 100°C for 5 minutes in a heating block, (ACCUBLOCKTM Digital Dry bath, Labnet International Inc. Global, UK) and centrifuged at maximum speed for 2 minutes at room temperature, (Eppendorf, centrifuge 5418, UK).

2.5.7 Electrophoresis

The gels were put inside the gel tank, (Biorad, UK) which was filled with 1X Tris-glycine running buffer (Table 2.2). The HyperPAGE pre-stained protein marker (Bioline, UK) and prepared samples were loaded to the SDS-PAGE gel. The gel was run at 80 V for 45 minutes and 150 V for 1 hour, (Biorad, UK) to separate proteins.

2.5.8 Electrotransfer

The wet transfer was performed to transfer the gel onto the nitrocellulose membrane, (GE Healthcare Life Science, AmershamTM ProtranTM 0.45 µM NC, UK). Four filter papers and one

nitrocellulose membrane were cut with 7 cm by 9 cm dimensions for each gel. The sponges, filter papers and nitrocellulose membrane were put into 1X transfer buffer (Table 2.2) to perform wet transfer. The glass plates were separated, and gel was retrieved. The transfer sandwich was created in the order of sponge, two filter papers, membrane, gel, two filter papers and sponge. The sandwich was put into the transfer tank and tank was filled with 1X transfer buffer until the transfer sandwich was covered. The transfer was carried out at 4°C at 80 V, 0.30 Amp for 3 hours or 20 V, 0.1 Amp for overnight, (Biorad, UK).

2.5.9 Blocking, antibody incubation and visualisation

The nitrocellulose membrane was washed with distilled water several times and stained with Ponceau S solution, concentration 0.1% (w/v) in 5% acetic acid, (Sigma- Aldrich, UK) to confirm the transfer. The membrane was washed with 1X TBST (Table 2.2) and water until the dye was cleared. This was then followed by blocking the membrane in 5% non-fat milk in 1X TBST at room temperature for 1 hour.

The membrane was incubated in the primary antibody overnight at 4°C on the roller, (Stuart, UK) and washed with 1X TBST 3 times, each time for 10 minutes on the rocker, (Stuart, UK). After the primary antibody incubation, the membrane was incubated in secondary antibody at room temperature for 1 hour on the roller. Both primary and secondary antibodies which were used throughout the project are in table 2.5. The membranes were then washed as previously mentioned after secondary antibody incubation.

LI-COR Odyssey® CLx was used to image the membranes and images were analysed by Image Studio Lite Ver 5.2 software, (Odyssey, UK). Then, ImageJ was used to quantify images with the normalisation to β-tubulin or GAPDH loading control by comparing the density of each band.

Table 2.5 Primary and secondary antibodies for western blot.

Antibody	*Species*	*Company*	*Catalogue Number*	*Dilution*
Primary Antibody Target				
PTEN	Rabbit	Cell Signalling	9188	1:1000
p-AKT(Thr308)	Rabbit	Cell Signalling	4056	1:1000
p-AKT(Ser473)	Rabbit	Cell Signalling	9271	1:1000
PARP	Rabbit	Cell Signalling	9532	1:1000
WDHD1	Rabbit	Sigma-Aldrich	HPA001122	1:500
Puromycin	Mouse	Sigma-Aldrich	MABE343	1:2000
RPS6 (C-8)	Mouse	Santa Cruz Biotechnology	sc-74459	1:500
eIF3β (A7)	Mouse	Santa Cruz Biotechnology	sc-374156	1:500
β-tubulin	Mouse	Cell Signalling	86298	1:1000
GAPDH	Rabbit	PROTEINTECH	10494-1-AP	1:10000
Secondary Antibody				
800CW	Rabbit	LI-COR	926-32211	1:5000
680CW	Mouse	LI-COR	926-68020	1:5000

2.6 QuantiNova™ SYBR green real time-polymerase chain reaction (RT-PCR)

2.6.1 RNA extraction

RNA extraction was performed using RNeasy® Mini Kit (Qiagen, UK) according to manufacturer's protocol. Media was removed from each well of 6-well plate and cells were washed twice with 1X PBS. 350 µl of Buffer RLT and 350 µl of 70% ethanol were added into the each well of 6-well plate, respectively and the lysates were mixed by pipetting. 700 µl of samples were transferred into RNeasy Mini spin column that was placed in a 2 ml collection tube and centrifuged for 30 seconds at maximum speed, (Eppendorf Centrifuge 5418, UK). Then, flow-through was discarded and 700 µl Buffer RW1 was transferred to the RNeasy spin column, which was then followed by centrifuging for 30 seconds at maximum speed and discarding flow-through. 500 µl of Buffer RPE was added to the RNeasy spin column and was followed by centrifuging and discarding the flow. 500 µl of Buffer RPE was added to the RNeasy spin column, column was centrifuged for 2 minutes at maximum speed, and flow-through was discarded. RNeasy spin column was placed in a new 2 ml collection tube and centrifuged at maximum speed for 1 minute. Finally, RNeasy spin column was placed in a new 1.5 ml collection tube and 40 µl of RNAse-free water was added to the spin column membrane and centrifuged for 1 minutes at maximum speed to elute the RNA. Nanodrop Spectrophotometer 2000c, (Thermo Fisher Scientific, UK) was used to quantify RNA concentration. RNA samples were kept at -80°C until they were required for further experiments.

2.6.2 RT-PCR analysis

QuantiNova™ SYBR Green RT-PCR, (Qiagen, UK) manufacturer's protocol was performed. 20 ng/µl RNA samples were prepared with RNAse-free water in 1.5 ml Eppendorf tubes. The reaction mixture was prepared in 1.5 ml Eppendorf tube, as stated in table 2.6. 9.5 µl from the reaction mixture was added into each well of 96-well plate and 0.5 µl of RNA from 20 ng/µl working stock was added into the wells containing the reaction mixture. *WDHD1* (QT00062244) and *ACTB* (β-actin, QT00096431) gene-specific primers, (QuantiTect Primer Assays, Qiagen, UK) were used. Real-time cycler was programmed as stated in table 2.7, the PCR plate was placed in the real-time cycler and the cycling program was run. Relative mRNA level of target gene was normalised to *ACTB*.

Table 2.6 Reaction mixture set up for RT-PCR.

Component	*Mixture/reaction*
2x QuantiNova SYBR Green RT-PCR Master Mix	5 µl
QN ROX Reference Dye	0.5 µl
QN SYBR Green RT-Mix	0.1 µl
Primer	0.5 µl
Template RNA	0.5 µl
RNase-Free water	3.4 µl
Total reaction volume	**10 µl**

Table 2.7 Real-time cycler conditions.

Step	*Time*	*Temperature*	*Ramp Rate*	*Cycle*
Holding Stage				
Reverse transcription	10 minutes	50°C	100%	
PCR initial activation step	2 minutes	95°C	100%	
Two-step Cycling				50
Denaturation	5 seconds	95°C	100%	
Combined annealing/extension	1 minute	60°C	100%	

2.7 Immunofluorescence microscopy

2.7.1 Plating cells

Slides and forceps were sterilised with sterile methanol and left to air dry. Three sterilised slides were put into each well of 6 well plate with forceps. MDA-MB-468-TR-PTEN cells were cultured for two weeks in absence or presence of DOX (100 ng/ml) as mentioned in section 2.4.1. MDA-MB-468-TR-PTEN cells in absence of DOX and presence of DOX were plated with the confluency of 35% and 45% into 6 well plate, respectively. Cells were plated in triplicates for each condition. DOX was added to the appropriate wells.

2.7.2 Fixing and staining cells

When the cells reached 80-90% confluency, media was removed and cells were gently washed with 1X PBS twice. 1 ml 4% PFA, (Thermo Fisher Scientific, UK) in 1X PBS was added to fix the cells for 15 minutes. PFA was removed and cells were washed with 1X PBS.

For permeabilisation of cells, 500 µl of 0.1% Tiron-X-100, (Thermo Fisher Scientific, UK) in 1X PBS was added to each well of 12 well plate and the slide was transferred from 6 well plate into 12 well plate and incubated in 0.1% Tiron-X-100 for 5 minutes on ice. This was followed by washing the slides with 1X PBS twice. Then, cells on the slides were blocked in 0.2% Fish Skin Gelatine, (Sigma Aldrich, UK) in 1X PBS for 60 minutes at room temperature. Meanwhile, anti-WDHD1 primary antibody was prepared in blocking buffer with 1:50 dilution and parafilm was put on the foil-wrapped container. To moist the container, wet tissue was also put into the side of the box. 45 µl of primary antibody was put on the parafilm and the excess buffer was removed from the slides and slides were put on the antibody upside down for 60 minutes at room temperature. 60 minutes after the primary antibody incubation, slides were flipped and put into 12 well plate and washed with 1X PBS 3 times, each time for 15 minutes on the rocker. Then, secondary antibody with 4'6-diamidino-2-pheylindole (DAPI), (Invitrogen, UK) was prepared in 1X PBS with the dilution of 1:400 and 1:1000, respectively. New parafilm was put into the box, 95 µl of secondary antibody was put onto parafilm, and slides were put onto parafilm upside down and incubated at room temperature for 60 minutes. Slides were washed with 1X PBS as previously by avoiding light exposure. 8 µl of mounting solution was added to the cover slip and slide was put on the cover slip upside down and left to air dry overnight by avoiding light exposure. Protein expression was detected using Alexa Fluor (1:400, Molecular Probes) for 20 minutes.

2.8 Cell viability assay by CellTiter-Glo® in 2D culture

CellTiter-Glo® Luminescent, (Promega, UK) cell viability assay was performed according to the manufacturer's protocol. siRNA transfected cells were plated into 96-well plate as mentioned in 2.4.2 and were allowed to grow for 96 hours. The experiment was set up with the control wells containing only medium for background luminescence. 96 hours post transfection, cells were kept at room temperature for 30 minutes and 100 µl of CellTiter-Glo® reagent was added to each well. The contents were mixed on the rocker for 2 minutes and plate was incubated at room temperature for 10 minutes. Then, the content was transferred into 96-well white plate, (Thermo Fischer Scientific, UK). GLOMAX MULTI+ DETECTION SYSTEM machine, (Promega, UK) was used to record luminescence with 0.5 second integration time per well.

2.9 Colony formation assay with crystal violet

siRNA transfection was performed as mentioned in 2.4.2 and 96 hours of post-transfection, cells were trypsinised and centrifuged at 500 x g for 5 minutes. Supernatant was removed and the cell pellets were re-suspended with an appropriate volume of media. Single cells were obtained by pipetting up and down and viable cells were counted with haemocytometer by using trypan blue, (Gibco® by life technology, UK). 3,000-5,000 cells were plated into each well of 6 well plate and cultured for two weeks until the colonies formed. Colonies were washed with 1X PBS and fixed with 4% PFA in 1X PBS for 30 minutes. This was followed by washing the colonies twice with distilled water and addition of 1 ml 0.5% crystal violet, (Thermo Fisher Scientific, UK) in 20% methanol for 30 minutes. Then, colonies were washed three times with distilled water and plates were left to air dry at room temperature overnight. Plates were scanned with EPSON PERFECTION V700 PHOTO, (Epson, UK). The intensity of colonies were analysed on ImageJ (Guzmán *et al.*, 2014).

2.10 Mammosphere formation assay

2.10.1 Plating 3D cell culture

siRNA transfection was performed in 2D cell culture (section 2.4.2). 96 hours post-transfection, adherent cells were typsinised and centrifuged at 500 x g for 5 minutes. Supernatant was removed and the cell pellets were re-suspended in mammosphere culture media, which was composed of 1:1 DMEM:F12 media, (Gibco® by life technology, UK) with 1% Penicillin/Streptomycin, 2% B27, (Gibco® by life technology, UK), 20 ng/ml EGF, (PEPROTECH, UK) and 20 ng/ml FGFb, (PEPROTECH, UK). Single cells were obtained by pipetting up and down. Viable cells were counted with haemocytometer by using trypan blue. Re-suspended single cells from TNBC cells were plated in 96-well ultralow attachment plate, (Corning, UK) in 100 µl of culture medium at plating densities between 3,000 and 7,000 cell per well. Cells were incubated at 37°C and 5% CO_2 for two weeks.

2.10.2 Mammosphere formation efficiency (MFE) and mammosphere volume analysis

The images were obtained under light microscope, EVOS, with 40X magnification after two weeks of incubation in 3D culture. ImageJ was used to determine the MFE and volume of sphere. The mammospheres that were equal or greater than 50 micrometre diameters were counted to calculate the MFE using equation 1 (shown below). Additionally, the volume of mammospheres were also calculated using equation 2 (shown below).

Equation 1. MFE (%)= (# of mammospheres per well) / (# of cells seeded per well) x 100

Equation 2. Volume = $(4/3)\pi r3$

2.10.3 Cell viability assay by CellTiter-Glo® in 3D culture

Cells were incubated at room temperature for 30 minutes and, CellTiter-Glo® cell viability assay was performed. 100 µl of CellTiter-Glo® reagent was added to each well and incubated at room temperature for 1 hour. Then, cells were gently mixed by pipetting up and down and transferred into 96-well white plate. GLOMAX MULTI+ DETECTION SYSTEM machine was used to record luminescence with 0.5 second integration time per well.

2.11 Immunohistochemical and haemotoxylin/eosin (H/E) staining and scoring

Dr. Huiquan Liu in China carried out H/E staining. Tissue microarray of TNBC patients with information of clinicopathological parameters was purchased from Outdo Biotech, (HBreD090Bc01; Shanghai, China). Tissue samples were pre-stained with Ki67. Paraffin-embedded sections of xenograft tissues were subjected to deparaffinization and rehydration. H/E staining of sections was carried out using H/E staining kit, (Beyotime, Shanghai, China) according to manufacturer's instructions. For immunohistochemical staining of tissue microarray and sections of xenograft, antigen retrieval, blocking of non-specific binding and incubation of primary antibody at 4°C overnight were sequentially conducted. The primary antibody of anti-WDHD1, (HPA001122, Sigma-Aldrich, 1:500) was used. After incubation with secondary goat anti-rabbit immunoglobulin conjugated to peroxidase-labelled dextran polymer, (SV0002; Boster) at 37°C for 1 hour, visualization, counterstaining with hematoxylin and mounting were performed. Semi-quantitative evaluations of protein expression were scored on the basis of the intensity and the percentage of WDHD1 positive tumour cells as previously described (Wang *et al.*, 2014; H. Liu *et al.*, 2019; Yihua Wang *et al.*, 2019; Liu *et al.*, 2020).

2.12 Flow cytometry

2.12.1 Plating cells

For cell cycle analysis, cells were plated into 6 well plate with the range between 30-45% confluency and transfected with *WDHD1* siRNA oligos along with RISC-Free siRNA oligo as mentioned in section 2.4.2.

2.12.2 Fixing cells

Cells were washed with 1X PBS and trypsinised 48 hours post transfection. Trypsinisation was stopped and cells were transferred into 1.5 ml Eppendorf tubes and mixed up and down to have single cells. Cells were centrifuged at 5,700 x g for 2 minutes at 4°C. All the steps were performed on ice after this step. Supernatant was removed and cell pellets were washed with 1X PBS by pipetting up and down. Cells were centrifuged as previously mentioned and supernatant was discarded. Pellets were re-suspended with 300 µl of 1X PBS and 700 µl of 100% ice cold ethanol was

added to the cells in a dropwise manner, cells were vortexed after each drop of ethanol. Cells were kept at 4°C up to 2 weeks until they were used for staining.

2.12.3 Propidium iodide (PI) staining and cell analysis

All steps were performed on ice. Cells were centrifuged as previously mentioned in section 2.12.2 and supernatant was removed. Pellets were re-suspended with 0.5 ml of 0.25% Triton-X-100 in 1X PBS and incubated on ice for 15 minutes. Cells were centrifuged as mentioned previously and supernatant was discarded. Pellets were re-suspended in 0.5 ml 1X PBS containing 200 µg/ml RNAse A, (Thermo Fisher Scientific, UK) and 50 µg/ml PI and incubated at room temperature in the dark for 30 minutes. Cell cycle analysis was performed by flow cytometry, Guava, (Millipore, UK).

2.13 Immunoprecipitation-mass spectrometry (IP-MS)

2.13.1 Immunoprecipitation

The cell lysis and protein quantification were performed as mentioned in 2.5.3 and 2.5.4, respectively. The protocol was performed on ice. 1 mg/ml protein samples were rotated with Protein G Sepharose beads, (GE Healthcare, UK) at 4°C for 1 hour. The samples were then centrifuged at 570 x g, at 4°C for 1 minute and this was followed by transferring 950 µl supernatant lysate into new 1.5 ml Eppendorf tube. The supernatants were rotated with 50 µl Protein G Sepharose and 0.4 µg/ml anti-WDHD1, (Sigma-Aldrich) or control immunoglobulin G (IgG), (Invitrogen, UK) antibodies for 16 hours at 4°C. Immunoprecipitates were washed four times with cold 1X PBS, each time centrifuging at 570 x g, at 4°C for 1 minute. Then, samples were prepared as mentioned in 2.5.5-2.5.9 to run western blot and confirm WDHD1 was successfully immunoprecipitated. This was then followed by mass spectrometry preparation and analysis (section 2.13.2, 2.13.3 and 2.13.4).

2.13.2 Sample preparations for mass spectrometry

Samples were prepared by Prof. Paul Skipp. Protein G Sepharose beads were re-suspended in 100 µL of 100 mM ammonium bicarbonate containing 0.25% Rapigest (Waters Corporation), heated at 70°C for 60 minutes, centrifuged at 13,000 x g for 5 minutes and the supernatant was collected.

Protein extracts were reduced with 0.5 µg DTT for 1 hour and then alkylated with 2.5 µg iodoacetamide (IAA) for 45 minutes in the dark, and digested with 0.5 µg sequencing grade modified trypsin (1/50 (w/w)) overnight at 37°C. Samples were acidified with 1% trifluoroacetic acid (v/v), centrifuged at 13,000 x g for 5 minutes and the supernatant was collected. Supernatants were lyophilised and re-suspended in 20 µL of buffer A (0.1% formic acid in water (v/v)) prior to mass spectrometry.

2.13.3 Mass spectrometry and database search

Mass spectrometry and database search were performed by Prof. Paul Skipp. 18 µL of peptide extracts in buffer A were separated on an Ultimate 3000 RSLC nano system, (Thermo Fisher Scientific, UK), using a PepMap C18 EASY-Spray LC column, 2 µm particle size, 75 µm x 75 cm column, (Thermo Fisher Scientific, UK), over 140 minutes (single run) linear gradient of 3–25% buffer B (0.1% formic acid in acetonitrile (v/v)) in buffer A at a flow rate of 300 nL/min. Peptides were introduced using an EASY-Spray source at 2000 V to a Fusion Tribrid Orbitrap mass spectrometer, (Thermo Fisher Scientific, UK). The ion transfer tube temperature was set to 275°C. Full MS spectra were recorded from 300 to 1500 m/z in the Orbitrap at 120,000 resolution with an automatic was performed using TopSpeed mode at a cycle time of 3 seconds. Peptide ions were isolated using an isolation width of 1.6 amu and trapped at a maximal injection time of 120 ms with an AGC target of 300,000. Higher-energy collisional dissociation (HCD) fragmentation was induced at an energy setting of 28 for peptides with a charge state of 2–4. Fragments were analysed in the orbitrap at 30,000 resolution.

Analysis of raw data was performed using Proteome Discoverer software (Thermo Scientific, UK), and the data was processed to generate reduced charge state and deisotoped precursor and associated product ion peak lists. These peak lists were searched against the human protein database. A maximum of one missed cleavage was allowed for tryptic digestion and the variable modification was set to contain oxidation of methionine and N-terminal protein acetylation. Carboxyamidomethylation of cysteine was set as a fixed modification. The false discovery rate (FDR) was estimated with randomised decoy database searches and were filtered to 1% FDR.

2.13.4 Immunoprecipitation-mass spectrometry (IP-MS) analysis

Two repeats of WDHD1 and two repeats of IgG control samples were combined in RStudio (version 3.4.4), and the proteins with *NA* values in more than two samples were removed. The average of

peptide numbers for WDHD1 and IgG control samples was calculated and the ratio of peptide numbers for each sample group was calculated. The proteins, which had two times higher peptide number in WDHD1 compared to the control samples were chosen as threshold, the codes are available in Appendix A1.7, and used to perform pathway analysis in ToppGene website as described in section 2.15.

2.14 Puromycin incorporation assay

2.14.1 Puromycin incorporation assay optimisation

MDA-MB-468-TR-PTEN cell line was cultured to optimise the concentration of puromycin and the incubation time of puromycin on cells. MDA-MB-468-TR-PTEN cells were plated into 6 well plate with 30% confluency. Three different 6 well plates with MDA-MB-468-TR-PTEN for the absence of DOX and another three 6 well plates for the presence of DOX were cultured. The cells for the presence of DOX were treated with DOX after 48 hours of plating at a final concentration of 100 ng/ml DOX and incubated further for 16 hours, which could be a positive control for puromycin incorporation assay. The following day different concentrations of puromycin (0 µM, 2.5 µM, 5 µM, 10 µM, 20 µM, 50 µM) was added to both DOX treated and untreated cells. Cells were incubated with puromycin for 5 minutes, 10 minutes and 30 minutes at 37°C and 5% CO_2. Then, cells were lysed with 8 M urea buffer to perform western blot and find the optimal puromycin concentration and incubation time by analysing puromycin protein level as mentioned in section 2.5.

2.14.2 *WDHD1* siRNA with puromycin incorporation assay

MDA-MB-468-TR-PTEN, BT20, MDA-MB-231, MDA-MB-468 and HCC1937 cells were plated into 6 well plates at 30% confluency with *WDHD1* siRNA oligos and RISC-Free negative control as mentioned in section 2.4.2. The following day, MDA-MB-468-TR-PTEN cells for the presence of DOX (DOX+) were treated with DOX at a final concentration of 100 ng/ml for 16 hours.

MDA-MB-468-TR-PTEN, BT20, MDA-MB-231, MDA-MB-468 and HCC1937 cells with *WDHD1* siRNA were cultured for 48 hours. Then, cells were treated with optimised puromycin concentration and duration time, at a final concentration of 2.5 µM puromycin for 5 minutes at 37°C and 5% CO_2. This was then followed by cell lysis with 8 M urea buffer and western blot as previously mentioned in section 2.5.

2.15 Pathway analysis

For pathway analysis, ToppGene Suite (https://toppgene.cchmc.org/) was used to detect functional enrichment of the mRNAs or proteins.

The pathway analysis for TCGA data was run with the significantly upregulated mRNAs in high *WDHD1* compared to the low *WDHD1* group and positively correlated mRNAs with *WDHD1*. The pathways were sorted from lowest *P* value and top 15 pathways were chosen for TCGA data. The histogram plot was produced with the top 15 pathways in GraphPad Prism 8.

The pathway analysis for IP-MS was run with the WDHD1 binding partners. The pathways for IP-MS data were sorted from lowest *P* value and the histogram was plotted with top four pathways in GraphPad Prism 8.

2.16 Subcellular localisation

MDA-MB-468-TR-PTEN were cultured in 60 cm^2 plate and cells for the presence of DOX (DOX+) were treated with DOX at a final concentration of 100 ng/ml for 16 hours. Media was discarded from the cells and cells were washed with 1X PBS and trypsinised. Trypsinisation was stopped as mentioned in section 2.2.2 and cells were transferred into a 15 ml falcon tubes and mixed up and down to have single cells. Viable cells were counted with haemocytometer by using trypan blue.

Approximately 1 million cells were transferred to 1.5 ml Eppendorf tube to be used as total lysates. Cells in the Eppendorf tubes for total lysates were centrifuged at 500 x g for 5 minutes and media was removed. Cell pellets were washed with 1X PBS, re-centrifuged and PBS was discarded. Cell lysis was performed with 150 µl of 8 M urea buffer as mentioned in section 2.5.2. Meanwhile, cytoplasm and nuclear extraction were performed by using the NE-PER® Nuclear and Cytoplasmic Extraction Reagents kit according to manufacturer's protocols, (Thermo Fisher Scientific, UK) with the remaining cells. Western blot was performed as mentioned in section 2.5 to confirm WDHD1 localisation in the presence or absence of DOX in MDA-MB-468-TR-PTEN cell lines.

2.17 Statistical analysis

Two tailed, unpaired Student's *t-test* for the TCGA data and two tailed, paired Student's *t-test* for the whole-genome siRNA screening data were performed in RStudio (version 3.4.4). Unless stated otherwise, comparison of two groups was statistically calculated by two paired, unpaired

Student's *t-test* in GraphPad Prism 8 software. Ordinary one-way ANOVA was conducted to statistically compare more than two groups in GraphPad Prism 8 software. Correlation analysis was conducted by Pearson's correlation in GraphPad Prism 8 software. χ^2 test was used to analyse the association of PTEN and *WDHD1* with clinical features of TNBC samples in the TCGA breast invasive carcinoma data in GraphPad Prism 8 software. χ^2 test or Fisher's exact test were used to evaluate the relationship of WDHD1 and clinicopathological parameters of TNBC patient samples in IHC using SPSS (version 19.0). Data were shown as box and whisker plot with minimum and maximum individual values, mean ± SD or mean ± SEM, indicated in figure legends.

Chapter 3 Bioinformatic analysis to reveal the candidate gene(s) that are essential for the survival of PTEN-inactive TNBC cells

3.1 Introduction

3.1.1 The Cancer Genome Atlas (TCGA)

Heterogeneity of cancer plays an important role in the complexity of the disease (Hanahan and Weinberg, 2011). There are at least 200 different cancer types that are divided into subtypes due to the variations in molecular profiles (Tomczak, Czerwińska and Wiznerowicz, 2015). Genetic alterations, copy-number, gene expression, somatic mutations, protein expression and epigenetic changes are different in each cancer type (Chin, Andersen and Futreal, 2011). Thus, treatment options vary across each cancer types and it is crucial to widen the knowledge about genome, and genetic changes in cancer for early diagnosis, prevention and treatment of cancer.

National Cancer Institute and National Human Genome Research Institute have been collaborating to launch TCGA project (http://cancergenome.nih.gov). Only three different cancer projects; ovary serous cystadenocarcinoma, glioblastoma multiforme (GBM) and lung squamous carcinoma were analysed in 2006 in TCGA project (O'Keefe, 2001; Tomczak, Czerwińska and Wiznerowicz, 2015; Hutter and Zenklusen, 2018). TCGA project has been improving, which included molecular characterisation of more than 11,000 primary cancer and matched normal samples of 33 different cancer types to create genomic data sets (Hutter and Zenklusen, 2018). The process of TCGA involves collection of sample, processing of sample, high-throughput sequencing and bioinformatic data analysis, in a sequence (Chin *et al.*, 2011). The high-throughput sequencing of TCGA project is based on next-generation sequencing (NGS) and microarray to analyse nucleic acids and both proteins and nucleic acids, respectively (Chin *et al.*, 2011). There are different high-throughput technologies, in this project we performed the analyses with RNA-sequencing (RNA-seq) for transcriptome and reverse-phase protein assay (RPPA) for large scale protein expression (Tomczak, Czerwińska and Wiznerowicz, 2015). RNA-seq identifies and quantifies non-coding RNAs, isoforms, gene fusion and transcripts including novel, rare and common (Tomczak, Czerwińska and Wiznerowicz, 2015; Calabrese *et al.*, 2020). Illumina system is used for TCGA transcriptome analysis and nucleotide sequence and gene expression information are shown in the TCGA data (Tomczak, Czerwińska and Wiznerowicz, 2015). Moreover, details of gene expression, junction or exon, sequence variants, and RNA-seq coverage can be obtained from RNA-seq alignment (Kukurba and

Montgomery, 2015). RPPA is an antibody-based technology, which is a very sensitive, high-throughput, reproducible, quantitative, and functional proteomics method (Spurrier, Ramalingam and Nishizuka, 2008). RPPA provides information to profile protein expression level and level of phosphorylated proteins (Zhang *et al.*, 2018). RPPA is an antibody-based technique that includes 500 different antibodies to analyse more than 1000 samples at a time (Tomczak, Czerwińska and Wiznerowicz, 2015).

To visualise generated cancer genomic data by array-based profiling technologies and NGS, visualisation tools are required. Although there are different tools to visualise the genomic data, UCSC Cancer Genomics Browser (https://genome-cancer.ucsc.edu/) and the cBioportal for Cancer Genomics (http://www.cbioportal.org/) were used in this project. Both UCSC Cancer Genomic Browser and cBioportal for Cancer Genomics are open-access web-based tools to visualise, analyse and obtain the genomic and proteomic data (Cerami *et al.*, 2014; Goldman *et al.*, 2015). UCSC Cancer Genomics Browser provides interactive views of genomic regions with annotated biological pathways and clinical features (Goldman *et al.*, 2015). In 2015, UCSC Cancer Genomics Browser included 526 datasets (somatic mutation copy number, DNA methylation, protein expression, gene and exon expression, phenotype data and PARADIGM pathway inference) from 31 different TCGA cancer types from genome –wide analyses (Goldman *et al.*, 2015). There are 69 cancer genomics in the cBioportal for Cancer Genomics that includes; DNA-copy number, DNA methylation, RPPA, miRNA, mRNA expression and a clinical data of the patients (Tomczak, Czerwińska and Wiznerowicz, 2015).

3.1.2 RNA interference (RNAi) whole-genome screening

RNAi was discovered by Andrew Fire and Craig Melo in 1998 by showing post-transcriptional gene silencing (PTGS) in *Caenorhabditis elegans* due to the double-stranded RNAs (dsRNAs) (Fire *et al.*, 1998). It was also shown that 21-22 nts dsRNAs can silence the gene expression in mammalian cells (Caplen *et al.*, 2001; Elbashir *et al.*, 2001). These discoveries showed that RNAi can be a powerful tool to study function of genes.

RNAi is a biological process that silences the gene expression by small RNAs; short hairpin RNA (shRNA) (Bernards, Brummelkamp and Beijersbergen, 2006) and siRNA (Surendranath *et al.*, 2013). dsRNAs incorporated into RNA-induced silencing complex (RISC) which unwind the strands and RISC bind to the guide strand to target the complementary or near-complementary region of target mRNA to supress the gene expression via mRNA degradation or mRNA translation blockage (Carthew and Sontheimer, 2009; Mohr *et al.*, 2014).

RNAi application is one of the efficient tools in high-throughput screen (HTS), which can be used in whole genome-wide scale studies in mammalian cells (Chang *et al.*, 2012). RNAi screen is also known as one of the synthetic lethal screening tools to identify potential synthetic lethal interactions which then can be validated with *in vitro* and *in vivo* work (Topatana *et al.*, 2020). Isogenic or patient-derived cell lines can be used to perform RNAi screening where the genes can be targeted with siRNAs and the cell viability or proliferation is measured. Then, the comparison of the impact of genes on cell viability or proliferation between the cell lines can identify the essential genes (Fece de la Cruz, Gapp and Nijman, 2014). RNAi screening is an effective tool to identify novel targets that can be potential biomarkers or used to develop a therapeutic treatment for cancer (Mohr, Bakal and Perrimon, 2013).

3.1.3 Summary of the chapter

In this chapter, we aimed to perform bioinformatic analysis to reveal the candidate gene(s) that are essential for the survival of PTEN-inactive TNBC cells.

Significantly different genes between high and low *PTEN* expressing TNBC patient samples were identified in TCGA data. In parallel to this, genes that showed significant killing effect between *PTEN*- and *PTEN*+ TNBC cell lines were discovered in whole genome siRNA screening data. The findings between TCGA and whole genome siRNA screening data sets were combined and the top hit gene(s) were identified. One of the identified genes was *WD repeat and high mobility group [HMG]-box DNA binding protein 1* (*WDHD1*).

3.2 Results

3.2.1 *PTEN* mutation associates with low PTEN expression

Previous studies showed that *PTEN* mutation is not common in breast cancer (Li *et al.*, 1997; Chang *et al.*, 2005) but PTEN protein expression loss is frequently observed in breast cancer (Chang *et al.*, 2005; Knudsen *et al.*, 2012). Thus, we decided to check whether *PTEN* mutation has an effect on both PTEN, protein and mRNA expression in breast invasive carcinoma data (TCGA, Provisional). To demonstrate this association, PTEN, protein and mRNA expression levels were analysed in *PTEN* WT and mutant samples in breast invasive carcinoma data (TCGA, Provisional). Both PTEN, protein and mRNA expression levels were significantly downregulated in *PTEN* mutant samples compared to *PTEN* WT samples in breast invasive carcinoma (TCGA, Provisional) patient cohort (Fig. 3.1A & Fig. 3.1B). Additionally, there was a significant positive correlation between PTEN, protein and mRNA expression levels (Fig. 3.1C; $r = 0.42$, $P = <0.0001$). This analysis showed that although the number of *PTEN* mutated samples was low, *PTEN* mutation is associated with low PTEN expression.

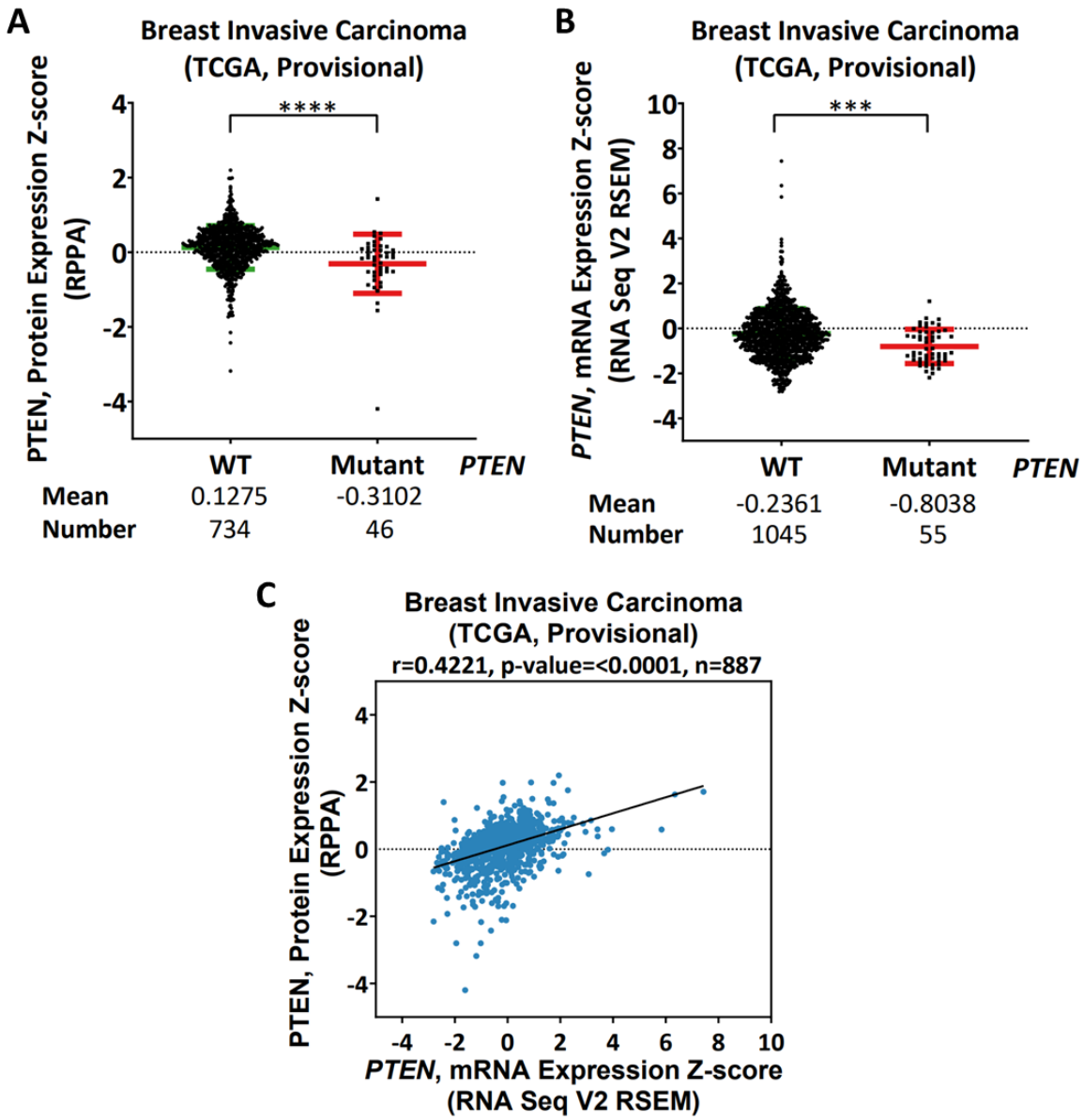

Figure 3.1 PTEN, protein and mRNA expression in *PTEN* WT and mutant breast invasive carcinoma samples (TCGA, Provisional) from cBioPortal.

PTEN, protein expression Z-score (RPPA) (**A**) and *PTEN,* mRNA expression Z-score (RNA Seq v2 RSEM) (**B**) in *PTEN* WT and mutant samples. Data are mean ± standard deviation (SD). Unpaired *t-test* was performed for statistical analysis. ***$P \leq 0.001$. ****$P \leq 0.0001$. **C)** The scatter plot for the correlation between *PTEN,* mRNA expression Z-score (RNA Seq V2 RSEM) and PTEN, protein expression Z-score (RPPA) (Pearson's correlation $r = 0.4221$; $P = <0.0001$; $n = 887$).

3.2.2 The link between PTEN, *PIK3CA* and the AKT activity

It has been known that the main downstream signalling pathway of PTEN is PI3K/AKT signalling pathway that has an important role in carcinogenesis (Carnero, 2010). To validate and show the association of PTEN and PI3K/AKT signalling in breast invasive carcinoma patient cohort (TCGA, Provisional), PTEN, protein expression and protein expression of phosphorylation sites of AKT at Thr308 and Ser473 (pAKT_308 and pAKT_473), which indicates the activation of AKT were extracted from cBioportal website. There was a significant negative correlation between PTEN and pAKT_308 protein expression levels (Fig. 3.2A; r = -0.19; P = <0.0001) but no significant correlation between PTEN and pAKT_473 protein expression was observed (Fig. 3.2B; r = -0.05; P = 0.1375). These results suggested that PTEN and pAKT_308 might be in the same signalling axis but PTEN and pAKT_473 might not be in the same signalling axis.

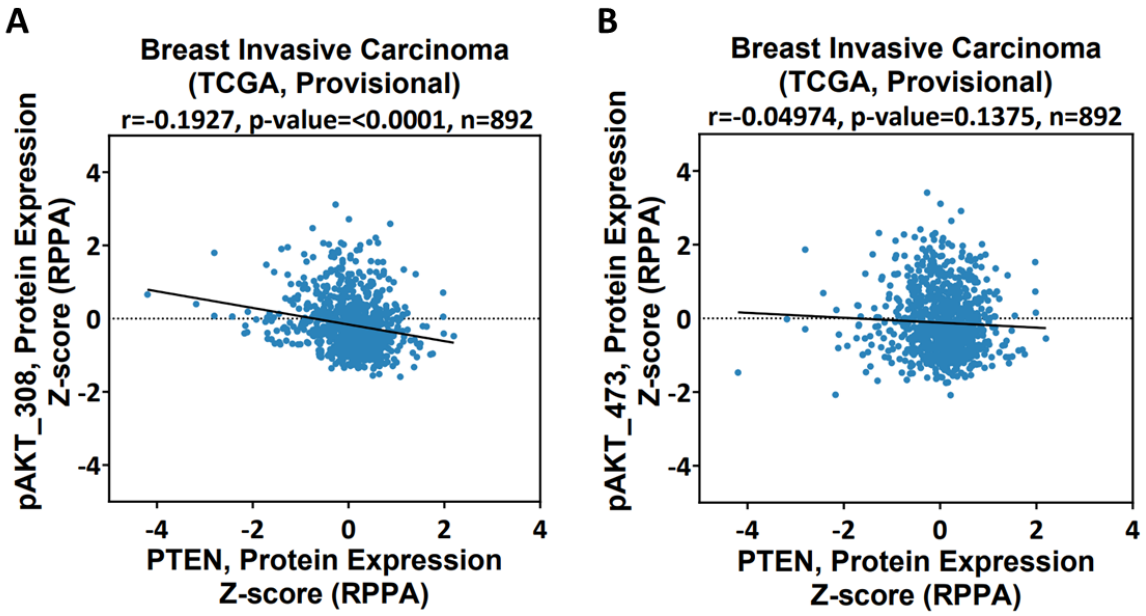

Figure 3.2 Correlation between PTEN, protein expression and phosphorylated forms of AKT (pAKT_308 and pAKT_473) in breast invasive carcinoma samples (TCGA, Provisional) from cBioPortal.

A) The scatter plot for the correlation between PTEN, protein expression Z-score (RPPA) and pAKT_308, protein expression Z-score (RPPA) (Pearson's correlation r = -0.1927; P = <0.0001; n = 892). **B)** The scatter plot for the correlation between PTEN, protein expression Z-score (RPPA) and pAKT_473, protein expression Z-score (RPPA) (Pearson's correlation r = -0.04974; P = 0.1375; n = 892).

The activated class I PI3Ks can phosphorylate PIP_2 into PIP_3, which then activates the AKT signalling pathway (Vanhaesebroeck, Stephens and Hawkins, 2012). It has also been shown that the isoform

of *PIK3CA* gene encoding p110α is frequently mutated in breast cancer (Bachman *et al.*, 2004; Samuels *et al.*, 2004; Alvarez-Garcia *et al.*, 2018). Mutation status of all the isoforms of PI3K was identified in breast invasive carcinoma data set (TCGA, Provisional), which showed *PIK3CA* was the highest mutated isoform (38%) and most of its mutations were associated with putative driver (Fig. 3.3). Thus, the following analysis was performed with *PIK3CA* isoform of PI3K to demonstrate the association between PTEN, PI3K and AKT activity. In *PIK3CA* mutant samples, protein expression of PTEN and pAKT_308 were significantly higher than *PIK3CA* WT (Fig. 3.4A-B).

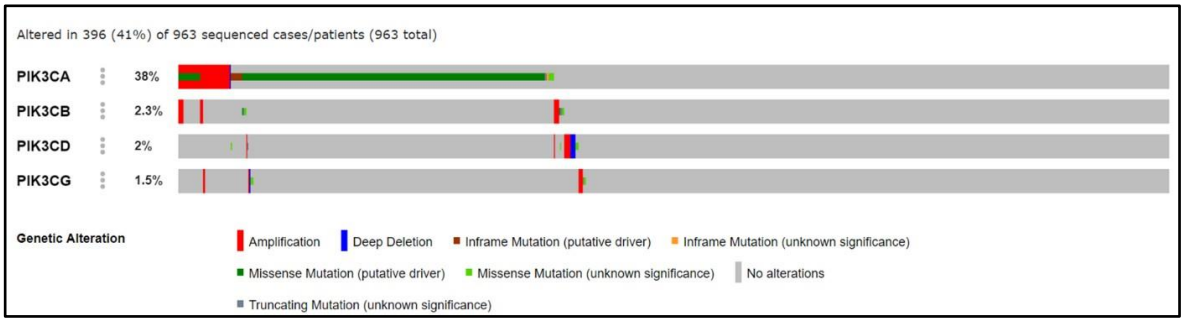

Figure 3.3 Mutation frequency of different PI3K isoforms in breast invasive carcinoma samples (TCGA, Provisional) from cBioPortal.

Highest genetic alteration was observed in *PIK3CA* (38%) which then followed by *PIK3CB* (2.3%), *PIK3CD* (2%) and *PIK3CG* (1.5%).

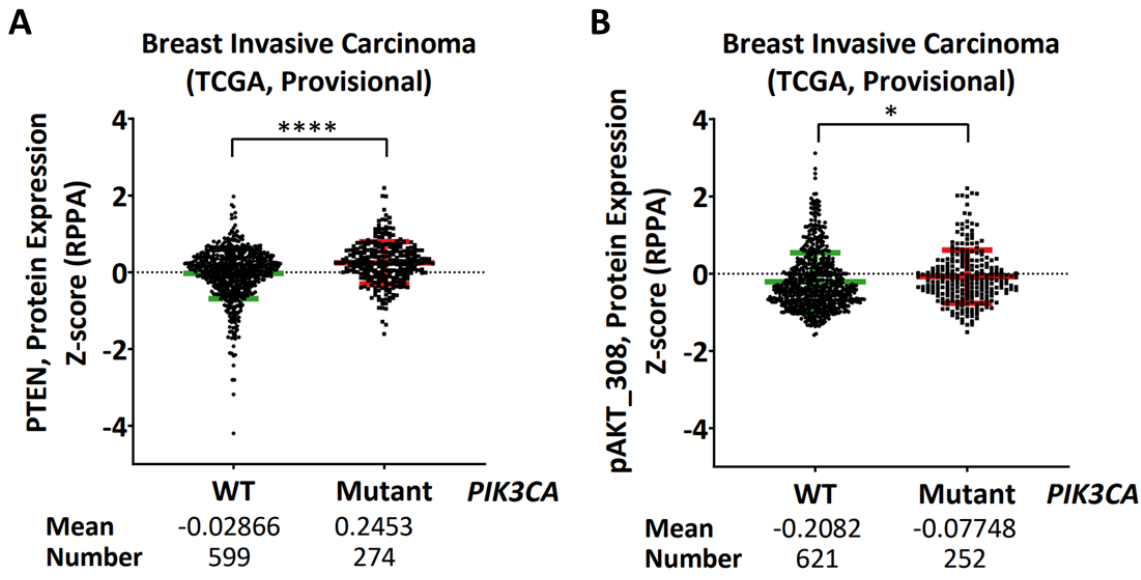

Figure 3.4 PTEN and pAKT_308, protein expression levels in *PIK3CA* WT and mutant breast invasive carcinoma samples (TCGA, Provisional) from cBioPortal.

PTEN, protein expression Z-score (RPPA) (**A**) and pAKT_308, protein expression Z-score (RPPA) (**B**) in *PIK3CA* WT and mutant samples. Data are mean ± standard deviation (SD). Unpaired *t-test* was performed for statistical analysis. **P* ≤ 0.05. *****P* ≤ 0.0001.

As our findings showed significant anti-correlation between PTEN, protein expression and pAKT_308, protein expression (Fig. 3.2A), the correlation of pAKT_308, protein expression and PTEN, protein expression was analysed in both *PIK3CA* WT and *PIK3CA* mutant samples. Significant anti-correlation between PTEN, protein expression and pAKT_308, protein expression was observed both in *PIK3CA* WT samples (Fig. 3.5A; r = -0.24; P = <0.0001) and *PIK3CA* mutant samples (Fig. 3.5B; r = -0.18; P = 0.0029). Additionally, lesser significance of the negative correlation between PTEN, protein expression and pAKT_308, protein expression was observed in *PIK3CA* mutant samples (Fig. 3.5B) compared to *PIK3CA* WT samples (Fig. 3.5A). This result might suggest that PTEN might slightly lost the defence to inhibit AKT activity in PI3KCA mutant samples compared to PI3KCA WT samples.

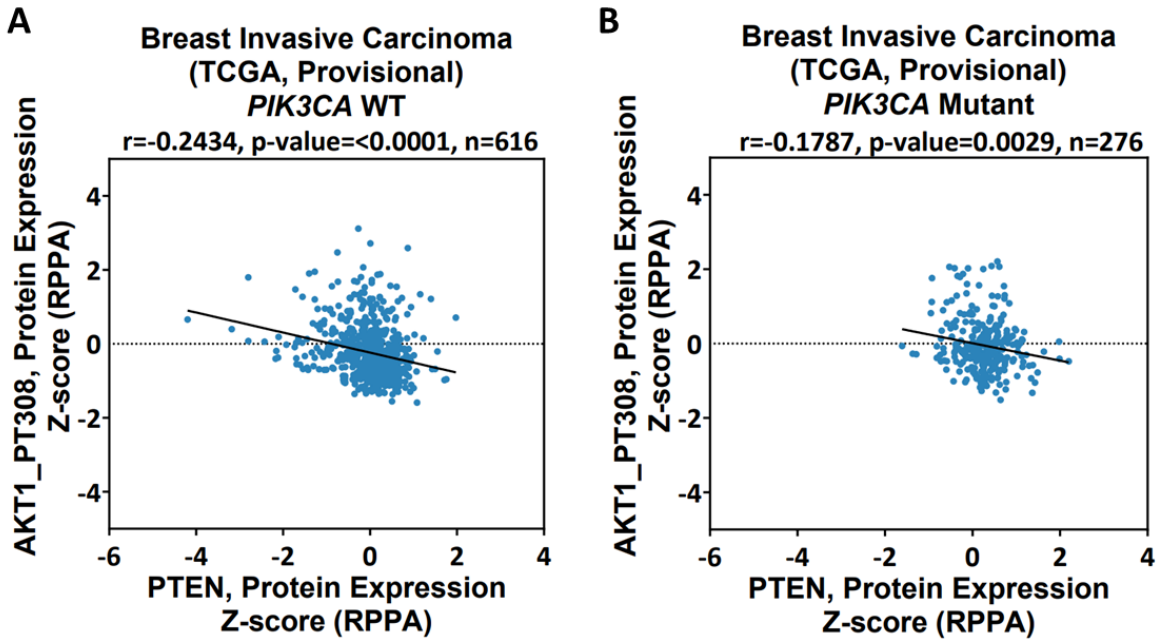

Figure 3.5 Correlation between PTEN, protein expression and pAKT_308, protein expression in *PIK3CA* WT and *PIK3CA* mutant breast invasive carcinoma samples (TCGA, Provisional) from cBioPortal.

A) The scatter plot shows the correlation between PTEN, protein expression Z-score (RPPA) and pAKT_308, protein expression Z-score (RPPA) in *PIK3CA* WT breast invasive carcinoma samples (TCGA, Provisional) (Pearson's correlation r = -0.2434; P <0.0001; n = 616). **B)** The scatter plot shows the correlation between PTEN, protein expression Z-score (RPPA) and pAKT_308, protein expression Z-score (RPPA) in *PIK3CA* mutant breast invasive carcinoma samples (TCGA, Provisional) (Pearson's correlation r = -0.1787; P = 0.0029; n = 276).

3.2.3 TCGA analysis confirms PTEN expression is decreased in TNBC

It has been stated that PTEN inactivation occurs more frequently in TNBC than the other subtypes of breast cancer (Beg *et al.*, 2015; S. Li *et al.*, 2017). To confirm this finding, clinical data of breast invasive carcinoma (TCGA, PanCancer) was obtained from cBioportal (https://www.cbioportal.org/). Both PTEN, protein and mRNA expression levels were analysed in the normal breast samples and each molecular subtype of breast cancer. *PTEN*, protein levels were significantly lower in TNBC compared to the luminal A, luminal B and HER2+ subtypes (Fig. 3.6A; $P < 0.05$; $P < 0.01$). Although PTEN, protein expression was lower in TNBC compared to the normal breast samples, no significant difference was observed (Fig. 3.6A). *PTEN*, mRNA levels were significantly lower in TNBC compared to the normal breast, luminal A, luminal B and HER2+ subtypes, although *PTEN* mutation frequency was similar (~6%) across all subtypes of breast cancer (Fig. 3.6B; $P < 0.0001$).

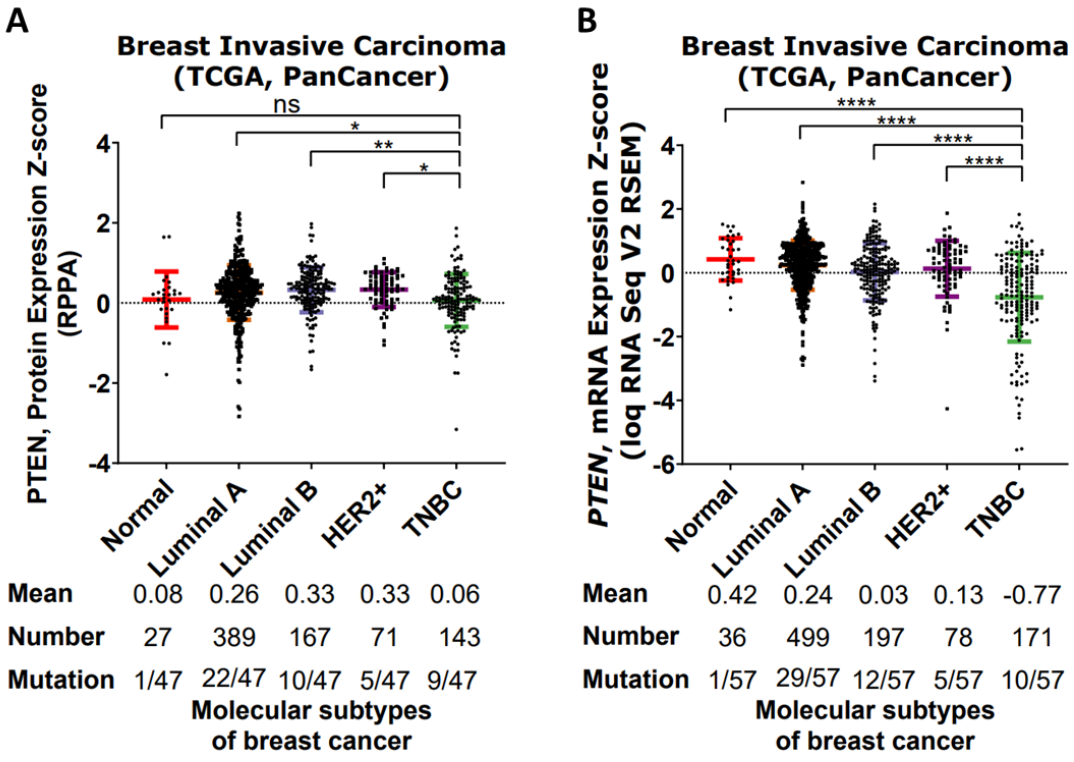

Figure 3.6 PTEN expression levels in different molecular subtypes of breast invasive carcinoma samples (TCGA, PanCancer) from cBioPortal.

A) Protein levels Z-score (RPPA) of PTEN in the TCGA samples from normal breast (n = 27), luminal A (n = 389), luminal B (n = 167), HER2+ (n = 71) and TNBC (n = 143). The total number of PTEN mutation in protein levels (RPPA) data was 47. **B)** mRNA levels Z-score (log RNA Seq V2 RSEM) of *PTEN* in the TCGA samples from normal breast (n = 36), luminal A (n = 499), luminal B (n = 197), HER2+ (n = 78) and TNBC (n = 171). The total number of PTEN mutation in mRNA levels (log RNA Seq V2 RSEM) data was 57. Data are mean ± standard deviation (SD). Ordinary one-way ANOVA was performed for statistical analysis. *$P \leq 0.05$. **$P \leq 0.01$. ****$P < 0.0001$. n.s. not significant.

3.2.4 TCGA analysis confirms the correlation between the loss of PTEN expression and clinical stages

Protein (RPPA) TCGA breast invasive carcinoma data from the UCSC Cancer Genome Browser (https://genome-cancer.ucsc.edu/) was obtained. The categorised TNBC samples (TCGA, Provisional) from the cBioportal website (*n* = 92) (See Appendix Table B.1) was aligned with the breast cancer samples in protein (RPPA) data (*n* = 410) and 43 common samples between the two data sets were obtained (Fig. 3.7). The identified 43 TNBC samples were also common in the mRNA (IlluminaHiSeq) data, which contains 1,215 breast cancer samples (Fig. 3.7).

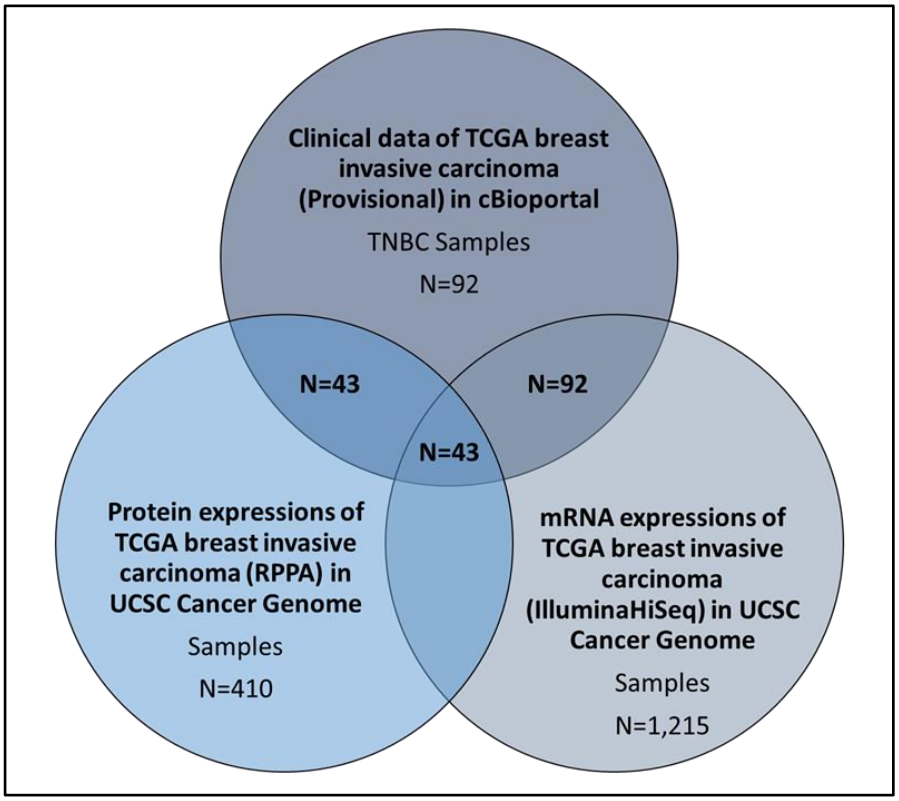

Figure 3.7 Venn chart for the combination of TCGA breast invasive carcinoma samples from different websites to identify common TNBC samples.

Codes are available in Appendix A.1.1.

In order to check the correlation between PTEN, protein and mRNA expression levels in TNBC samples, correlation analysis was performed. A significant correlation between mRNA and protein levels of PTEN was observed in TNBC samples (Fig. 3.8; $r = 0.55$; $P = 0.0001$), which suggested that PTEN inactivation in TNBC occurs at the transcriptional level.

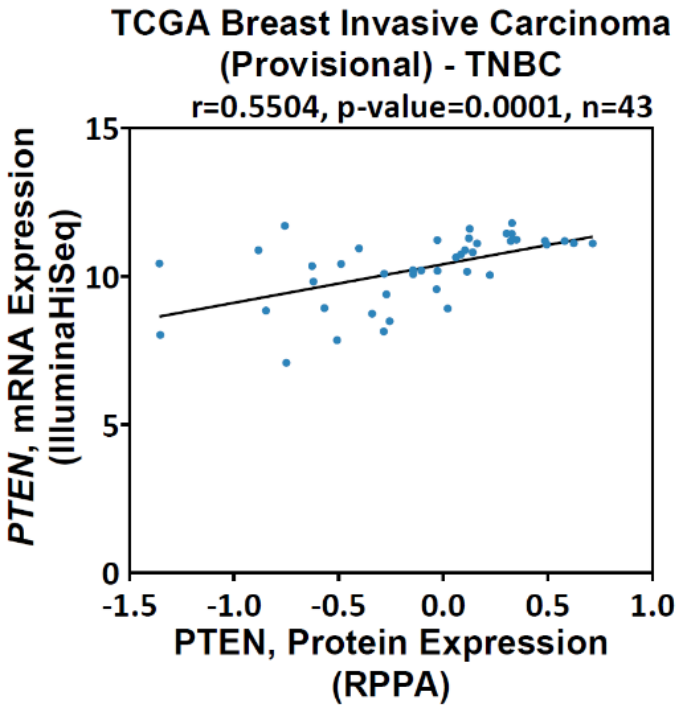

Figure 3.8 Correlation between PTEN, protein expression and *PTEN*, mRNA expression in TNBC samples (TCGA, Provisional) from cBioPortal.

The scatter plot for the correlation of TNBC samples between PTEN, protein expression (RPPA) and *PTEN,* mRNA expression (IlluminaHiSeq) in the TCGA breast invasive carcinoma (Pearson's correlation r = 0.5504; P = 0.0001; n = 43). Codes are available in Appendix A.1.1.

To evaluate the association between PTEN, protein level and clinicopathological features in TNBC patients, clinical data from the cBiportal website was extracted. PTEN, protein expression was narrowly distributed across all TNBC samples (See Appendix Fig. B.1); therefore, approximately the top 40% and bottom 40% samples were defined as high and low PTEN, respectively. As top 40% and bottom 40% samples were analysed, 16 samples were in the high PTEN, protein expression group and 16 samples were in the low PTEN, protein expression group (See Appendix Table B.2 and B.3). Table 3.1 shows the association between TNBC patients' clinicopathological features and PTEN, protein expression from TCGA data set. There was no significant association between PTEN, protein expression and the age, location, lymph node and metastatic characteristics of TNBC patients (Table 3.1). On the other hand, the number of patients with Stage II and above, or T2 and above, in PTEN high TNBC samples was significantly lower than the PTEN low group (Table 3.1; Fig. 3.9A-B; $P < 0.05$). These findings demonstrated that reduced PTEN levels correlate with advanced clinical stages.

Table 3.1 The relationship between TNBC patients' clinicopathological characteristics and PTEN, protein expression in TCGA data.

Characteristics	N	PTEN		*P* value
		Low expression	High expression	
Age	32			
≤ 50	15	6	9	
＞50	17	10	7	0.288
Location	32			
Left breast	18	9	9	
Right breast	14	7	7	>0.999
Stage	30			
Stage I	4	0	4	
≥Stage II	26	15	11	***0.032***
Size	32			
<T2	4	0	4	
≥T2	28	16	12	***0.033***
Positive LN	32			
<N2	27	13	14	
≥N2	5	3	2	0.626
Metastasis	32			
<M1	31	15	16	
≥M1	1	1	0	0.310

P values were calculated by χ2 test. Numbers in bold-italics mean *P* values less than 0.05 and are statistically significant. LN: lymph node.

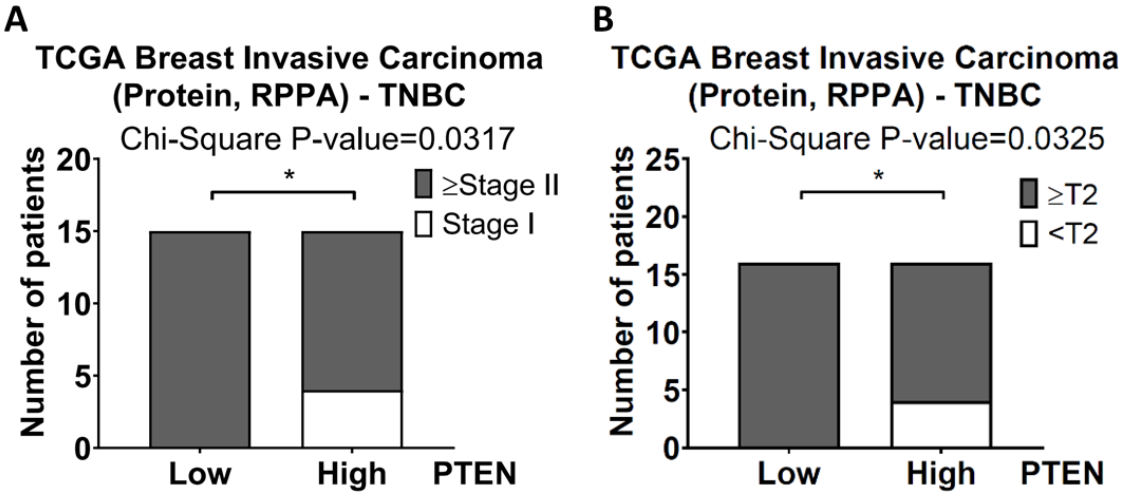

Figure 3.9 The association between PTEN, protein expression (RPPA) and clinicopathological features of TNBC samples in TCGA data from UCSC Cancer browser.

A) The graph shows the number of TNBC patients (TCGA) with Stage II and above or Stage I in the low or high PTEN group. **B)** The graph shows the number of TNBC patients (TCGA) with T2 and above or < T2 in the low or high PTEN group. Statistical significance was determined by χ2 analysis. **P* < 0.05. Codes are available in Appendix A.1.2.

3.2.5 Negative correlation between PTEN expression levels and AKT activity in TNBC

As pAKT_308 is the main downstream mediator of PTEN (Carnero, 2010), pAKT_308, protein expression levels were analysed in the normal breast samples and each molecular subtype of breast cancer. pAKT_308, protein levels were significantly higher in TNBC compared to the luminal A and luminal B subtypes (Fig. 3.10; $P < 0.05$; $P < 0.0001$). Although pAKT_308, protein levels were higher in TNBC compared to the HER2+ samples, no significant difference was observed (Fig. 3.10).

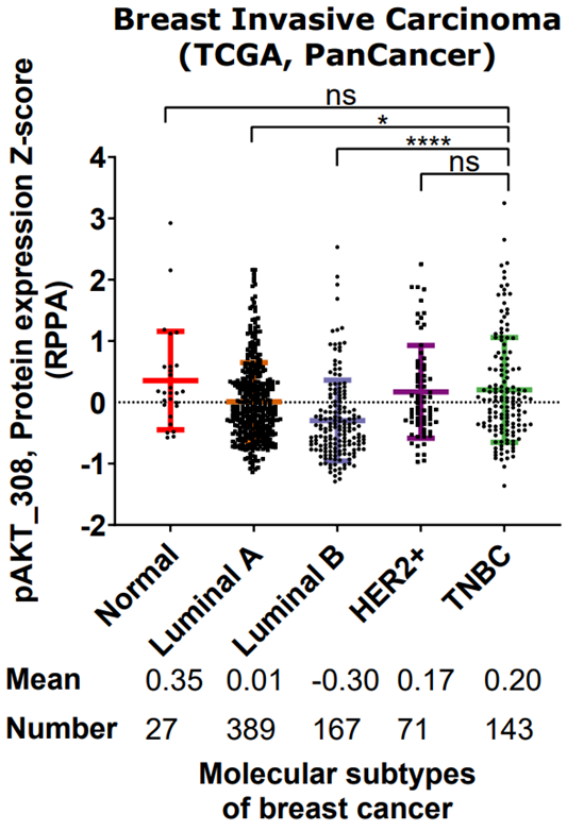

Figure 3.10 pAKT_308, protein levels in different molecular subtypes of breast invasive carcinoma samples (TCGA, PanCancer) from cBioPortal.

A) Protein levels Z-score (RPPA) of pAKT_308 in the TCGA samples from normal breast (n = 27), luminal A (n = 389), luminal B (n = 167), HER2+ (n = 71) and TNBC (n = 143). Data are mean ± standard deviation (SD). One-way ANOVA was performed for statistical analysis. *$P \leq 0.05$. ****$P < 0.0001$. n.s. not significant. Codes are available in Appendix A.1.1.

To determine the effect of PTEN on AKT activity in TNBC, correlation analysis was performed between PTEN and pAKT_308, protein expression levels. Functionally, decreased PTEN levels were responsible for the high AKT activity in TNBC, since there was a significant negative correlation between the levels of phosphorylated AKT (pAKT_308, a main downstream molecule of PTEN (Carnero, 2010)) and PTEN in TNBC (Fig. 3.11; $r = -0.55$; $P = 0.0001$).

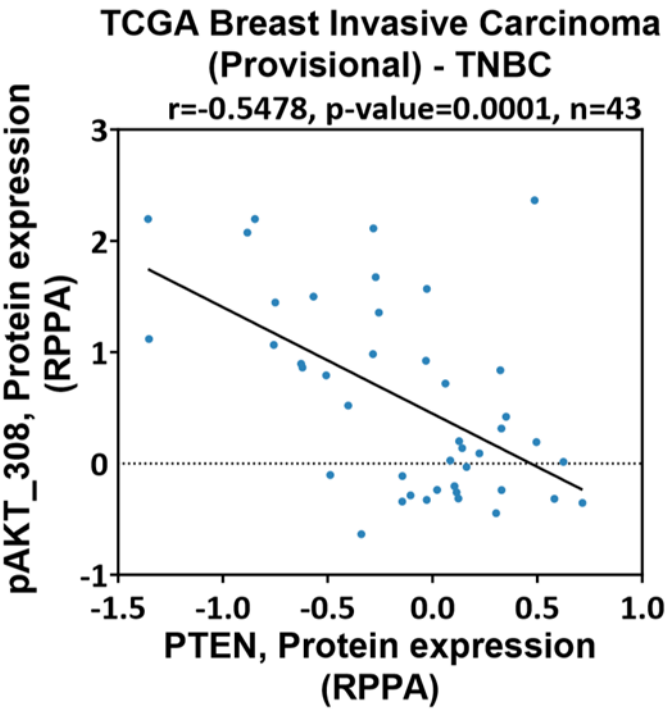

Figure 3.11 Correlation between PTEN, protein expression and pAKT_308, protein expression in TNBC samples (TCGA, Provisional) from cBioPortal.

The scatter plot for the correlation of TNBC samples between PTEN, protein expression Z-score (RPPA) and pAKT_308, protein expression Z-score (RPPA) in the TCGA breast invasive carcinoma data (Pearson's correlation r = -0.5478; P = 0.0001; n = 43). Codes are available in Appendix A.1.1.

3.2.6 Candidate gene(s) essential for the survival of PTEN-inactive TNBC cells are identified by the TCGA analysis and a whole-genome siRNA screen

mRNA expressions (IlluminaHiSeq) of TCGA breast invasive carcinoma data was obtained from Cancer Genome Browser that contained 1,215 samples and 20,530 genes. After the alignment of mRNA expressions (IlluminaHiSeq) data and TNBC samples from cBioPortal website, 92 TNBC samples were identified in both data sets (Fig. 3.7 and 3.12).

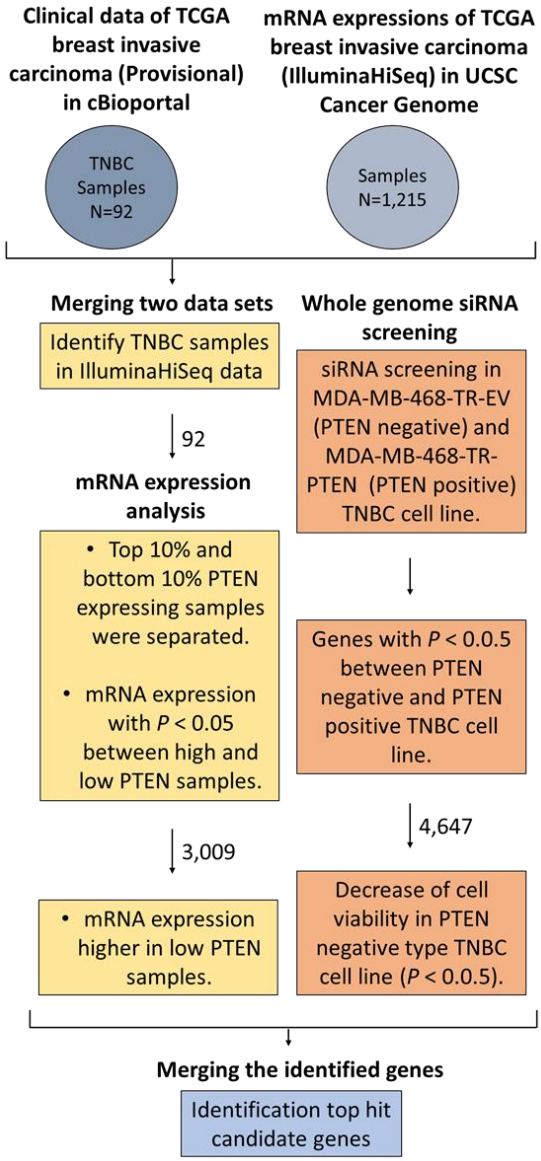

Figure 3.12 Workflow of TCGA and whole genome siRNA high-throughput screening analysis to identify candidate gene(s) essential for the survival of PTEN-inactive TNBC cells.

The analysis of TCGA and whole genome siRNA screening data sets was performed by **Ayse Ertay**. **(Whole genome siRNA screening data was generated by Dr. Yihua Wang)**. Codes are available in Appendix A.1.1-A.1.5.

PTEN, mRNA expression was widely distributed across all TNBC samples (Fig. 3.13A); therefore, approximately the top 10% and bottom 10% samples were defined as high and low *PTEN*, respectively. As top 10% and bottom 10% samples were analysed, 10 samples were in the high *PTEN*, mRNA expression group and 10 samples were in the low *PTEN*, mRNA expression group. In all, 3,009 mRNAs were identified as differentially expressed in the high *vs.* low *PTEN* groups (Fig. 3.13B; $P < 0.05$). The heat-map shows the hierarchical clustering of significantly different mRNAs between the high and low *PTEN* groups.

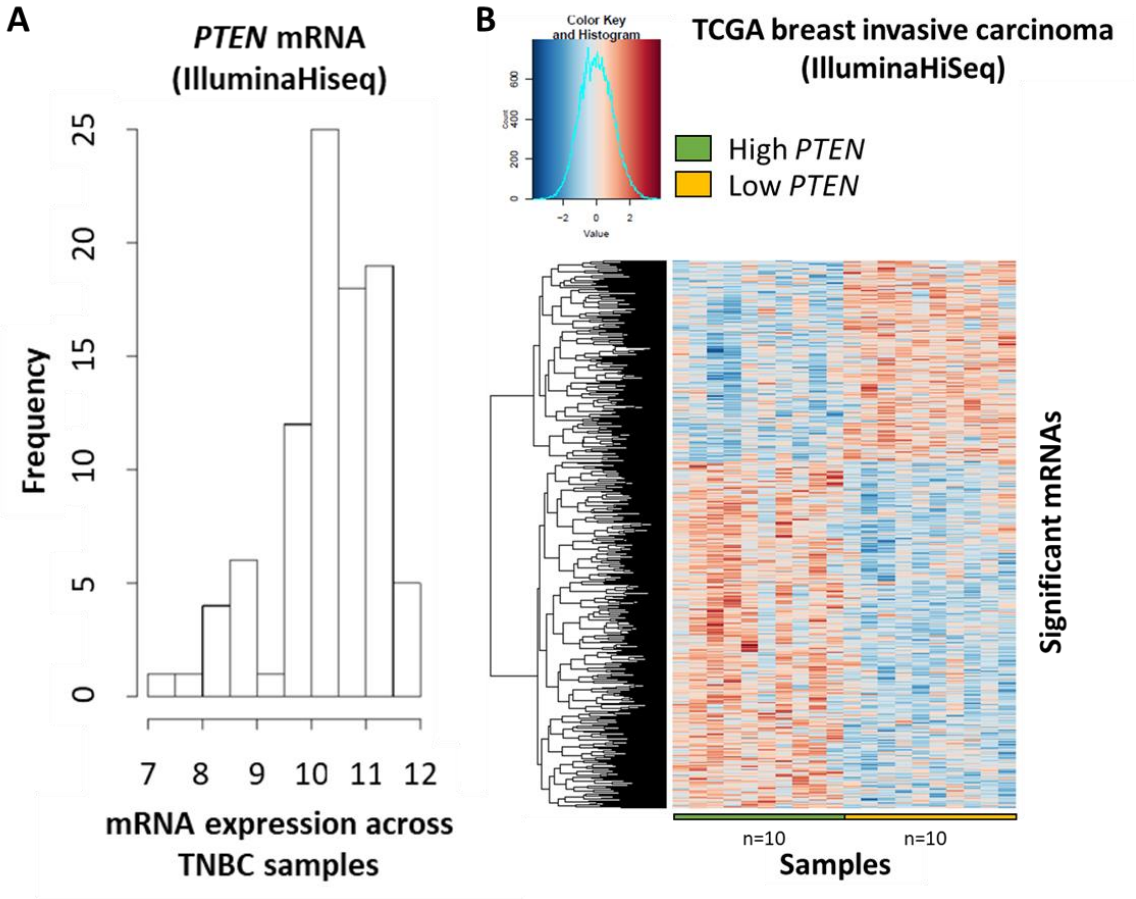

Figure 3.13 Identifying significantly different mRNAs between the high and low *PTEN* groups in TCGA (IlluminaHiSeq) TNBC samples.

A) Frequency distribution of *PTEN*, mRNA levels across TNBC samples in TCGA breast invasive carcinoma data (IlluminaHiSeq). Histograms of *PTEN* frequency expressed in all TNBC samples. X-axis shows *PTEN*, mRNA expression and y-axis shows the frequency of samples that have each expression level. **B)** The heat-map shows 3,009 significantly different mRNAs between the high and low *PTEN* expressing TNBC samples obtained from the TCGA analysis. Rows show the individual mRNAs and columns show the individual TNBC samples in the high and low *PTEN* groups across each gene. Red indicates up-regulation and blue indicates down-regulation. Un-paired *t-test* was performed to find the significantly different mRNAs. *P*-value < 0.05. *n* = 10 per group. Codes are available in Appendix A.1.3.

Previously generated whole genome siRNA screening data, by Dr. Yihua Wang, contained 21,121 genes and two main groups; isogenic GFP-labelled (*PTEN*-) cells and CherryFP-labelled (*PTEN*+) cells.

For PTEN-inducible cells, MDA-MB-468 cell line was used as it is PTEN null type TNBC cell and does not express PTEN expression. MDA-MB-468 cells were also stably transfected with a Tet-inducible PTEN vector (MDA-MB-468-TR-PTEN) and Tet-inducible parent vector (MDA-MB-468-TR-EV). To fluorescently label MDA-MB-468-TR-PTEN and MDA-MB-468-TR-EV cells, pCherryFP-N1 and p-EGFP-N1 were stably transfected into them, respectively. Single clones were picked and sorted by FACS, and named as MDA-MB-468-TR-PTEN/CherryFP or MDA-MB-468-TR-EV/GFP (Fig. 3.14A).

To optimise the concentration of DOX, MDA-MB-468-TR-PTEN and MDA-MB-468-TR-EV cell lines were treated with different concentrations of DOX to induce PTEN expression. MCF10A is a non-tumorigenic triple negative breast cell line. PTEN expression was induced with the treatment of DOX in MDA-MB-468-TR-PTEN cell line compared to the DOX untreated cell line (control). No PTEN induction was observed with the treatment of DOX in MDA-MB-468-TR-EV cell line. Endogenous PTEN expression was observed in MCF10A cells (Fig. 3.14B). Similar levels of PTEN induction were observed in different DOX concentration treatments with MCF10A cells (Fig. 3.14B). As expected, PTEN induction led to reduced levels of phospho-AKT (p-AKT), but not phospho-ERK (p-ERK) (Fig. 3.14B). For the following studies, we used 100 ng/ml DOX to induce PTEN in MDA-MB-468-TR-PTEN cells.

DOX-treated MDA-MB-468-TR-PTEN/CherryFP (*PTEN*+) or MDA-MB-468-TR-EV/GFP (*PTEN*-) cells were mixed and transfected at a 1:1 ratio in 96-well plates. To evaluate the cell numbers in *PTEN*+ or *PTEN*- cells, cells were fixed and cherryFP or GFP fluorescence was read, respectively, as mentioned in section 2.3. Overall, four patterns were observed, including “No effects”, “Non-selective cytotoxic”, “Cytotoxic hits for *PTEN*+” and “Cytotoxic hits for *PTEN*-” (Fig. 3.14C).

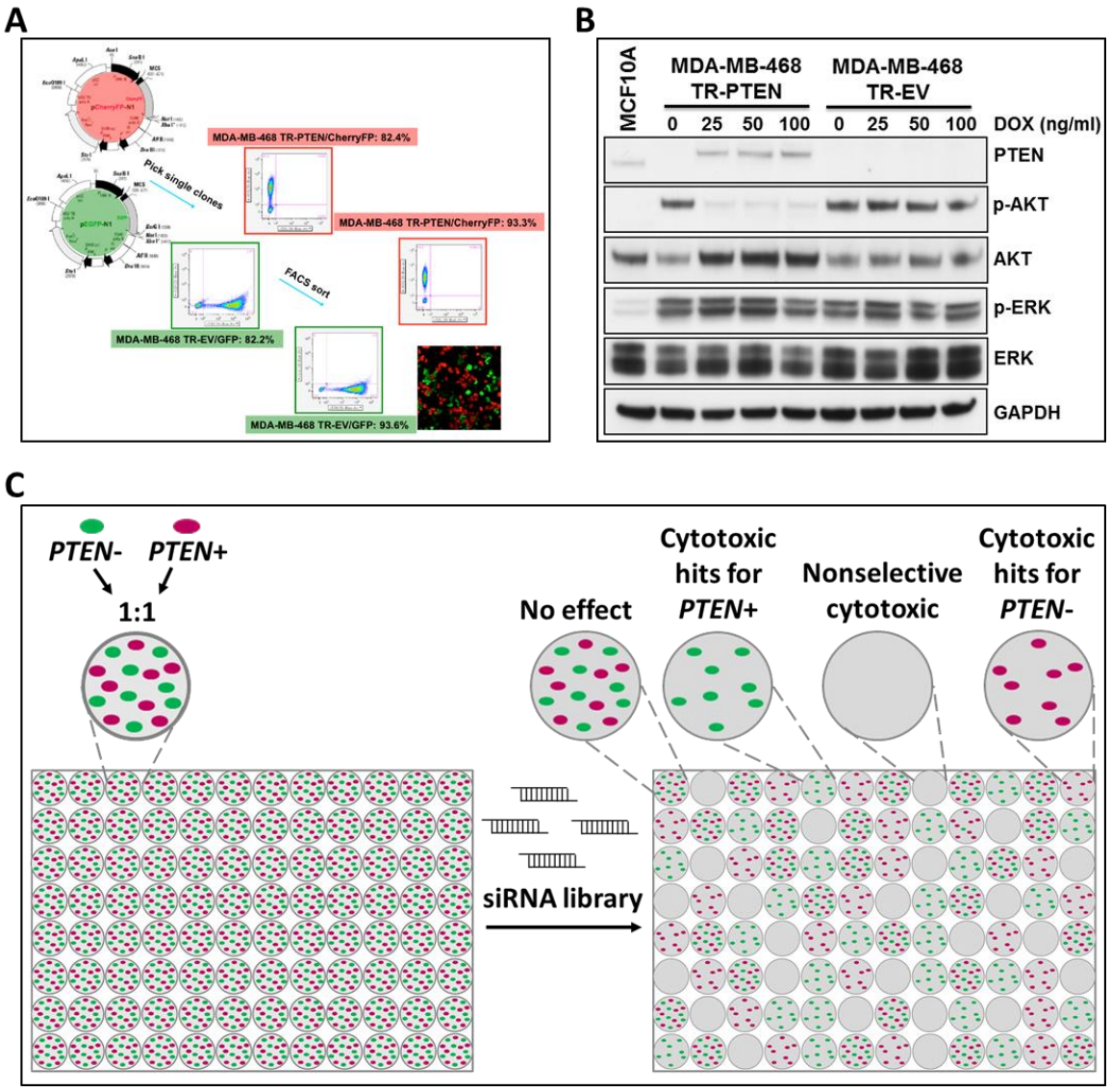

Figure 3.14 Workflow showing the whole genome siRNA screen in isogenic *PTEN*-positive or -negative TNBC cells.

A) The schematic diagram shows fluorescent labelling of MDA-MB-468-TR-PTEN and MDA-MB-468-TR-EV cells. Plasmids pCherryFP-N1 or p-EGFP-N1 were stably transfected into these two cell lines, respectively. Single clones were picked and sorted by FACS, and named as MDA-MB-468-TR-PTEN/CherryFP or MDA-MB-468-TR-EV/GFP. **(Generated by Dr. Yihua WANG)**. **B)** Protein expressions of PTEN, phospho-AKT (p-AKT), AKT, phospho-ERK (p-ERK) and ERK expression in MCF10A, MDA-MB-468-TR-PTEN and MDA-MB-468-TR-EV with indicated treatments. GAPDH was used as a loading control. **(Generated by Dr. Yihua WANG)**. **C)** The schematic diagram shows the whole genome siRNA screen in *PTEN*+ and *PTEN*- cell lines. DOX-treated MDA-MB-468-TR-PTEN/CherryFP (*PTEN*+) or MDA-MB-468-TR-EV/GFP (*PTEN*-) cells were mixed and transfected at a 1:1 ratio in 96-well plates. Cells were fixed with 4% PFA at 96 h post transfection. Fluorescence was read on an EnVision 2102 Plate-reader. [Information collected from (Prendergast, 2001)].

Each cell line group in whole genome siRNA screening contained three biological repeats. The correlation analysis between each replicate in each cell line group showed reproducible results (Fig. 3.15A; $r = 0.8$; $P < 0.001$), which means each replicate was positively correlated with each other. In all, 4,647 genes were identified as showing differential effects on cell viability in *PTEN*- *vs. PTEN*+ cells (Fig.15B). The heat-map shows the hierarchical clustering of the significantly different genes that have killing effect between *PTEN*- and *PTEN*+ cell lines.

By cross-referencing TCGA analysis (significantly high expression of mRNA in the low *PTEN* group) with the whole-genome siRNA screen (genes that showed significant decrease of cell viability in *PTEN*- cells), 47 candidate genes essential for the survival of *PTEN*-inactive TNBC cells were identified (Fig. 3.16A-B; Tables 3.2 and 3.3.). Among them, *WD repeat and high mobility group [HMG]-box DNA binding protein 1* (*WDHD1*) expression was increased in the low *vs.* high *PTEN* TNBC samples (Table 3.2; $P = 0.04$). It was also the top candidate gene whose knockdown significantly inhibited cell viability in *PTEN*- cells (Z-score = −1.26) with mild effects on *PTEN*+ cells (Table 3.3; Z-score = −0.32; $P = 0.009$).

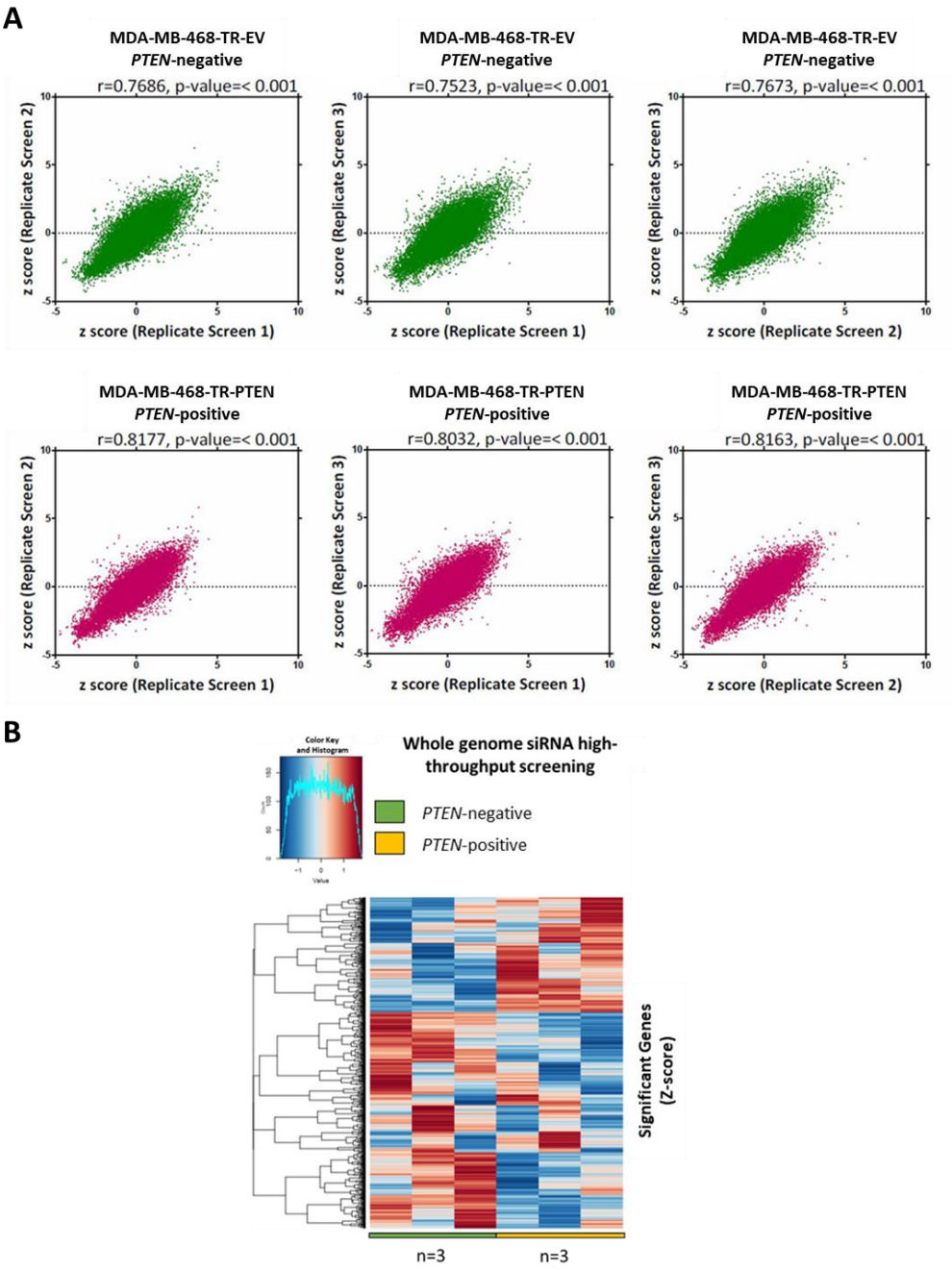

Figure 3.15 Candidate genes essential for the survival of PTEN-inactive TNBC cells are identified by a whole genome siRNA screen.

A) The response of cell lines to 21,121 siRNA pools in 3 replicate screens based on Z-score was analysed by Pearson's correlation. Individual dot indicates the pool of siRNA. Top and bottom panels show reproducibility analysis between the replicates in *PTEN*- cells and *PTEN*+ cells, respectively. **B)** The heat-map shows 4,647 genes that have significant decrease in cell viability between *PTEN*+ and *PTEN*- TNBC cells obtained from the whole genome siRNA screen. Rows indicate the Z-score value of the normalised intensity of signal in each well, which represents cell number for each gene in whole genome siRNA screening. Columns indicate the individual paired replicate in GFP labelled *PTEN*- MDA-MB-468 cell lines and red-cherry fluorescence labelled *PTEN*+ MDA-MB-468 cell lines. Red indicates the high Z-score and blue indicates low Z-score. Paired *t-test* was performed to identify the statistically different genes in whole genome siRNA screening. *P*-value < 0.05. *n* = 3 per group. Codes are available in Appendix A.1.4.

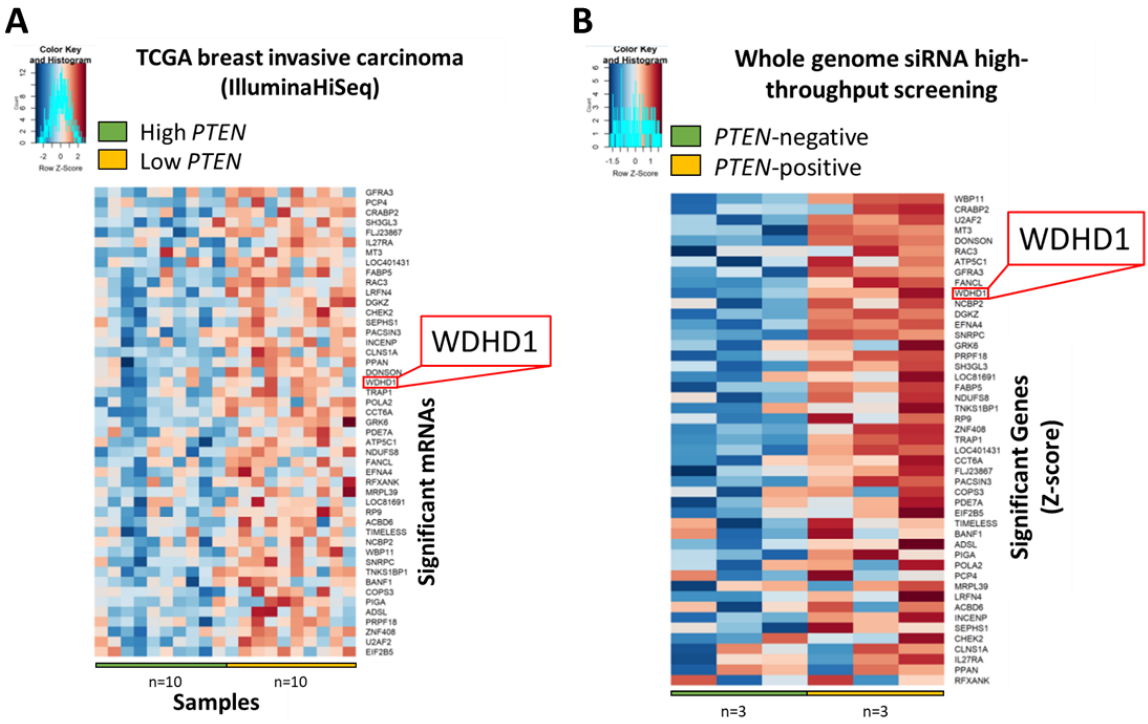

Figure 3.16 Candidate genes essential for the survival of PTEN-inactive TNBC cells are identified by the TCGA analysis and a whole-genome siRNA screen.

A) The heatmap shows 47 candidate mRNAs that are over-expressed in TNBC samples with the low *PTEN* compared to those with the high *PTEN* from TCGA analysis. Red indicates up-regulation and blue indicates down-regulation. *n* = 10 per group. **B)** The heatmap shows 47 candidate genes that are required for the survival of *PTEN*- TNBC cells from a whole-genome siRNA screen. Red indicates high Z-score and blue for low Z-score. *n* = 3 per group. Codes are available in Appendix A.1.5.

Table 3.2 Expressions of 47 candidate mRNAs essential for the survival of PTEN-inactive TNBC cells in the TCGA samples with the high *vs.* low *PTEN* expression.

mRNAs	High *PTEN*	Low *PTEN*	*P*-value	Fold change, log2 (Low *PTEN* - High *PTEN*)
GFRA3	3.32229	6.5785	0.014064183	3.25621
PCP4	1.36775	3.78875	0.00466737	2.421
CRABP2	10.68019	13.03127	0.007714491	2.35108
SH3GL3	2.4853	4.24452	0.026716662	1.75922
FLJ23867	9.4979	11.17481	0.005161797	1.67691
IL27RA	8.76325	10.19964	0.032904368	1.43639
MT3	1.13247	2.53807	0.035024884	1.4056
LOC401431	4.47207	5.82061	0.04807528	1.34854
FABP5	6.85297	8.19205	0.009847354	1.33908
RAC3	7.44451	8.75014	0.0008484	1.30563
LRFN4	8.387	9.64319	0.003183923	1.25619
DGKZ	9.45414	10.50187	0.000461961	1.04773
CHEK2	7.99384	8.99476	0.004217383	1.00092
SEPHS1	10.51725	11.49549	0.003070291	0.97824
PACSIN3	9.49668	10.45725	0.029142294	0.96057
INCENP	8.89947	9.82412	0.008724304	0.92465
CLNS1A	10.57214	11.49	0.000467946	0.91786
PPAN	8.55198	9.45596	0.010342268	0.90398
DONSON	8.35511	9.25394	0.022255134	0.89883
WDHD1	8.18826	9.01551	0.036629183	0.82725
TRAP1	10.75074	11.55342	0.008508955	0.80268
POLA2	8.68987	9.49169	0.001641816	0.80182
CCT6A	12.23387	13.0295	0.000673169	0.79563
GRK6	9.54469	10.33608	0.004664026	0.79139
PDE7A	10.26377	11.03673	0.035189517	0.77296
ATP5C1	11.77915	12.54962	0.02654747	0.77047
NDUFS8	9.53725	10.29363	0.019548691	0.75638
FANCL	8.51811	9.27367	0.010129573	0.75556
EFNA4	8.77033	9.5131	0.048641277	0.74277
RFXANK	9.43467	10.13543	0.033319336	0.70076
MRPL39	8.65615	9.34307	0.045338789	0.68692
LOC81691	6.87459	7.50888	0.048787488	0.63429
RP9	7.38021	8.01249	0.003893487	0.63228
ACBD6	8.68409	9.31465	0.01936246	0.63056
TIMELESS	9.76789	10.36352	0.049713733	0.59563
NCBP2	10.99242	11.58552	0.040725009	0.5931
WBP11	11.14879	11.73598	0.002336989	0.58719
SNRPC	10.37165	10.9568	0.009112171	0.58515
TNKS1BP1	12.01617	12.58796	0.006976547	0.57179
BANF1	11.06916	11.63137	0.034312404	0.56221
COPS3	9.92573	10.43557	0.028305322	0.50984
PIGA	7.9605	8.45298	0.049582049	0.49248
ADSL	9.92541	10.39989	0.047262923	0.47448
PRPF18	8.92899	9.37873	0.038169988	0.44974
ZNF408	8.01857	8.42282	0.004283212	0.40425
U2AF2	11.43756	11.77608	0.042453125	0.33852
EIF2B5	10.27008	10.54917	0.049506103	0.27909

Table 3.3 Forty-seven candidate genes essential for the survival of PTEN-inactive TNBC cells are identified by a whole genome siRNA screen.

Genes	*PTEN-*	*PTEN+*	*P*-value	ΔZ Score (*PTEN+* - *PTEN* -)
WBP11	-0.416666667	1.514	0.003782644	1.930666667
CRABP2	-0.295333333	1.284333333	0.042450798	1.579666667
U2AF2	-0.375	1.105	0.017624149	1.48
MT3	-0.134	1.144333333	0.035554253	1.278333333
DONSON	-0.618333333	0.521333333	0.002206531	1.139666667
RAC3	0.546	1.680666667	0.044216827	1.134666667
ATP5C1	-0.069	1.061	0.044216827	1.13
GFRA3	0.143333333	1.242	0.042534134	1.098666667
FANCL	0.013333333	1.018	0.037311343	1.004666667
WDHD1	-1.258333333	-0.316666667	0.00910254	0.941666667
NCBP2	-0.447333333	0.456	0.025800729	0.903333333
DGKZ	-0.747333333	0.152333333	0.005879834	0.899666667
EFNA4	-0.219666667	0.576666667	0.010309804	0.796333333
SNRPC	-0.074	0.693	1.42E-05	0.767
GRK6	-0.061333333	0.684333333	0.016073649	0.745666667
PRPF18	-0.851333333	-0.17	0.020964327	0.681333333
SH3GL3	0.194333333	0.861333333	0.025292942	0.667
LOC81691	-0.211666667	0.443333333	0.002605788	0.655
FABP5	1.265666667	1.915666667	0.041573112	0.65
NDUFS8	-0.326666667	0.31	0.043265062	0.636666667
TNKS1BP1	0.331333333	0.967666667	0.002651125	0.636333333
RP9	1.792666667	2.425333333	0.025308458	0.632666667
ZNF408	-0.131333333	0.493333333	0.030292668	0.624666667
TRAP1	-0.475	0.119	0.012566733	0.594
LOC401431	-0.062333333	0.528666667	0.01272895	0.591
CCT6A	-1.743333333	-1.225333333	0.007401735	0.518
FLJ23867	-0.768666667	-0.281	0.039704313	0.487666667
PACSIN3	1.061666667	1.543666667	0.006248231	0.482
COPS3	0.893666667	1.333333333	0.000957949	0.439666667
PDE7A	-0.724666667	-0.285333333	0.015073112	0.439333333
EIF2B5	0.168666667	0.591333333	0.014744277	0.422666667
TIMELESS	-0.907333333	-0.487333333	0.045342768	0.42
BANF1	0.068	0.479333333	0.005922966	0.411333333
ADSL	-0.326	0.083333333	0.039375916	0.409333333
PIGA	-0.920333333	-0.516333333	0.047175111	0.404
POLA2	-0.175	0.221	0.016811612	0.396
PCP4	-0.638	-0.247	0.002751103	0.391
MRPL39	-0.309333333	0.077333333	0.043702746	0.386666667
LRFN4	-0.872	-0.498333333	0.046242021	0.373666667
ACBD6	0.242666667	0.612333333	0.000295832	0.369666667
INCENP	-2.337333333	-2.023	0.049530855	0.314333333
SEPHS1	-1.733333333	-1.450666667	0.019625008	0.282666667
CHEK2	0.488666667	0.766333333	0.03952613	0.277666667
CLNS1A	-0.431666667	-0.171666667	0.043820346	0.26
IL27RA	0.454	0.651666667	0.029789901	0.197666667
PPAN	0.087	0.261666667	0.021409989	0.174666667
RFXANK	0.103333333	0.257333333	0.048160881	0.154

3.3 Discussion

Data presented in this chapter validated that PI3K/AKT is the downstream of PTEN. TCGA data analysis illustrated that *PTEN*, mRNA expression is decreased in TNBC compared to the normal breast and other subtypes of breast cancer samples. Additionally, the number of patients with higher tumour stage and larger tumour size, in PTEN low TNBC samples was significantly higher than the PTEN high group and also low PTEN, protein expression level increased the activity of AKT. Cross-referencing the analysis between the TCGA and whole genome siRNA screening, *WDHD1* was one of the identified candidate synthetic essential genes in PTEN-inactive TNBC cells (Fig. 3.17).

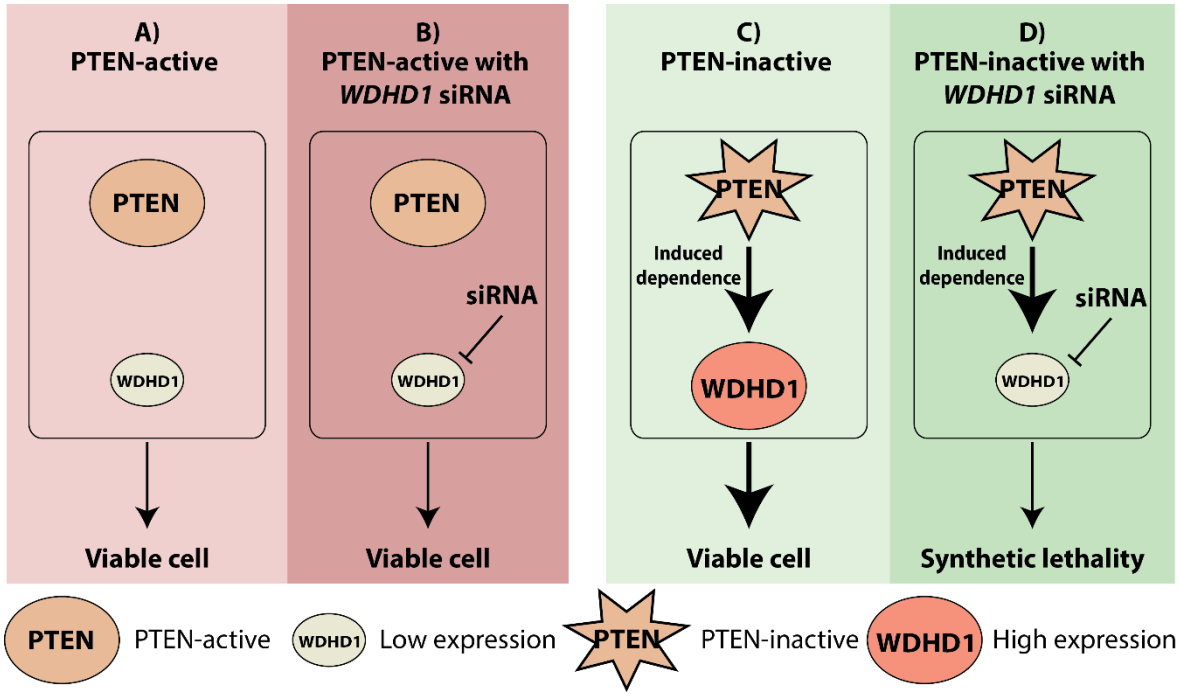

Figure 3.17 *WDHD1* as a synthetic essential gene in PTEN-inactive TNBC cells.
A) *WDHD1* expression is low in PTEN-active TNBC. **B)** Knockdown of *WDHD1* with siRNA does not decrease the cell survival in PTEN-active TNBC cells. **C)** PTEN-inactive TNBC cells increase *WDHD1* expression and the survival of cells. **D)** Inhibition of *WDHD1* with siRNA in PTEN-inactive TNBC leads to synthetic lethality (cell death). The star represents the inactive PTEN. Arrows indicate induction. Bold arrows indicate higher induction. PTEN: phosphatase and tensin homolog; WDHD1: WD repeat and high mobility group [HMG]-box DNA binding protein 1.

The PTEN, protein and mRNA expression levels were significantly lower in *PTEN* mutant samples compared to the *PTEN* WT breast invasive carcinoma samples (Fig. 3.1A-B). It was previously shown that *PTEN* mutation is rare in breast cancer (<5%) (Hollander, Blumenthal and Dennis, 2011). This was also confirmed with the TCGA analysis in this chapter, which showed that *PTEN* mutation is around 5% in all breast cancer samples in this patient cohort (TCGA, Provisional). However, the

number of patients in *PTEN* mutant and *PTEN* WT groups could be the limitation of this cohort as the number of *PTEN* mutant samples were 15-20 times less than the *PTEN* WT samples (Fig. 3.1A-B). Different number of patients in each group could lead to bias observed result due to the grouping effect of the samples. Therefore, different publicly available data set such as METABRIC could also be used to check the similar result can be obtained in a different data.

The correlation analysis between PTEN, protein expression and pAKT_308, protein expression showed significant anti-correlation (Fig. 3.2A) but no significant anti-correlation was observed with pAKT_473, protein expression (Fig. 3.2B). It was discovered that PDK1 (Sarbassov *et al.*, 2005; Carnero, 2010) that is found in the PTEN/AKT axis (Fig 1.4), can phosphorylate Thr308 to activate AKT activity but Ser473 is phosphorylated by mTORC2 (Sarbassov *et al.*, 2005), which is not in the same axis with PTEN (Fig 1.4).

Protein expression levels of PTEN and pAKT_308 were significantly higher in *PIK3CA* mutant breast invasive carcinoma samples than WT samples (Fig 3.4). The significant higher expression of PTEN in *PIK3CA* mutant breast cancer samples might indicate that the activity of PTEN is not affected by *PIK3CA* mutation as PTEN can be regulated by different mechanisms (Fig. 1.5) (Salmena, Carracedo and Pandolfi, 2008; Song, Salmena and Pandolfi, 2012). Additionally, significant negative correlation was observed between pAKT_308 and PTEN, protein expression levels in both *PIK3CA* WT and *PIK3CA* mutant samples. These findings suggest that PTEN can function to regulate AKT activity regardless of presence or absence of *PI3KCA* mutation.

The TCGA data analysis validated that PTEN expression is lower in TNBC compared to the other subtypes of breast cancer (Fig. 3.6), which was also shown by previous studies (López-Knowles *et al.*, 2010; Beg *et al.*, 2015; S. Li *et al.*, 2017). Moreover, significant positive correlation between PTEN, protein expression and *PTEN*, mRNA expression in TNBC samples (Fig. 3.8) suggested that PTEN inactivation in TNBC occurs at the transcriptional level. Li *et al.,* 2017 demonstrated that loss of PTEN expression in TNBC is associated with poor prognosis, larger tumour size, high tumour grade, lymph node metastasis and tumour recurrence (S. Li *et al.*, 2017). We also partially validated these findings by showing significantly higher number of patients with T2 and above, or Stage II and above, in the PTEN low TNBC samples compared to the PTEN high group (Fig. 3.9). In addition to the negative correlation between pAKT_308 level and PTEN level in all breast cancer samples (Fig. 3.2A), similar correlation was also observed in TNBC samples (Fig. 3.11) as pAKT_308 is the main downstream mediator of PTEN (Carnero, 2010). Thus, the association between PTEN and AKT activity is also observed in TNBC. These findings confirm that reduced PTEN levels correlate with advanced clinical stages and a high AKT activity in TNBC.

Molecular biomarkers that are identified by clinicopathological features such as TNM staging, can predict the cancer progression and treatment response but do not represent the complex mechanisms of cancer (Sheng *et al.*, 2020). Therefore, identifying inaccurate biomarkers or targeted therapies in cancer show the heterogeneity in cancer subtypes (Lawrence *et al.*, 2014). High-throughput techniques such as RNA-Seq have been developed to identify the gene expression signatures associated with cancer progression. RNA-seq technique can show poor reproducible signatures due to the variability between different cohorts (Sheng *et al.*, 2020). Loss-of-function screen using RNAi screening is high-throughput tool to identify gene functions and their effect on the cell viability in cancer (Mohr, Bakal and Perrimon, 2013). However, RNAi screening can also have limitations such as isogenic cell lines have artificially created genetic background that might not reflect the same cellular state of "normal" cancer cell (Nijman, 2011) and also off-target effects that might contribute to false-positive results (Mohr, Bakal and Perrimon, 2013). As TNBC is heterogeneous, cross-referencing two different data sets (RNA-Seq and RNAi screening) can overcome these limitations to identify novel biomarkers or therapeutic targets by understanding the molecular heterogeneity of cancer (Mohr, Bakal and Perrimon, 2013; Sheng *et al.*, 2020). Discovering PTEN synthetic lethal interactions in TNBC may provide potential biomarkers or targeted therapies for this breast cancer type that does not have successful treatment options. Thus, RNA-Seq from TCGA and whole genome siRNA screening analyses were cross-referenced to identify the candidate genes that are required for the survival of PTEN-inactive TNBC. The total of 47 top hit candidate genes were identified which were highly expressed in PTEN-inactive TNBC cells and these genes could be a potential targeted therapy for PTEN-inactive TNBC. Among the identified candidate genes, *WDHD1* expression was increased in the low *vs.* high PTEN TNBC samples (Fig. 3.16A; Table 3.2). It was also the top candidate gene whose knockdown significantly inhibited cell viability in *PTEN*- cells (Fig. 3.16B; Table 3.3).

Overall, this chapter identified *WDHD1* as a candidate gene, which might play an important role for the survival of PTEN-inactive TNBC. To validate the obtained bioinformatic results from this chapter and functionally characterise *WDHD1*, functional assays were performed in Chapter 4 and Chapter 5, respectively.

Chapter 4 Validation of bioinformatic analysis findings with *in vitro* work and patients' samples in PTEN-inactive TNBC

4.1 Introduction

4.1.1 *WD repeat and high mobility group [HMG]-box DNA binding protein 1* (*WDHD1*)

WDHD1 is the mammalian orthologue of budding yeast (*Saccharomyces cerevisiae*) chromosome transmission fidelity 4 (*ctf4)* (Kouprina *et al.*, 1992; Hanna *et al.*, 2001)*, Drosophilia ctf4* (Gosnell and Christensen, 2011) and fission yeast (*Schizosaccharomyces pombe*) mini-chromosome loss 1 (*Mcl1)* (Williams and Mcintosh, 2002). *WDHD1* is also known as acidic and nucleoplasmic DNA binding protein 1 (*AND-1*) in humans (Zhu *et al.*, 2007; Im *et al.*, 2009; Bermudez *et al.*, 2010; Kang *et al.*, 2013).

4.1.2 Structure of WDHD1

Ctf4, which was first discovered as chromosome transmission fidelity mutant in *Saccharomyces cerevisiae* (Kouprina *et al.*, 1992; Hanna *et al.*, 2001), is present in different eukaryotes as mentioned in section 4.1.1. WD40 repeats at the N-terminus and the central conserved domain (SepB) are present in all species (Gosnell and Christensen, 2011). However, high mobility group (HMG) box domain at the C-terminus is only present in vertebrates (Gosnell and Christensen, 2011). WD40 repeats has a role to facilitate protein-protein interactions (Stirnimann *et al.*, 2010) and HMG box domain has DNA binding activity (Köehler, Schmidt-Zachmann and Franke, 1997).

Guan *et al.,* 2017 reported the structure of a human orthologue of Ctf4, WDHD1, which is larger than other species with 1129 amino acids (Guan *et al.*, 2017). WDHD1 contains three functional domains; N-terminal WD40 domain, SepB domain and C-terminal HMG DNA binding domain, that are linked with two flexible loops (Fig. 4.1) (Guan *et al.*, 2017). WD40 domain has seven blades (blade i-vii) that form a ring-like β-propeller structure (Guan *et al.*, 2017). SepB domain includes β-propeller subdomain that contains six blades (blades I-VI) and a helical subdomain, which contains five helixes (α1-5). It was also identified that SepB domain mediates trimerisation of WDHD1 and

includes binding motifs (Guan *et al.*, 2017). HMG domain is involved in the role of chromatin assembly, transcription and replication (Köehler, Schmidt-Zachmann and Franke, 1997).

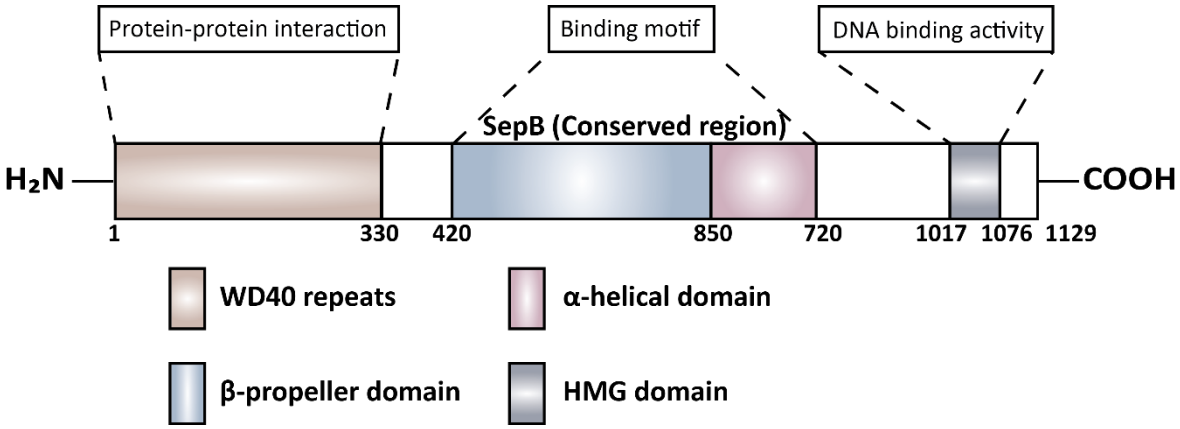

Figure 4.1 WDHD1 protein domain structure.
WDHD1 has three main domains: N-terminal WD40 domain (residues 1-330), SepB domain (residues 420-850) and C-terminal HMG-box region (residues 1017-1076). WD40 repeats facilitate protein-protein interaction, SepB domain has binding motif and HMG-box region has DNA binding activity. [Information collected from (Guan *et al.*, 2017)].

4.1.3 Function of WDHD1

WDHD1 is an adaptor molecule, which ensures the replisome complex integrity and the efficiency of DNA replication (Zhu *et al.*, 2007; Im *et al.*, 2009; Bermudez *et al.*, 2010; Kang *et al.*, 2013). In addition, WDHD1 controls cell cycle, DNA damage response and DNA repair (Yoshizawa-Sugata and Masai, 2009; Y. Li *et al.*, 2017). The roles of WDHD1 in cell cycle, DNA replication and DNA repair are mentioned in sections 4.1.3.2 and 4.1.3.3.

Previous studies also showed that WDHD1 can play a role in malignant oesophageal carcinogenesis, lung cancer (Sato *et al.*, 2010), cervical cancer (Zhou *et al.*, 2016) and cholangiocarcinoma (B. Liu *et al.*, 2019), which are mentioned in section 4.1.4 below.

4.1.3.1 Cell cycle

Cell cycle is a complex process that includes DNA replication, chromosome segregation and cell division. There are two main parts of cell cycle: interphase and mitotic phase (Barnum and O'Connell, 2014).

Interphase is divided into three parts; G_1 phase, S phase and G_2 phase in an order where the chromosomes are not detectable under light microscope. G_1 phase is known as the first gap phase where the cells are metabolically active and growing. In S phase, synthesis phase, DNA replication occurs. In G_2 phase, second gap phase, cells continue to grow and synthesis of proteins takes place so cells are prepared for division (Nurse, 2000). M phase, mitotic phase includes mitosis (nuclear division-karyokinesis) and cytokinesis (cell division). In M phase, cells stop growing and divide into two daughter cells. M phase is also divided into five phases: prophase, pro-metaphase, metaphase, anaphase and telophase. Each stage of mitosis is visible under the light microscope. In prophase, chromatin is condensed into chromosome and nucleolus disappears. In pro-metaphase, nuclear membrane breaks down, kinetochores form during the attachment of proteins to the centromeres and chromosomes start to move due to the attachment of microtubules to the kinetochores. In metaphase, chromosomes align to the centre of the nucleus (metaphase plate). In anaphase, sister chromatids (chromosome) move to the opposite poles. In telophase, nuclear membrane reforms around the group of chromosomes at each pole. Finally, cell divides into two daughter cells in the cytokinesis (Yanagida, 2014). Additionally, the cells, which stop dividing enter G_0 phase that is known as quiescence (Malumbres and Barbacid, 2002).

The cell cycle progression, transition from one to another phase of the cell cycle, is carried out by the protein complexes; cyclins (A, B, D, E) that bind to cyclin dependent protein kinases (CDKs) (Malumbres and Barbacid, 2009). CDK4 and CDK6 are activated by cyclin D and cells enter and progress in the G_1 phase (Malumbres and Barbacid, 2005). Then, cyclin E interacts with CDK2 for the progression of the G_1 to the S phase (Malumbres and Barbacid, 2002). Association between CDK2 and cyclin A leads to the S phase progression (Lowe *et al.*, 2002). In the G_2 phase, cyclin A-CDK1 association leads the entry of cells into the M phase (Malumbres and Barbacid, 2005). Finally, CDK1 is activated by cyclin B and helps the progression in the M phase (Lowe *et al.*, 2002).

Synthesis and degradation of cyclins regulate the cyclin-CDK complex formation and activity in cell cycle. This regulation occurs by the binding of the cell cycle inhibitory proteins (CDK inhibitors (CKI)) to the cyclin-CDK complexes or by the phosphorylation status of CDK (Malumbres and Barbacid, 2009).

Additionally, checkpoints in cell cycle play an important role for the accurate cell cycle progression during DNA synthesis and chromosome segregation. When there is DNA damage, checkpoints in cell cycle can be activated at G_1/S transition, intra-S phase or G_2/M boundary (Bartek, Lukas and Lukas, 2004).

4.1.3.2 DNA replication

DNA replication is the biological process that two identical DNA replicas form from the original DNA molecule in normal dividing cells to maintain genomic integrity in each cell cycle. Therefore, it is crucial to have faithful DNA replication to prevent genomic alterations: genomic rearrangements and accumulation of mutations, which can lead to genomic instability (Abe *et al.*, 2018).

Eukaryotic DNA replication, a stepwise manner process, requires protein complexes that are assembled on chromatin (Kang *et al.*, 2013). DNA replication initiation requires the pre-replicative complex (pre-RC) assembly, pre-RC activation and replisome formation (Takeda and Dutta, 2005; Sclafani and Holzen, 2007).

Pre-RC starts with binding of origin recognition complex (ORC) to replication origins and recruits cell division cycle 6 (Cdc6) and cdc10-dependent transcript 1 (Cdt1). Then, Cdc6 and Cdt1 recruit mini chromosome maintenance 2-7 (Mcm2-7) complex and multiple Mcm2-7 complexes are loaded as a head-to-head dimer along the chromatin (Fig. 4.2). Pre-RC assembly occurs during late M and early G_1 phases of the cell cycle to prepare the DNA for replication during S phase (Bell and Dutta, 2002).

During G_1/S phase transition, Pre-RC is activated with the assembly of new replication initiation factors whose actions are facilitated by CDKs and dumbbell former 4 (Dbf4)-dependent cell division cycle 7 (Cdc7) kinases (Cdc7-Dbf4 (DDKs)) (Fig. 4.2) (Diffley, 2004; Kang *et al.*, 2013). The new replication initiation factors facilitate the interaction between cell division cycle protein 45 (Cdc45) and go ichi ni san complex (GINS) with Mcm2-7 complex, which then activates Mcm2-7 (Fig. 4.2) (Moyer, Lewis and Botchan, 2006). This interaction leads to the formation of replicative DNA Cdc45-Mcm2-7-GINS (CMG) complex, which is an important component of the replisome progression complex (RPC) at the replication forks (Fig. 4.2) (Gambus *et al.*, 2006). Mcm10, RecQ protein like 4 (RecQL4) and WDHD1 are replication initiation factors and have a role to form CMG complex in humans (Zhu *et al.*, 2007; Im *et al.*, 2009; Thu and Bielinsky, 2013).

CMG complex has hetero-hexameric structure, which has a role to unwind the double strand DNA by forming active DNA helicase (Fig. 4.2) (Pacek and Walter, 2004; Shechter, Ying and Gautier, 2004). Then, new strands of DNA are synthesised according to the complementary base pairing rule alongside of the leading and lagging strands. Both polymerase epsilon (Pol ϵ) and polymerase delta (Pol δ) require proliferating cell nuclear antigen (pCNA) to maintain their function (Garg and Burgers, 2005). Pol ϵ directly binds to the CMG complex and contributes to continuous DNA replication on the leading strand (Langston *et al.*, 2014). However, lagging strand requires primase, polymerase alpha (Pol α), and Pol δ, which form discontinuous Okazaki fragments (Guan *et al.*,

2017). During the process, primase synthesises a short RNA primer (~10 nts) (177), Pol α extends the primer to approximately 20 nts (Perera *et al.*, 2013) and Pol δ elongates the primer (Wideman, Zautra and Edwards, 2012). In contrast to Pol ϵ, Pol α and Pol δ cannot directly bind to CMG complex so they require adaptor proteins such as WDHD1 for the replisome complex integrity and replication process efficiency (Fig. 4.2) (Zhu *et al.*, 2007; Im *et al.*, 2009; Bermudez *et al.*, 2010; Kang *et al.*, 2013; Guan *et al.*, 2017).

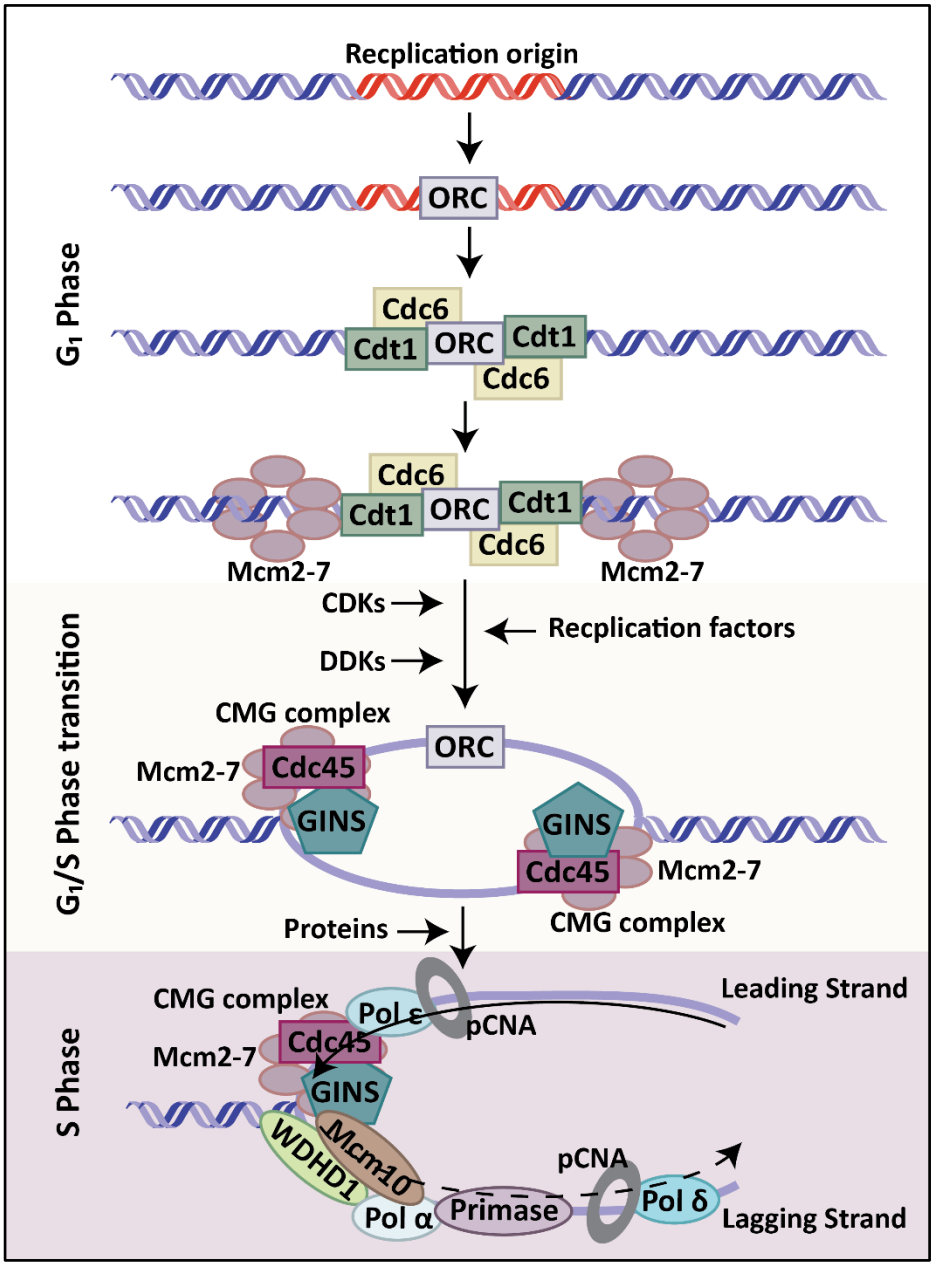

Figure 4.2 Diagram illustrating the process of DNA replication.
For Pre-RC assembly, ORC is recruited to the replication origin in G_1 phase. Then, Cdc6, Cdt1 and Mcm2-7 bind to ORC to allow replication licensing. In G_1/S phase transition, DDKs, CDK and several replication factors are recruited to the origin for the interaction of Cdc45 and GINS with Mcm2-7 to form CMG complex. Then, Mcm2-7 helicase is activated and dissociated into two Mcm2-7 hexamers to unwind DNA. In S phase, DNA unwinds by activated helicase. Mcm2-7 activation recruits several other proteins such as DNA polymerases and pCNA to form functional replication forks and move to the opposite directions along with replisome such as WDHD1 from activated origin. Pre-RC: Pre-replicative complex; ORC: origin recognition complex; Cdc6: cell division cycle 6; Cdt1; CDC10-dependent transcript 1; Mcm2-7: mini-chromosome maintenance 2-7; DDKs: cyclin dependent and cell division cycle 7 (Cdc7)-dumbbell former 4 (Dbf4) kinases; CDK: cyclin-dependent kinase; Cdc45: cell division cycle protein 45; GINS: go ichi ni san complex; CMG: Cdc45-Mcm2-7-GINS; pCNA: proliferating cell nuclear antigen; WDHD1: WD repeat and high mobility group [HMG]-box DNA binding protein 1. [Information collected from (Takeda and Dutta, 2005; Zheng *et al.*, 2018; Boavida *et al.*, 2021)].

4.1.3.3 WDHD1 maintains genomic integrity

WDHD1 is important for initiation of DNA replication and sister chromatid cohesion due to the interaction between WDHD1 and Mcm10 (Zhu *et al.*, 2007; Errico *et al.*, 2009; Im *et al.*, 2009; Tanaka *et al.*, 2009; Yoshizawa-Sugata and Masai, 2009; Bermudez *et al.*, 2010; Li *et al.*, 2012). WDHD1 is loaded on chromatin after Mcm10, at the same time with DNA polymerase α during S phase in *Xenopus* egg extract and it also stabilises p180 subunit of DNA polymerase α in human cells (Zhu *et al.*, 2007). It was shown that WDHD1 interacts with Mcm10 that is known to associate with Mcm2-7 and p180 subunit of DNA polymerase α (Zhu *et al.*, 2007). Moreover, RecQL4 is required for the interaction of WDHD1 and Mcm10 in human cells and this interaction of RecQL4/WDHD1/Mcm10 is controlled by CDK and DDK, which are S phase promoting kinases (Im *et al.*, 2015). The recruitment and stabilisation of WDHD1 and DNA polymerase α on the chromatin can be regulated by CTC1-STN1-TEN1 (CST), which also interacts with Mcm2-7 (Yilin Wang *et al.*, 2019).

WDHD1 is also associated with cohesion and replication fork components such as Smc1, Smc3, Rad21, and Mcm7 (Yoshizawa-Sugata and Masai, 2009). In *Xenopus laevis* egg extract, And-1 was identified as Tipin-binding partner and form Tipin/Tim/And-1 complex that stabilises the replication fork and maintain sister chromatin cohesion (Errico *et al.*, 2009; Tanaka *et al.*, 2009).

WDHD1 also plays an important role for the formation of CMG complex that activates DNA polymerase α and ϵ and links Mcm2-7 and DNA polymerase α-primase complex (Im *et al.*, 2009; Bermudez *et al.*, 2010; Kang *et al.*, 2013). On the other hand, human cell studies showed that WDHD1 is assembled onto chromatin in late mitosis and early G_1 phase, which recruits and forms a complex with Mcm2-7 during pre-RC assembly and plays a role in Cdt1 and Mcm7 interaction (Li *et al.*, 2012).

Further mechanistic studies of WDHD1 demonstrated that WDHD1 can bind to DNA polymerase α via its SepB domain (Guan *et al.*, 2017; Kilkenny *et al.*, 2017). It was also shown that WDHD1 binds to DNA via its C-terminal HMG domain (Köehler, Schmidt-Zachmann and Franke, 1997; Guan *et al.*, 2017) but another study showed that WDHD1-DNA binding is not via HMG domain, and it is via the intermediate region of SepB and HMG domains (Kilkenny *et al.*, 2017). Guan *et al.,* 2017 concluded that the interaction between WDHD1 and CMG complex was unknown and further mechanistic WDHD1 function in DNA replication is required in human (Guan *et al.*, 2017). A recent study indicated that the interaction between WDHD1 and CMG complex is due to the binding of WDHD1 SepB domain to the site of Cdc45 and GINS in human (Rzechorzek *et al.*, 2020).

Abe *et al.,* 2018 demonstrated that while the HMG domain of WDHD1 is required for fast replication fork speed, WD40 domain is essential to protect resected fork, which is essential for cell proliferation to maintain genomic integrity (Abe *et al.*, 2018). A recent study confirmed that WDHD1 is required for the cell proliferation in early mouse embryogenesis (Fan *et al.*, 2021).

WDHD1 facilitates DNA replication checkpoint signalling by stabilising Chk1, which is an effector kinase involved in S/G_2 checkpoints (Yoshizawa-Sugata and Masai, 2009; Hao *et al.*, 2015; Chen *et al.*, 2017). Another study also demonstrated that WDHD1 interacts with Timeless, Tipin and Claspin proteins that are involved in the DNA replication checkpoint (Hao *et al.*, 2015). In the presence of DNA replication stress, ATR phosphorylates WDHD1 and WDHD1 is recruited to the DNA damage site and mediates the interaction between Claspin (Chk1 interacting protein) and Chk1 (Hao *et al.*, 2015). It was also shown that WDHD1 contributes to mismatch repair pathway (MMR) as WDHD1 was identified as a binding partner of MSH2 (important protein in MMR pathway) (Chen *et al.*, 2016). Moreover, WDHD1 interacts with CtIP (positive regulator of DNA end-resection) to maintain DNA damage checkpoint via homologous recombination DNA double strand breaks (Chen *et al.*, 2017).

The findings mentioned above, indicated the important roles of WDHD1 in DNA replication, sister chromatid cohesion, checkpoint activation and DNA damage repair to maintain genomic integrity.

4.1.4 WDHD1 in cancer

WDHD1 is known as a DNA replication initiation factor and maintains genomic integrity via different mechanisms as mentioned in section 4.1.3.3. However, further studies are required for better understanding of WDHD1 function and mechanism in cancer. There have been studies that highlighted the role of WDHD1 in cancer progression.

It has been previously shown that WDHD1 expression was higher in lung carcinoma, oesophageal carcinoma, colorectal carcinoma, melanoma, cholangiocarcinoma and cervical cancer compared to their normal cell lines or tissues as shown in table 4.1.

Table 4.1 The expression of WDHD1 in different cancer tissue or cell lines.

Cancer Types	Tissue Samples	Cell lines
Lung carcinoma	↑ (Sato *et al.*, 2010; Gong *et al.*, 2020)	↑ (Sato *et al.*, 2010; Li, A. N. Jaramillo-Lambert, *et al.*, 2011; Gong *et al.*, 2020)
Oesophageal carcinoma	↑ (Sato *et al.*, 2010; N. Chen *et al.*, 2020)	↑ (Sato *et al.*, 2010)
Colorectal carcinoma	↑ (Li, A. N. Jaramillo-Lambert, *et al.*, 2011)	-
Melanoma	-	↑ (Li, A. N. Jaramillo-Lambert, *et al.*, 2011)
Cholangiocarcinoma	↑ (B. Liu *et al.*, 2019)	↑ (B. Liu *et al.*, 2019)
Cervical cancer	↑ (S. Chen *et al.*, 2020)	-

↑ indicates higher expression

The higher expression of WDHD1 was negatively correlated with the survival rate in lung and oesophageal carcinoma patients' samples (Sato *et al.*, 2010; Gong *et al.*, 2020). Moreover, the knockdown of *WDHD1* in lung carcinoma (Sato *et al.*, 2010; Gong *et al.*, 2020), oesophageal carcinoma (Sato *et al.*, 2010; N. Chen *et al.*, 2020) and acute myeloid leukaemia (Wermke *et al.*, 2015) cells impaired the growth and viability compared to the control cells. *WDHD1* has a growth promoting effect on lung carcinoma, oesophageal carcinoma and cholangiocarcinoma cell lines, which was also confirmed with the delayed entry of cells to S phase, decreased cell cycle progression (DNA replication) and induced cell death with the knockdown of *WDHD1* (Zhu *et al.*,

2007; Yoshizawa-Sugata and Masai, 2009; Bermudez *et al.*, 2010; Sato *et al.*, 2010; B. Liu *et al.*, 2019).

Sato *et al.,* 2010 reported that AKT phosphorylates and stabilises WDHD1, which could be involved in the downstream of PI3K/AKT pathway and might be a biomarker and therapeutic target in pulmonary and oesophageal carcinoma as a regulator of cell cycle (Sato *et al.*, 2010). It was also discovered that inhibition of *WDHD1* significantly increased both protein and mRNA expression levels of E-cadherin and decreased N-cadherin, Vimentin, MMP-9, Snail and Twist protein and mRNA levels compared to the control group and reduced cholangiocarcinoma cell invasion and migration (B. Liu *et al.*, 2019). E-cadherin, N-cadherin, Vimentin, MMP-9, Snail and Twist are EMT markers thus, the study showed that WDHD1 has a role in EMT in cholangiocarcinoma (B. Liu *et al.*, 2019).

WDHD1 expression was also upregulated in E7-expressing cells (Zhou *et al.*, 2016). E7 is an oncoprotein that has a function in human papillomavirus (HPV)-induced carcinogenesis; cervical cancer, which abolishes G_1 checkpoint and contributes to re-replication (Zhou *et al.*, 2016). The knockdown of *WDHD1* induced G_1 arrest and decreased S phase in E7-expressing cells (Zhou *et al.*, 2016). Further studies showed that G_1 checkpoint abrogation in E7-expressing cells is facilitated by WDHD1/GCN5/AKT axis as WDHD1 is correlated with AKT activity and general control non-derepressible (GCN5) (Zhou *et al.*, 2020), the association between WDHD1 and GCN5 are mentioned in the paragraph below.

Apart from the role of WDHD1 and the association between WDHD1 and AKT in cancer, studies also showed the mechanism of WDHD1 interaction with other proteins or genes in cancer. Liu *et al.,* 2019 showed that miR494 is negatively correlated with WDHD1 in cholangiocarcinoma; overexpression of miR494 inhibits WDHD1 which then suppresses EMT in cholangiocarcinoma cells (B. Liu *et al.*, 2019). Although further mechanistic studies are required, it was shown that signal transducers and activators of transcription 3 (STAT3) binds to the promoter region of *WDHD1* and regulates the transcription of *WDHD1*, which then leads to DNA replication (Zhou and Chen, 2021).

WDHD1 can stabilise GCN5, which is a histone acetyltransferase and prevents the interaction between GCN5 and Cdc10-dependent transcript 2 (Cdt2), thus overexpression of GCN5 leads to tumorigenesis (Li, A. Jaramillo-Lambert, *et al.*, 2011; Li, A. N. Jaramillo-Lambert, *et al.*, 2011). Moreover, it has been shown that overexpression of WDHD1 is also correlated with histone H3 acetylation; H3K9AC and H3K56AC in lung carcinoma and melanoma cell lines (Li, A. N. Jaramillo-Lambert, *et al.*, 2011). A recent study demonstrated microtubule-associated protein RP/EB family member 2 (MAPRE2) can be one of the target proteins of WDHD1 as WDHD1 ubiquitinates and

degrades MAPRE2 and decreases the sensitivity of lung adenocarcinoma to cisplatin (Gong *et al.*, 2020).

There have been various studies about *WDHD1* in different cancer types, however there are no studies of WDHD1 in PTEN-inactive TNBC. Therefore, this project is the first study to check the effect of WDHD1 in cell viability and clinicopathological features (Chapter 4) and functionally characterise WDHD1 (Chapter 5) in PTEN-inactive TNBC cells.

4.1.5 Summary of the chapter

In this chapter, the aim was to validate the bioinformatic analysis findings with *in vitro* work and patients' samples in PTEN-inactive TNBC.

We showed that WDHD1 expression were higher in PTEN-inactive TNBC cell lines compared to the PTEN-active TNBC cells and can be regulated by AKT signalling pathway. The bioinformatic findings from Chapter 3 was validated, which demonstrated that WDHD1 is essential for the survival of PTEN null TNBC cells. WDHD1 levels were increased in TNBC compared to normal breast tissues, and associated with tumour size and proliferation.

4.2 Results

4.2.1 WDHD1 expression is affected by PTEN status in TNBC cell lines

TCGA analysis suggested that *WDHD1* expression is higher in the low *vs.* high *PTEN* TNBC samples (Chapter 3; Fig. 3.16A; Table 3.2). To validate this finding, both protein and mRNA levels of WDHD1 were measured in a panel of TNBC cell lines, either PTEN WT (HCC1806, BT20, MDA-MB-157 and MDA-MB-231) or PTEN null (MDA-MB-468, HCC1395, HCC1937 and HCC38). We found that WDHD1 was highly expressed at both the protein (Fig. 4.3A-B; $P < 0.05$) and mRNA (Fig. 4.3C-D; $P < 0.01$) level in PTEN null *vs.* WT TNBC cell lines. Phosphorylated AKT (pAKT Thr308 and Ser473) expression levels were also measured in PTEN WT and null type TNBC cells. pAKT expression of MDA-MB-468 showed higher pAKT expression than the other PTEN null type and PTEN WT (HCC1806 and BT20) TNBC cells (See Appendix Fig. C.1). Moreover, MDA-MB-157 and MDA-MB-231 PTEN WT TNBC cells do not express pAKT (See Appendix Fig. C.1).

To further confirm the relationship between PTEN and WDHD1 expression levels, we introduced a regulable PTEN construct into MDA-MB-468 cells (PTEN null) that is conditionally responsive to DOX. Addition of DOX induces PTEN expression in MDA-MB-468 cells expressing TR-PTEN (MDA-MB-468-TR-PTEN) to a similar level in a non-tumorigenic triple negative human breast epithelial cell line MCF10A (Fig. 3.14B). MDA-MB-468-TR-PTEN cell line was treated with different concentrations of DOX to find the optimum DOX concentration to induce PTEN expression. PTEN was expressed with the treatment of DOX compared to the DOX untreated cell line, control. The treatment with different concentrations of DOX showed that 100 ng/ml DOX induced higher expression of PTEN than 25 ng/ml and 50 ng/ml DOX (Fig. 4.4). Therefore, following studies were carried out by using 100 ng/ml DOX.

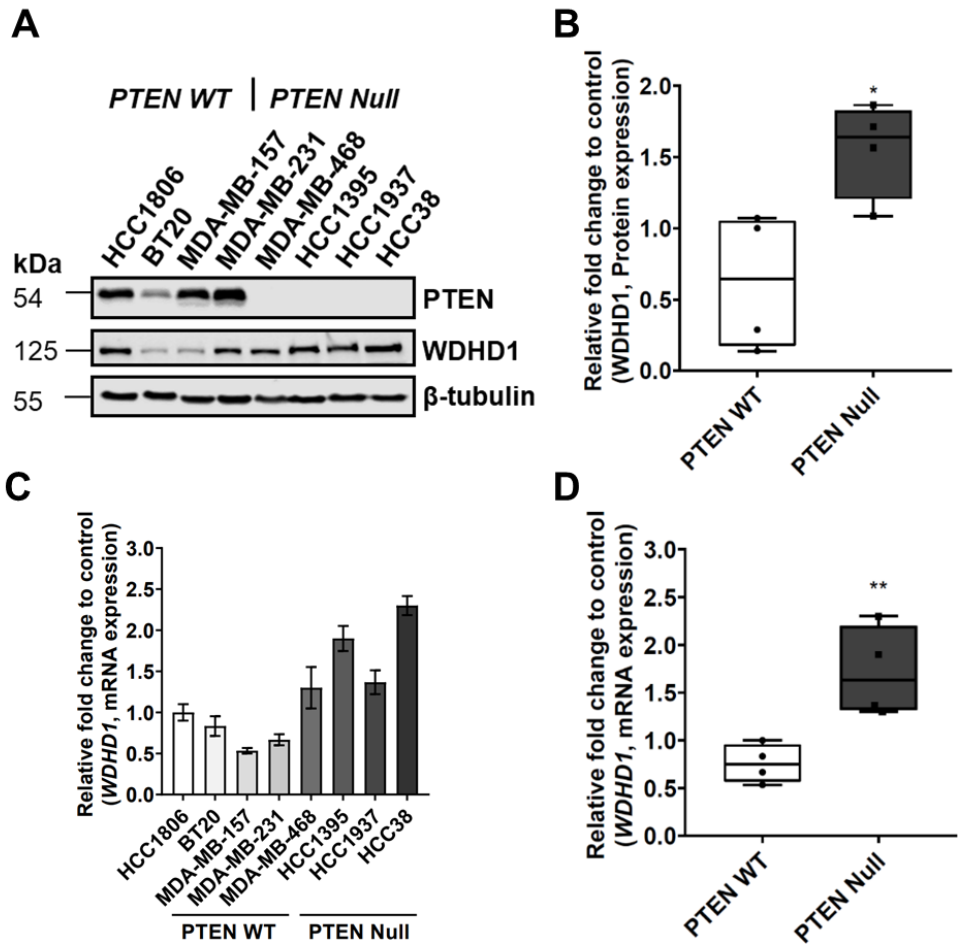

Figure 4.3 WDHD1 is highly expressed in PTEN-inactive TNBC cells.

A) TNBC cell lines with PTEN WT or PTEN null were lysed with 8 M urea buffer and 30 µg of protein was used to check protein expression of PTEN and WDHD1 by western blot. β-tubulin was used as a loading control. **B)** The graph shows protein levels of WDHD1 in PTEN WT or PTEN null TNBC cell lines. Unpaired *t-test* was performed for statistical analysis. $*P < 0.05$. **C)** Fold change in mRNA levels of *WDHD1* in the indicated PTEN WT or PTEN null TNBC cell lines by performing qRT-PCR. *WDHD1*, mRNA expression was normalised to a housekeeping gene, *β-actin*. Data are mean ± SEM. $n = 3$ per group. **D)** The graph shows mRNA levels of *WDHD1* in PTEN WT or PTEN null TNBC cell lines. Unpaired *t-test* was performed for statistical analysis. $**P < 0.01$. Data in (**B**) and (**D**) are individual values with mean, and error bars indicate minimum and maximum individual values. $n = 4$ per group. The quantification of each sample was performed by normalisation to the loading control, β-tubulin (**B**) and housekeeping gene*, β-actin* (**C**-**D**).

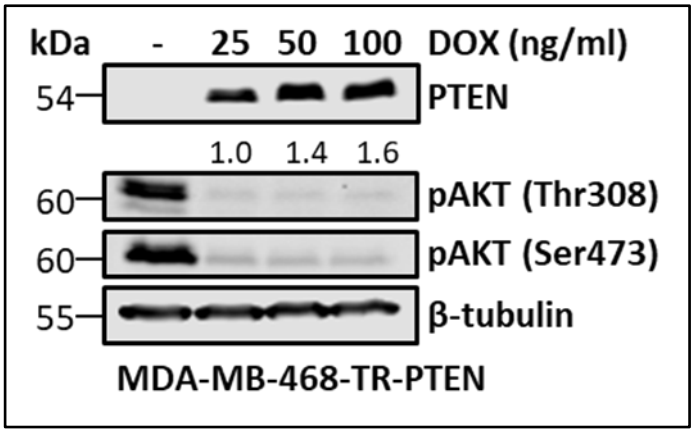

Figure 4.4 Optimising the concentration of DOX for MDA-MB-468-TR-PTEN cell line to induce PTEN expression.

Previously generated MDA-MB-468-TR-PTEN cell line was treated with different concentrations of DOX (25 ng/ml, 50 ng/ml and 100 ng/ml) and cells were lysed with 8 M urea buffer six hours post DOX treatment. After the cell lysis, 40 µg of protein was run for western blot to analyse PTEN, pAKT (ThrT308) and pAKT (Ser473) expression. β-tubulin was used as a loading control. Quantified numbers were normalised to optical density of β-tubulin.

PTEN is the upstream of AKT signalling pathway and affects the apoptosis and cell viability of cells (Sato *et al.*, 2010; B. Liu *et al.*, 2019). Therefore, pAKT (Thr308), pAKT (Ser473), cleaved PARP protein expression, both WDHD1 protein expression and mRNA expression levels and cell viability were analysed in two weeks DOX treated MDA-MB-468-TR-PTEN cell lines. Figure 4.5A and Figure 4.6A show the representative western blot images of DOX untreated (*PTEN*-) and two weeks DOX treated (*PTEN*+) MDA-MB-468-TR-PTEN cell line. The results showed that while the expression of pAKT (Thr308) and pAKT (Ser473) were lower, cleaved PARP was higher in the presence of DOX compared to the absence of DOX (Fig. 4.5A). Moreover, cell viability of DOX treated cell line was significantly decreased compared to the DOX untreated cell line (Fig. 4.5B). As shown in Figure 4.6, WDHD1 levels were significantly reduced upon PTEN expression (DOX+) in MDA-MB-468-TR-PTEN cells at both protein and mRNA levels, as demonstrated by the results from the western blot (Fig. 4.6A-B; $P < 0.01$), qRT-PCR (Fig. 4.6C; $P < 0.0001$) and immunofluorescence staining of WDHD1 (Fig. 4.6D). These results showed that inducing PTEN expression in TNBC cell lines has negative impact on AKT activity, cell viability and WDHD1 expression, and positive impact on apoptosis.

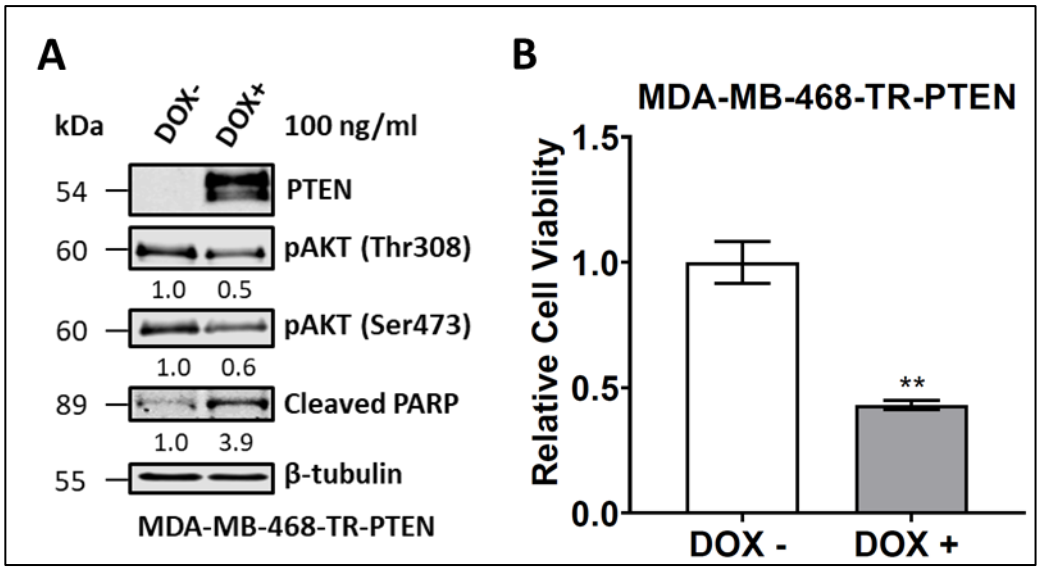

Figure 4.5 The effect of PTEN on the AKT signalling pathway in TNBC cells.

A-B) MDA-MB-468-TR-PTEN cell line was treated with 100 ng/ml DOX for two weeks in 2D cultures. **A)** Cell lysis with 8 M urea buffer was performed and 40 µg of protein was run for western blot to analyse the protein expression of PTEN, pAKT (Thr308), pAKT (Ser473) and cleaved PARP. β-tubulin was used as a loading control. **B)** Graph shows relative cell viability in MDA-MB-468-TR-PTEN cell line with indicated treatment. Cell-Titer Glo® assay was performed to measure cell viability. Data are mean ± SEM. Unpaired *t-test* was performed for statistical analysis. $^{**}P \leq 0.01$.

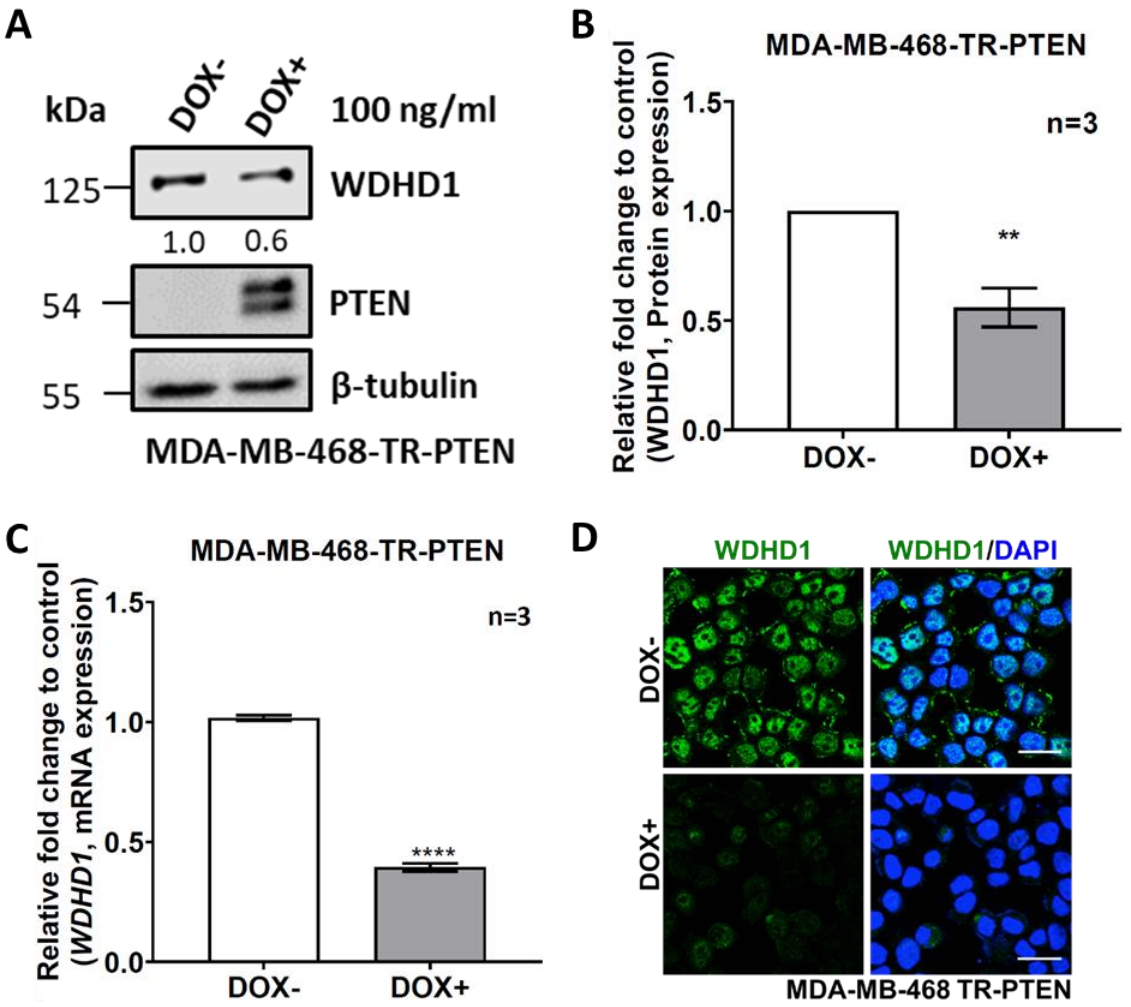

Figure 4.6 WDHD1 levels are reduced upon PTEN expression in MDA-MB-468 cells.
A-D) MDA-MB-468-TR-PTEN cell line was treated with 100 ng/ml DOX for two weeks in 2D cultures. **A)** Cell lysis with 8 M urea buffer was performed and 40 µg of protein was run for western blot to analyse the protein expression of cleaved PARP, WDHD1 and PTEN. β-tubulin was used as a loading control. The graphs show protein (**B**) or mRNA (**C**) levels of WDHD1 in MDA-MB-468-TR-PTEN cells treated with (DOX+) or without DOX (DOX−). Data are mean ± SEM. Unpaired *t-test* was performed for statistical analysis. $^{**}P < 0.01$. $^{****}P < 0.0001$. $n = 3$ per group. **F)** Immunofluorescence staining of WDHD1 (green) in MDA-MB-468-TR-PTEN cells treated with (DOX+) or without DOX (DOX−). 4'6-diamidino-2-pheylindole (DAPI) (blue) was used to stain nuclei. Scale bars: 20 µm.

4.2.2 WDHD1 expression is affected by PTEN status in TNBC cells via AKT signalling pathway

According to our findings, PTEN and AKT activity is negatively correlated in TNBC (Fig. 3.11) and we decided to determine whether AKT is involved in the regulation of WDHD1 expression in TNBC cell lines. An AKT inhibitor (AKT VIII) was used to treat PTEN null type TNBC cell lines MDA-MB-468 (Fig. 4.7A), HCC1395 (Fig. 4.7B), HCC1937 (Fig. 4.7C) and HCC38 (Fig. 4.7D). AKT activity, monitored by the levels of phosphorylated AKT (pAKT Thr308 and Ser473), was inhibited following the treatment with AKT VIII in all PTEN null type TNBC cell lines (Fig. 4.7A–D). Subsequently, WDHD1 levels were significantly reduced upon AKT inhibition in these cells (Fig. 4.7A–D; $P < 0.05$). These findings suggested that AKT signalling effect WDHD1 expression in PTEN null type TNBC cells.

As inhibition of AKT activity decreased WDHD1 protein expression (Fig. 4.7A-D), we investigated whether WDHD1 expression has an effect on AKT activity. *WDHD1* expression was knocked-down with two individual siRNA oligos and protein expression of pAKT (Thr308) was detected in PTEN WT: HCC1806 (Fig. 4.8A) and BT20 (Fig. 4.8B) and PTEN null type: MDA-MB-468 (Fig. 4.8C), HCC1395 (Fig. 4.8D), HCC1937 (Fig. 4.8E) and HCC38 (Fig. 4.8F) TNBC cell lines. We observed no significant change in pAKT (Thr308) expression in PTEN WT TNBC cell lines when *WDHD1* was knocked-down compared to the control group (Fig. 4.8A-B). In PTEN null type MDA-MB-468 TNBC cell line, pAKT (Thr308) protein expression was significantly downregulated with two individual siRNA oligos compared to the control group (Fig. 4.8C). In PTEN null type HCC1937 cell lines, *WDHD1* siRNA oligo 1# showed significant decrease in pAKT (Thr308) compared to control group (Fig. 4.8E). However, there was no significant change with *WDHD1* siRNA oligos in HCC1395 and HCC38 PTEN null type TNBC cell line (Fig. 4.8D and F). The combination of individual siRNA oligos in PTEN WT and PTEN null type TNBC cell lines showed significant decrease of pAKT (Thr308) in PTEN null type cells compared to PTEN WT cell lines with *WDHD1* siRNA oligo 1# (Fig. 4.8G). Although no significant decrease was observed with oligo 2# between PTEN WT and null type combined groups, there was a decreasing pattern of pAKT (Thr308) in PTEN null type TNBC cell lines compared to PTEN WT cell lines (Fig. 4.8G). These results demonstrated that WDHD1 can affect AKT activity in PTEN null TNBC cells but this association might be cell specific.

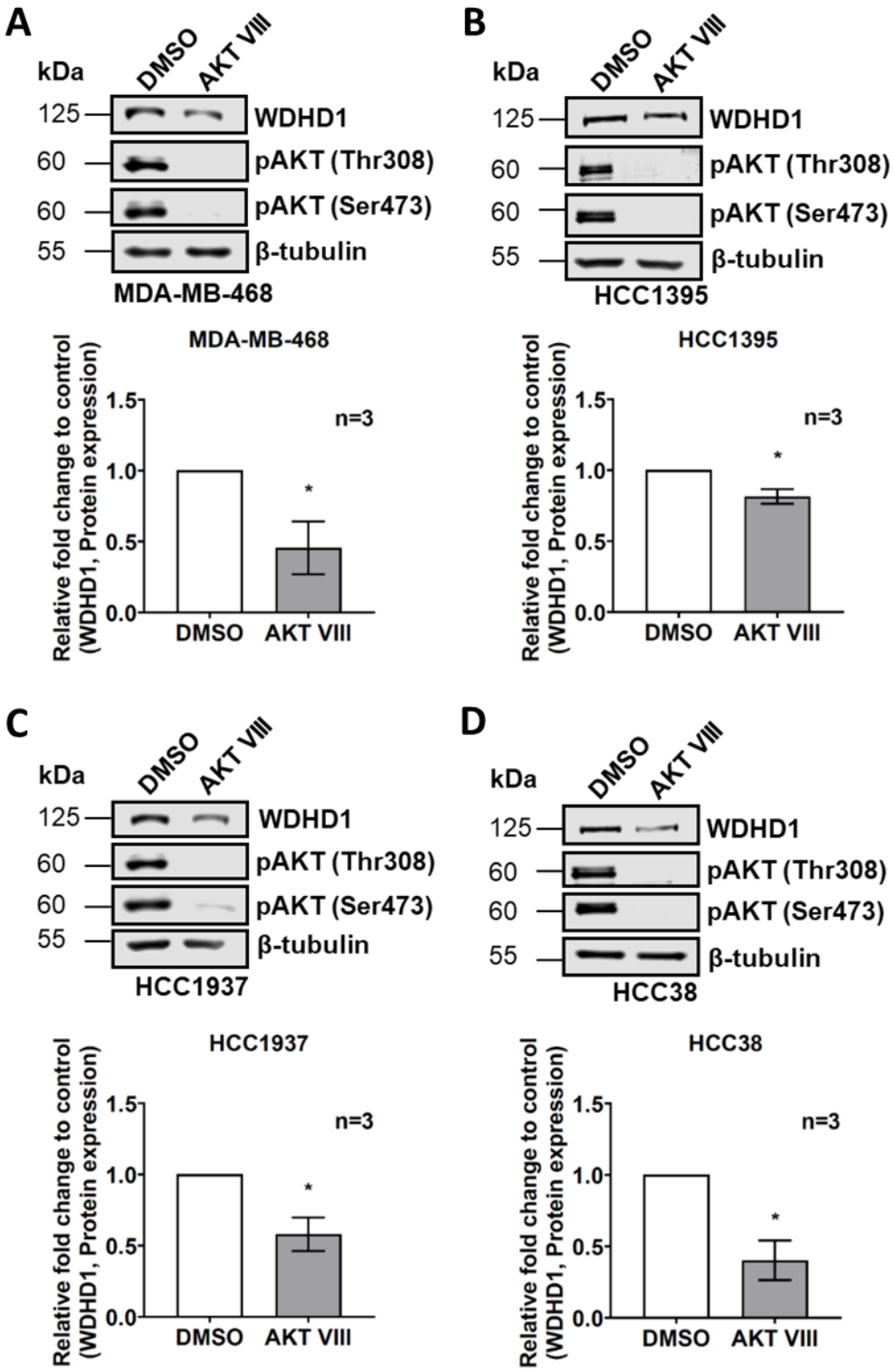

Figure 4.7 WDHD1 levels are reduced upon AKT inhibition in PTEN null TNBC cells.
Protein expression of WDHD1, phospho-AKT (pAKT) (Thr308) and pAKT (Ser473) in MDA-MB-468 (**A**), HCC1395 (**B**), HCC1937 (**C**) and HCC38 (**D**) treated with DMSO (negative control) or an AKT inhibitor, AKT VIII (10 µM). Cell lysis was performed with 8 M urea buffer 24 hours post treatment and 20 µg of protein was run for western blot. β-tubulin was used as a loading control. The graphs show protein levels of WDHD1 in MDA-MB-468 (**A**), HCC1395 (**B**), HCC1937 (**C**) and HCC38 (**D**) treated with DMSO or AKT VIII. Data are mean ± SEM. Paired *t-test* was performed for statistical analysis. *$P < 0.05$. $n = 3$ per group.

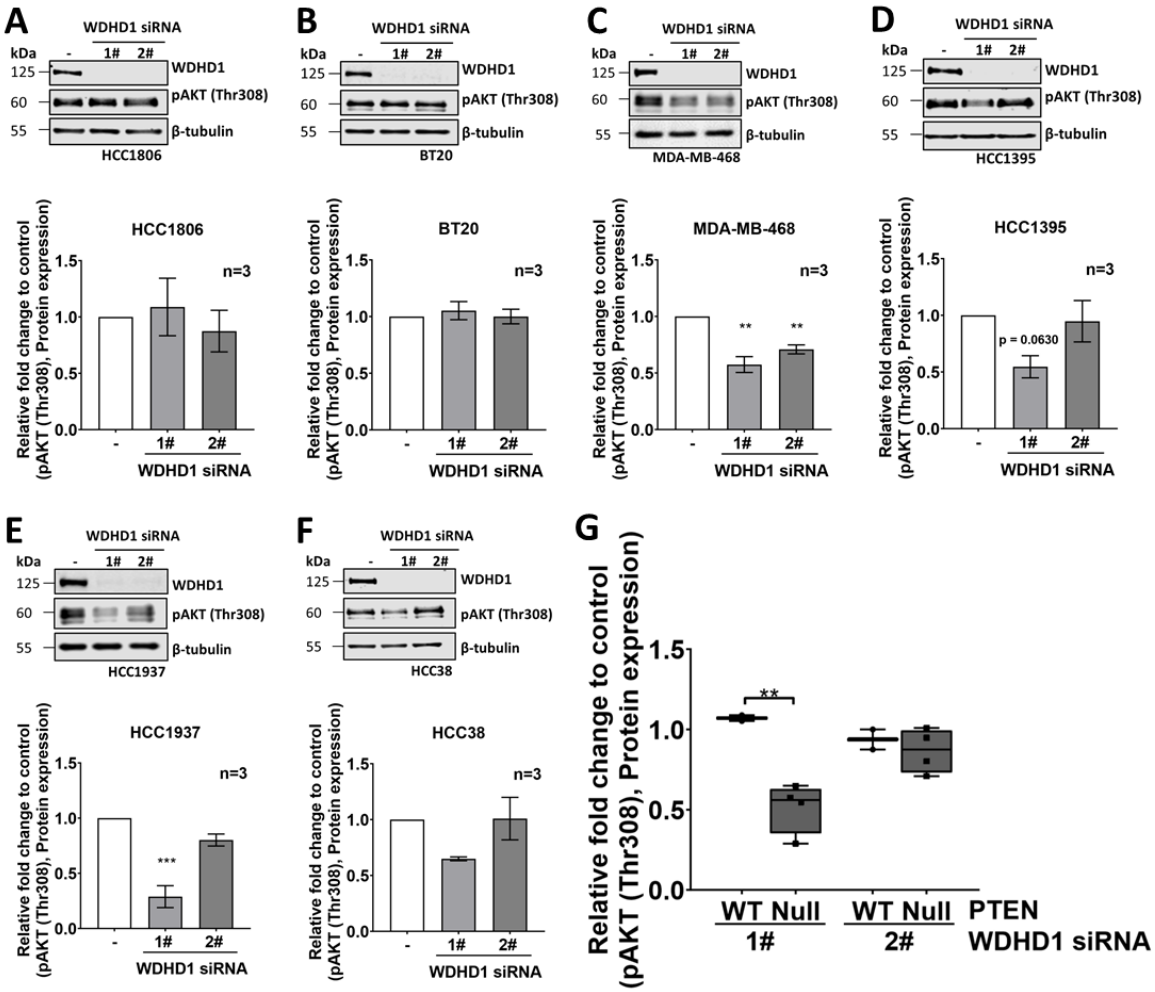

Figure 4.8 pAKT (Thr308) levels are reduced upon *WDHD1* knockdown in PTEN null TNBC cell lines. WDHD1 expression was knocked-down with two different *WDHD1* siRNA oligos along with RISC-Free negative control siRNA oligo in HCC1806 (**A**), BT20 (**B**), MDA-MB-468 (**C**), HCC1395 (**D**), HCC1937 (**E**) and HCC38 (**F**). 8 M urea buffer was used for cell lysis following 96 hours of knockdown and 15 µg protein was run for western blot. WDHD1 and pAKT (Thr308) protein expression were observed with the indicated transfections. β-tubulin was used as a loading control. The graphs show protein levels of pAKT (Thr308) in HCC1806 (**A**), BT20 (**B**), MDA-MB-468 (**C**), HCC1395 (**D**), HCC1937 (**E**) and HCC38 (**F**) with indicated transfections cultured in 2D cultures. Data are mean ± SEM. Ordinary one-way ANOVA was performed for statistical analysis. $^{**}P \leq 0.01$. $^{***}P \leq 0.001$. $n = 3$ per group. **G)** The combination of each *WDHD1* siRNA oligo in both PTEN WT and null type TNBC cell lines. Data are individual values with mean, and error bars indicate minimum and maximum individual values. Unpaired *t-test* was performed for statistical analysis. $^{**}P \leq 0.01$.

The impact of PTEN-AKT signalling on WDHD1 expression was further confirmed by the TCGA analysis. To reflect the functional consequence of PTEN status, we decided to check pAKT_308 levels and the correlation with *WDHD1*, mRNA expression in TCGA TNBC samples. We demonstrated that there was a significant positive correlation between *WDHD1*, mRNA expression and pAKT_308 levels in the TCGA dataset (Fig. 4.9; $r = 0.3321$, $P = 0.0296$).

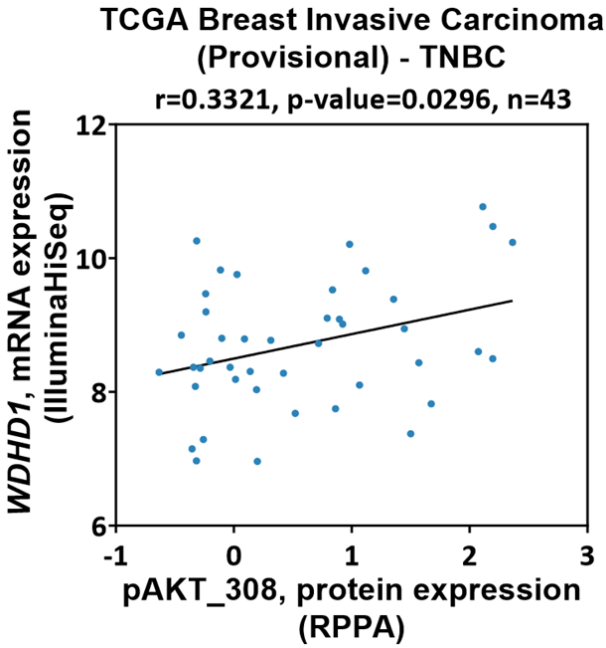

Figure 4.9 Correlation between pAKT_308, protein expression and *WDHD1*, mRNA level in TNBC samples (TCGA, Provisional) from cBioPortal.

The scatter plot for the correlation of TNBC samples between pAKT_308, protein expression (RPPA) and *WDHD1*, mRNA expression (IlluminaHiSeq) in the TCGA breast invasive carcinoma (Provisional) data (Pearson's correlation (r) = 0.3321; $P = 0.0296$; $n = 43$). Codes are available in Appendix A.1.1.

4.2.3 WDHD1 is required for the survival of PTEN null TNBC cells cultured in 2D and 3D

The initial whole-genome siRNA screen suggested that *WDHD1* depletion selectively inhibits cell viability in *PTEN- vs. PTEN*+ TNBC cells. To validate this observation, *WDHD1* expression was down-regulated by two individual siRNA oligos in the aforementioned panel of TNBC cell lines and cell viability was measured by Cell-Titer Glo® assays (Fig. 4.10). Knockdown of *WDHD1* in PTEN WT TNBC cell lines (HCC1806, BT20, MDA-MB-157 and MDA-MB-231) showed mild, but not significant, effects on cell viability (Fig. 4.10A–D; $P > 0.05$). On the other hand, *WDHD1* knockdown in PTEN null type TNBC cell lines (MDA-MB-468, HCC1395 and HCC1937) showed a significant decrease in cell viability (Fig. 4.10E–G). Although there was a reduction in cell viability with *WDHD1* knockdown in HCC38 cells, no significant difference was observed (Fig. 4.10H). In general, consistent with the whole-genome siRNA screen, depletion of *WDHD1* selectively inhibited cell viability in PTEN null *vs.* WT TNBC cells with two individual siRNA oligos against *WDHD1*, although statistical significance for oligo 1# was not reached ($P = 0.054$) (Fig. 4.10I).

To further validate the cell viability assay, colony formation assay with crystal violet was also performed in 2D cell culture with PTEN null type TNBC cell lines (HCC1937 and HCC38) (Fig. 4.11). Four days post-treatment of *WDHD1* knockdown with two individual siRNA oligos, single cells were cultured in 2D environment up to two weeks. *WDHD1* knockdown in HCC1937 (Fig. 4.11A) and HCC38 (Fig. 4.11B) significantly decreased the cell proliferation.

It is known that 3D cell cultures represent their *in vivo* counterparts better than 2D monolayer cell culture models (Pampaloni, Reynaud and Stelzer, 2007; Yamada and Cukierman, 2007). To further validate the effects of *WDHD1* knockdown in TNBC cells, 3D mammosphere assays with PTEN WT (BT20 and MDA-MB-231) and null type (HCC1395 and HCC1937) TNBC cell lines were performed. Images of spheres were analysed for sphere formation efficiency and sphere volume, and cell viability was determined using Cell-Titer Glo® assays. *WDHD1* depletion in PTEN WT TNBC cell lines (BT20 and MDA-MB-231) showed minimal effects on sphere formation efficiency, sphere volume and cell viability (Fig. 4.12A-B). Oligo 1# of *WDHD1* siRNA significantly decreased the cell viability in MDA-MB-231 cell line (Fig. 4.12B). In contrast, a significant decrease in sphere formation efficiency, sphere volume and cell viability with two individual siRNA oligos against *WDHD1* was observed in HCC1395 (Fig. 4.12C; $P < 0.05$) and HCC1937 (Fig. 4.12D; $P < 0.05$), both of which are PTEN null type TNBC cell lines.

These findings showed that WDHD1 is preferentially required by PTEN-inactive TNBC cells for survival, but not for those harbouring WT PTEN.

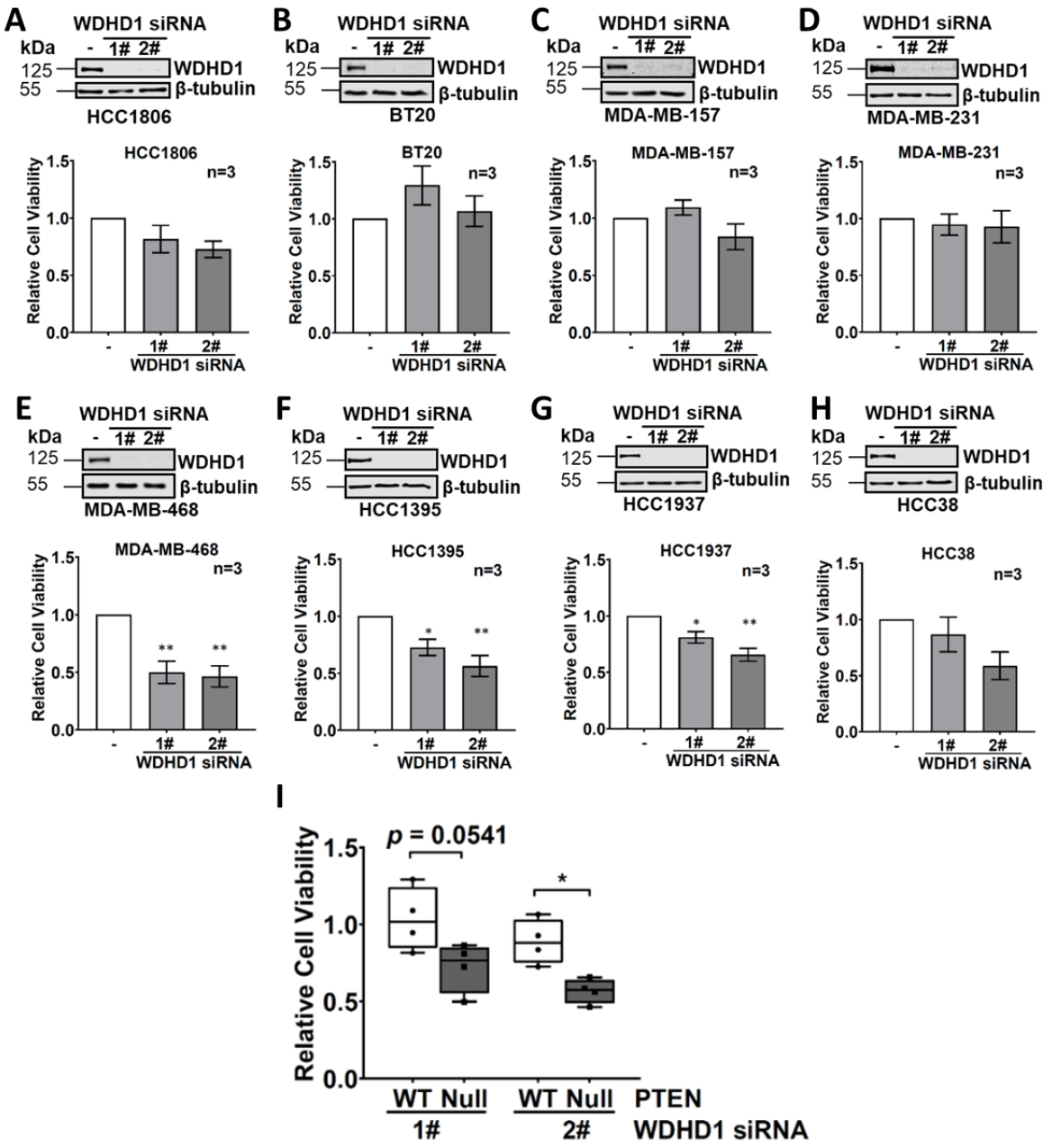

Figure 4.10 WDHD1 is required for the survival of PTEN null TNBC cells.

Protein expression of WDHD1 in PTEN WT TNBC cell line HCC1806 (**A**), BT20 (**B**), MDA-MB-157 (**C**) or MDA-MB-231 (**D**) and PTEN null type TNBC cell line MDA-MB-468 (**E**), HCC1395 (**F**), HCC1937 (**G**) or HCC38 (**H**) with indicated transfections in 2D cultures. β-tubulin was used as a loading control. The graphs show relative cell viability in HCC1806 (**A**), BT20 (**B**), MDA-MB-157 (**C**), MDA-MB-231 (**D**), MDA-MB-468 (**E**), HCC1395 (**F**), HCC1937 (**G**) and HCC38 (**H**) with indicated transfections. Cell-Titer Glo® assay was performed to measure cell viability following 96 hours of *WDHD1* knockdown. Data are mean ± SEM. Ordinary one-way ANOVA was performed for statistical analysis. *n* = 3 per group. **I)** Each *WDHD1* siRNA oligo in both PTEN WT and null type TNBC cell line was combined to compare the cell viability effect of *WDHD1* knockdown between PTEN WT and null type TNBC cell lines. Data are mean ± SEM. Unpaired *t-test* was performed for statistical analysis. **P* ≤ 0.05. ***P* ≤ 0.01. *n* = 4 per group.

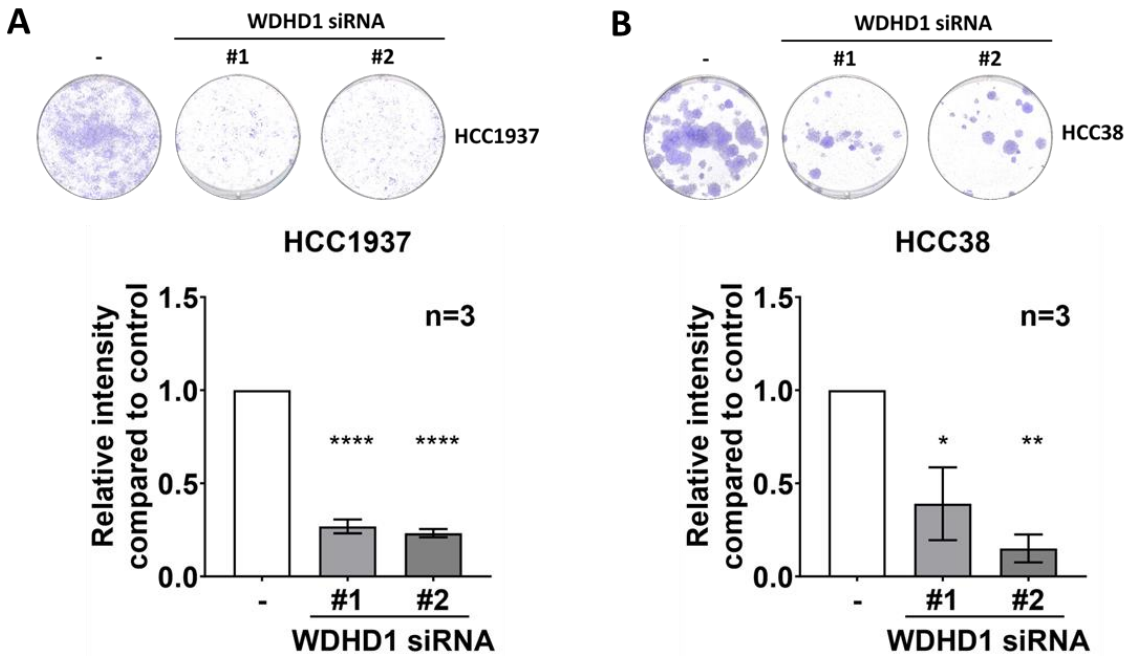

Figure 4.11 *WDHD1* knockdown reduces the proliferation of PTEN null TNBC cells cultured in 2D. *WDHD1* expression was knocked-down with two individual *WDHD1* siRNA oligos along with RISC-Free negative control siRNA oligo in PTEN null type TNBC cell line HCC1937 (**A**) or HCC38 (**B**). Cells were plated into new 6 well/plate following four days of *WDHD1* knockdown and grown for up to two weeks in 2D cell culture to observe the cell proliferation by crystal violet staining assay. Images were observed with EPSON PERFECTION V700 PHOTO. Images were analysed on ImageJ (Guzmán *et al.*, 2014). Data are mean ± SEM. Ordinary one-way ANOVA was performed for statistical analysis. **P* ≤ 0.05. ***P* ≤ 0.01. *****P* ≤ 0.0001. *n* = 3 samples per group.

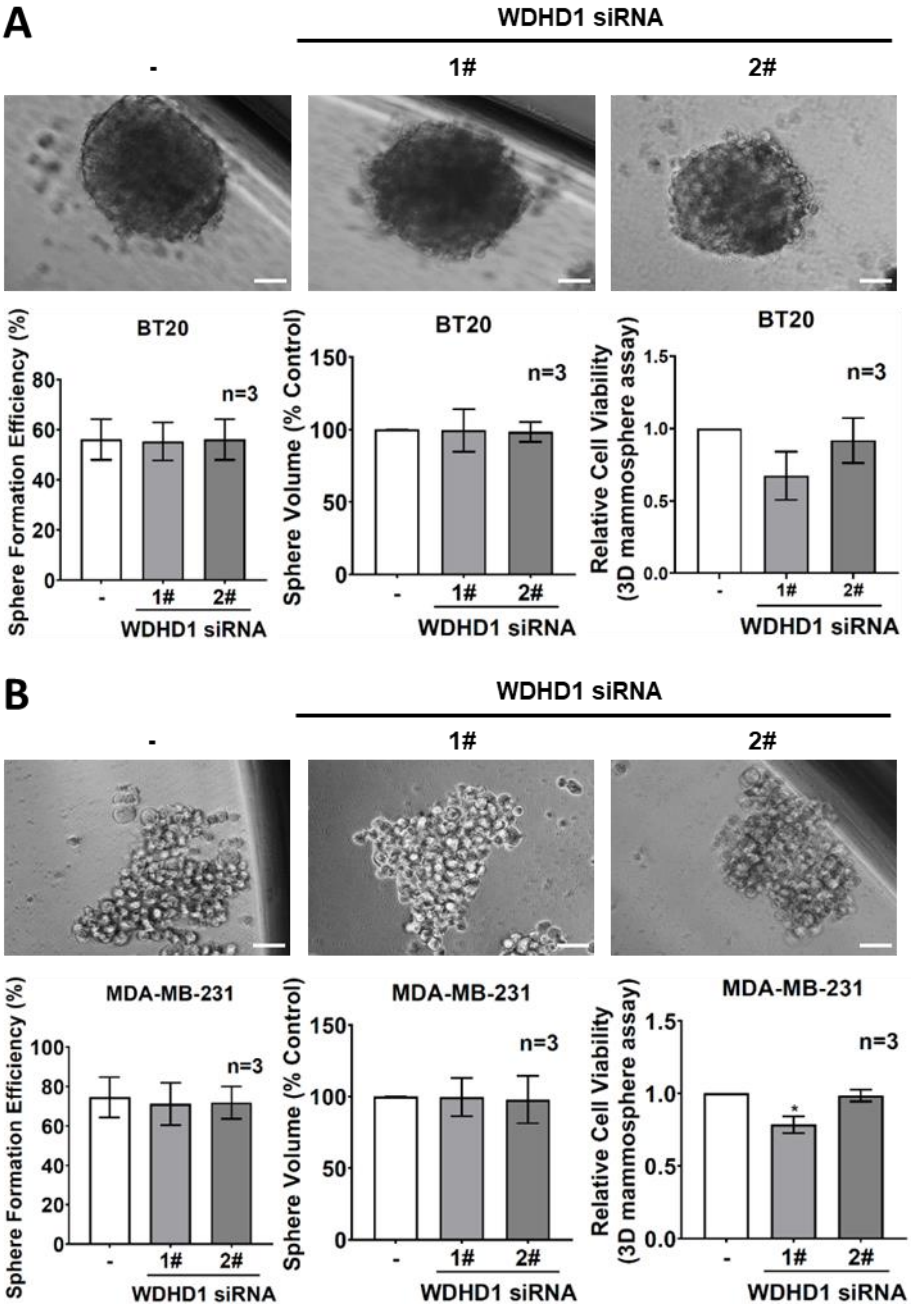

Figure 4.12 *(Figure and legend continued on next page).*

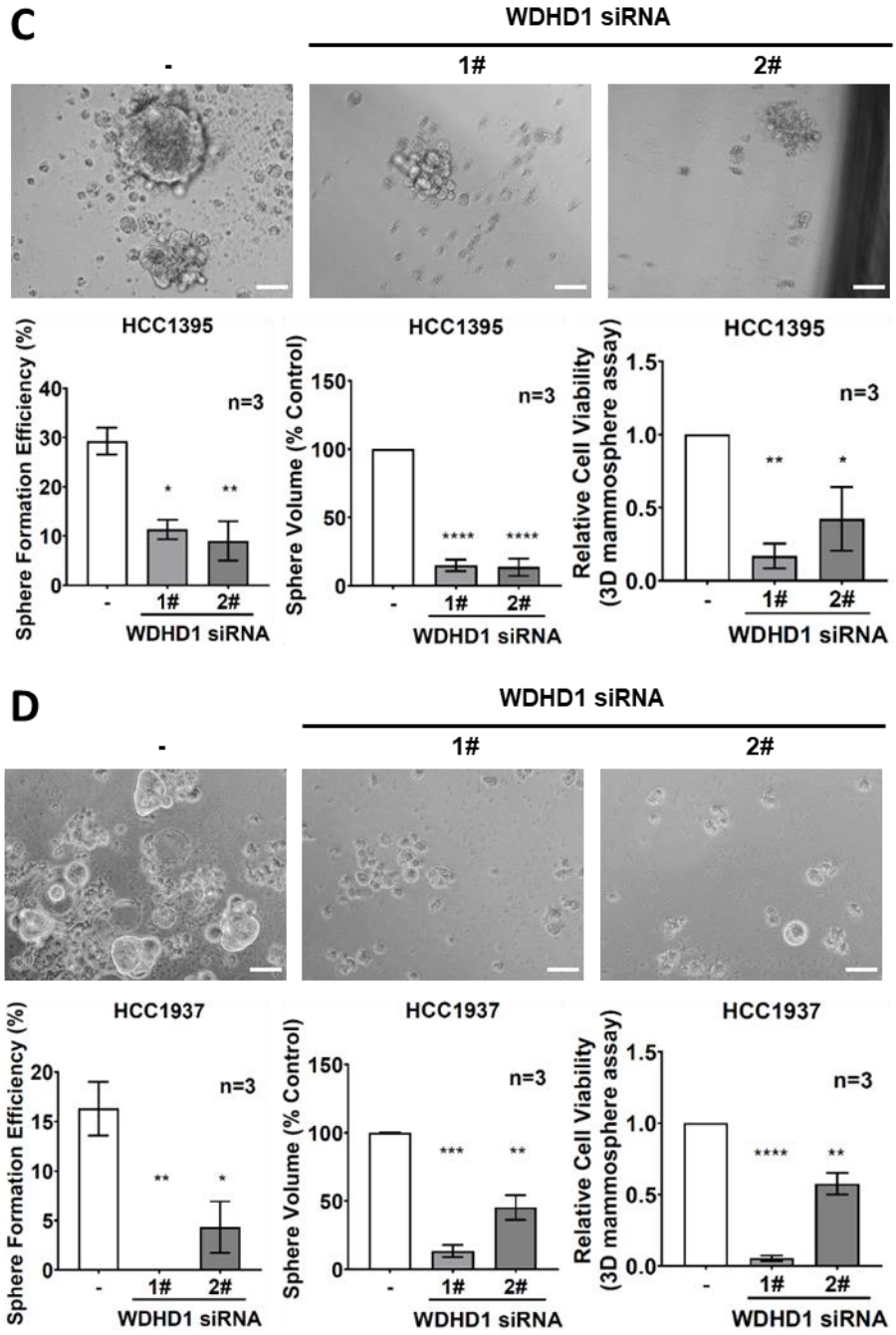

Figure 4.12 WDHD1 is required for the survival of PTEN null TNBC cells cultured in 3D.
(Figure and legend continued from previous page).
WDHD1 expression was knocked-down with two individual *WDHD1* siRNA oligos along with RISC-Free negative control siRNA oligo in PTEN WT TNBC cell line BT20 (**A**) or MDA-MB-231 (**B**) and PTEN null type TNBC cell line HCC1395 (**C**) or HCC1937 (**D**). Cells were plated into low attachment 96 well/plate following four days of *WDHD1* knockdown and grown for up to two weeks in 3D cell culture. Images were observed under light microscope, EVOS, with 40 X magnification. Scale bar: 50 µm. The graphs show sphere formation efficiency, sphere volume and cell viability (Cell-Titer Glo® assay) in BT20 (**A**), MDA-MB-231 (**B**), HCC1395 (**C**) and HCC1937 (**D**) with indicated transfections cultured in 3D. Data are mean ± SEM. Ordinary one-way ANOVA was performed for statistical analysis. **P* ≤ 0.05. ***P* ≤ 0.01. ****P* ≤ 0.001. *****P* ≤ 0.0001. *n* = 3 samples per group.

4.2.4 WDHD1 levels are increased in TNBC compared to normal breast tissues, and associated with tumour size and proliferation

We decided to analyse *WDHD1*, mRNA expression between normal breast samples and TNBC samples. From TCGA analysis, *WDHD1*, mRNA levels were significantly higher in TNBC than the normal breast samples (Fig. 4.13; $P < 0.0001$).

To evaluate the association between *WDHD1* and clinicopathological features in TNBC patients, clinical data from the cBiportal website was extracted (See Appendix Table C.1 and C.2). Table 4.2 shows the association between TNBC patients' clinicopathological features and *WDHD1* expression from TCGA data set. There was no significant association between *WDHD1* expression and the age, location, lymph node and metastatic characteristics of TNBC patients (Table 4.2). On the other hand, the number of patients with Stage II and above, or T2 and above, in the high *WDHD1* TNBC samples was significantly larger than the low *WDHD1* group (Table 4.2; Fig. 4.14A-B; $P < 0.05$).

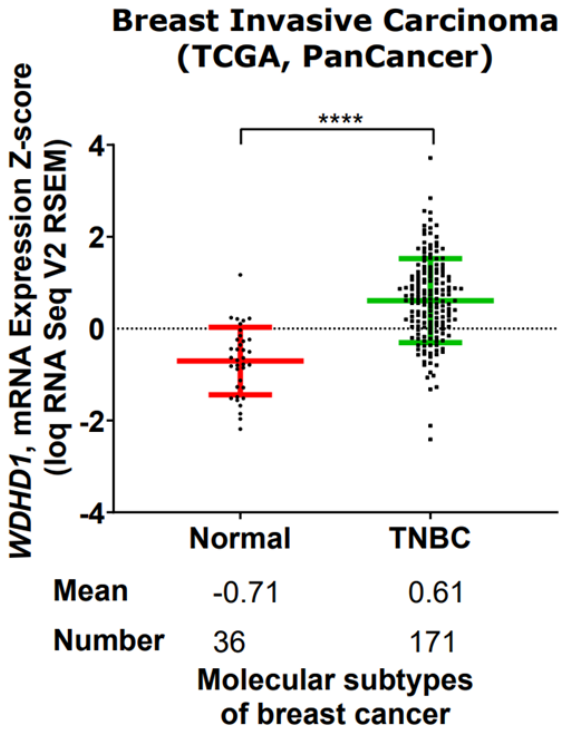

Figure 4.13 *WDHD1*, mRNA expression in normal breast and TNBC samples in TCGA (PanCancer) data from cBioPortal.

The graph shows *WDHD1*, mRNA levels Z-score (log RNA Seq V2 RSEM) in the normal breast ($n = 36$) and TNBC ($n = 171$) samples obtained from the TCGA data. Data are mean ± SD. Unpaired *t-test* was performed for statistical analysis. ****$P < 0.0001$.

Table 4.2 The relationship between TNBC patients' clinicopathological characteristics and *WDHD1* expression in TCGA data.

Characteristics	N	*WDHD1*		*P* value
		Low expression	High expression	
Age	22			
≤ 50	8	5	3	
＞50	14	6	8	0.375
Location	22			
Left breast	7	3	4	
Right breast	15	8	7	0.647
Stage	21			
Stage I	4	4	0	
≥Stage II	17	7	10	***0.034***
Size	22			
<T2	4	4	0	
≥T2	18	7	11	***0.027***
Positive LN	22			
<N2	17	8	9	
≥N2	5	3	2	0.611
Metastasis	22			
<M1	21	10	11	
≥M1	1	1	0	0.306

P values were calculated by χ2 test. Numbers in bold-italics mean *P* values less than 0.05 and are statistically significant. LN: lymph node.

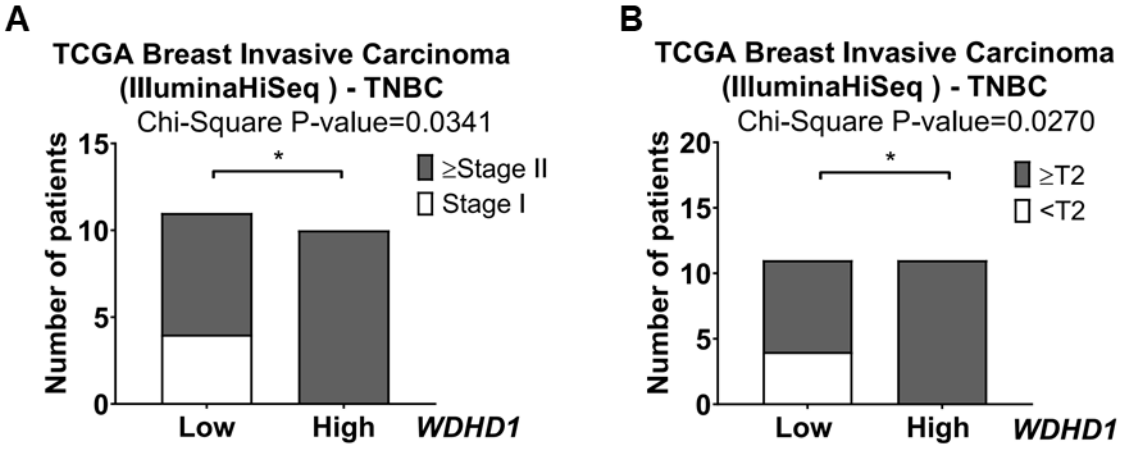

Figure 4.14 The association between *WDHD1* and clinicopathological features for TNBC samples in TCGA (IlluminaHiSeq) data from UCSC Cancer browser.

A) The graph shows the number of TNBC patients (TCGA) with Stage II and above or Stage I in the low or high *WDHD1* group. Statistical significance was determined by χ2 analysis. **P* < 0.05. **B)** The graph shows the number of TNBC patients (TCGA) with T2 and above or < T2 in the low or high *WDHD1* group. Statistical significance was determined by χ2 analysis. **P* < 0.05. Codes are available in Appendix A.1.6.

The association between WDHD1 and clinicopathological features in TNBC patients was further investigated by IHC staining of WDHD1 in a TNBC tissue microarray. We found that tumour grade ($P = 0.03$) and tumour size ($P = 0.016$) were significantly correlated with WDHD1 expression (Table 4.3). Representative images of high and low expression of WDHD1 in TNBC are shown in Figure 4.15A. Moreover, a positive correlation between WDHD1 expression levels (reflected by its IHC scores) and Ki67 percentage (a proliferation marker) was observed in TNBC (Fig. 4.15B; Pearson's correlation $r = 0.3714$; $P = 0.0004$). These findings showed that high WDHD1 levels correlate with advanced clinical stages in TNBC.

Table 4.3 The relationship between TNBC patients' clinicopathological characteristics and WDHD1 expression in tissue microarray.

(Generated by Dr. Huiquan LIU)

Characteristics	N	WDHD1		*P* value
		Low expression	High expression	
Age	90			
≤ 50	46	26	20	
＞50	44	23	21	0.686
Location	90			
Left breast	46	25	21	
Right breast	44	24	20	0.985
Grade	90			
I-II	36	25	11	
III	54	24	30	***0.030***
Size	86			
≤ 2cm	37	26	11	
＞2cm	49	21	28	***0.016***
Positive LN	35			
≤ 2	21	9	12	1.000
＞2	14	6	8	

P values were calculated by χ2 test. Numbers in bold-italics mean *P* values less than 0.05 and are statistically significant. LN: lymph node.

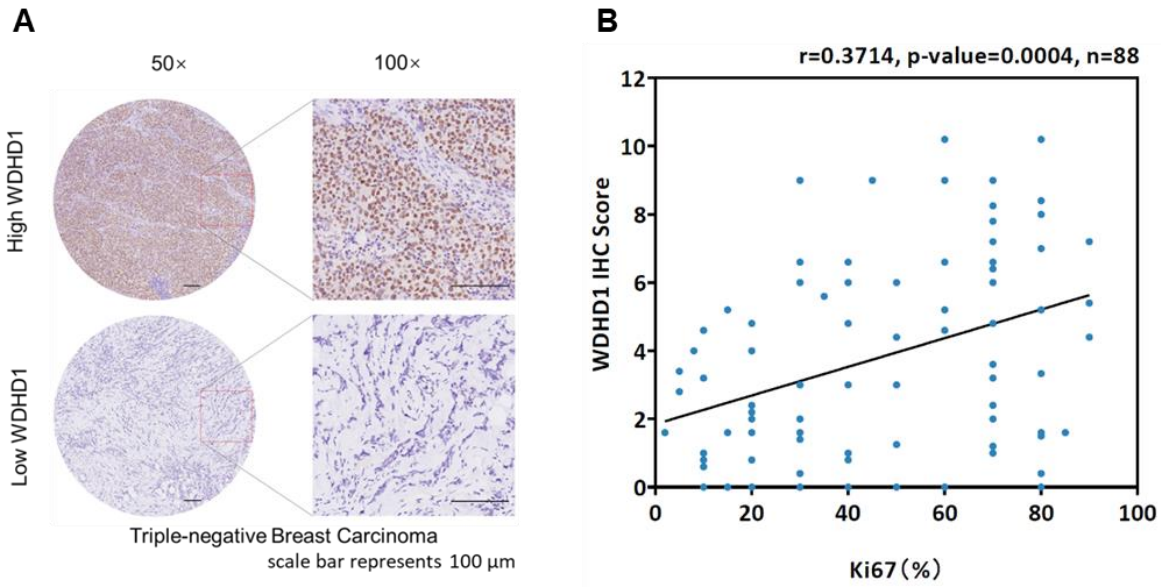

Figure 4.15 WDHD1 is associated with TNBC proliferation.

A) Representative WDHD1 staining pattern (high or low WDHD1) in TNBC tissue microarray cores. Scale bar: 100 µm. **B)** The scatter plot for the correlation between WDHD1 IHC scores and percentage of Ki67-positive cells in TNBC samples (Pearson's correlation $r = 0.3714$; $P = 0.0004$; $n = 88$). **(Generated by Dr. Huiquan LIU)**.

4.3 Discussion

This chapter validated the bioinformatic analysis findings obtained from Chapter 3. We showed that PTEN-inactive TNBC cell lines express higher WDHD1 expression level than PTEN-active TNBC cell lines. *In vitro* work demonstrated that AKT signalling pathway can regulate the expression of WDHD1 in PTEN null TNBC cell lines (Fig. 4.16). Additionally, this chapter validated that WDHD1 is essential for the survival of PTEN null TNBC cells (Fig. 4.16). Both TCGA and tissue microarray findings also showed that WDHD1 is associated with tumour size, stage and proliferation.

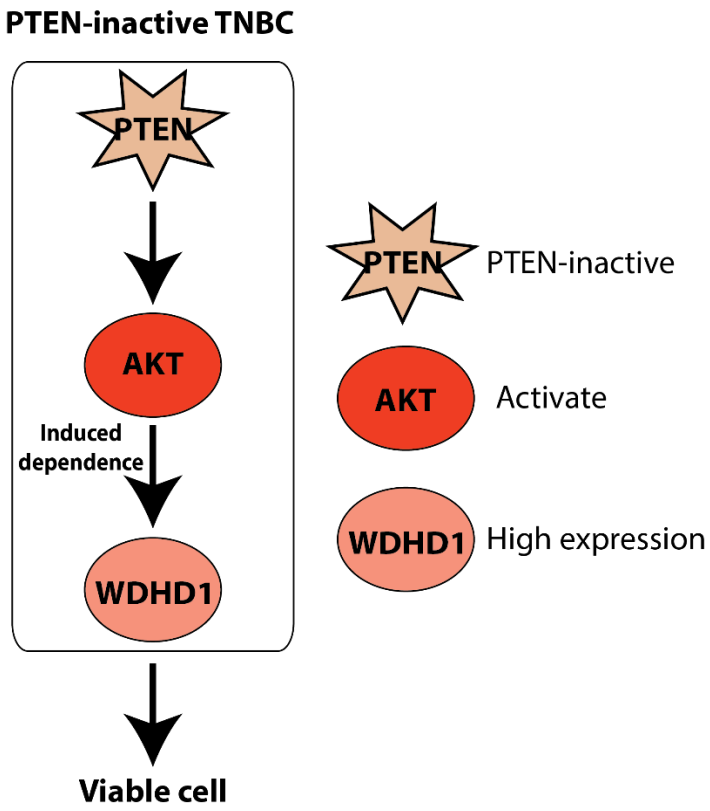

Figure 4.16 WDHD1 is essential for the survival of PTEN-inactive TNBC via the AKT signalling pathway.

Inactive PTEN activates AKT signalling pathway, which then increases WDHD1 expression and leads to the survival of PTEN-inactive TNBC. The star represents the inactive PTEN. Arrows indicate induction. PTEN: phosphatase and tensin homolog; TNBC: triple negative breast cancer; WDHD1: WD repeat and high mobility group [HMG]-box DNA binding protein 1.

We found that AKT activity is different between each TNBC cell line regardless of PTEN status; WT or null (See Appendix Fig. C.1) that may indicate the genetic differences between each cell line. Although BT20 is PTEN WT TNBC cell line, AKT activity is higher than the other PTEN WT TNBC cell lines and this could be because PTEN expression is lower in BT20 compared to other cell lines (Fig. 4.3). Moreover, *PI3KCA* is mutated in BT20 cell line (Weigelt, Warne and Downward, 2011) and we

also showed that AKT activity is higher in *PI3KCA* mutant compared to *PI3KCA* WT samples in Chapter 3 (Fig. 3.4B). Another reason of high AKT activity in BT20 could be due to the amplification of EGFR (Lebeau and Goubin, 1987), which activates AKT signalling pathway. Highest AKT activity was observed in MDA-MB-468 PTEN null TNBC cell line (See Appendix Fig. C.1) and apart from being PTEN null, this cell line also has EGFR amplification (Filmus *et al.*, 1985) that might lead to higher AKT activity compared to the other cell lines.

As mentioned in Chapter 1, section 1.3.4, PTEN inhibits oncogenic AKT signalling pathway, which then leads to reduction of cell growth, proliferation and induction of apoptosis (Myers *et al.*, 1997; Cantley and Neel, 1999). Consistent with this knowledge, we demonstrated that induction of PTEN with two weeks DOX treatment in MDA-MB-468-TR-PTEN cell line, decreased AKT activity, increased cleaved PARP (a marker for apoptosis) and decreased cell viability (Fig. 4.5).

We found that WDHD1 expression is significantly higher in PTEN-inactive TNBC cell lines than PTEN-active TNBC cell lines (Fig. 4.3 and Fig. 4.6). A previous study suggested that AKT can phosphorylate and stabilise WDHD1 expression in different cancers (Sato *et al.*, 2010). To demonstrate whether AKT has an effect on WDHD1 expression in PTEN null TNBC cells, AKT inhibitor was used to inhibit AKT activity. We observed significantly lower WDHD1 expression when AKT activity was inhibited (Fig. 4.7). Similar to the effect of AKT on WDHD1 in PTEN null TNBC cells, we observed a significant positive correlation between AKT activity and *WDHD1*, mRNA levels in TCGA TNBC patients' samples (Fig. 4.9). Taken together, WDHD1 expression is affected by PTEN status in TNBC cells and this is mainly achieved by the AKT signalling. Furthermore, we also showed a reduction of AKT activity when *WDHD1* was knocked-down with two individual siRNA oligos in PTEN null MDA-MB-468 TNBC cells (Fig. 4.8C), which suggests a feedback loop between AKT and WDHD1. Similarly, knockdown of *WDHD1* decreased AKT activity in E7 expressing cells (Zhou *et al.*, 2020). However, only 1 siRNA oligo against WDHD1 showed a significant decrease of AKT activity in HCC1937 PTEN null TNBC cells (Fig 4.8E) and also no significant difference was observed with two individual siRNA oligos in other PTEN null TNBC cells HCC1395 (Fig. 4.8D) and HCC38 (Fig. 4.8F). The reason of these inconsistent results between the cell lines for AKT activity could be due to the different levels of pAKT expression across the cell lines (See Appendix Fig. C.1). As HCC1395, HCC1937 and HCC38 showed lower expression of pAKT than MDA-MB-468 (See Appendix Fig. C.1), the effect of WDHD1 on AKT activity in these cell lines might not be as strong as shown in MDA-MB-468 and it might depend on the AKT expression level.

The reduction of PTEN null TNBC cell viability and proliferation with the knockdown of *WDHD1* in 2D cell culture (Fig. 4.10-4.11), suggested that WDHD1 is essential for the survival of PTEN-inactive TNBC cells. These findings were also supported by 3D cell culture (Fig. 4.12). Both 2D and 3D cell

culture *in vitro* work validated the results obtained from the cross-referencing TCGA and whole genome siRNA screening in Chapter 3, Fig. 3.16.

As shown in table 4.1, WDHD1 expression was higher in lung carcinoma, oesophageal carcinoma, colorectal carcinoma tissue, melanoma, cholangiocarcinoma and cervical cancer compared to their normal cell lines or tissues (Sato *et al.*, 2010; Li, A. N. Jaramillo-Lambert, *et al.*, 2011; B. Liu *et al.*, 2019; Gong *et al.*, 2020; N. Chen *et al.*, 2020; S. Chen *et al.*, 2020). In this study we also observed higher *WDHD1* expression in TNBC compared to normal breast samples in TCGA data (Fig. 4.13). The association between WDHD1 expression and clinical features; tumour size and stage was observed in TCGA TNBC patients' samples (Table 4.2; Fig. 4.14), which was then confirmed with TNBC tissue microarray (Table 4.3). The importance of WDHD1 expression on different clinical features in non-small cell lung carcinoma patients' samples was also discovered previously (Sato *et al.*, 2010). Additionally, TNBC tissue microarray confirmed the link between WDHD1 and Ki67 (Fig. 4.15B). Ki67 is one of the proliferation markers, which is used in various malignancies (Sahebjam *et al.*, 2011). For instance, it has been shown that there was a positive correlation between c-kit expression and Ki67 expression, which suggested high expression of c-kit leads to increased cell proliferation (Brunetti *et al.*, 2014; Fonseca-Alves *et al.*, 2017). Thus, higher expression of WDHD1 leads to increased cell proliferation in TNBC, suggesting a role of WDHD1 in regulating cell viability, in consistence with *in vitro* cell viability or crystal violet assays in PTEN null TNBC cells.

In summary, data presented in this chapter validated the findings identified in Chapter 3, showing that *WDHD1* is required for the survival of PTEN-inactive TNBC cells via the AKT signalling pathway. The data further showed the importance of WDHD1 in clinical features in TNBC. However, functional characterisation of WDHD1 is required, which is presented in Chapter 5.

Chapter 5 Functional characterisation of WDHD1 in PTEN-inactive TNBC

5.1 Introduction

5.1.1 Target proteins of WDHD1 in cancer

Histone acetylation by histone acetyltransferases is one of the post-translational modifications (Shahbazian and Grunstein, 2007). GCN5 as mentioned in section 4.1.4 is one of the histone acetyltransferases, which plays an important role in survival of cancer cells and regulation of oncogenic gene expression (Liu *et al.*, 2003; Nagy and Tora, 2007; Kikuchi *et al.*, 2011). However, the regulation of GCN5 protein was not well known and it was found that WDHD1 has an important role to regulate GCN5 as well as histone H3 acetylation, as mentioned in section 4.1.4 (Li, A. Jaramillo-Lambert, *et al.*, 2011; Li, A. N. Jaramillo-Lambert, *et al.*, 2011). Those studies showed the mechanism between WDHD1 and GCN5, suggesting that in the absence of WDHD1, $CRL4^{Cdt2}$ E3-ligase complexes (composed of a scaffold protein Cullin 4 (Cul4), the adaptor protein DNA damage-binding protein 1 (DDB1), and a substrate receptor protein Cdt2) can interact with GCN5, leading to GCN5 degradation and reduced histone H3 acetylation (Li, A. Jaramillo-Lambert, *et al.*, 2011; Li, A. N. Jaramillo-Lambert, *et al.*, 2011).

One of the major challenges of lung adenocarcinoma is the resistance of tumours to cisplatin but this resistance mechanism was not clear (Gong *et al.*, 2020). A recent study showed that the resistance mechanism could be due to protein ubiquitination and WDHD1 was identified as a ubiquitin ligase (Gong *et al.*, 2020). As mentioned in section 4.1.4, it was also shown that WDHD1 causes cisplatin resistance in lung adenocarcinoma due to the ubiquitination and degradation of MAPRE2 by WDHD1 (Gong *et al.*, 2020).

These studies suggested the mechanisms of WDHD1 that are important for cancer treatment. Thus, it is important to understand its functional role, target proteins or downstream signalling to discover a successful targeted therapy for cancer.

5.1.2 WDHD1 and PTEN/AKT signalling in TNBC

It is well known that PTEN/PI3K/AKT signalling pathway phosphorylates downstream signalling proteins to regulate cell survival, protein synthesis, angiogenesis, EMT/metastasis, cell proliferation and glucose metabolism (Fig. 1.4) (Manning and Cantley, 2007), as mentioned in section 1.3.4.

In this study, *WDHD1* was identified as a top hit gene that might be essential for PTEN-inactive TNBC (Chapter 3). This was then validated with *in vitro* work and patient samples in Chapter 4. Importantly, we showed that WDHD1 is involved in the AKT signalling pathway and its expression is influenced by PTEN status in TNBC cells.

Although the mechanisms of WDHD1 with its target proteins in different cancer types were identified as mentioned in section 5.1.1, those mechanisms could be cell or tissue specific (Gong *et al.*, 2020). Therefore, it is crucial to functionally characterise WDHD1, discover the target proteins or downstream signalling of WDHD1 in PTEN-inactive TNBC, as there are no studies in this field.

The aim of Chapter 5 is to functionally characterise WDHD1 and understand the downstream signalling of WDHD1 in PTEN-inactive TNBC cells.

5.1.3 Summary of the chapter

In this chapter, the aim was to functionally characterise WDHD1 in PTEN-inactive TNBC.

The potential role of WDHD1 in cell cycle and protein translation was observed in PTEN null TNBC cell lines by performing TCGA analysis and IP/MS analysis, respectively. It was discovered that RPS6 and eIF3β are the target proteins of WDHD1 in PTEN null TNBC cell lines.

5.2 Results

5.2.1 Essential role of WDHD1 in cell cycle in PTEN null TNBC cell lines

In order to find the role of *WDHD1* in TNBC, we analysed the data from the TCGA project. As mentioned in section 3.2.6, 92 TNBC samples were identified in mRNA expression (IlluminaHiSeq) of TCGA breast invasive carcinoma data. *WDHD1*, mRNA expression was widely distributed across all TNBC samples (See Appendix Fig. D.1); therefore, the top 10% and bottom 10% samples were separated into two groups: high and low *WDHD1* expressing samples, respectively.

The unpaired *t*-test was performed to identify the significantly different mRNAs between the high and low *WDHD1* groups and those genes with *P* values < 0.05 were considered as differentially expressed genes (DEGs). A heat-map of 3,796 DEGs in the high *vs.* low *WDHD1* groups ($P < 0.05$) is shown in Figure 5.1A. To investigate whether the significantly upregulated 2,069 genes in the high *WDHD1* were enriched in certain cellular functions, ToppGene, (https://toppgene.cchmc.org/) was used. We found that the regulation of cell cycle was enriched in the high *WDHD1* TNBC samples (Fig. 5.1B).

To further validate the findings of *WDHD1* role in cell cycle, hierarchical cluster was performed on the highly correlated genes with *WDHD1* though Pearson analysis in all TNBC samples in TCGA breast invasive carcinoma data set to check whether similar pathways could be observed, as shown in Figure 5.1B. Pearson analysis was performed to find the significantly correlated and anti-correlated mRNAs with *WDHD1*. Figure 5.1C shows the top 50 positively and negatively correlated mRNAs with *WDHD1*. 3,306 positively correlated mRNAs were used in ToppGene for pathway analysis. The pathway analysis for the correlation analysis also showed similar results with Fig. 5.1B, indicating that cell cycle is regulated (Fig. 5.1D).

The identified 47 top hit genes from Chapter 3 (Fig. 3.16) were aligned with 3,306 positively correlated mRNAs with *WDHD1* to check whether there is any overlay between the genes. We observed that 17 genes including WDHD1 were overlay between the identified 47 top hit genes and the genes that were positively correlated with *WDHD1* (Fig. 5.2A-B). This two different analyses showed 17 common genes and supported the findings that obtained from each analysis.

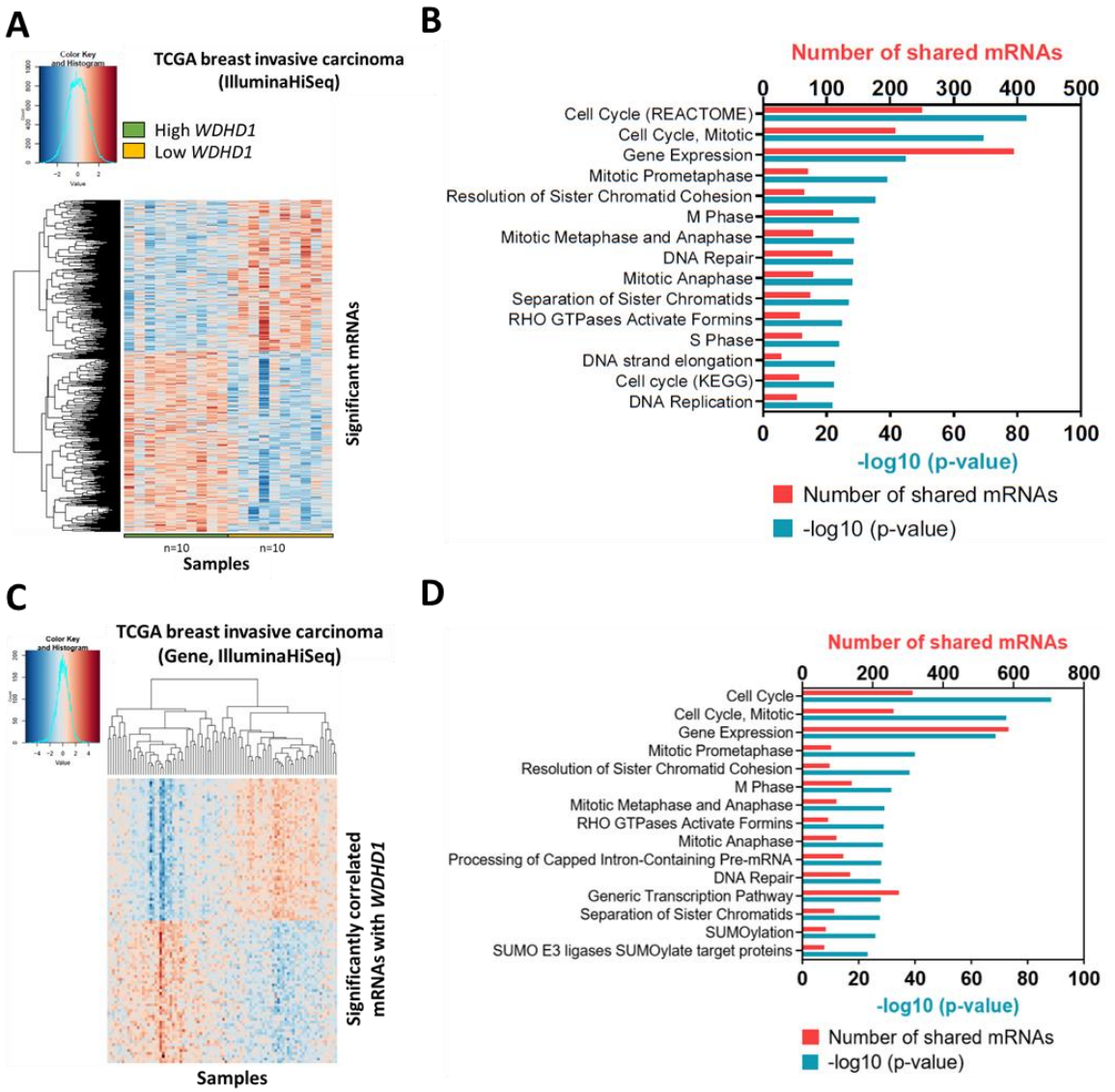

Figure 5.1 TCGA analysis suggests an important role of *WDHD1* in cell cycle regulation.
A) The heat-map shows 3,796 differentially expressed mRNAs between the high and low *WDHD1* expressing TNBC samples obtained from the TCGA analysis. Rows show the individual mRNAs and columns show the individual TNBC samples in the high and low *WDHD1* groups across each mRNA. Red indicates up-regulation and blue indicates down-regulation. Un-paired *t-test* was performed to find the significantly different mRNAs. *P*-value < 0.05. *n* = 10 per group. **B)** Functional enrichment (ToppGene) of up-regulated mRNAs in the high *WDHD1* group was visualised on a bar chart, showing number of shared mRNAs (genes) and -Log10 (*P* value). **C)** The heat-map shows the top 50 genes that had a significantly positive or negative correlation with *WDHD1*. Rows show the individual mRNA and columns show the individual TNBC samples (*n* = 92). Red indicates up-regulation and blue indicates down-regulation. Hierarchical cluster with Pearson analysis was performed. *P*-value < 0.05. **D)** Functional enrichment (ToppGene) of positively correlated mRNAs with *WDHD1* was visualised on a bar chart, showing number of shared mRNAs (genes) and -Log10 (*P* value). Codes are available in Appendix A.1.6.

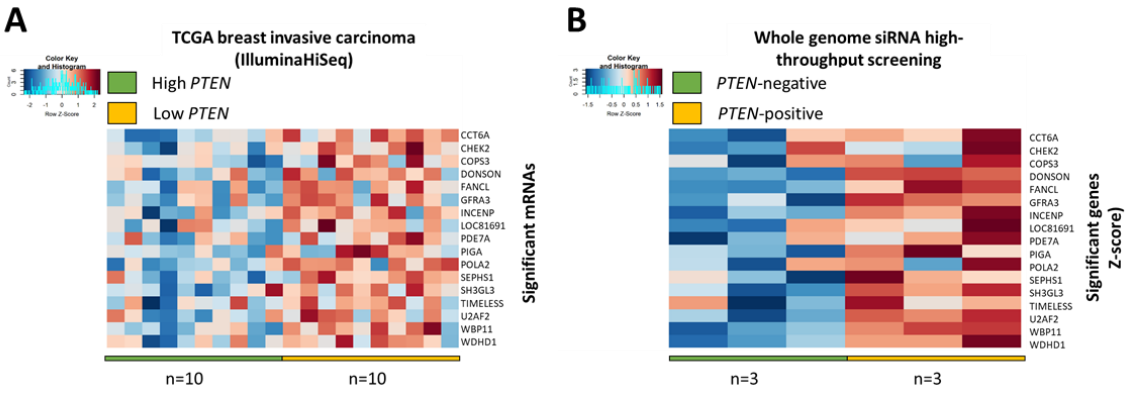

Figure 5.2 Overlay genes between identified top hit genes and genes that were positively correlated with *WDHD1*.

A) The heatmap shows 17 mRNAs that are over-expressed in TNBC samples with the low *PTEN* compared to those with the high *PTEN* from TCGA analysis. Red indicates up-regulation and blue indicates down-regulation. *n* = 10 per group. **B)** The heatmap shows 17 candidate genes that are required for the survival of *PTEN*- TNBC cells from a whole-genome siRNA screen. Red indicates high Z-score and blue for low Z-score. *n* = 3 per group. Codes are available in Appendix A.1.6.

To validate these findings from the TCGA analysis (Fig. 5.1B and D), *WDHD1* expression was depleted by two individual siRNA oligos in TNBC cell lines, followed by cell cycle analysis based on flow cytometry (Fig. 5.3). Depletion of *WDHD1* did not show any significant change in each phase of cell cycle; G_1, S and G_2/M phases in PTEN WT TNBC cell lines: HCC1806 (Fig. 5.3A), BT20 (Fig. 5.3B), MDA-MB-157 (Fig. 5.3C) and MDA-MB-231 (Fig. 5.3D). We observed that G_1 phase was significantly increased with *WDHD1* siRNA 1# oligo in MDA-MB-468 (Fig. 5.3E) and HCC1395 (Fig. 5.3F). Interestingly, depletion of *WDHD1* with two individual siRNA oligos significantly reduced the percentage of cells in S phase in PTEN null TNBC cells: MDA-MB-468 (Fig. 5.3E) and HCC1395 (Fig. 5.3F). These results suggested an important role of WDHD1 in cell cycle regulation in PTEN null TNBC cell lines, consistent with the findings in cell viability assays.

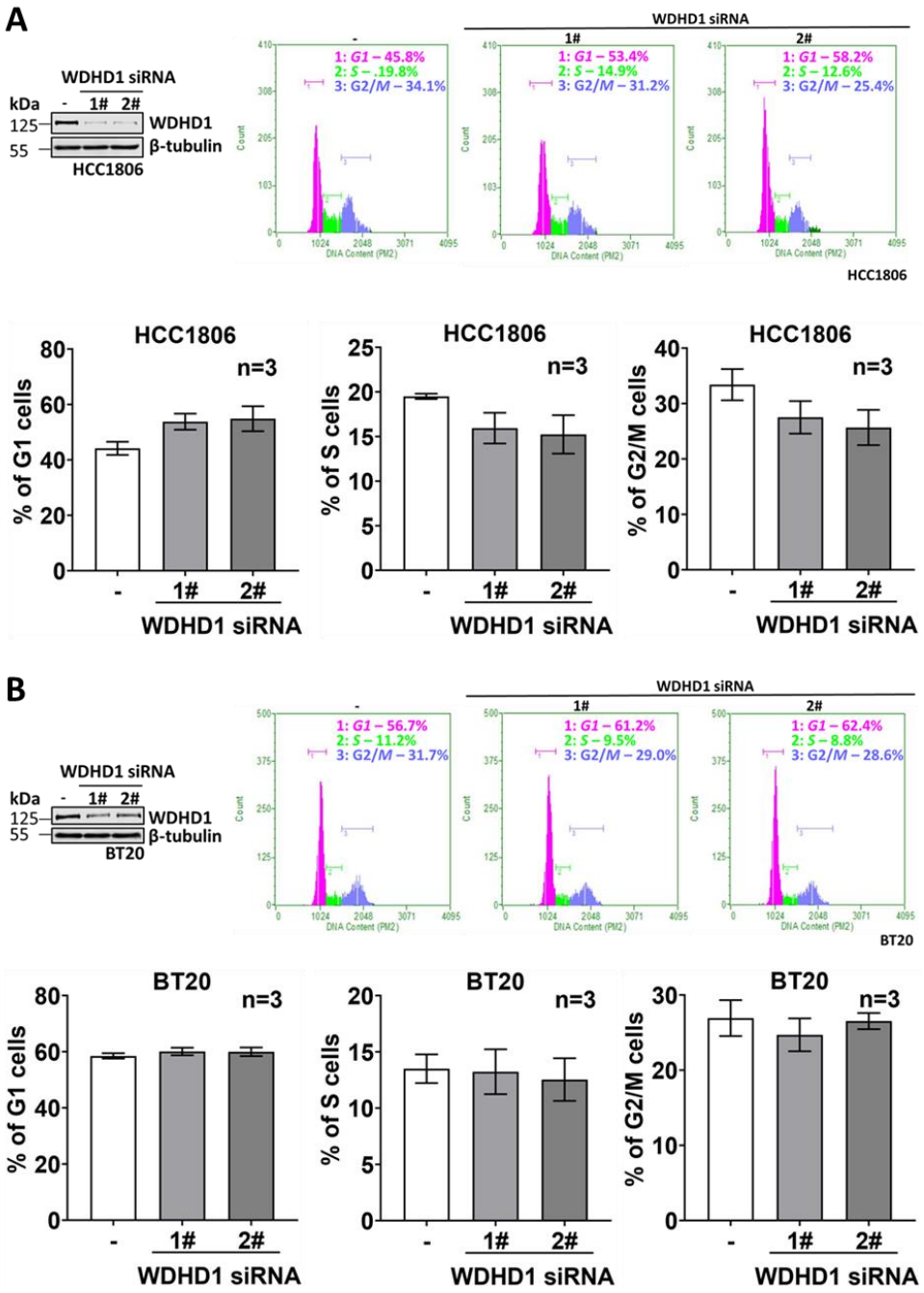

Figure 5.3 *(Figure and legend continued on next pages).*

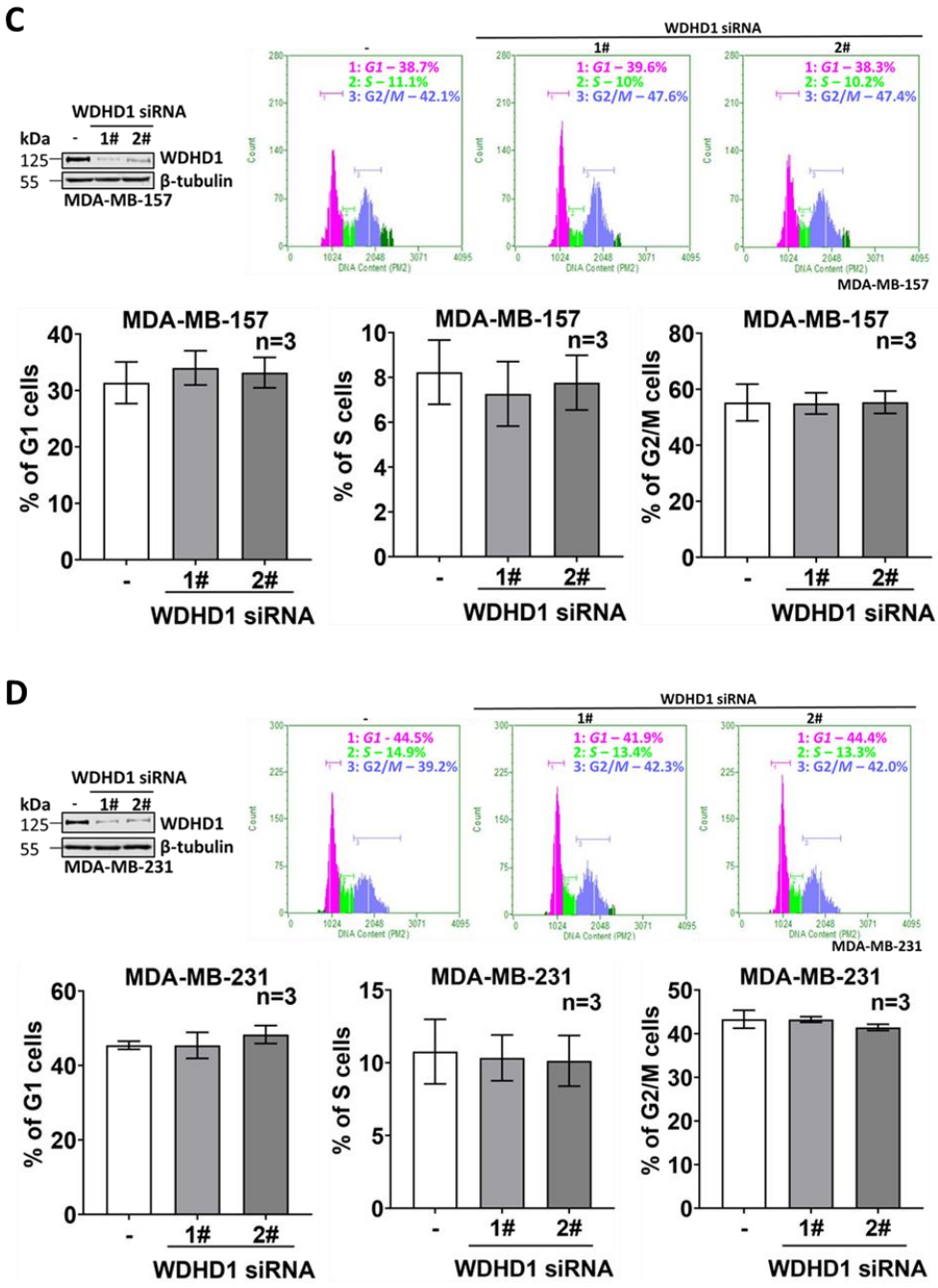

Figure 5.3 *(Figure and legend continued on next page).*

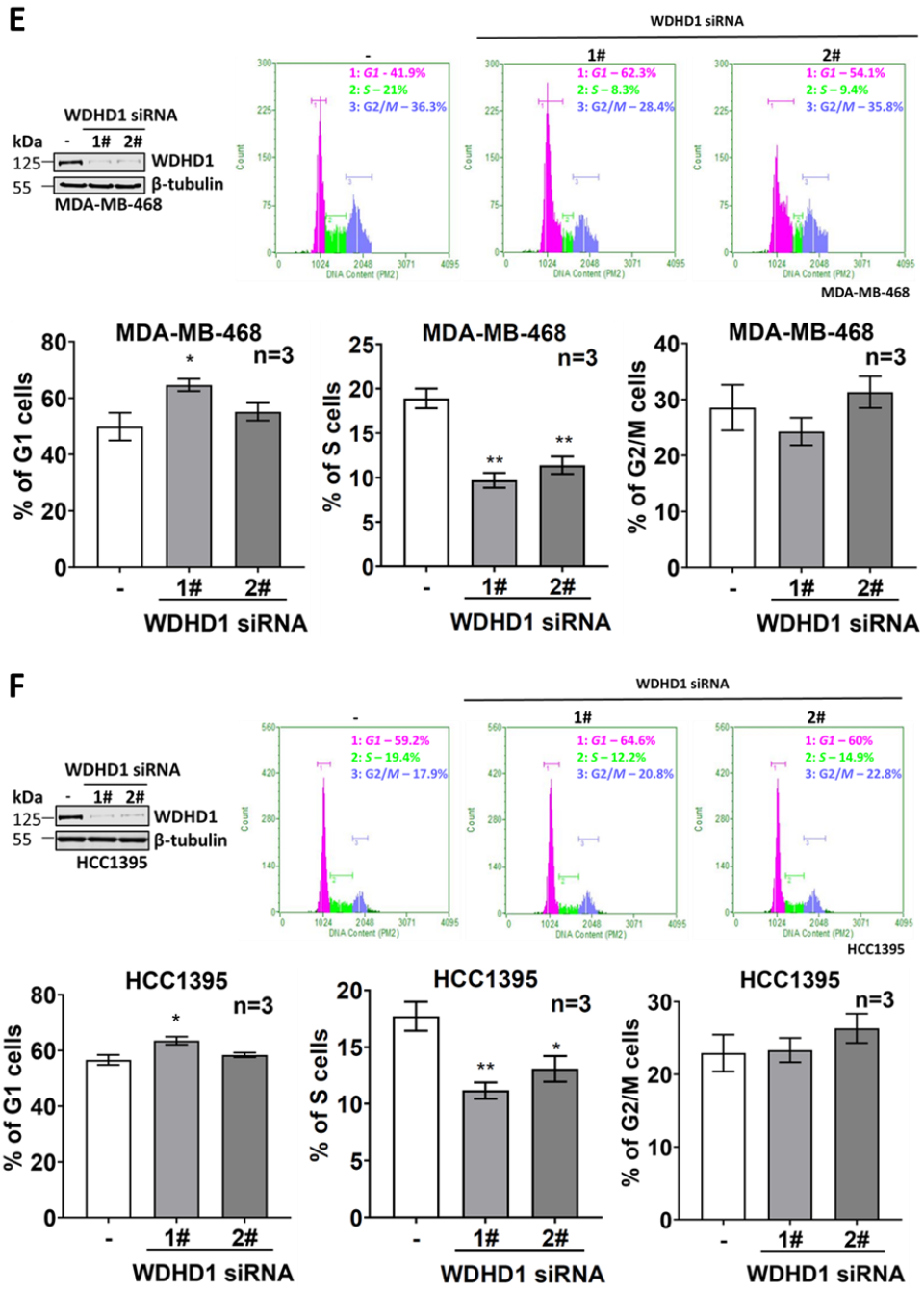

Figure 5.3 Essential roles of WDHD1 in cell cycle in PTEN null TNBC cell lines.

(Figure and legend continued from previous pages).

WDHD1 expression was knocked-down with two individual *WDHD1* siRNA oligos along with RISC-Free negative control siRNA oligo for two days in PTEN WT TNBC cell line HCC1806 (**A**), BT20 (**B**), MDA-MB-157 (**C**) or MDA-MB-231 (**D**) and PTEN null type TNBC MDA-MB-468 (**E**) or HCC1395 (**F**). The top left panels show WDHD1, protein level with indicated transfections by western blot. β-tubulin was used as a loading control. After two days of *WDHD1* siRNA oligo incubation, cells were treated with triton X-100, RNAse A and PI and analysed by flow cytometry, Guava. The top right panels indicate the representative percentage of cells in each phase of cell cycle; G_1, S and G_2/M phases with indicated transfections. The graphs show the percentage of cells in G_1, S or G_2/M phases from HCC1806 (**A**), BT20 (**B**), MDA-MB-157 (**C**), MDA-MB-231 (**D**), MDA-MB-468 (**E**) and HCC1395 (**F**) with indicated transfections. Data are mean ± SEM. Ordinary one-way ANOVA was performed for statistical analysis. **P* < 0.05. ***P* < 0.01. *n* = 3 samples per group.

5.2.2 IP-MS analysis reveals the role of WDHD1 in protein translation in PTEN-inactive TNBC cell lines

Our study investigated that WDHD1 plays an important role in the PTEN/AKT signalling pathway and affects the cell viability/cell cycle. However, to further understand the unknown mechanism of WDHD1 in PTEN-inactive TNBC cell line, endogenous WDHD1 was immunoprecipitated along with control IgG as a negative control in MDA-MB-468 cell lines and mass spectrometry was performed as shown in Figure 5.4.

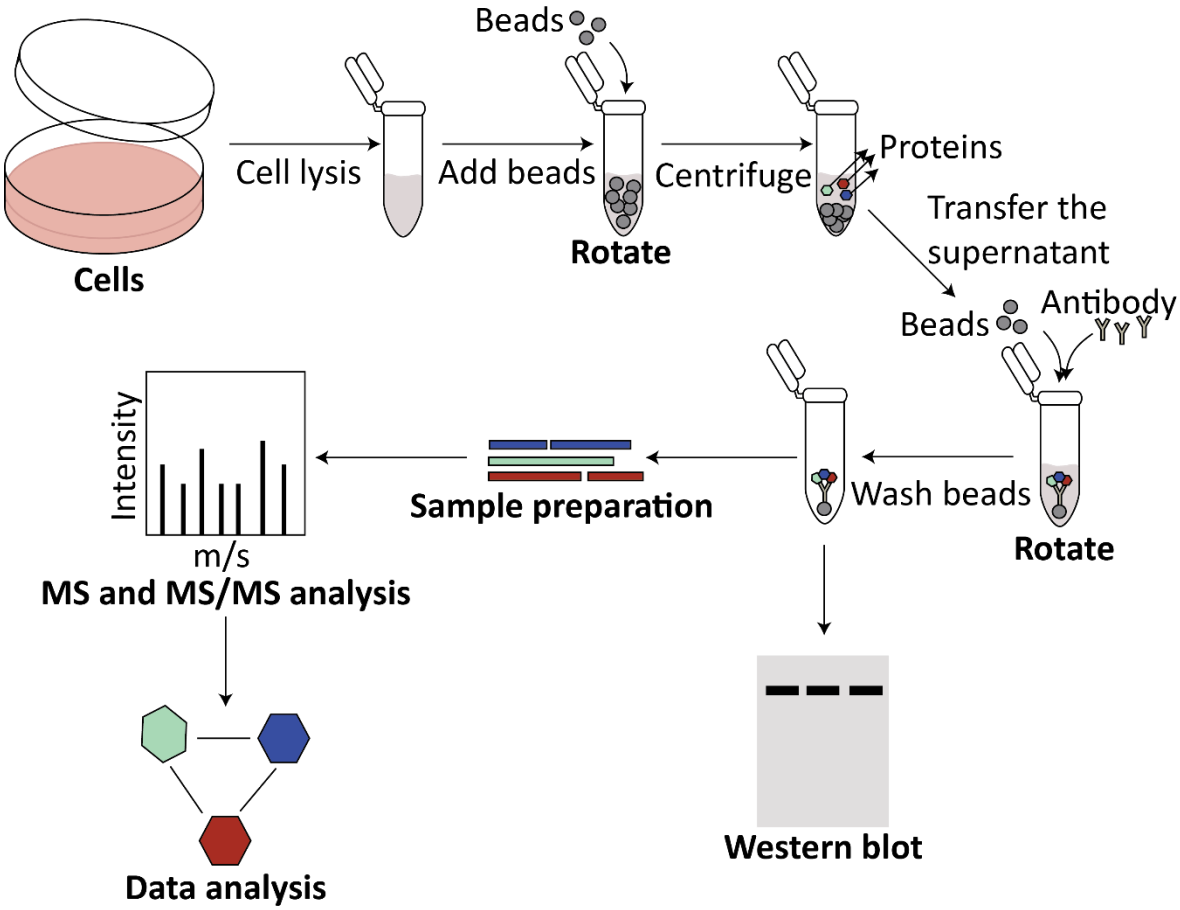

Figure 5.4 Workflow to identify WDHD1 binding partners in PTEN-inactive TNBC cell line. Details are provided in sections 2.13 and 2.15.

Figure 5.5 shows that WDHD1 was successfully immunoprecipitated. WDHD1 pull down and IgG negative control samples were run in mass spectrometry. By performing IP-MS analysis, we identified 64 proteins as WDHD1 binding partners in PTEN null MDA-MB-468 cells (See Appendix Table D.1). Functional enrichment (ToppGene) of WDHD1 binding partners showed a total of 17 functions identified (Table 5.1). The top four functions are shown in Figure 5.6, with protein translation as the top function (Fig. 5.6), which suggests a role of WDHD1 in protein translation in PTEN null TNBC cells.

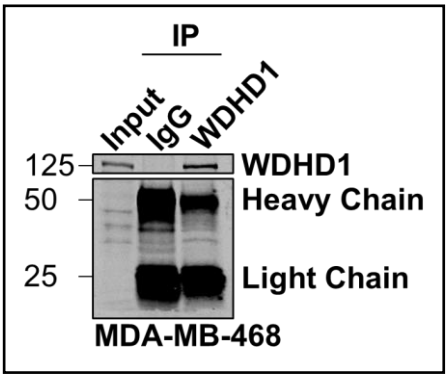

Figure 5.5 WDHD1 is immunoprecipitated in MDA-MB-468, a PTEN null type TNBC cell line.
MDA-MB-468 cells were lysed with pNAS lysis buffer and western blot was run. 40 µg of input and 1 mg/ml immunoprecipitated (IP) samples were run for western blot. Total cell lysates from MDA-MB-468 cell were immunoprecipitated with an anti-WDHD1 antibody or control IgG. WDHD1, IgG heavy and light chains are indicated.

Table 5.1 Functional enrichment (ToppGene) of WDHD1 binding partners identified via IP-MS. Codes are available in Appendix A.1.7.

Pathways	Number of shared proteins	-log10 (*P*-value)	Hit Count in Query List
Translation			
	6	4.2761340355565	RPL35A, EIF2S3, RPS6, RPS16, EIF3B, SEC61A1
MAP00640 Propanoate metabolism			
	3	4.15939212099071	ACAT1, ALDH3A2, MMUT
Formation of the ternary complex, and subsequently, the 43S complex			
	4	4.14472319616991	EIF2S3, RPS6, RPS16, EIF3B
GTP hydrolysis and joining of the 60S ribosomal subunit			
	5	3.92628164965388	RPL35A, EIF2S3, RPS6, RPS16, EIF3B
L13a-mediated translational silencing of Ceruloplasmin expression			
	5	3.92628164965388	RPL35A, EIF2S3, RPS6, RPS16, EIF3B
Ribosomal scanning and start codon recognition			
	4	3.91292879409346	EIF2S3, RPS6, RPS16, EIF3B
Translation initiation complex formation			
	4	3.88639084892697	EIF2S3, RPS6, RPS16, EIF3B
Activation of the mRNA upon binding of the cap-binding complex and eIFs, and subsequent binding to 43S			
	4	3.86012091359876	EIF2S3, RPS6, RPS16, EIF3B
Cap-dependent translation initiation			
	5	3.79317412396815	RPL35A, EIF2S3, RPS6, RPS16, EIF3B
Eukaryotic translation initiation			
	5	3.79317412396815	RPL35A ,EIF2S3, RPS6, RPS16, EIF3B
Gene expression			
	18	3.67223251009727	PPP2R2A, H2BC15, RPL35A, MT-CO2, MARS1, EIF2S3, COX5B, RPS6, CBX3, RPS16, MSH2, EIF3B, NUP93, SEC61A1, MOV10, HNRNPL, HNRNPR, CPSF7
Propanoate metabolism			
	3	3.49566508819754	ACAT1, ALDH3A2, MMUT
Lysine degradation			
	2	3.23965292147009	ACAT1, ALDH3A2
Valine, leucine and isoleucine degradation			
	3	3.12418661116024	ACAT1, ALDH3A2, MMUT
Formation of a pool of free 40S subunits			
	4	3.03254563181726	RPL35A, RPS6, RPS16, EIF3B
Valine, leucine and isoleucine degradation			
	3	3.01327304066878	ACAT1, ALDH3A2, MMUT
Propanoate metabolism			
	2	2.97963871735229	ACAT1, MMUT

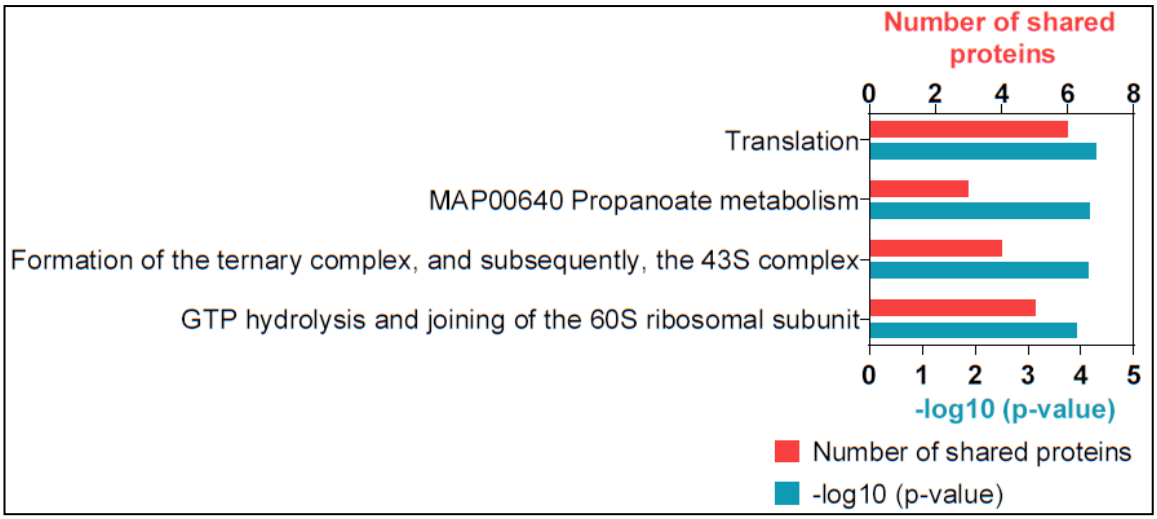

Figure 5.6 WDHD1 plays an important role in translation in MDA-MB-468, a PTEN null type TNBC cell line.

Mass spectrometry with the total cell lysates which were immunoprecipitated with an anti-WDHD1 antibody or control IgG in MDA-MB-468 cells were performed **(by Prof. Paul SKIPP)**. Functional enrichment (ToppGene) of WDHD1 binding partners identified from an IP-MS experiment is visualised on a bar chart, showing number of shared proteins and −Log10 (*P* value). *P*-values < 0.0001 are shown.

5.2.3 WDHD1 depletion reduced the protein translation in PTEN-inactive TNBC cell lines

The pathway analysis showed that WDHD1 might be involved in translation in PTEN null TNBC cells. To verify this finding, puromycin incorporation assay was performed to measure protein synthesis. Puromycin is commonly used to study translation (Dermit, Dodel and Mardakheh, 2017; Hidalgo, Jose and Signer, 2019). Puromycin incorporation stops translation elongation and subsequently induces the release of puromycylated peptides from the ribosome (Nathans, 1964). Unlike radiolabelled amino acids and non-canonical amino acid analogues, puromycin incorporation is not significantly impacted by the endogenous methionine concentration nor the methionine content of proteins (Hidalgo, Jose and Signer, 2019). Puromycin thus incorporates relatively equally into all nascent polypeptides, making it a reliable tool for measuring global protein synthesis.

To optimise the concentration and incubation time point of puromycin, MDA-MB-468-TR-PTEN cell line was cultured. DOX was added to the one set of MDA-MB-468-TR-PTEN cells to induce PTEN expression overnight, which could be a positive control. The following day different concentration of puromycin were added to the cells, in absence or presence of DOX. After 5, 10 and 30 minutes of puromycin incubation, cells were lysed to perform a western blot and identify which puromycin concentration and puromycin incubation time was sufficient for the experiment. Representative images of puromycin incorporation assay for 5 minutes, 10 minutes and 30 minutes are shown in Figure 5.7A-C. Puromycin labelling intensity decreased in the presence of DOX compared to the absence of DOX (Fig. 5.7A-C), indicating reduction of global protein translation. It has been found that 2.5 µM puromycin for 5 minutes incubation showed the biggest reduction of global protein translation compared to the other concentrations and time points (Fig. 5.7D). Therefore, further studies of puromycin incorporation assay were performed with 2.5 µM puromycin for 5 minutes incubation.

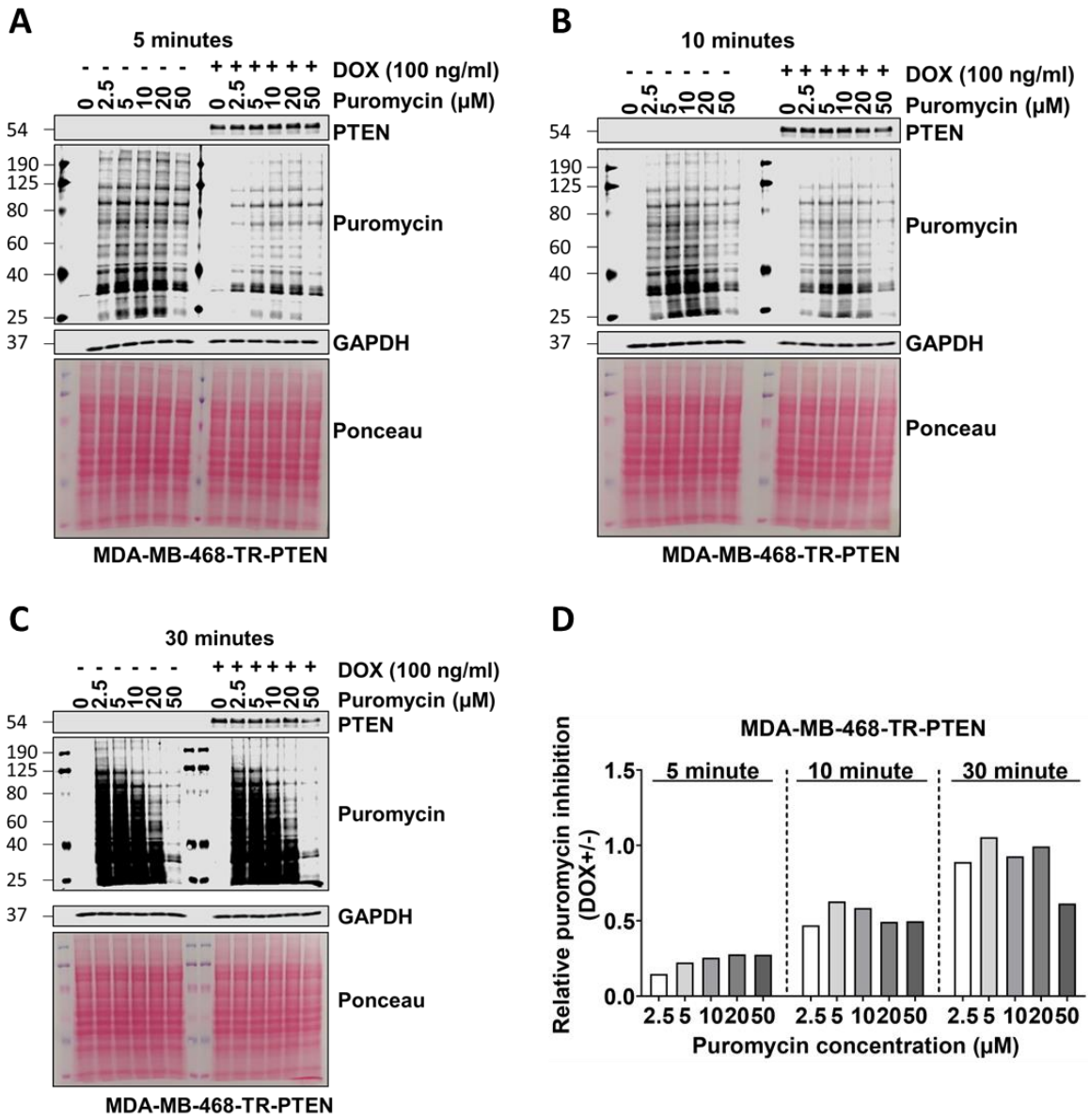

Figure 5.7 Optimisation of puromycin incorporation assay.

MDA-MB-468-TR-PTEN cell line was plated into 6 well plate and 100 ng/ml DOX was added in the following day to the wells (DOX+) and incubated overnight. Following overnight DOX treatment, the cells were treated with different concentration of puromycin (0 µM, 2.5 µM, 5 µM, 10 µM, 20 µM and 50 µM). The cells were incubated with puromycin for 5 minutes (**A**), 10 minutes (**B**) and 30 minutes (**C**). 8 M urea lysis buffer was used for cell lysis after each incubation time period. 30 µg protein was run for western blot to analyse PTEN and puromycin. Puromycin labelling was used to measure protein synthesis in MDA-MB-468-TR-PTEN cells with indicated treatments. GAPDH was used as a loading control. Ponceau S staining shows total protein levels. **D)** The graph shows the quantification of relative puromycin protein inhibition to GAPDH loading control between the absence and presence of DOX in MDA-MB-468-TR-PTEN at different time points for each puromycin concentration.

To observe the effect of WDHD1 expression on translation, *WDHD1* expression was depleted by two individual siRNA oligos in MDA-MB-468-TR-PTEN cells, in the presence (*PTEN*+) (Fig. 5.8A-B) or absence of DOX (*PTEN*-) (Fig. 5.8C-D). We utilised the puromycin incorporation assay, in which cells were treated with 2.5 μM puromycin for 5 minutes before sample collection. Representative images of puromycin incorporation assay with the indicated treatments are shown in Figure 5.8A and Figure 5.8C. There was no reduction in global protein translation when *WDHD1* was depleted in *PTEN*+ cells (Fig. 5.8A-B). As a positive control, PTEN expression was induced in MDA-MB-468-TR-PTEN cells by addition of DOX (Fig. 5.8C). Interestingly, the phosphorylation level of mTOR was not affected by WDHD1 status in *PTEN*- cells (Fig. 5.8C). We were able to show a 25−30% reduction in global protein translation upon PTEN re-introduction (DOX+) compared to the DOX- cells or *WDHD1* depletion in DOX- (Fig. 5.8C-D; $P < 0.05$). As shown in Figure 5.8C and D, depletion of *WDHD1* with two individual siRNA oligos significantly inhibited global protein translation in DOX untreated MDA-MB-468-TR-PTEN cells, reflected by the reductions in the puromycin labelling intensity (Fig. 5.8D; $P < 0.05$).

To further confirm the global protein translation findings obtained from MDA-MB-468-TR-PTEN cells, parental PTEN WT and null TNBC cells were also used for puromycin incorporation assay. Protein translation was measured after *WDHD1* expression was down-regulated with two individual siRNA oligos in PTEN WT (BT20 and MDA-MB-231) and PTEN null (MDA-MB-468 and HCC1937) TNBC cell lines. Knockdown of *WDHD1* in PTEN WT TNBC cell lines did not show a significant change in global protein translation, which was observed with puromycin labelling intensity (Fig. 5.9A-B). *WDHD1* knockdown in PTEN null type TNBC cell lines showed a significant decrease in global protein translation (Fig. 5.9C-D). Thus, consistent with *PTEN*- MDA-MB-46-TR-PTEN cells, parental PTEN null TNBC cell lines showed a reduction of global protein translation with *WDHD1* knockdown.

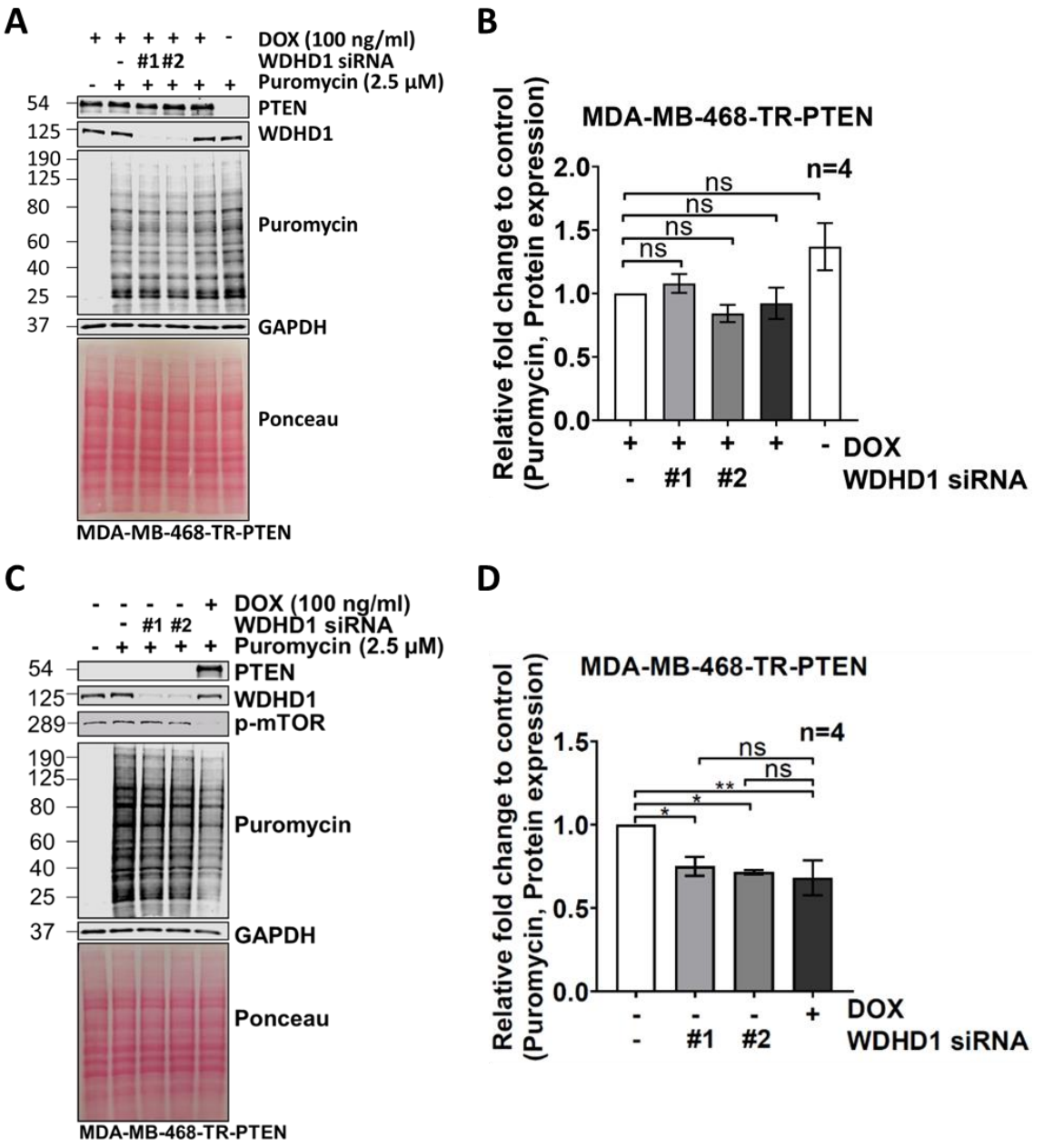

Figure 5.8 Essential roles of WDHD1 in protein translation in *PTEN*-negative TNBC cells.
WDHD1 was knocked-down with two individual *WDHD1* siRNA oligos along with RISC-Free negative control siRNA oligo in MDA-MB-468-TR-PTEN cell line in the presence (*PTEN*+) (**A-B**) or absence (*PTEN*-) (**C-D**) of DOX. 100 ng/ml DOX was added in the following day to the well (DOX+) and incubated overnight. **A)** and **C)** 8 M urea buffer was used to lyse cells after 5 minutes of 2.5 µM puromycin incubation. 30 µg protein was analysed by western blotting showing the levels of PTEN, WDHD1, phospho-mTOR (p-mTOR) and puromycin labelling. GAPDH was used as a loading control. Ponceau S staining shows total protein levels. **B)** and **D)** the graphs show relative puromycin labelling intensity in MDA-MB-468-TR-PTEN cells with indicated treatments. Data are mean ± SEM. Ordinary one-way ANOVA was performed for statistical analysis. **P* ≤ 0.05. ***P* ≤ 0.01 n.s. not significant. *n* = 4 samples per group.

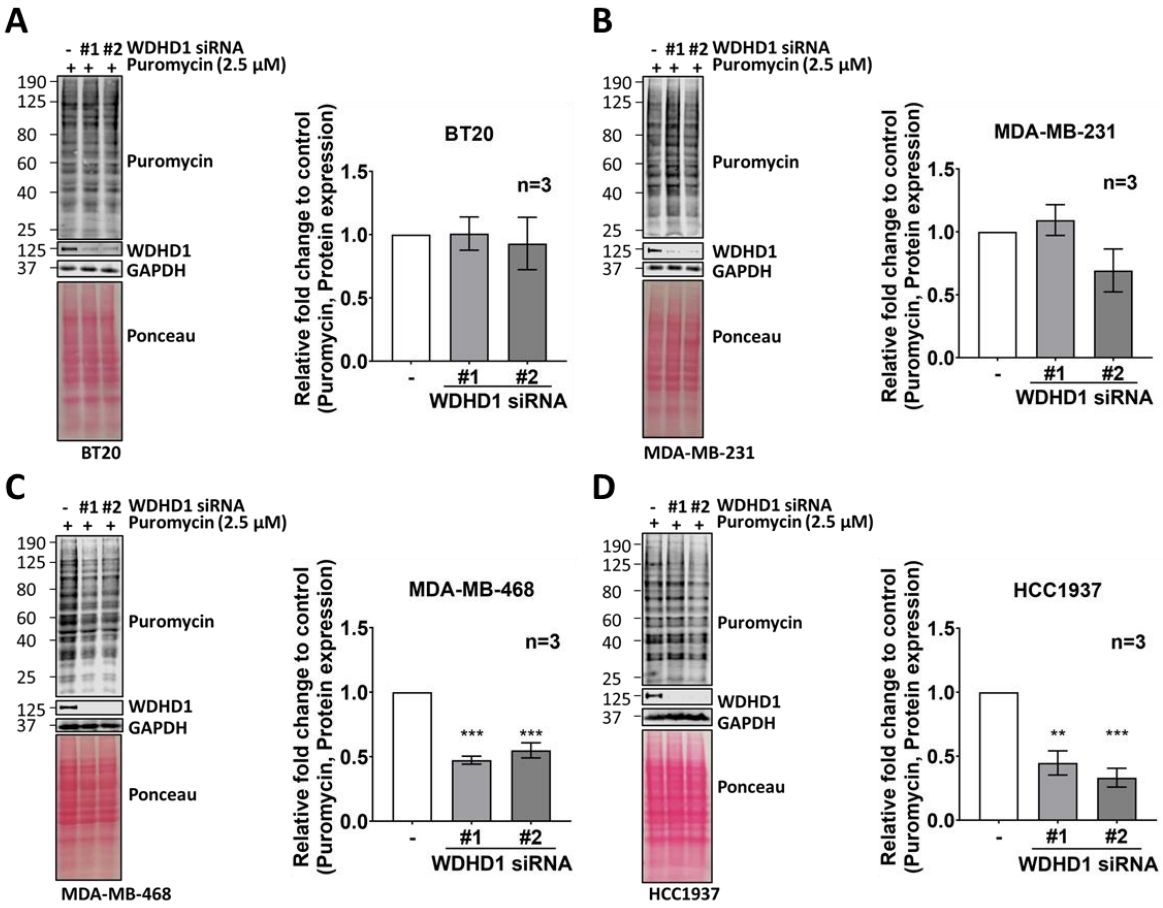

Figure 5.9 *WDHD1* knockdown reduces global protein translation in PTEN null type TNBC cell line. *WDHD1* was knocked-down with two individual *WDHD1* siRNA oligos along with RISC-Free negative control siRNA oligo in PTEN WT TNBC cells BT20 (**A**) and MDA-MB-231 (**B**) and PTEN null type TNBC cells MDA-MB-468 (**C**) and HCC1937 (**D**). Two days after transfection, the cells were treated with 2.5 µM puromycin for 5 minutes. 8 M urea buffer was used to lyse cells and 30 µg protein was analysed by western blotting showing the levels of WDHD1 and puromycin labelling. GAPDH was used as a loading control. Ponceau S staining shows total protein levels. The graphs show relative puromycin labelling intensity in BT20 (**A**), MDA-MB-231 (**B**), MDA-MB-468 (**C**) and HCC1937 (**D**) with indicated treatments. Data are mean ± SEM. Ordinary one-way ANOVA was performed for statistical analysis. $^{**}P \leq 0.01$. $^{***}P \leq 0.001$. $n = 3$ samples per group.

5.2.4 RPS6 and eIF3β are the target proteins of WDHD1 in PTEN null TNBC cell lines

IP-MS analysis identified six WDHD1 potential binding partners that are involved in translation (Table 5.1). Thus, we decided to investigate the interactions of WDHD1 with identified binding partners (including ribosomal protein S6 (RPS6) and eukaryotic translation initiation factor 3 subunit beta (eIF3β)) by performing Co-IP. We validated that RPS6 and eIF3β are potential binding partners of WDHD1 in PTEN null MDA-MB-468 TNBC cell (Fig. 5.10), highlighting the interactions between WDHD1 and the components of translational machinery.

To determine whether WDHD1 can regulate the expression of RPS6 and eIF3β, *WDHD1* was down-regulated with two individual siRNA oligos in PTEN null TNBC cell lines (MDA-MB-468 and HCC1937) and the protein expression of RPS6 and eIF3β was examined with western blot. *WDHD1* knockdown in MDA-MB-468 (Fig. 5.11A) and HCC1937 (Fig. 5.11B) showed a significant decrease in the protein expression of RPS6 and eIF3β compared to the control group.

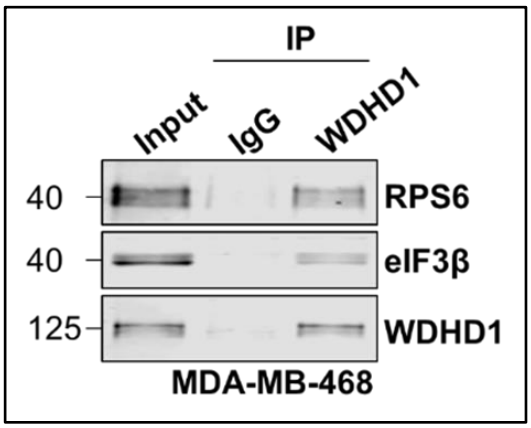

Figure 5.10 WDHD1 interacts with RPS6 and eIF3β in MDA-MB-468 PTEN null TNBC cell line.
MDA-MB-468 cells were lysed with pNAS lysis buffer and western blot was run. Total cell lysates from MDA-MB-468 cells were immunoprecipitated with an anti-WDHD1 antibody or control IgG. RPS6, eIF3β and WDHD1 are indicated. **(Generated by Dr. Huiquan Liu)**.

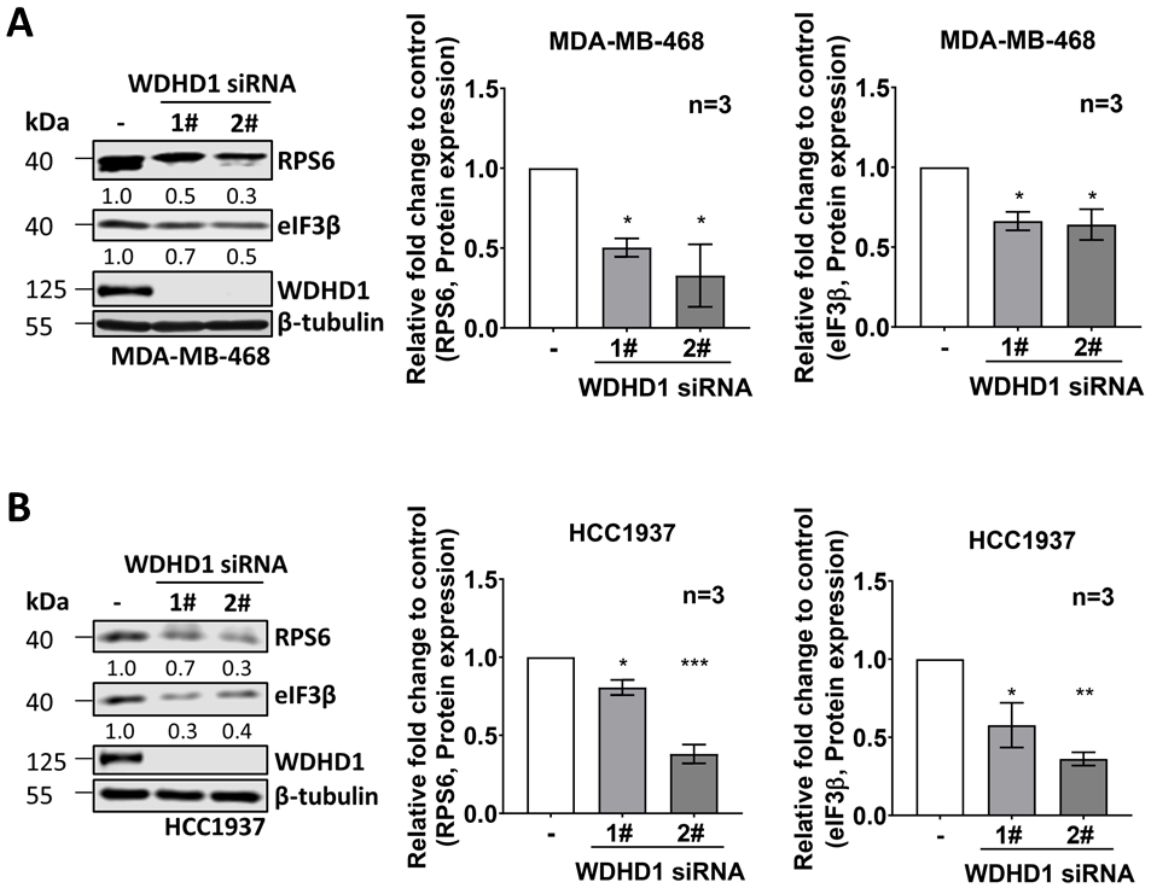

Figure 5.11 RPS6 and eIF3β levels are reduced upon *WDHD1* knockdown in PTEN null TNBC cell lines.

WDHD1 expression was knocked-down with two individual *WDHD1* siRNA oligos along with RISC-Free negative control siRNA oligo in MDA-MB-468 (**A**) and HCC1937 (**B**). 8 M urea buffer was used for cell lysis following 96 hours of knockdown and 15 µg protein was run for western blot. WDHD1, RPS6 and eIF3β protein expression levels were investigated with the indicated transfections. β-tubulin was used as a loading control. The graphs show the protein levels of RPS6 and eIF3β in MDA-MB-468 (**A**) and HCC1937 (**B**) with indicated transfections cultured in 2D cultures. Data are mean ± SEM. Ordinary one-way ANOVA was performed for statistical analysis. **P* ≤ 0.05. ***P* ≤ 0.01. ****P* ≤ 0.001. *n* = 3 per group.

5.3 Discussion

In this chapter, WDHD1 was functionally characterised in PTEN-inactive TNBC cells (Fig. 5.12). TCGA data analysis showed that cell cycle regulation was enriched in the high *WDHD1* TNBC samples and this finding was validated with flow cytometry, which showed that cell cycle is regulated by WDHD1 in PTEN null TNBC cells. Using IP-MS analysis followed by bioinformatic analysis, we identified a potential, yet unknown function of WDHD1 in protein translation in PTEN null TNBC cells. In this chapter, we further showed the potential signalling axis of WDHD1 in protein translation, where WDHD1 can affect the expression of components of translation machinery; RPS6 and eIF3β.

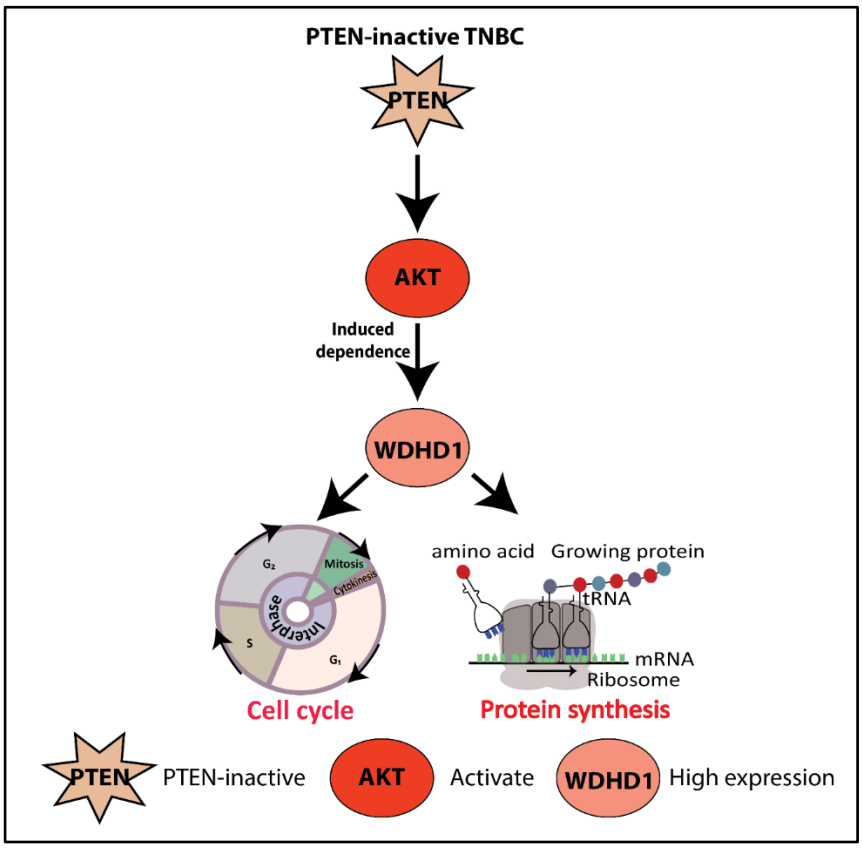

Figure 5.12 Function of WDHD1 in cell cycle and protein translation in PTEN-inactive TNBC cells. High expression of WDHD1 regulates cell cycle and protein translation in PTEN-inactive TNBC cells. The star represents the inactive PTEN. Arrows indicate induction. PTEN: phosphatase and tensin homolog; WDHD1: WD repeat and high mobility group [HMG]-box DNA binding protein 1; TNBC: triple negative breast cancer.

Several studies showed the reduction of cell growth and viability in different cancer types when *WDHD1* was knocked-down (Sato *et al.*, 2010; Wermke *et al.*, 2015; Gong *et al.*, 2020; N. Chen *et al.*, 2020). However, it was not clear how *WDHD1* affect the cell survival in PTEN-inactive TNBC. To understand the mechanism between *WDHD1* and cell survival, TCGA analysis which was then followed by pathway analysis were performed. These analyses identified *WDHD1* might regulate

cell cycle (Fig. 5.1), which was then further validated in 2D cell culture environment (Fig. 5.3) showing a reduction of S phase with *WDHD1* knockdown in PTEN null TNBC cells. It was also previously confirmed that *WDHD1* knockdown decreased the percentage of cells in S phase in lung carcinoma, oesophageal carcinoma and cholangiocarcinoma cell lines (Zhu *et al.*, 2007; Yoshizawa-Sugata and Masai, 2009; Bermudez *et al.*, 2010; Sato *et al.*, 2010; B. Liu *et al.*, 2019). These results suggested an important role of WDHD1 in cell cycle regulation in PTEN null TNBC cell lines, consistent with the findings in cell viability assays in Chapter 3 (Fig. 3.16B; Table 3.3.).

PTEN expression was induced in MDA-MB-468-TR-PTEN cells by addition of DOX and used as a positive control for puromycin assay, since it is known that PTEN inhibits protein translation through negative regulation of mammalian target of rapamycin (mTOR) (Fig. 5.8C) (Simpson and Parsons, 2001). The inhibitory effect of *WDHD1* depletion on protein translation was similar to those achieved by re-introducing PTEN in MDA-MB-468 cells (Fig. 5.8C-D), indicating a potential role of WDHD1 in protein translation in PTEN null TNBC cells. However, knockdown of *WDHD1* did not change the phosphorylation level of mTOR in *PTEN*- TNBC cell lines (Fig. 5.8C), indicating that the impact of WDHD1 on protein translation is independent of mTOR and potentially via directly interacting with the translational machinery. The possible direct interaction of WDHD1 with the translation machinery is supported with Co-IP and down-regulation of WDHD1 experiments in PTEN null TNBC cells (Fig. 5.10 and 5.11), which highlighted that depletion of *WDHD1* reduced the expression of the translation machinery components; RPS6 and eIF3β (Fig 5.11). However, performing the Co-IP experiment (Fig. 5.10) with PTEN null TNBC cell might reflect the limitation of the experiment as it did not show that the potential role of WDHD1 in translation is specific to PTEN null TNBC cells and not to PTEN WT TNBC cells. To discard this limitation, the experiment could be performed both with *PTEN*- and *PTEN*+ TNBC cells.

mTOR is known as the regulator of protein translation, cell growth and metabolism (Schmelzle and Hall, 2000). mTORC1 is one of the catalytic subunit of protein complexes that mTOR forms and acts downstream of AKT signalling pathway (Inoki et al., 2002). RPS6 is a downstream protein of mTORC1, which mediates the function of mTORC1 by promoting translation (Ma et al., 2008). RPS6 is one of the ribosomal proteins of the 40S ribosomal subunit and the phosphorylated form of RPS6 upregulates protein synthesis (Gressner and Wool, 1974). Moreover, one of the key subunits of the translation initiation factor 3 (eIF3) is eIF3β, which is known as a scaffold protein (Feng, Li and Liu, 2018). eIF3β is located into 40S subunit of ribosome, prevents premature joining of 40S and 60S ribosomal subunits, stimulates mRNA binding to 43S pre-initiation complex and initiates the codon recognition (Simonetti et al., 2016).

High expression of RPS6 was observed in various cancer types such as oesophageal squamous cell carcinoma (Kim et al., 2013), oral squamous cell carcinoma (Chaisuparat, Rojanawatsirivej and Yodsanga, 2013), non-small cell lung carcinoma (Chen et al., 2014, 2015), cervical cancer (Campos-Parra et al., 2016) and epithelial ovarian cancer (Yang et al., 2020). It was shown that down-regulation of RPS6 inhibits proliferation and EMT via inducing G_0/G_1 phase arrest and decrease in S phase in epithelial ovarian cancer (Yang et al., 2020) and non-small cell lung carcinoma (Chen et al., 2014). As we also observed the reduction of cells in S phase after *WDHD1* knockdown and the interaction between WDHD1 and RPS6, this might suggest that WDHD1 might affect cell cycle directly and/or indirectly via RPS6. eIF3β expression is also higher in many cancer types; breast cancer (Lin et al., 2001), gastric cancer (Chen and Burger, 2004; L. Wang et al., 2019), colon cancer (Wang et al., 2012), prostate cancer (Wang et al., 2013), bladder cancer (Wang et al., 2013), oesophageal squamous cell carcinoma (Xu et al., 2016, 2019), osteosarcoma (Choi et al., 2017), clear cell renal cell carcinoma (Zang et al., 2017), non-small cell lung carcinoma (C. Liu et al., 2020), and pancreatic cancer (Zhu et al., 2021), and leads to carcinogenesis. Thus, it is considered as an oncogene in different cancer types. PTEN was one of the identified downstream proteins of eIF3β in pancreatic cancer (Zhu et al., 2021) and AKT signalling was identified as a downstream signalling pathway of eIF3β in oesophageal squamous cell carcinoma (Xu et al., 2019) and gastric carcinoma (L. Wang et al., 2019). Although the mechanism of eIF3β in carcinogenesis is not clear yet, these studies suggested that eIF3β affects the progression of cancer cells via feedback loop of AKT signalling pathway. Although our study showed the potential interaction between WDHD1 and RPS6 and eIF3β, further studies, which are mentioned in Chapter 6 are required to support these findings and understand the exact mechanism of WDHD1 in translation within PTEN-inactive TNBC cells.

In this study, we identified the important role of WDHD1 in cell cycle and protein translation (Chapter 5) in PTEN-inactive TNBC cells. As mentioned in Chapter 4, WDHD1 has DNA binding properties and is involved in cell cycle. Moreover, our study showed the role of WDHD1 in protein translation in PTEN null TNBC cells for the first time. Therefore, to verify the subcellular localisation of endogenous WDHD1 in MDA-MB-468-TR-PTEN cells, western blot was performed after NE-PER Nuclear and Cytoplasmic Extraction. Appendix Figure D.2 shows that WDHD1 is abundantly localised in nucleus and weakly localised in cytoplasm both in *PTEN*- and *PTEN*+ TNBC cells and this finding was also supported by previous findings in a study using a lung cancer cell line (Sato *et al.*, 2010). It is well known that protein translation occurs on the ribosomes or endoplasmic reticulum in cytoplasm (Jackson, Hellen and Pestova, 2015). Therefore, our study suggested that WDHD1 is localised in the cytoplasm for its protein translation function and might move to nucleus to control the cell cycle in PTEN-inactive TNBC cells.

In conclusion, data presented in this chapter showed the role of WDHD1 in cell cycle and an unknown potential role of WDHD1 in protein translation via targeting RPS6 and eIF3β that are translation machinery components in PTEN-inactive TNBC.

Chapter 6 Overall Discussion

TNBC lacks all three targetable receptors and has a limited response to chemotherapy. Thus, identifying biomarkers for TNBC early detection or therapeutic treatment strategies to improve response rates are crucial. For instance, one of the well-known targeted therapies is imatinib (small molecule kinase inhibitor) for chronic myeloid leukaemia (CML), which targets BCR-ABL1 fusion protein. Imatinib improved the 10-year survival rate of patients from 20% to approximately 83% (Hochhaus *et al.*, 2017). Moreover, trastuzumab is the first FDA approved targeted therapy for HER2+ breast cancer, which was combined with first-line chemotherapy and improved overall survival rate, delayed the disease progression and improved the response rate and response duration (Slamon *et al.*, 2001).

Targeted therapies are specific to special genes or proteins in cancer cells, which lead to lower toxicity to the normal cells (Padma, 2015). However, the main problem of the targeted therapy might be the drug resistance due to the different mechanisms (Ke and Shen, 2017). One of the resistance mechanisms is alterations or mutations of functional targets (Saijo, 2012). Activation of various signalling pathways is possible while targeting specific genes or proteins; targeting the upstream of the signalling pathway might lead to mutation of other genes/proteins in the downstream of the signalling pathway or vice versa (Ke and Shen, 2017). For instance, although trastuzumab is the gold standard treatment option for HER2+ breast cancer, some patients with HER2+ breast cancer showed resistance to trastuzumab (Vu and Claret, 2012; Maximiano *et al.*, 2016). This resistance mechanism could be due to the structural modification of HER2 protein such that mutated HER2 changes its structure to a truncated receptor that lacks extracellular domain, leads to oncogenic signalling activation, and prevents the effect of trastuzumab (Scaltriti *et al.*, 2007). Moreover, trastuzumab upregulates the expression of *c-MET in vitro,* which encodes hepatocyte growth factor receptor and leading to abnormal activation of PI3K pathway (Shattuck *et al.*, 2008). Another trastuzumab resistance mechanism is the intracellular changes in the downstream signalling of HER2, which includes loss of PTEN and mutation of PI3K and this leads to activation of PI3K/AKT signalling pathway (Berns *et al.*, 2007; Kataoka *et al.*, 2010). Therefore, understanding the signalling pathway in cancer is very important for the effect and response of a potential drug. To overcome these problems, combination treatment to block different pathways or different genes in a signalling pathway may be required to achieve better treatment response (Stratikopoulos *et al.*, 2015).

As TNBC is difficult to be targeted and is molecularly heterogeneous, further stratification is needed. TNBC was subdivided into six distinct subtypes: BL1, BL2, IM, M, MSL and LAR (Lehmann *et al.*, 2011). Another study re-classified TNBC into five stable subtypes: BL1, IM, M, MSL and LAR (Bareche *et al.*, 2018). PTEN inactivation was observed in the BL1 subtype (Bareche *et al.*, 2018), which was further confirmed in a recent *in silico* analysis, showing exceedingly poor clinical outcome (D. Y. Wang *et al.*, 2019). Therefore, understanding the molecular basis of TNBC heterogeneity is important to discover a possible novel biomarker or targeted therapy for this disease. Moreover, there are various studies on signal transduction pathways to identify new treatment, for instance, Atezolizumab is the first immunotherapy, which is combined with chemotherapy for PD-L1 positive TNBC (Cyprian *et al.*, 2019).

As mentioned in Chapter 1, section 1.5.1, inactive tumour suppressor genes can alter the downstream signalling pathways. Therefore, targeting downstream signalling pathway, known as synthetic lethality, is an alternative approach to treat cancers that have inactive tumour suppressor genes. In this study, using TCGA analysis coupled with a whole-genome siRNA screen in isogenic *PTEN*- and *PTEN*+ TNBC cells, we identified *WDHD1* as a synthetic essential gene in PTEN-inactive TNBC cells.

WDHD1, an orthologue of Ctf4 in budding yeast (Kang *et al.*, 2013) and Mcl1 in fission yeast (Williams and Mcintosh, 2002), is a DNA-binding protein (Köehler, Schmidt-Zachmann and Franke, 1997) that is known to play important roles in DNA replication and cell cycle (Zhu *et al.*, 2007; Bermudez *et al.*, 2010; Sato *et al.*, 2010; Kang *et al.*, 2013; Zhou *et al.*, 2016; Guan *et al.*, 2017; Kilkenny *et al.*, 2017; Abe *et al.*, 2018).

We found WDHD1 expression is significantly higher in PTEN-inactive TNBC cells than in PTEN-active cells. A previous report suggested that AKT kinase seems to phosphorylate and stabilise the WDHD1 protein in cancer cells (Sato *et al.*, 2010). In addition to the reported effects of AKT on WDHD1 protein stability, we found the mRNA levels of WDHD1 are also regulated by the PTEN-AKT pathway. Thus, WDHD1 expression is influenced by PTEN-AKT signalling in TNBC cells at both mRNA and protein levels.

We also observed an important role of WDHD1 in cell cycle, especially in PTEN-inactive TNBC cells. The selective killing of *WDHD1* depletion in PTEN-inactive TNBC cells was further validated in both 2D and 3D cultures. In addition, using IP-MS analysis followed by bioinformatic analysis, we identified a potential, yet unknown function of WDHD1 in protein translation in PTEN null TNBC cells, which was further validated with puromycin incorporation assay to measure global protein synthesis. Depletion of *WDHD1* significantly inhibits global protein translation in PTEN null TNBC cells, which is independent of mTOR inhibition and potentially via directly interacting with the

translational machinery. WDHD1 has a potential to affect the translation via regulating the translation machinery components; RPS6 and eIF3β. The impact of *WDHD1* depletion on global protein translation is similar to the effect achieved by re-introducing PTEN. PTEN inactivation in TNBC leads to a high activity of mTOR (Ní Bhaoighill and Dunlop, 2019), which is linked to a high rate of protein synthesis, creating an "Achilles heel" of TNBC. Indeed, several clinical trials on Everolimus (a mTOR inhibitor) in TNBC are ongoing (clinicaltrials.gov), some of which showed positive results (Singh *et al.*, 2014; Lee *et al.*, 2019). However, a common pattern seen in trial data is a modest response to rapalog (rapamycin and its analogues) monotherapy, which does not lead to a significant improvement in patient outcomes. One of the likely reasons is that it is caused by reactivation of signalling pathways that drive the high rate of protein synthesis required by tumour growth. Inhibition of WDHD1 in a PTEN-inactive background reduces protein translation, suggesting that such a "synthetic sickness" approach may be applicable to PTEN-deficient tumours when rapalog resistance happens.

Although further studies are required (mentioned in section 6.1), our and previous findings suggest that WDHD1 affects the survival of PTEN null TNBC cells via the AKT signalling pathway by regulating the cell cycle and translation machinery components; RPS6 and eIF3β (Fig. 6.1).

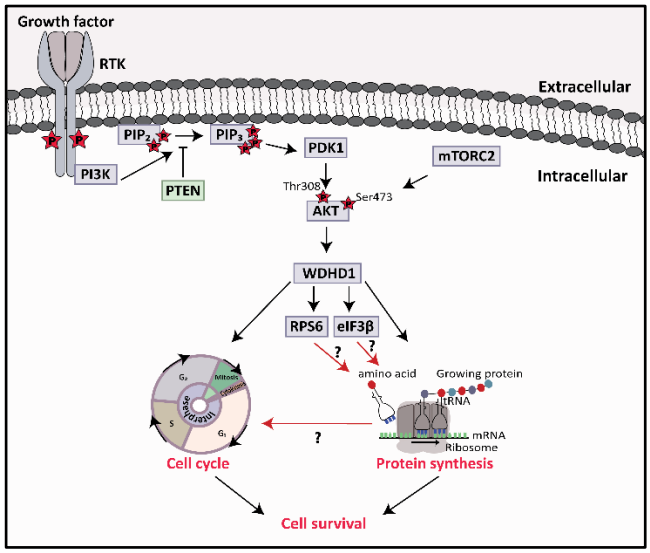

Figure 6.1 Potential novel signalling pathway of WDHD1 in PTEN-inactive TNBC cells.
WDHD1 is overexpressed via the AKT signalling pathway in PTEN-inactive TNBC cells that has an impact on cell cycle and protein synthesis. Red arrows with the question mark represent the unknown part of the signalling pathway, which require further studies. P in red star indicates phosphorylation. Arrows indicate induction. PTEN: phosphatase and tensin homolog; RTK: receptor tyrosine kinase; PI3K: phosphoinositide 3-kinase; PIP_2: phosphatidylinositol 4,5-bisphosphate; PIP_3: phosphatidylinositol 3,4,5-triphosphate; PDK1: phosphoinositide-dependent kinase 1; mTORC2: mammalian target of rapamycin complex 2; WDHD1: WD repeat and high mobility group [HMG]-box DNA binding protein 1; RPS6: ribosomal protein S6; eIF3β: eukaryotic translation initiation factor 3 subunit beta.

A potential role of WDHD1 in regulating the stemness of PTEN-inactive TNBC cells was investigated using a mammosphere formation assay, which is one of the assays used to determine cell stemness (Nalla, Kalia and Khairnar, 2019). Given the impact of WDHD1 on cell cycle and protein translation, both of which play important roles in regulating cell stemness (Tahmasebi, Amiri and Sonenberg, 2019), we presume that WDHD1 may control stemness in PTEN-inactive TNBC cells via its ability to regulate cell cycle and protein translation; however, this remains to be elucidated.

A recent report demonstrated that overexpression of WDHD1 leads to cisplatin resistance in lung adenocarcinoma (Gong *et al.*, 2020). Moreover, cisplatin is also used to treat TNBC but the resistance of the cells to the drug is also the main problem (Carey *et al.*, 2012; Nedeljkovic and Damjanovic, 2019). Although further studies are required to confirm these findings (mentioned in Section 6.1) in TNBC, the data presented here suggest that inhibitors that can disrupt the interactions between WDHD1 and the protein synthesis machinery could target some of the most intractable tumour types, such as TNBC with PTEN-deficiency. The relatively mild effects of WDHD1 depletion in *PTEN*+ cells suggests that on-target inhibition of this factor may also be relatively free from unwanted side effects.

6.1 Future studies

- **Evaluate whether WDHD1 can control stemness in PTEN-inactive TNBC cells**

In this study, we observed that down-regulation of *WDHD1* decreased the cell viability, sphere volume and MFE in 3D cell culture (Fig. 4.12). *In vitro* 3D cell culture is known to mimic the stemness features of cancer cells (Serrano-oviedo *et al.*, 2020). Thus, investigating the expression of WDHD1 in PTEN WT and null type cells in 3D cell culture is important to compare the expression of WDHD1 between 2D and 3D cell culture environment.

- **Examine the expression of RPS6 and eIF3β in PTEN-inactive TNBC cells**

As we observed the interaction between WDHD1 and RPS6 and eIF3β in PTEN null TNBC cells, it is important to examine the expression of RPS6 and eIF3β in parental PTEN WT and null and isogenic *PTEN*- and *PTEN*+ TNBC cell lines by western blot.

- **Further investigation of WDHD1, RPS6 and eIF3β signalling axis in PTEN null TNBC cells**

Down-regulation of WDHD1 reduced the expression of translation machinery components; RPS6 and eIF3β (Fig. 5.11). To further investigate whether there is a positive feedback loop between WDHD1 and translation machinery components, RPS6 and eIF3β can be downregulated by using siRNA oligos and the expression of WDHD1 and pAKT can be examined.

To validate that RPS6 and eIF3β are the downstream proteins of AKT, AKT inhibitor VIII can be used to inhibit AKT activity and check its effect on RPS6 and eIF3β expression.

To further understand that WDHD1 affects the cell viability of PTEN-inactive TNBC (in the control group and WDHD1 overexpression group) via directly affecting translation machinery, cell viability assay can be performed after RPS6 and eIF3β siRNA transfection.

- **Investigate whether the disruption of interactions between WDHD1 and the protein synthesis machinery could target PTEN-inactive TNBC cells.**

Our study demonstrated that depletion of *WDHD1* reduced the global protein translation via potential interaction with translation machinery. Thus, PTEN-inactive TNBC cells can be treated with mTOR inhibitor, as mentioned in Chapter 6, with the combination of *WDHD1* knockdown to investigate whether the reduction of *WDHD1* can sensitise PTEN-inactive TNBC cells to the mTOR inhibitor.

As mentioned in Chapter 6, cisplatin is also used to treat TNBC but the disease develops a resistance mechanism. Therefore, it might be important to investigate the response of PTEN-inactive TNBC to cisplatin and if the cells are resistant to cisplatin, this could be due to the overexpression of WDHD1 in PTEN-inactive TNBC. Thus, down-regulation of *WDHD1* might help to overcome the cisplatin resistance in PTEN-inactive TNBC cells.

- **Validate the findings with *in vivo* studies**

It would be important to validate the findings obtained from this study in a mouse model. The functional role of WDHD1 in mammals with mice work is not well-known. The validation of WDHD1 role in PTEN-inactive TNBC with *in vivo* work could be performed with the CRISPR/Cas9-mediated genome editing system which was used in a recent study (Fan *et al.*, 2021).

List of References

Abbotts, R. *et al.* (2014) 'Targeting human apurinic/apyrimidinic endonuclease 1 (APE1) in phosphatase and tensin homolog (PTEN) deficient melanoma cells for personalized therapy', *Oncotarget*, 5(10), pp. 3273–3286. doi: 10.18632/oncotarget.1926.

Abe, T. *et al.* (2018) 'AND-1 fork protection function prevents fork resection and is essential for proliferation', *Nature Communications*, 9(1), p. 3091. doi: 10.1038/s41467-018-05586-7.

Acevedo-Gadea, C. *et al.* (2015) 'Sirolimus and trastuzumab combination therapy for HER2-positive metastatic breast cancer after progression on prior trastuzumab therapy', *Breast Cancer Research and Treatment*, 150(1), pp. 157–167. doi: 10.1007/s10549-015-3292-8.

Agrawal, S., Pilarski, R. and Eng, C. (2005) 'Different splicing defects lead to differential effects downstream of the lipid and protein phosphatase activities of PTEN', *Human Molecular Genetics*, 14(16), pp. 2459–2468. doi: 10.1093/hmg/ddi246.

Al Ajmi, K. *et al.* (2020) 'Association of nongenetic factors with breast cancer risk in genetically predisposed groups of women in the UK biobank cohort', *JAMA Network Open*, 3(4), p. e203760. doi: 10.1001/jamanetworkopen.2020.3760.

Al-Khouri, A. M. *et al.* (2005) 'Cooperative phosphorylation of the tumor suppressor phosphatase and tensin homologue (PTEN) by casein kinases and glycogen synthase kinase 3β', *Journal of Biological Chemistry*, 280(42), pp. 35195–35202. doi: 10.1074/jbc.M503045200.

Al-Subhi, N. *et al.* (2018) 'Targeting ataxia telangiectasia-mutated- and Rad3-related kinase (ATR) in PTEN-deficient breast cancers for personalized therapy', *Breast Cancer Research and Treatment*, 169(2), pp. 277–286. doi: 10.1007/s10549-018-4683-4.

Al-Tamimi, D. *et al.* (2009) 'Distribution of molecular breast cancer subtypes in Middle Eastern-Saudi Arabian women: A pilot study', *Ultrastructural Pathology*, 33(4), pp. 141–150. doi: 10.1080/01913120903183135.

Alimonti, A. *et al.* (2010) 'Subtle variations in Pten dose determine cancer susceptibility', *Nature Genetics*, 42(5), pp. 454–458. doi: 10.1038/ng.556.

Allred, D. C. *et al.* (2008) 'Ductal carcinoma in situ and the emergence of diversity during breast cancer evolution', *Clinical Cancer Research*, 14(2), pp. 370–378. doi: 10.1158/1078-0432.CCR-07-1127.

Alvarez-Garcia, V. *et al.* (2018) 'A simple and robust real-time qPCR method for the detection of PIK3CA mutations', *Scientific Reports*, 8(1), p. 4290. doi: 10.1038/s41598-018-22473-9.

Amin, M. B., Edge, S., *et al.* (2017) *AJCC CANCER STAGING MANUAL*. 8th Editio. New York: Springer.

Amin, M. B., Greene, F. L., *et al.* (2017) 'The Eighth Edition AJCC Cancer Staging Manual: Continuing to build a bridge from a population-based to a more "personalized" approach to cancer staging', *CA: A Cancer Journal for Clinicians*, 67(2), pp. 93–99. doi: 10.3322/caac.21388.

Amodio, N. *et al.* (2010) 'Oncogenic role of the E3 ubiquitin ligase NEDD4-1, a PTEN negative regulator, in non-small-cell lung carcinomas', *American Journal of Pathology*, 177(5), pp. 2622–2634. doi: 10.2353/ajpath.2010.091075.

Anderson, M. W. *et al.* (1992) 'Role of Proto-oncogene activation in carcinogenesis', *Environmental Health Perspectives*, 98, pp. 13–24. doi: 10.1289/ehp.929813.

André, F. *et al.* (2014) 'Everolimus for women with trastuzumab-resistant, HER2-positive, advanced breast cancer (BOLERO-3): A randomised, double-blind, placebo-controlled phase 3 trial', *The Lancet Oncology*, 15(6), pp. 580–591. doi: 10.1016/S1470-2045(14)70138-X.

André, F. *et al.* (2019) 'Alpelisib for PIK3CA -Mutated, Hormone Receptor–Positive Advanced Breast Cancer', *New England Journal of Medicine*, 380(20), pp. 1929–1940. doi: 10.1056/nejmoa1813904.

Anjum, F., Razvi, N. and Masood, M. A. (2017) 'Breast cancer therapy: A mini review', *MOJ Drug Design Development & Therapy*, 1(2), pp. 35–38. doi: 10.15406/MOJDDT.2017.1.00006.

Antoniou, A. *et al.* (2003) 'Average risks of breast and ovarian cancer associated with BRCA1 or BRCA2 mutations detected in case series unselected for family history: A combined analysis of 22 studies', *American Journal of Human Genetics*, 72(5), pp. 1117–1130. doi: 10.1086/375033.

Aquila, S. *et al.* (2020) 'The tumor suppressor PTEN as molecular switch node regulating cell metabolism and autophagy: Implications in immune system and tumor microenvironment', *Cells*, 9(7), p. 1725. doi: 10.3390/cells9071725.

Van Asten, K. *et al.* (2014) 'Aromatase inhibitors in the breast cancer clinic: focus on exemestane', *Endocrine-Related Cancer*, 21(1), pp. R31–R49. doi: 10.1530/ERC-13-0269.

Bachman, K. E. *et al.* (2004) 'The PIK3CA gene is mutated with high frequency in human breast cancers', *Cancer Biology and Therapy*, 3(8), pp. 772–775. doi: 10.4161/cbt.3.8.994.

Backman, S. A. *et al.* (2001) 'Deletion of Pten in mouse brain causes seizures, ataxia and defects in soma size resembling Lhermitte-Duclos disease', *Nature Genetics*, 29(4), pp. 396–403. doi:

10.1038/ng782.

Balko, J. M. *et al.* (2014) 'Molecular profiling of the residual disease of triple-negative breast cancers after neoadjuvant chemotherapy identifies actionable therapeutic targets', *Cancer Discovery*, 4(2), pp. 232–245. doi: 10.1158/2159-8290.CD-13-0286.

Banks, E. *et al.* (2003) 'Breast cancer and hormone-replacement therapy in the Million Women Study', *Lancet*, 362(9382), pp. 419–427. doi: 10.1016/S0140-6736(03)14065-2.

Bardia, A. *et al.* (2021) 'Sacituzumab govitecan in metastatic triple-negative breast cancer', *New England Journal of Medicine*, 384(16), pp. 1529–1541. doi: 10.1056/nejmoa2028485.

Bareche, Y. *et al.* (2018) 'Unravelling triple-negative breast cancer molecular heterogeneity using an integrative multiomic analysis', *Annals of Oncology*, 29(4), pp. 895–902. doi: 10.1093/annonc/mdy024.

Barnum, K. J. and O'Connell, M. J. (2014) 'Cell cycle regulation by checkpoints', *Methods in Molecular Biology*, 1170, pp. 29–40. doi: 10.1007/978-1-4939-0888-2_2.

Bartek, J., Lukas, C. and Lukas, J. (2004) 'Checking on DNA damage in S phase', *Nature Reviews Molecular Cell Biology*, 5(10), pp. 792–804. doi: 10.1038/nrm1493.

Baselga, J., Campone, M., *et al.* (2012) 'Everolimus in postmenopausal hormone- receptor–positive advanced breast cancer', *The New England Journal of Medicine*, 366(6), pp. 520–529. doi: 10.1056/NEJMoa1109653.

Baselga, J., Cortés, J., *et al.* (2012) 'Pertuzumab plus trastuzumab plus docetaxel for metastatic breast cancer', *New England Journal of Medicine*, 366(2), pp. 109–119. doi: 10.1056/NEJMoa1113216.

Baselga, J. *et al.* (2017) 'Buparlisib plus fulvestrant versus placebo plus fulvestrant in postmenopausal, hormone receptor-positive, HER2-negative, advanced breast cancer (BELLE-2): a randomised, double-blind, placebo-controlled, phase 3 trial', *Lancet Oncology*, 18(7), pp. 904–916. doi: 10.1016/S1470-2045(17)30376-5.

Bassi, C. *et al.* (2013) 'Nuclear PTEN controls DNA repair and sensitivity to genotoxic stress', *Science*, 341(6144), pp. 395–399. doi: 10.1126/science.1236188.

Bazzichetto, C. *et al.* (2019) 'Pten as a prognostic/predictive biomarker in cancer: An unfulfilled promise?', *Cancers*, 11(4), p. 435. doi: 10.3390/cancers11040435.

Beg, S. *et al.* (2015) 'Loss of PTEN expression is associated with aggressive behavior and poor

prognosis in Middle Eastern triple-negative breast cancer', *Breast Cancer Research and Treatment*, 151(3), pp. 541–553. doi: 10.1007/s10549-015-3430-3.

Bell, S. P. and Dutta, A. (2002) 'DNA replication in eukaryotic cells', *Annual Review of Biochemistry*, 71, pp. 333–374. doi: 10.1146/annurev.biochem.71.110601.135425.

Benitez, J. A. *et al.* (2017) 'PTEN regulates glioblastoma oncogenesis through chromatin-associated complexes of DAXX and histone H3.3', *Nature Communications*, 8, p. 15223. doi: 10.1038/ncomms15223.

Benz, C. C. (2008) 'Impact of aging on the biology of breast cancer', *Critical Reviews in Oncology/Hematology*, 66(1), pp. 65–74. doi: 10.1016/j.critrevonc.2007.09.001.

Beral, V. *et al.* (1997) 'Breast cancer and hormone replacement therapy: Collaborative reanalysis of data from 51 epidemiological studies of 52,705 women with breast cancer and 108,411 women without breast cancer', *Lancet*, 350(9084), pp. 1047–1059. doi: 10.1016/S0140-6736(97)08233-0.

Bermudez, V. P. *et al.* (2010) 'Influence of the human cohesion establishment factor Ctf4/AND-1 on DNA replication', *Journal of Biological Chemistry*, 285(13), pp. 9493–9505. doi: 10.1074/jbc.M109.093609.

Bernards, R., Brummelkamp, T. R. and Beijersbergen, R. L. (2006) 'shRNA libraries and their use in cancer genetics', *Nature Methods*, 3(9), pp. 701–706. doi: 10.1038/nmeth921.

Berns, K. *et al.* (2007) 'A functional genetic approach identifies the PI3K pathway as a major determinant of trastuzumab resistance in breast cancer', *Cancer Cell*, 12(4), pp. 395–402. doi: 10.1016/j.ccr.2007.08.030.

Bianchini, G. *et al.* (2016) 'Triple-negative breast cancer: challenges and opportunities of a heterogeneous disease', *Nature Reviews Clinical Oncology*, 13(11), pp. 674–690. doi: 10.1038/nrclinonc.2016.66.

Bissel, M. J. and Radisky, D. (2001) 'Putting tumors in context', *Nature Reviews Cancer*, 1(1), pp. 46–54. doi: 10.1038/35094059.

Bloom, H. J. and Richardson, W. W. (1957) 'Histological grading and prognosis in breast cancer a study of 1409 cases of which 359 have been followed for 15 years', *British Journal of Cancer*, 11(3), pp. 359–377. doi: 10.1038/bjc.1957.43.

Blows, F. M. *et al.* (2010) 'Subtyping of breast cancer by immunohistochemistry to investigate a relationship between subtype and short and long term survival: A collaborative analysis of data for

10,159 cases from 12 studies', *PLoS Medicine*, 7(5), p. e1000279. doi: 10.1371/journal.pmed.1000279.

Boavida, A. *et al.* (2021) 'Functional coupling between DNA replication and sister chromatid cohesion establishment', *International Journal of Molecular Sciences*, 22(6), p. 2810. doi: 10.3390/ijms22062810.

Boffetta, P. and Hashibe, M. (2006) 'Alcohol and cancer', *Lancet Oncology*, 7(2), pp. 149–156. doi: 10.1016/S1470-2045(06)70577-0.

Bonneterre, J. *et al.* (2000) 'Anastrozole versus tamoxifen as first-line therapy for advanced breast cancer in 668 postmenopausal women: Results of the tamoxifen or arimidex randomized group efficacy and tolerability study', *Journal of Clinical Oncology*, 18(22), pp. 3748–3757. doi: 10.1200/JCO.2000.18.22.3748.

Bonneterre, J. *et al.* (2001) 'Anastrozole is superior to tamoxifen as first-line therapy in hormone receptor positive advanced breast carcinoma', *Cancer*, 92(9), pp. 2247–2258. doi: 10.1002/1097-0142(20011101)92:9<2247::aid-cncr1570>3.0.co;2-y.

Bosch, A. *et al.* (2016) 'PI3K inhibition results in enhanced estrogen receptor function and dependence in hormone receptor-positive breast cancer', *Science Translational Medicine*, 7(283), p. 283ra51. doi: 10.1126/scitranslmed.aaa4442.

Bose, S. *et al.* (1998) 'Allelic loss of chromosome 10q23 is associated with tumor progression in breast carcinomas', *Oncogene*, 17(1), pp. 123–127. doi: 10.1038/sj.onc.1201940.

Boutros, M., Brás, L. P. and Huber, W. (2006) 'Analysis of cell-based RNAi screens', *Genome Biology*, 7(7), p. R66. doi: 10.1186/gb-2006-7-7-r66.

Bray, F. *et al.* (2018) 'Global cancer statistics 2018: GLOBOCAN estimates of incidence and mortality worldwide for 36 cancers in 185 countries.', *CA: a cancer journal for clinicians*, 68(6), pp. 394–424. doi: 10.3322/caac.21492.

Breast Cancer Statistics (2017) *Cancer Research UK*.

Brenton, J. D. *et al.* (2005) 'Molecular classification and molecular forecasting of breast cancer: Ready for clinical application?', *Journal of Clinical Oncology*, 23(29), pp. 7350–7360. doi: 10.1200/JCO.2005.03.3845.

Brewer, H. R. *et al.* (2017) 'Family history and risk of breast cancer: an analysis accounting for family structure', *Breast Cancer Research and Treatment*, 165(1), pp. 193–200. doi: 10.1007/s10549-017-

4325-2.

Bronisz, A. *et al.* (2012) 'Reprogramming of the tumour microenvironment by stromal PTEN-regulated miR-320', *Nature Cell Biology*, 14(2), pp. 159–167. doi: 10.1038/ncb2396.

Brough, R. *et al.* (2011) 'Functional Viability Profiles of Breast Cancer', *Cancer Discovery*, 1(3), pp. 260–273. doi: 10.1158/2159-8290.CD-11-0107.

Brummelkamp, T. R. and Bernards, R. (2003) 'New tools for functional mammalian cancer genetics', *Nature Reviews Cancer*, 3(10), pp. 781–789. doi: 10.1038/nrc1191.

Brunen, D. and Bernards, R. (2017) 'Drug therapy: Exploiting synthetic lethality to improve cancer therapy', *Nature Reviews Clinical Oncology*, 14(6), pp. 331–332. doi: 10.1038/nrclinonc.2017.46.

Brunetti, B. *et al.* (2014) 'CD117 expression influences proliferation but not survival in canine mammary tumours', *Journal of Comparative Pathology*, 151(2–3), pp. 202–206. doi: 10.1016/j.jcpa.2014.04.018.

Bryant, H. E. *et al.* (2005) 'Specific killing of BRCA2-deficient tumours with inhibitors of poly(ADP-ribose) polymerase', *Nature*, 434(7035), pp. 913–917. doi: 10.1038/nature03443.

Burnett, J. P. *et al.* (2015) 'Trastuzumab resistance induces EMT to transform HER2 + PTEN' to a triple negative breast cancer that requires unique treatment options', *Scientific Reports*, 5(22), pp. 1–13. doi: 10.1038/srep15821.

Burstein, H. J. *et al.* (2004) 'Ductal Carcinoma in Situ of the Breast', *The New England Journal of Medicine*, 350(14), pp. 1430–1441. doi: 10.1056/NEJMra031301.

Calabrese, C. *et al.* (2020) 'Genomic basis for RNA alterations in cancer', *Nature*, 578(7793), pp. 129–136. doi: 10.1038/s41586-020-1970-0.

Cameron, D. *et al.* (2013) 'Adjuvant bevacizumab-containing therapy in triple-negative breast cancer (BEATRICE): Primary results of a randomised, phase 3 trial', *The Lancet Oncology*, 14(10), pp. 933–942. doi: 10.1016/S1470-2045(13)70335-8.

Campbell, R. B., Liu, F. and Ross, A. H. (2003) 'Allosteric activation of PTEN phosphatase by phosphatidylinositol 4,5-bisphosphate', *Journal of Biological Chemistry*, 278(36), pp. 33617–33620. doi: 10.1074/jbc.C300296200.

Cantley, L. C. and Neel, B. G. (1999) 'New insights into tumor suppression: PTEN suppresses tumor formation by restraining the phosphoinositide 3-kinase/AKT pathway', *Proceedings of the National Academy of Sciences of the United States of America*, 96(8), pp. 4240–4245. doi:

10.1073/pnas.96.8.4240.

Capelan, M. *et al.* (2013) 'Pertuzumab: New hope for patients with HER2-positive breast cancer', *Annals of Oncology*, 24(2), pp. 273–282. doi: 10.1093/annonc/mds328.

Caplen, N. J. *et al.* (2001) 'Specific inhibition of gene expression by small double-stranded RNAs in invertebrate and vertebrate systems', *Proceedings of the National Academy of Sciences of the United States of America*, 98(17), pp. 9742–9747. doi: 10.1073/pnas.171251798.

Carey, L. A. *et al.* (2006) 'Race, breast cancer subtypes, and survival in the Carolina Breast Cancer Study', *JAMA*, 295(21), pp. 2492–2502. doi: 10.1001/jama.295.21.2492.

Carey, L. A. *et al.* (2012) 'TBCRC 001: Randomized phase II study of cetuximab in combination with carboplatin in stage IV triple-negative breast cancer', *Journal of Clinical Oncology*, 30(21), pp. 2615–2623. doi: 10.1200/JCO.2010.34.5579.

Carnero, A. (2010) 'The PKB/AKT pathway in cancer', *Current pharmaceutical design*, 16(1), pp. 34–44. doi: 10.2174/138161210789941865.

Carthew, R. W. and Sontheimer, E. J. (2009) 'Origins and Mechanisms of miRNAs and siRNAs Richard', *Cell*, 136(4), pp. 642–655. doi: 10.1016/j.cell.2009.01.035.

Castrellon, A. B. *et al.* (2017) 'The role of carboplatin in the neoadjuvant chemotherapy treatment of triple negative breast cancer', *Oncology Reviews*, 11(1), pp. 7–12. doi: 10.4081/oncol.2017.324.

Cerami, E. *et al.* (2014) 'The cBio cancer genomics portal: An open platform for exploring multidimensional cancer genomics data', *Cancer Discovery*, 2(5), pp. 401–404. doi: 10.1158/2159-8290.CD-12-0095.

Chalhoub, N. and Baker, S. J. (2008) 'PTEN and the PI3-Kinase Pathway in Cancer', *Annual Review of Pathology: Mechanisms of Disease*, 4(1), pp. 127–150. doi: 10.1146/annurev.pathol.4.110807.092311.

Chan, J. J., Tan, T. J. Y. and Dent, R. A. (2019) 'Novel therapeutic avenues in triplenegative breast cancer: PI3K/AKT inhibition, androgen receptor blockade, and beyond', *Therapeutic Advances in Vaccines*, 11, p. 1758835919880429. doi: 10.1177/1758835919880429.

Chandarlapaty, S. *et al.* (2011) 'AKT inhibition relieves feedback suppression of receptor tyrosine kinase expression and activity', *Cancer Cell*. Elsevier Inc., 19(1), pp. 58–71. doi: 10.1016/j.ccr.2010.10.031.

Chang, C. H. *et al.* (2012) 'An efficient RNA interference screening strategy for gene functional

analysis', *BMC Genomics*, 13, p. 491. doi: 10.1186/1471-2164-13-491.

Chang, S. H. *et al.* (2005) 'Loss of PTEN expression in breast cancers', *The Korean Journal of Pathology*, 39(4), pp. 236–241.

Chatterjee, N. *et al.* (2019) 'Synthetic essentiality of metabolic regulator PDHK1 in PTEN deficient cells and cancers', *Cell Reports*, 28(9), pp. 2317–2330. doi: 10.1016/j.celrep.2019.07.063.

Chaudhary, L. N., Wilkinson, K. H. and Kong, A. (2018) 'Triple-negative breast cancer: who should receive neoadjuvant chemotherapy?', *Surgical Oncology Clinics of North America*, 27(1), pp. 141–153. doi: 10.1016/j.soc.2017.08.004.

Chen, N. *et al.* (2020) 'Identification of key modules and hub genes involved in esophageal squamous cell carcinoma tumorigenesis using WCGNA', *Cancer Control*, 27(1), p. 1073274820978817. doi: 10.1177/1073274820978817.

Chen, P. *et al.* (2019) 'Symbiotic macrophage-glioma cell interactions reveal synthetic lethality in PTEN null glioma', *Cancer Cell*, 35(6), pp. 868–884. doi: 10.1016/j.ccell.2019.05.003.

Chen, S. *et al.* (2020) 'Identification of Prognostic miRNA Signature and Lymph Node Metastasis-Related Key Genes in Cervical Cancer', *Frontiers in Pharmacology*, 11(May), p. 544. doi: 10.3389/fphar.2020.00544.

Chen, S. and Parmigiani, G. (2007) 'Meta-analysis of BRAC1 and BRAC2 penetrance', *Journal of Clinical Oncology*, 25(11), pp. 1329–1333. doi: 10.1200/JCO.2006.09.1066.

Chen, Y. *et al.* (2017) 'And-1 coordinates with CtIP for efficient homologous recombination and DNA damage checkpoint maintenance', *Nucleic Acids Research*, 45(5), pp. 2516–2530. doi: 10.1093/nar/gkw1212.

Chen, Z. *et al.* (2016) 'Proteomic analysis reveals a novel mutator S (MutS) partner involved in mismatch repair pathway', *Molecular and Cellular Proteomics*, 15(4), pp. 1299–1308. doi: 10.1074/mcp.M115.056093.

Chien, A. J. *et al.* (2016) 'A phase 1b study of the Akt-inhibitor MK-2206 in combination with weekly paclitaxel and trastuzumab in patients with advanced HER2-amplified solid tumor malignancies', *Breast Cancer Research and Treatment*, 155(3), pp. 521–530. doi: 10.1007/s10549-016-3701-7.

Chin, L. *et al.* (2011) 'Making sense of cancer genomic data', *Genes & Development*, 25(6), pp. 534–555. doi: 10.1101/gad.2017311.

Chin, L., Andersen, J. N. and Futreal, P. A. (2011) 'Cancer genomics: From discovery science to

personalized medicine', *Nature Medicine*, 17(3), pp. 297–303. doi: 10.1038/nm.2323.

Chow, J. Y. C. *et al.* (2007) 'RAS/ERK modulates TGFβ-regulated PTEN expression in human pancreatic adenocarcinoma cells', *Carcinogenesis*, 28(11), pp. 2321–2327. doi: 10.1093/carcin/bgm159.

Chow, L. M. L. and Baker, S. J. (2006) 'PTEN function in normal and neoplastic growth', *Cancer Letters*, 241(2), pp. 184–196. doi: 10.1016/j.canlet.2005.11.042.

Chung, J. H., Ginn-Pease, M. E. and Eng, C. (2005) 'Phosphatase and tensin homologue deleted on chromosome 10 (PTEN) has nuclear localization signal-like sequences for nuclear import mediated by major vault protein', *Cancer Research*, 65(10), pp. 4108–4116. doi: 10.1158/0008-5472.CAN-05-0124.

Ciuffreda, Ludovica Sanza, C. Di *et al.* (2012) 'The mitogen-activated protein kinase (MAPK) cascade controls phosphatase and tensin homolog (PTEN) expression through multiple mechanisms', *Journal of Molecular Medicine (Berlin, Germany)*, 90(6), pp. 667–679. doi: 10.1007/s00109-011-0844-1.

Clemons, M. and Gross, P. (2001) 'Estrogen and the risk of breast cancer', *The New England journal of medicineEnglish Journal*, 344(4), pp. 276–285. doi: 10.1056/NEJM200101253440407.

Cobain, E. F., Milliron, K. J. and Merajver, S. D. (2016) 'Updates on breast cancer genetics: Clinical implications of detecting syndromes of inherited increased susceptibility to breast cancer', *Seminars in Oncology*, 43(5), pp. 528–535. doi: 10.1053/j.seminoncol.2016.10.001.

Coccia, M. (2013) 'The effect of country wealth on incidence of breast cancer', *Breast Cancer Research and Treatment*, 141, pp. 225–229. doi: 10.1007/s10549-013-2683-y.

Costa, C. *et al.* (2020) 'Pten loss mediates clinical cross-resistance to CDK4/6 and PI3Kα inhibitors in breast cancer', *Cancer Discovery*, 10(1), pp. 72–85. doi: 10.1158/2159-8290.CD-18-0830.

Criscitiello, C. *et al.* (2012) 'Understanding the biology of triple-negative breast cancer', *Annals of Oncology*, 23(SUPPL. 6), pp. vi13–vi18. doi: 10.1093/annonc/mds188.

Cristofanilli, M. *et al.* (2016) 'Fulvestrant plus palbociclib versus fulvestrant plus placebo for treatment of hormone-receptor-positive, HER2-negative metastatic breast cancer that progressed on previous endocrine therapy (PALOMA-3): final analysis of the multicentre, double-blind, phas', *The Lancet Oncology*, 17(4), pp. 425–439. doi: 10.1016/S1470-2045(15)00613-0.

Di Cristofano, A. *et al.* (1998) 'Pten is essential for embryonic development and tumor suppression',

Nature Genetics, 19(4), pp. 348–355. doi: 10.1038/1235.

Cyprian, F. S. *et al.* (2019) 'Targeted immunotherapy with a checkpoint inhibitor in combination with chemotherapy: A new clinical paradigm in the treatment of triple-negative breast cancer', *Bosnian Journal of Basic Medical Sciences*, 19(3), pp. 227–233. doi: 10.17305/bjbms.2019.4204.

Dai, X. *et al.* (2015) 'Breast cancer intrinsic subtype classification, clinical use and future trends', *American Journal of Cancer Research*, 5(10), pp. 2929–2943.

Das, S., Dixon, J. E. and Cho, W. (2003) 'Membrane-binding and activation mechanism of PTEN', *Proceedings of the National Academy of Sciences of the United States of America*, 100(13), pp. 7491–7496. doi: 10.1073/pnas.0932835100.

Datta, S. R. *et al.* (1997) 'Akt phosphorylation of BAD couples survival signals to the cell- intrinsic death machinery', *Cell*, 91(2), pp. 231–241. doi: 10.1016/S0092-8674(00)80405-5.

Dent, R. *et al.* (2020) 'Abstract 1390-Final results of the double-blind placebo (PBO)-controlled randomised phase II LOTUS trial of first-line ipatasertib (IPAT) + paclitaxel (PAC) for inoperable locally advanced/metastatic triple-negative breast cancer (mTNBC)', *Annals of Oncology*, 31(Suppl_2), pp. S62–S82. doi: 10.1016/annonc/annonc122.

Dermit, M., Dodel, M. and Mardakheh, F. K. (2017) 'Methods for monitoring and measurement of protein translation in time and space', *Molecular BioSystems*, 13(12), pp. 2477–2488. doi: 10.1039/c7mb00476a.

Dhankhar, R. *et al.* (2010) 'Advances in novel drug delivery strategies for breast cancer therapy', *Artificial Cells, Blood Substitutes, and Biotechnology*, 38(5), pp. 230–249. doi: 10.3109/10731199.2010.494578.

Dickler, M. N. *et al.* (2018) 'Phase II study of taselisib (GDC-0032) in combination with fulvestrant in patients with HER2-negative, hormone receptor positive advanced breast cancer', *Clinical Cancer Research*, 24(18), pp. 4380–4387. doi: 10.1158/1078-0432.CCR-18-0613.

Diehl, J. A. *et al.* (1998) 'Glycogen synthase kinase-3b regulates cyclin D1 proteolysis and subcellular localization', *Genes & Development*, 12(22), pp. 3499–3511. doi: 10.1101/gad.12.22.3499.

Diepen, M. Van *et al.* (2009) 'MyosinV controls PTEN function and neuronal cell size', *Nature Cell Biology*, 11(10), pp. 1191–1196. doi: 10.1038/ncb1961.

Diffley, J. F. X. (2004) 'Regulation of early events in chromosome replication', *Current Biology*, 14(18), pp. 778–786. doi: 10.1016/j.cub.2004.09.019.

Dodd, K. M. *et al.* (2015) 'mTORC1 drives HIF-1α and VEGF-A signalling via multiple mechanisms involving 4E-BP1, S6K1 and STAT3', *Oncogene*, 34(17), pp. 2239–2250. doi: 10.1038/onc.2014.164.

Doye, V. and Hurt, E. C. (1995) 'Genetic approaches to nuclear pore structure and function', *Trends in Genetics*, 11(6), pp. 235–241. doi: 10.1016/S0168-9525(00)89057-5.

Dutta, U. and Pant, K. (2008) 'Aromatase inhibitors: Past, present and future in breast cancer therapy', *Medical Oncology*, 25(2), pp. 113–124. doi: 10.1007/s12032-007-9019-x.

Elbashir, S. M. *et al.* (2001) 'Duplexes of 21-nucleotide RNAs mediate RNA interference in cultured mammalian cells', *Nature*, 411(6836), pp. 494–498. doi: 10.1038/35078107.

Elenbaas, B. and Weinberg, R. A. (2001) 'Heterotypic signaling between epithelial tumor cells and fibroblasts in carcinoma formation', *Experimental Cell Research*, 264(1), pp. 169–184. doi: 10.1006/excr.2000.5133.

Elston, C. W. and Ellis, I. O. (1991) 'Pathological prognostic factors in breast cancer: experience from a large study with long-term follow-up', *Histopathology*, 19, pp. 403–410. Available at: http://dx.doi.org/10.1111/j.1365-2559.1991.tb00229.x.

Errico, A. *et al.* (2009) 'Tipin/Tim1/And1 protein complex promotes Polα chromatin binding and sister chromatid cohesion', *The EMBO Journal*, 28(23), pp. 3681–3692. doi: 10.1038/emboj.2009.304.

Escrivà, M. *et al.* (2008) 'Repression of PTEN Phosphatase by Snail1 Transcriptional Factor during Gamma Radiation-Induced Apoptosis', *Molecular and Cellular Biology*, 28(5), pp. 1528–1540. doi: 10.1128/mcb.02061-07.

Evans, J. C. and Mizrahi, V. (2015) 'The application of tetracyclineregulated gene expression systems in the validation of novel drug targets in Mycobacterium tuberculosis', *Frontiers in Microbiology*, 6, p. 812. doi: 10.3389/fmicb.2015.00812.

Fan, C. *et al.* (2006) 'Concordance among gene-expression-based predictors for breast cancer', *New England Journal of Medicine*, 355(6), pp. 560–569. doi: 10.1056/NEJMoa052933.

Fan, H. H. *et al.* (2021) 'Wdhd1 is essential for early mouse embryogenesis', *Biochimica et Biophysica Acta - Molecular Cell Research*, 1868(6), p. 119011. doi: 10.1016/j.bbamcr.2021.119011.

Fanning, A. S. and Anderson, J. M. (1999) 'Protein modules as organizers of membrane structure', *Current Opinion in Cell Biology*, 11(4), pp. 432–439. doi: 10.1016/S0955-0674(99)80062-3.

Farmer, H. *et al.* (2005) 'Targeting the DNA repair defect in BRCA mutant cells as a therapeutic

strategy', *Nature*, 434(1991), pp. 917–921. doi: 10.1038/nature03445.

Fece de la Cruz, F., Gapp, B. V. and Nijman, S. M. B. (2014) 'Synthetic lethal vulnerabilities of cancer', *Annual Review of Pharmacology and Toxicology*, 55(1), pp. 513–531. doi: 10.1146/annurev-pharmtox-010814-124511.

Feng, Y. *et al.* (2018) 'Breast cancer development and progression: Risk factors, cancer stem cells, signaling pathways, genomics, and molecular pathogenesis', *Genes and Diseases*. Elsevier Ltd, 5(2), pp. 77–106. doi: 10.1016/j.gendis.2018.05.001.

Fidler, I. J. (2003) 'The pathogenesis of cancer metastasis: the "seed and soil" hypothesis revisited', *Nature Reviews Cancer*, 3(1), pp. 453–458. doi: 10.1111/j.1937-5956.1995.tb00040.x.

Filmus, J. *et al.* (1985) 'MDA-468, a human breast cancer cell line with a high number of epidermal growth factor (EGF) receptors, has an amplified EGF receptor gene and is growth inhibited by EGF', *Biochemical and Biophysical Research Communications*, 128(2), pp. 898–905. doi: 10.1016/0006-291x(85)90131-7.

Fine, B. *et al.* (2005) 'Activation of the PI3K pathway in cancer through inhibition of PTEN by exchange factor P-REX2a', *Science*, 325(5945), pp. 1-71261–1265. doi: 10.1126/science.1173569.

Finn, R. S. *et al.* (2016) 'Palbociclib and letrozole in advanced breast cancer', *New England Journal of Medicine*, 375(20), pp. 1925–1936. doi: 10.1056/NEJMoa1607303.

Fire, A. *et al.* (1998) 'Potent and specific genetic interference by double-stranded RNA in Caenorhabditis elegans', *Nature*, 391(6669), pp. 806–811. doi: 10.1038/35888.

Fonseca-Alves, C. E. *et al.* (2017) 'Investigation of c-KIT and Ki67 expression in normal, preneoplastic and neoplastic canine prostate', *BMC Veterinary Research*, 13(1), pp. 1–9. doi: 10.1186/s12917-017-1304-0.

Freedman, O. C. *et al.* (2015) 'Adjuvant endocrine therapy for early breast cancer: a systematic review of the evidence for the 2014 Cancer Care Ontario systemic therapy guideline', *Current Oncology*, 22, pp. S95–S113. doi: 10.3747/co.22.2326.

Freeman, D. J. *et al.* (2003) 'PTEN tumor suppressor regulates p53 protein levels and activity through phosphatase-dependent and -independent mechanisms', *Cancer Cell*, 3(2), pp. 117–130. doi: 10.1016/S1535-6108(03)00021-7.

Freihoff, D. *et al.* (1999) 'Exclusion of a major role for the PTEN tumour-suppressor gene in breast carcinomas', *British Journal of Cancer*, 79(5–6), pp. 754–758. doi: 10.1038/sj.bjc.6690121.

Gambus, A. *et al.* (2006) 'GINS maintains association of Cdc45 with MCM in replisome progression complexes at eukaryotic DNA replication forks', *Nature Cell Biology*, 8(4), pp. 358–366. doi: 10.1038/ncb1382.

Garcia-cao, I. *et al.* (2012) 'Systemic elevation of PTEN induces a tumor suppressive metabolic state', *Cell*, 149(1), pp. 49–62. doi: 10.1016/j.cell.2012.02.030.

García, J. M. *et al.* (2004) 'Promoter methylation of the PTEN gene is a common molecular change in breast cancer', *Genes Chromosomes Cancer*, 41(2), pp. 117–124. doi: 10.1002/gcc.20062.

Garg, P. and Burgers, P. M. J. (2005) 'DNA polymerases that propagate the eukaryotic DNA replication fork', *Critical Reviews in Biochemistry and Molecular Biology*, 40(2), pp. 115–128. doi: 10.1080/10409230590935433.

Georgescu, M. M. *et al.* (1999) 'The tumor-suppressor activity of PTEN is regulated by its carboxyl-terminal region', *Proceedings of the National Academy of Sciences of the United States of America*, 96(18), pp. 10182–10187. doi: 10.1073/pnas.96.18.10182.

Gil, A. *et al.* (2006) 'Nuclear localization of PTEN by a Ran-dependent mechanism enhances apoptosis: Involvement of an N-Terminal nuclear localization domain and multiple nuclear exclusion motifs', *Molecular biology of the cell*, 17(9), pp. 4002–4013. doi: 10.1091/mbc.e06-05-0380.

Gimm, O. *et al.* (2000) 'Differential nuclear and cytoplasmic expression of PTEN in normal thyroid tissue, and benign and malignant epithelial thyroid tumors', *American Journal of Pathology*, 156(5), pp. 1693–1700. doi: 10.1016/S0002-9440(10)65040-7.

Ginn-pease, M. E. and Eng, C. (2003) 'Increased nuclear phosphatase and tensin homologue deleted on chromosome 10 is associated with G0-G1 in MCF-7 cells', *Cancer Research*, 63(2), pp. 282–286.

Goetz, M. P. *et al.* (2017) 'MONARCH 3: Abemaciclib as initial therapy for advanced breast cancer', *Journal of Clinical Oncology*, 35(32), pp. 3638–3646. doi: 10.1200/JCO.2017.75.6155.

Goldman, M. *et al.* (2015) 'The UCSC cancer genomics browser: Update 2015', *Nucleic Acids Research*, 43(D1), pp. D812–D817. doi: 10.1093/nar/gku1073.

Gong, L. *et al.* (2020) 'WDHD1 leads to cisplatin resistance by promoting MAPRE2 ubiquitination in lung adenocarcinoma', *Frontiers in Oncology*, 10, p. 461. doi: 10.3389/fonc.2020.00461.

Gosnell, J. A. and Christensen, T. W. (2011) 'Drosophila Ctf4 is essential for efficient DNA replication and normal cell cycle progression', *BMC Molecular Biology*, 12(13). doi: 10.1186/1471-2199-12-13.

Goss, P. E. and Sierra, S. (1998) 'Current perspectives on radiation-induced breast cancer', *J Clin Oncol*, 16(1), pp. 338–347. doi: 10.1200/JCO.1998.16.1.338.

Greenwalt, I. *et al.* (2020) 'Precision medicine and targeted therapies in breast cancer', *Surgical Oncology Clinics of North America*, 29(1), pp. 51–62. doi: 10.1016/j.soc.2019.08.004.

Gu, J. *et al.* (1999) 'Shc and FAK differentially regulate cell motility and directionality modulated by PTEN', *Journal of Cell Biology*, 146(2), pp. 389–403. doi: 10.1083/jcb.146.2.389.

Gu, J., Tamura, M. and Yamada, K. M. (1998) 'Tumor suppressor PTEN inhibits integrin- and growth factor-mediated mitogen-activated protein (MAP) kinase signaling pathways', *The Journal of Cell Biology*, 143(5), pp. 1375–83. doi: 10.1083/jcb.143.5.1375.

Guan, C. *et al.* (2017) 'The structure and polymerase-recognition mechanism of the crucial adaptor protein AND-1 in the human replisome', *Journal of Biological Chemistry*, 292(23), pp. 9627–9636. doi: 10.1074/jbc.m116.758524.

Guerin, M. *et al.* (2017) 'PIKHER2: A phase IB study evaluating buparlisib in combination with lapatinib in trastuzumab-resistant HER2-positive advanced breast cancer', *European Journal of Cancer*, 86, pp. 28–36. doi: 10.1016/j.ejca.2017.08.025.

El Guerrab, A. *et al.* (2020) 'Co-targeting EGFR and mTOR with gefitinib and everolimus in triple-negative breast cancer cells', *Scientific Reports*, 10(1), p. 6367. doi: 10.1038/s41598-020-63310-2.

Guzmán, C. *et al.* (2014) 'ColonyArea: An ImageJ plugin to automatically quantify colony formation in clonogenic assays', *PLoS ONE*, 9(3), p. e92444. doi: 10.1371/journal.pone.0092444.

Haar, E. Vander *et al.* (2007) 'Insulin signalling to mTOR mediated by the Akt/PKB substrate PRAS40', *Nature Cell Biology*, 9(3), pp. 316–323. doi: 10.1038/ncb1547.

Hanahan, D. and Weinberg, R. A. (2000) 'The hallmarks of cancer', *Cell*, 100(1), pp. 57–70. doi: 10.1016/s0092-8674(00)81683-9.

Hanahan, D. and Weinberg, R. A. (2011) 'Hallmarks of cancer: The next generation', *Cell*, 144(5), pp. 646–674. doi: 10.1016/j.cell.2011.02.013.

Hanna, J. S. *et al.* (2001) 'Saccharomyces cerevisiae CTF18 and CTF4 Are Required for Sister Chromatid Cohesion', *Molecular and Cellular Biology*, 21(9), pp. 3144–3158. doi: 10.1128/mcb.21.9.3144-3158.2001.

Hao, J. *et al.* (2015) 'And-1 coordinates with Claspin for efficient Chk1 activation in response to replication stress', *The EMBO Journal*, 34(15), pp. 2096–2110. doi: 10.15252/embj.201488016.

Hartwell, L. H. *et al.* (1997) 'Integrating genetic approaches into the discovery of anticancer drugs', *Science*, 278(5340), pp. 1064–1068. doi: 10.1126/science.278.5340.1064.

Haruta, T. *et al.* (2000) 'A rapamycin-sensitive pathway down-regulates insulin signaling via phosphorylation and proteasomal degradation of insulin receptor substrate-1', *Molecular Endocrinology*, 14(6), pp. 783–794. doi: 10.1210/mend.14.6.0446.

He, L. *et al.* (2010) 'Shank-interacting protein-like 1 promotes tumorigenesis via PTEN inhibition in human tumor cells', *Journal of Clinical Investigation*, 120(6), pp. 2094–2108. doi: 10.1172/JCI40778.

He, L. *et al.* (2011) 'α-Mannosidase 2C1 attenuates PTEN function in prostate cancer cells', *Nature Communications*, 2(1), p. 307. doi: 10.1038/ncomms1309.

Heer, E. *et al.* (2020) 'Global burden and trends in premenopausal and postmenopausal breast cancer: a population-based study', *The Lancet Global Health*. World Health Organization, 8(8), pp. e1027–e1037. doi: 10.1016/S2214-109X(20)30215-1.

Heiden, M. G. V., Cantley, L. C. and Thompson, C. B. (2009) 'Understanding the warburg effect: The metabolic requirements of cell proliferation', *Science*, 324(5930), pp. 1029–1033. doi: 10.1126/science.1160809.

Hennessy, B. T. *et al.* (2005) 'Exploiting the PI3K/AKT pathway for cancer drug discovery', *Nature Reviews Drug Discovery*, 4(12), pp. 988–1004. doi: 10.1038/nrd1902.

Hettinger, K. *et al.* (2007) 'c-Jun promotes cellular survival by suppression of PTEN', *Cell Death and Differentiation*, 14(2), pp. 218–229. doi: 10.1038/sj.cdd.4401946.

Hidalgo, L., Jose, S. and Signer, R. A. J. (2019) 'Cell-type-specific quantification of protein synthesis in vivo', *Nature Protocols*, 14(2), pp. 441–460. doi: 10.1038/s41596-018-0100-z.

Hinds, P. W. and Weinberg, R. A. (1994) 'Tumor suppressor genes', *Current Opinion in Genetics and Development*, 4(1), pp. 135–141. doi: 10.1016/0959-437X(94)90102-3.

Hochhaus, A. *et al.* (2017) 'Long-Term Outcomes of Imatinib Treatment for Chronic Myeloid Leukemia', *New England Journal of Medicine*, 376(10), pp. 917–927. doi: 10.1056/NEJMoa1609324.

Hodel, M. R., Corbett, A. H. and Hodel, A. E. (2001) 'Dissection of a nuclear localization signal', *Journal of Biological Chemistry*, 276(2), pp. 1317–1325. doi: 10.1074/jbc.M008522200.

Hollander, M. C., Blumenthal, G. M. and Dennis, P. A. (2011) 'PTEN loss in the continuum of common cancers, rare syndromes and mouse models', *Natural Review Cancer*, 11(4), pp. 289–301. doi: 10.1038/nrc3037.

Horie, Y. *et al.* (2004) 'Hepatocyte-specific Pten deficiency results in steatohepatitis and hepatocellular carcinomas', *Journal of Clinical Investigation*, 113(12), pp. 1774–1783. doi: 10.1172/JCI20513.

Hortobagyi, G. N. *et al.* (2016) 'Ribociclib as first-line therapy for HR-positive, advanced breast cancer', *New England Journal of Medicine*, 375(18), pp. 1738–1748. doi: 10.1056/NEJMoa1609709.

Howlader, N. *et al.* (2014) 'US incidence of breast cancer subtypes defined by joint hormone receptor and HER2 status', *Journal of the National Cancer Institute*, 106(5), pp. 1–8. doi: 10.1093/jnci/dju055.

Hudis, C. *et al.* (2013) 'A phase 1 study evaluating the combination of an allosteric AKT inhibitor (MK-2206) and trastuzumab in patients with HER2-positive solid tumors', *Breast Cancer Research*, 15(6), p. R110. doi: 10.1186/bcr3577.

Hunter, D. J. *et al.* (1997) 'Non-dietary factors as risk factors for breast cancer, and as effect modifiers of the association of fat intake and risk of breast cancer', *Cancer Causes and Control: CCC*, 8(1), pp. 49–56. doi: 10.1023/A:1018431104786.

Hurvitz, S. A. *et al.* (2015) 'Combination of everolimus with trastuzumab plus paclitaxel as first-line treatment for patients with HER2-positive advanced breast cancer (BOLERO-1): A phase 3, randomised, double-blind, multicentre trial', *The Lancet Oncology*, 16(7), pp. 816–829. doi: 10.1016/S1470-2045(15)00051-0.

Hutter, C. and Zenklusen, J. C. (2018) 'The Cancer Genome Atlas: Creating Lasting Value beyond Its Data', *Cell*, 173(2), pp. 283–285. doi: 10.1016/j.cell.2018.03.042.

Im, J.-S. *et al.* (2009) 'Assembly of the Cdc45-Mcm2-7-GINS complex in human cells requires the Ctf4/And-1, RecQL4, and Mcm10 proteins', *Proceedings of the National Academy of Sciences*, 106(37), pp. 15628–15632. doi: 10.1073/pnas.0908039106.

Im, J. S. *et al.* (2015) 'RecQL4 is required for the association of Mcm10 and Ctf4 with replication origins in human cells', *Cell Cycle*, 14(7), pp. 1001–1009. doi: 10.1080/15384101.2015.1007001.

Inoki, K. *et al.* (2002) 'TSC2 is phosphorylated and inhibited by Akt and suppresses mTOR signalling', *Nature Cell Biology*, 4(9), pp. 648–657. doi: 10.1038/ncb839.

Iqbal, Nida and Iqbal, Naveed (2014) 'Human Epidermal Growth Factor Receptor 2 (HER2) in Cancers: Overexpression and Therapeutic Implications', *Molecular Biology International*, 2014, pp. 1–9. doi: 10.1155/2014/852748.

Jackson, R. J., Hellen, C. U. . and Pestova, T. V. (2015) 'The mechanism of eukaryotic translation initiation and principles of its regulation', *Nature Reviews Molecular Cell Biology*, 11(2), pp. 113–127. doi: 10.1038/nrm2838.

Javier, R. T. and Butel, J. S. (2008) 'The history of tumor virology', *Cancer Research*, 68(19), pp. 7693–7706. doi: 10.1158/0008-5472.CAN-08-3301.

Jerde, T. J. (2015) 'Phosphatase and tensin homologue: Novel regulation by developmental signaling', *Journal of Signal Transduction*, 2015, p. 282567. doi: 10.1155/2015/282567.

Juric, D. *et al.* (2015) 'Convergent loss of PTEN leads to clinical resistance to a PI3Kα inhibitor', *Nature*, 518(7538), pp. 240–244. doi: 10.1038/nature13948.

Kalluri, R. and Zeisberg, M. (2006) 'Fibroblasts in cancer', *Nature Reviews Cancer*, 6(5), pp. 392–401. doi: 10.1038/nrc1877.

Kang, Y.-H. *et al.* (2013) 'Interaction between human Ctf4 and the Cdc45/Mcm2-7/GINS (CMG) replicative helicase', *Proceedings of the National Academy of Sciences*, 110(49), pp. 19760–19765. doi: 10.1073/pnas.1320202110.

Kang, Y. and Pantel, K. (2014) 'Tumor cell dissemination: emerging biological insights from animal models and cancer patients', *Cancer Cell*, 23(5), pp. 573–581. doi: 10.1016/j.ccr.2013.04.017.

Kappler, C. S. *et al.* (2014) 'Oncogenic signaling in amphiregulin and EGFR-expressing PTEN-null human breast cancer', *Molecular Oncology*, 9(2), pp. 527–43. doi: 10.1016/j.molonc.2014.10.006.

Kataoka, Y. *et al.* (2010) 'Association between gain-of-function mutations in PIK3CA and resistance to HER2-targeted agents in HER2-amplified breast cancer cell lines', *Annals of Oncology*, 21(2), pp. 255–262. doi: 10.1093/annonc/mdp304.

Ke, X. and Shen, L. (2017) 'Molecular targeted therapy of cancer: The progress and future prospect', *Frontiers in Laboratory Medicine*, 1(2), pp. 69–75. doi: 10.1016/j.flm.2017.06.001.

Kechagioglou, P. *et al.* (2014) 'Tumor suppressor PTEN in breast cancer: heterozygosity, mutations and protein expression', *Anticancer Research*, 34(3), pp. 1387–1400.

Key, T. J. *et al.* (2002) 'Endogenous sex hormones and breast cancer in postmenopausal women: Reanalysis of nine prospective studies', *Journal of the National Cancer Institute*, 94(8), pp. 606–616. doi: 10.1093/jnci/94.8.606.

Khan, F. *et al.* (2018) 'Loss of PTEN in high grade advanced stage triple negative breast ductal cancers in African American women', *Pathology Research and Practice*, 214(5), pp. 673–678. doi:

10.1016/j.prp.2018.03.020.

Kikuchi, H. *et al.* (2011) 'GCN5 regulates the activation of PI3K/Akt survival pathway in B cells exposed to oxidative stress via controlling gene expressions of Syk and Btk', *Biochemical and Biophysical Research Communications*. Elsevier Inc., 405(4), pp. 657–661. doi: 10.1016/j.bbrc.2011.01.088.

Kilkenny, M. L. *et al.* (2017) 'The human CTF4-orthologue AND-1 interacts with DNA polymerase a/primase via its unique C-Terminal HMG box', *Open Biology*, 7(11), p. 170217. doi: 10.1098/rsob.170217.

Kim, S.-B. *et al.* (2017) 'Ipatasertib plus paclitaxel versus placebo plus paclitaxel as firstline therapy for metastatic triple-negative breast cancer (LOTUS): a multicentre, randomised, double-blind, placebocontrolled, phase 2 trial', *The Lancet Oncology*, 18(10), pp. 1360–1372. doi: 10.1016/S1470-2045(17)30450-3.

Kim, Y.-C. *et al.* (2009) 'Oxidation of DJ-1-dependent cell transformation through direct binding of DJ-1 to PTEN', *International Journal of Oncology*, 35(6), pp. 1331–1341. doi: 10.3892/ijo_00000458.

Kim, Y., Yoo, K. Y. and Goodman, M. T. (2015) 'Differences in incidence, mortality and survival of breast cancer by regions and countries in Asia and contributing factors', *Asian Pacific Journal of Cancer Prevention*, 16(7), pp. 2857–2870. doi: 10.7314/APJCP.2015.16.7.2857.

Kittaneh, M., Montero, A. J. and Glück, S. (2013) 'Molecular Profiling for Breast Cancer: A Comprehensive Review', *Biomarkers in Cancer*, 5(1), pp. 61–70. doi: 10.4137/bic.s9455.

Klassen, A. C. and Smith, K. C. (2011) 'The enduring and evolving relationship between social class and breast cancer burden: A review of the literature', *Cancer Epidemiology*, 35(3), pp. 217–234. doi: 10.1016/j.canep.2011.02.009.

Klippel, A. *et al.* (1997) 'A specific product of phosphatidylinositol 3-kinase directly activates the protein kinase Akt through its pleckstrin homology domain.', *Molecular and Cellular Biology*, 17(1), pp. 338–344. doi: 10.1128/mcb.17.1.338.

Knudsen, E. S. *et al.* (2012) 'Retinoblastoma and phosphate and tensin homolog tumor suppressors: Impact on ductal carcinoma in situ progression', *Journal of the National Cancer Institute*, 104(23), pp. 1825–1836. doi: 10.1093/jnci/djs446.

Koboldt, D. C. *et al.* (2012) 'Comprehensive molecular portraits of human breast tumours', *Nature*, 490(7418), pp. 61–70. doi: 10.1038/nature11412.

Köehler, A., Schmidt-Zachmann, M. S. and Franke, W. W. (1997) 'AND-1, a natural chimeric DNA-binding protein, combines an HMG-box with regulatory WD-repeats', *Journal of Cell Science*, 110(9), pp. 1051–1062. doi: 10.1242/jcs.110.9.1051.

Koh, J. and Kim, M. J. (2019) 'Introduction of a new staging system of breast cancer for radiologists: An emphasis on the prognostic stage', *Korean Journal of Radiology*, 20(1), pp. 69–82. doi: 10.3348/kjr.2018.0231.

Konecny, G. E. and Kristeleit, R. S. (2016) 'PARP inhibitors for BRCA1/2-mutated and sporadic ovarian cancer: Current practice and future directions', *British Journal of Cancer*, 115(10), pp. 1157–1173. doi: 10.1038/bjc.2016.311.

Kotelevets, L. *et al.* (2005) 'Implication of the MAGI-1b/PTEN signalosome in stabilization of adherens junctions and suppression of invasiveness', *The FASEB Journal*, 19(1), pp. 115–117. doi: 10.1096/fj.04-1942fje.

Kouprina, N. *et al.* (1992) 'CTF4 (CHL15) mutants exhibit defective DNA metabolism in the yeast Saccharomyces cerevisiae', *Molecular and Cellular Biology*, 12(12), pp. 5736–5747. doi: 10.1128/mcb.12.12.5736.

Krishnamurthy, J. and Kumar, P. S. (2016) 'Significance of prognostic indicators in infiltrating duct carcinoma breast: Scenario in developing country', *Indian Journal of Cancer*, 53(1), pp. 34–38. doi: 10.4103/0019-509X.180834.

Kukurba, K. R. and Montgomery, S. B. (2015) 'RNA sequencing and analysis', *Cold Spring Harbor protocols*, 2015(11), pp. 951–69. doi: 10.1101/pdb.top084970.

Kulkarni, A. *et al.* (2019) 'Breast cancer incidence and mortality by molecular subtype: Statewide age and racial/ethnic disparities in New Jersey.', *Cancer health disparities*, 3, pp. e1–e17. doi: 10.9777/chd.2019.1012.

Kurose, K. *et al.* (2002) 'Frequent somatic mutations in PTEN and TP53 are mutually exclusive in the stroma of breast carcinomas', *Nature Genetics*, 32(3), pp. 355–357. doi: 10.1038/ng1013.

Lambert, A. W., Pattabiraman, D. R. and Weinberg, R. A. (2017) 'Emerging Biological Principles of Metastasis', *Cell*, 168(4), pp. 670–691. doi: 10.1016/j.cell.2016.11.037.

Langston, L. D. *et al.* (2014) 'CMG helicase and DNA polymerase ε form a functional 15-subunit holoenzyme for eukaryotic leading-strand DNA replication', *Proceedings of the National Academy of Sciences of the United States of America*, 111(43), pp. 15390–15395. doi: 10.1073/pnas.1418334111.

Lawrence, M. S. *et al.* (2014) 'Discovery and saturation analysis of cancer genes across 21 tumor types', *Nature*, 505(7484), pp. 495–501. doi: 10.1038/nature12912.

Lebeau, J. and Goubin, G. (1987) 'Amplification of the epidermal growth factor receptor gene in the BT20 breast carcinoma cell line', *International Journal of Cancer*, 40(2), pp. 189–191. doi: 10.1002/ijc.2910400210.

Lee, A. and Djamgoz, M. B. A. (2018) 'Triple negative breast cancer: Emerging therapeutic modalities and novel combination therapies', *Cancer Treatment Reviews*, 62, pp. 110–122. doi: 10.1016/j.ctrv.2017.11.003.

Lee, J. O. *et al.* (1999) 'Crystal structure of the PTEN tumor suppressor: Implications for its phosphoinositide phosphatase activity and membrane association', *Cell*, 99(3), pp. 323–334. doi: 10.1016/S0092-8674(00)81663-3.

Lee, J. S. *et al.* (2019) 'Phase I clinical trial of the combination of eribulin and everolimus in patients with metastatic triple-negative breast cancer', *Breast Cancer Research*. Breast Cancer Research, 21(1), p. 119. doi: 10.1186/s13058-019-1202-4.

Lee, J. T. *et al.* (2013) 'RFP-mediated ubiquitination of PTEN modulates its effect on AKT activation', *Cell Research*, 23(4), pp. 552–564. doi: 10.1038/cr.2013.27.

Lee, J. Y. *et al.* (2009) 'Id-1 activates Akt-mediated Wnt signaling and p27Kip1 phosphorylation through PTEN inhibition', *Oncogene*, 28(6), pp. 824–831. doi: 10.1038/onc.2008.451.

Lee, S. R. *et al.* (2002) 'Reversible inactivation of the tumor suppressor PTEN by H2O2', *Journal of Biological Chemistry*, 277(23), pp. 20336–20342. doi: 10.1074/jbc.M111899200.

Lee, Y. R., Chen, M. and Pandolfi, P. P. (2018) 'The functions and regulation of the PTEN tumour suppressor: new modes and prospects', *Nature Reviews Molecular Cell Biology*, 19(9), pp. 547–562. doi: 10.1038/s41580-018-0015-0.

Leevers, S. J., Vanhaesebroeck, B. and Waterfield, M. D. (1999) 'Signalling through phosphoinositide 3-kinases: the lipids take centre stage', *Current Opinion in Cell Biology*, 11(2), pp. 219–225. doi: 10.1016/s0955-0674(99)80029-5.

Lehmann, B. D. *et al.* (2011) 'Identification of human triple-negative breast cancer subtypes and preclinical models for selection of targeted therapies', *Journal of Clinical Investigation*, 121(7), pp. 2750–2767. doi: 10.1172/JCI45014.

Leslie, N. and Foti, M. (2011) 'Non-genomic loss of PTEN function in cancer: not in my genes', *Trends*

in Pharmacological SciencesPharmacol Sci, 32(3), pp. 131–140. doi: 10.1016/j.tips.2010.12.005.

Leslie, N. R. and Downes, C. P. (2004) 'PTEN function: how normal cells control it and tumour cells lose it', *Biochemical Journal*, 382(1), pp. 1–11. doi: 10.1042/BJ20040825.

Li, D. M. and Sun, H. (1997) 'TEP1, encoded by a candidate tumor suppressor locus, is a novel protein tyrosine phosphatase regulated by transforming growth factor β', *Cancer research*, 57(11), pp. 2124–2129.

Li, D. M. and Sun, H. (1998) 'PTEN/MMAC1/TEP1 suppresses the tumorigenicity and induces G1 cell cycle arrest in human glioblastoma cells', *Proceedings of the National Academy of Sciences of the United States of America*, 95(26), pp. 15406–15411. doi: 10.1073/pnas.95.26.15406.

Li, J. *et al.* (1997) 'PTEN, a putative protein tyrosine phosphatase gene mutated in human brain, breast, and prostate cancer', *Science*, 275(5308), pp. 1943–1947. doi: 10.1126/science.275.5308.1943.

Li, K. *et al.* (2018) 'ATM inhibition induces synthetic lethality and enhances sensitivity of PTEN-deficient breast cancer cells to cisplatin', *Experimental Cell Research*, 366(1), pp. 24–33. doi: 10.1016/j.yexcr.2018.03.006.

Li, M. *et al.* (2020) 'Monitoring TNM stage of female breast cancer and survival across the South Australian population, with national and international TNM benchmarking: A population-based cohort study', *BMJ Open*, 10(6), p. e037069. doi: 10.1136/bmjopen-2020-037069.

Li, S. *et al.* (2017) 'Loss of PTEN expression in breast cancer: association with clinicopathological characteristics and prognosis', *Oncotarget*, 8(19), pp. 32043–32054. doi: 10.18632/oncotarget.16761.

Li, Y., Jaramillo-Lambert, A. N., *et al.* (2011) 'And-1 is required for the stability of histone acetyltransferase Gcn5', *Oncogene*, 31(5), pp. 643–652. doi: 10.1038/onc.2011.261.

Li, Y., Jaramillo-Lambert, A., *et al.* (2011) 'The stability of histone acetyltransferase general control non-derepressible (Gcn) 5 is regulated by Cullin4-RING E3 ubiquitin ligase', *Journal of Biological Chemistry*, 286(48), pp. 41344–41352. doi: 10.1074/jbc.M111.290767.

Li, Y. *et al.* (2012) 'The involvement of acidic nucleoplasmic DNA-binding protein (and-1) in the regulation of prereplicative complex (pre-RC) assembly in human cells', *Journal of Biological Chemistry*, 287(51), pp. 42469–42479. doi: 10.1074/jbc.M112.404277.

Li, Y. *et al.* (2017) 'And-1 is required for homologous recombination repair by regulating DNA end

resection', *Nucleic Acids Research*, 45(5), pp. 2531–2545. doi: 10.1093/nar/gkw1241.

Li, Z. *et al.* (2005) 'Regulation of PTEN by Rho small GTPases', *Nature Cell Biology*, 7(4), pp. 399–404. doi: 10.1038/ncb1236.

Liaw, D. *et al.* (1997) 'Germline mutations of the PTEN gene in Cowden disease, an inherited breast and thyroid cancer syndrome', *Nature Genetics*, 16(1), pp. 64–67. doi: 10.1038/ng0597-64.

Liliental, J. *et al.* (2000) 'Genetic deletion of the Pten tumor suppressor gene promotes cell motility by activation of Rac1 and Cdc42 GTPases', *Current Biology*, 10(7), pp. 401–404. doi: 10.1016/S0960-9822(00)00417-6.

Lima-Fernandes, E. *et al.* (2011) 'Distinct functional outputs of PTEN signalling are controlled by dynamic association with β 2-arrestins', *The EMBO Journal*, 30(13), pp. 2557–2568. doi: 10.1038/emboj.2011.178.

Lin, Z. *et al.* (2021) 'PTEN loss correlates with T cell exclusion across human cancers', *BMC Cancer*. BMC Cancer, 21(1), p. 429. doi: 10.1186/s12885-021-08114-x.

Liu, B. *et al.* (2019) 'MicroRNA-494-dependent WDHDI inhibition suppresses epithelial-mesenchymal transition, tumor growth and metastasis in cholangiocarcinoma', *Digestive and Liver Disease*, 51(3), pp. 397–411. doi: 10.1016/j.dld.2018.08.021.

Liu, D. *et al.* (2020) 'ASPP1 deficiency promotes epithelial-mesenchymal transition, invasion and metastasis in colorectal cancer', *Cell Death and Disease*, 11(4), p. 224. doi: 10.1038/s41419-020-2415-2.

Liu, F. *et al.* (2005) 'PTEN enters the nucleus by diffusion', *Journal of Cellular Biochemistry*, 96(2), pp. 221–234. doi: 10.1002/jcb.20525.

Liu, H. *et al.* (2019) 'SGLT1 is required for the survival of triple-negative breast cancer cells via potentiation of EGFR activity', *Molecular Oncology*, 13(9), pp. 1874–1886. doi: 10.1002/1878-0261.12530.

Liu, J. C. *et al.* (2018) 'Identification of CDC25 as a Common Therapeutic Target for Triple-Negative Breast Cancer', *Cell Reports*, 23(1), pp. 112–126. doi: 10.1016/j.celrep.2018.03.039.

Liu, X. *et al.* (2003) 'c-Myc transformation domain recruits the human STAGA complex and requires TRRAP and GCN5 acetylase activity for transcription activation', *The Journal of Biological Chemistry*, 278(22), pp. 20405–20412. doi: 10.1074/jbc.M211795200.

Liu, X. S. *et al.* (2011) 'Polo-like kinase 1 facilitates loss of Pten tumor suppressorinduced prostate

cancer formation', *Journal of Biological Chemistry*, 286(41), pp. 35795–35800. doi: 10.1074/jbc.C111.269050.

López-Knowles, E. *et al.* (2010) 'PI3K pathway activation in breast cancer is associated with the basal-like phenotype and cancer-specific mortality', *International Journal of Cancer*, 126(5), pp. 1121–1131. doi: 10.1002/ijc.24831.

Lowe, E. D. *et al.* (2002) 'Specificity determinants of recruitment peptides bound to phospho-CDK2/cyclin A', *Biochemistry*, 41(52), pp. 15625–15634. doi: 10.1021/bi0268910.

Lu, J. *et al.* (2009) 'Stem cell factor SALL4 represses the transcriptions of PTEN and SALL1 through an epigenetic repressor complex', *PLoS ONE*, 4(5), pp. 1–13. doi: 10.1371/journal.pone.0005577.

Luo, J. L. *et al.* (2007) 'Nuclear cytokine-activated IKKα controls prostate cancer metastasis by repressing Maspin', *Nature*, 446(7136), pp. 690–694. doi: 10.1038/nature05656.

Maddams, J., Utley, M. and Møller, H. (2012) 'Projections of cancer prevalence in the United Kingdom, 2010-2040', *British Journal of Cancer*, 107(7), pp. 1195–1202. doi: 10.1038/bjc.2012.366.

Maehama, T. and Dixon, J. E. (1998) 'The Tumor Suppressor, PTEN/ MMAC1, Dephosphorylates the Lipid Second Messenger, Phosphatidylinositol 3,4,5-Trisphosphate', *The Journal of Biological Chemistry*, 273(22), pp. 13375–13379. doi: 10.1074/jbc.273.22.13375.

Mahimainathan, L. *et al.* (2006) 'Mesangial cell hypertrophy by high glucose is mediated by downregulation of the tumor suppressor PTEN', *Diabetes*, 55(7), pp. 2115–2125. doi: 10.2337/db05-1326.

Makki, J. (2015) 'Diversity of breast carcinoma: Histological subtypes and clinical relevance', *Clinical Medicine Insights: Pathology*, 8(1), pp. 23–31. doi: 10.4137/CPath.s31563.

Malhotra, G. K. *et al.* (2010) 'Histological, molecular and functional subtypes of breast cancers', *Cancer Biology and Therapy*, 10(10), pp. 955–960. doi: 10.4161/cbt.10.10.13879.

Malumbres, M. and Barbacid, M. (2002) 'To cycle or not to cycle: a critical decision in cancer', *Nature Reviews Cancer*, 1(3), pp. 222–231. doi: 10.1038/35106065.

Malumbres, M. and Barbacid, M. (2005) 'Mammalian cyclin-dependent kinases', *Trends in Biochemical Sciences*, 30(11), pp. 630–641. doi: 10.1016/j.tibs.2005.09.005.

Malumbres, M. and Barbacid, M. (2009) 'Cell cycle, CDKs and cancer: A changing paradigm', *Nature Reviews Cancer*, 9(3), pp. 153–166. doi: 10.1038/nrc2602.

Manning, B. D. and Cantley, L. C. (2007) 'AKT/PKB Signaling: Navigating Downstream', *Cell*, 129(7), pp. 1261–1274. doi: 10.1016/j.cell.2007.06.009.

Marsh, D. J. *et al.* (1998) 'Mutation spectrum and genotype-phenotype analyses in Cowden disease and Bannayan-Zonana syndrome, two hamartoma syndromes with germline PTEN mutation', *Human Molecular Genetics*, 7(3), pp. 507–515. doi: 10.1093/hmg/7.3.507.

Marsh, D. J. *et al.* (1999) 'PTEN mutation spectrum and genotype-phenotype correlations in Bannayan-Riley-Ruvalcaba syndrome suggest a single entity with Cowden syndrome', *Human Molecular Genetics*, 8(8), pp. 1461–1472. doi: 10.1093/hmg/8.8.1461.

Martin-Belmonte, F. *et al.* (2007) 'PTEN-mediated apical segregation of phosphoinositides controls rpithelial morphogenesis through Cdc42', *Cell*, 128(2), pp. 383–397. doi: 10.1016/j.cell.2006.11.051.

Martin, A. and Weber, B. L. (2000) 'Genetic and Hormonal Risk Factors in Breast Cancer', *Journal of the National Cancer Institute*, 92(14), pp. 1126–1135. doi: 10.1093/jnci/92.14.1126.

Martin, V. *et al.* (2012) 'Molecular characterization of EGFR and EGFR-downstream pathways in triple negative breast carcinomas with basal like features', *Histology and Histopathology*, 27(6), pp. 785–792. doi: 10.14670/HH-27.785.

Maximiano, S. *et al.* (2016) 'Trastuzumab in the treatment of breast cancer', *BioDrugs*, 30(2), pp. 75–86. doi: 10.1007/s40259-016-0162-9.

Mayo, L. D. and Donner, D. B. (2001) 'A phosphatidylinositol 3-kinase/Akt pathway promotes translocation of Mdm2 from the cytoplasm to the nucleus', *Proceedings of the National Academy of Sciences of the United States of America*, 98(20), pp. 11598–11603. doi: 10.1073/pnas.181181198.

McCabe, N. *et al.* (2015) 'Mechanistic rationale to target PTEN-deficient tumor cells with inhibitors of the DNA damage response kinase ATM', *Cancer Research*, 75(11), pp. 2159–2165. doi: 10.1158/0008-5472.CAN-14-3502.

Mehenni, H. *et al.* (2005) 'LKB1 interacts with and phosphorylates PTEN: A functional link between two proteins involved in cancer predisposing syndromes', *Human Molecular Genetics*, 14(15), pp. 2209–2219. doi: 10.1093/hmg/ddi225.

Meisel, J. L. *et al.* (2018) *Evolution of Targeted Therapy in Breast Cancer : Where Precision Medicine Began*, *American Society of Clinical Oncology Educational Book*. doi: 10.1200/EDBK_201037.

Melchor, L. and Benítez, J. (2013) 'The complex genetic landscape of familial breast cancer', *Human Genetics*, 132(8), pp. 845–863. doi: 10.1007/s00439-013-1299-y.

Mendes-Pereira, A. M. *et al.* (2009) 'Synthetic lethal targeting of PTEN mutant cells with PARP inhibitors', *EMBO Molecular Medicine*, 1(6–7), pp. 315–322. doi: 10.1002/emmm.200900041.

Mendes-Pereira, A. M., Lord, C. J. and Ashworth, A. (2012) 'NLK Is a novel therapeutic target for PTEN deficient tumour cells', *PLoS ONE*, 7(10), p. e47249. doi: 10.1371/journal.pone.0047249.

Meng, F. *et al.* (2007) 'MicroRNA-21 regulates expression of the PTEN tumor suppressor gene in human hepatocellular cancer', *Gastroenterology*, 133(2), pp. 647–658. doi: 10.1053/j.gastro.2007.05.022.

Mereniuk, T. R. *et al.* (2013) 'Synthetic lethal targeting of PTEN-deficient cancer cells using selective disruption of polynucleotide kinase/phosphatase', *Molecular Cancer Therapeutics*, 12(10), pp. 2135–2144. doi: 10.1158/1535-7163.MCT-12-1093.

Metcalfe, K. A. *et al.* (2009) 'Breast cancer risks in women with a family history of breast or ovarian cancer who have tested negative for a BRCA1 or BRCA2 mutation', *British Journal of Cancer*, 100(2), pp. 421–425. doi: 10.1038/sj.bjc.6604830.

Miller, S. J. *et al.* (2002) 'Direct identification of PTEN phosphorylation sites', *FEBS Letters*, 528(1–3), pp. 145–153. doi: 10.1016/S0014-5793(02)03274-X.

Miller, T. W. *et al.* (2009) 'Loss of Phosphatase and tensin homologue deleted on chromosome 10 engages ErbB3 and insulin-like growth factor-I receptor signaling to promote antiestrogen resistance in breast cancer', *Cancer Research*, 69(10), pp. 4192–4201. doi: 10.1158/0008-5472.CAN-09-0042.

Miller, T. W. *et al.* (2010) 'Hyperactivation of phosphatidylinositol-3 kinase promotes escape from hormone dependence in estrogen receptor-positive human breast cancer', *Journal of Clinical Investigation*, 120(7), pp. 2406–2413. doi: 10.1172/JCI41680.

Von Minckwitz, G. *et al.* (2019) 'Trastuzumab emtansine for residual invasive HER2-positive breast cancer', *New England Journal of Medicine*, 380(7), pp. 617–628. doi: 10.1056/NEJMoa1814017.

Mirmohammadsadegh, A. *et al.* (2006) 'Epigenetic silencing of the PTEN gene in melanoma', *Cancer Research*, 66(13), pp. 6546–6552. doi: 10.1158/0008-5472.CAN-06-0384.

Mohamed, A. *et al.* (2013) 'Targeted therapy for breast cancer', *American Journal of Pathology*. American Society for Investigative Pathology, 183(4), pp. 1096–1112. doi:

10.1016/j.ajpath.2013.07.005.

Mohr, S., Bakal, C. and Perrimon, N. (2013) 'Genomic screening with RNAi: results and challenges', *Annual Review of Biochemistry*, 79(1), pp. 37–64. doi: 10.1146/annurev-biochem-060408-092949.

Mohr, S. E. *et al.* (2014) 'RNAi screening comes of age: improved techniques and complementary approaches', *Nature Reviews Molecular Cell Biology*, 15(9), pp. 591–600. doi: 10.1038/nrm386.

Molinari, F. and Frattini, M. (2014) 'Functions and regulation of the PTEN gene in colorectal cancer', *Frontiers in Oncology*, 3, p. 326. doi: 10.3389/fonc.2013.00326.

Moorehead, R. A. *et al.* (2003) 'Insulin-like growth factor-II regulates PTEN expression in the mammary gland', *Journal of Biological Chemistry*, 278(50), pp. 50422–50427. doi: 10.1074/jbc.M306894200.

Morani, F. *et al.* (2014) 'PTEN regulates plasma membrane expression of glucose transporter 1 and glucose uptake in thyroid cancer cells', *Journal of Molecular Endocrinology*, 53(2), pp. 247–258. doi: 10.1530/JME-14-0118.

Morrow, P. K. *et al.* (2011) 'Phase I/II study of trastuzumab in combination with everolimus (RAD001) in patients with HER2-overexpressing metastatic breast cancer who progressed on trastuzumab-based therapy', *Journal of Clinical Oncology*, 29(23), pp. 3126–3132. doi: 10.1200/JCO.2010.32.2321.

Mosser, V. A., Li, Y. and Quon, M. J. (2001) 'PTEN does not modulate GLUT4 translocation in rat adipose cells under physiological conditions', *Biochemical and Biophysical Research Communications*, 288(4), pp. 1011–1017. doi: 10.1006/bbrc.2001.5876.

Mouridsen, H. *et al.* (2003) 'Phase III study of letrozole versus tamoxifen as first-line therapy of advanced breast cancer in postmenopausal women: analysis of survival and update of efficacy from the International Letrozole Breast Cancer Group', *Journal of Clinical Oncology*, 21(11), pp. 2101–2109. doi: 10.1200/JCO.2003.04.194.

Moyer, S. E., Lewis, P. W. and Botchan, M. R. (2006) 'Isolation of the Cdc45/Mcm2-7/GINS (CMG) complex, a candidate for the eukaryotic DNA replication fork helicase', *Proceedings of the National Academy of Sciences of the United States of America*, 103(27), pp. 10236–10241. doi: 10.1073/pnas.0602400103.

Mu, P. *et al.* (2009) 'Genetic dissection of the miR-17-92 cluster of microRNAs in Myc-induced B-cell lymphomas', *Genes and Development*, 23(24), pp. 2806–2811. doi: 10.1101/gad.1872909.

Musgrove, E. A. and Sutherland, R. L. (2009) 'Biological determinants of endocrine resistance in breast cancer', *Nature Reviews Cancer*, 9(9), pp. 631–643. doi: 10.1038/nrc2713.

Myal, Y., Leygue, E. and Blanchard, A. A. (2010) 'Claudin 1 in breast tumorigenesis: revelation of a possible novel "claudin high" subset of breast cancers', *Journal of Biomedicine and Biotechnology*, 2010, p. 956897. doi: 10.1155/2010/956897.

Myers, M. P. *et al.* (1997) 'P-TEN, the tumor suppressor from human chromosome 10q23, is a dual-specificity phosphatase', *Proceedings of the National Academy of Sciences*, 94(17), pp. 9052–9057. doi: 10.1073/pnas.94.17.9052.

Myers, M. P. *et al.* (1998) 'The lipid phosphatase activity of PTEN is critical for its tumor supressor function', *Proceedings of the National Academy of Sciences of the United States of America*, 95(23), pp. 13513–13518. doi: 10.1073/pnas.95.23.13513.

Nabholtz, J. M. *et al.* (2000) 'Anastrozole is superior to tamoxifen as first-line therapy for advanced breast cancer in postmenopausal women: results of a North American multicenter randomized trial. Arimidex Study Group', *Journal of Clinical Oncology*, 18(22), pp. 3758–3767. doi: 10.1200/JCO.2000.18.22.3758.

Nagata, C. *et al.* (1997) 'Associations of alcohol, height, and reproductive factors with serum hormone concentrations in postmenopausal Japanese women. Steroid hormones in Japanese postmenopausal women', *Breast Cancer Research and Treatment*, 44(3), pp. 235–241. doi: 10.1023/A:1005831220205.

Nagata, Y. *et al.* (2004) 'PTEN activation contributes to tumor inhibition by trastuzumab, and loss of PTEN predicts trastuzumab resistance in patients', *Cancer Cell*, 6(2), pp. 117–127. doi: 10.1016/j.ccr.2004.06.022.

Nagy, Z. and Tora, L. (2007) 'Distinct GCN5/PCAF-containing complexes function as co-activators and are involved in transcription factor and global histone acetylation', *Oncogene*, 26(37), pp. 5341–5357. doi: 10.1038/sj.onc.1210604.

Nakamura, N. *et al.* (2000) 'Forkhead transcription factors are critical effectors of cell death and cell cycle arrest downstream of PTEN', *Molecular and Cellular Biology*, 20(23), pp. 8969–8982. doi: 10.1128/mcb.20.23.8969-8982.2000.

Nakashima, N. *et al.* (2000) 'The tumor suppressor PTEN negatively regulates insulin signaling in 3T3-L1 adipocytes', *The Journal of Biological Chemistry*, 275(17), pp. 12889–12895. doi: 10.1074/jbc.275.17.12889.

Nalla, L. V., Kalia, K. and Khairnar, A. (2019) 'Self-renewal signaling pathways in breast cancer stem cells', *International Journal of Biochemistry and Cell Biology*, 107, pp. 140–153. doi: 10.1016/j.biocel.2018.12.017.

Nathans, D. (1964) 'Puromycin inhibition of protein synthesis: Incorporation of puromycin into peptide chains', *Proceedings of the National Academy of Sciences of the United States of America*, 51(4), pp. 585–592. doi: 10.1073/pnas.51.4.585.

Nedeljkovic, M. and Damjanovic, A. (2019) 'Mechanisms of Chemotherapy Resistance in Triple-Negative Breast Cancer — How We Can Rise to the Challenge', *Cells*, 8(9), p. 957. doi: 10.3390/cells8090957.

Ní Bhaoighill, M. and Dunlop, E. A. (2019) 'Mechanistic target of rapamycin inhibitors: successes and challenges as cancer therapeutics', *Cancer Drug Resistance*, 2, pp. 1069–1085. doi: 10.20517/cdr.2019.87.

Nijman, S. M. B. (2011) 'Synthetic lethality: General principles, utility and detection using genetic screens in human cells', *FEBS Letters*, 585(1), pp. 1–6. doi: 10.1016/j.febslet.2010.11.024.

Nounou, M. I. *et al.* (2015) 'Breast cancer: Conventional diagnosis and treatment modalities and recent patents and technologies', *Breast cancer : Basic and Clinical Research*, 9(Suppl 2), pp. 17–34. doi: 10.4137/BCBCR.S29420.

Nurse, P. (2000) 'A long twentieth century of the cell cycle and beyond', *Cell*, 100(1), pp. 71–78. doi: 10.1016/S0092-8674(00)81684-0.

O'Keefe, B. (2001) 'The future of cancer treatment', *Fortune*, 144(2), p. 80. doi: 10.1038/nm.3801.

O'Neil, N. J., Bailey, M. L. and Hieter, P. (2017) 'Synthetic lethality and cancer', *Nature Reviews Genetics*, 18(10), pp. 613–623. doi: 10.1038/nrg.2017.47.

O'Reilly, K. E. *et al.* (2006) 'mTOR inhibition induces upstream receptor tyrosine kinase signaling and activates Akt', *Cancer Research*, 66(3), pp. 1500–1508. doi: 10.1158/0008-5472.CAN-05-2925.

Ogawara, Y. *et al.* (2002) 'Akt enhances Mdm2-mediated ubiquitination and degradation of p53', *Journal of Biological Chemistry*, 277(24), pp. 21843–21850. doi: 10.1074/jbc.M109745200.

Okumura, K. *et al.* (2005) 'Cellular transformation by the MSP58 oncogene is inhibited by its physical interaction with the PTEN tumor suppressor', *Proceedings of the National Academy of Sciences of the United States of America*, 102(8), pp. 2703–2706. doi: 10.1073/pnas.0409370102.

Okumura, K. *et al.* (2006) 'PCAF modulates PTEN activity', *Journal of Biological Chemistry*, 281(36),

pp. 26562–26568. doi: 10.1074/jbc.M605391200.

Oliveira, M. *et al.* (2019) 'FAIRLANE, a double-blind placebo-controlled randomized phase II trial of neoadjuvant ipatasertib plus paclitaxel for early triple-negative breast cancer', *Annals of Oncology*, 30(8), pp. 1289–1297. doi: 10.1093/annonc/mdz177.

Oluogun, W. A. *et al.* (2019) 'Histological classification, grading, staging, and prognostic indexing of female breast cancer in an African population: A 10-year retrospective study', *International journal of health sciences*, 13(4), pp. 3–9.

Ortega-Molina, A. *et al.* (2012) 'Pten positively regulates brown adipose function, energy expenditure, and longevity', *Cell Metabolism*, 15(3), pp. 382–394. doi: 10.1016/j.cmet.2012.02.001.

Owusu-Brackett, N. *et al.* (2020) 'Targeting PI3Kβ alone and in combination with chemotherapy or immunotherapy in tumors with PTEN loss', *Oncotarget*, 11(11), pp. 969–981. doi: 10.18632/oncotarget.27503.

Pacek, M. and Walter, J. C. (2004) 'A requirement for MCM7 and Cdc45 in chromosome unwinding during eukaryotic DNA replication', *EMBO Journal*, 23(18), pp. 3667–3676. doi: 10.1038/sj.emboj.7600369.

Padma, V. V. (2015) 'An overview of targeted cancer therapy', *BioMedicine*, 5(4), p. 19. doi: 10.7603/s40681-015-0019-4.

Paik, S. *et al.* (2004) 'A multigene assay to predict recurrence of tamoxifen-treated, node-negative breast cancer', *The New England Journal of Medicine*, 351(27), pp. 2817–2826. doi: 10.1056/NEJMoa041588.

Pampaloni, F., Reynaud, E. G. and Stelzer, E. H. K. (2007) 'The third dimension bridges the gap between cell culture and live tissue', *Nature Reviews Molecular Cell Biology*, 8(10), pp. 839–845. doi: 10.1038/nrm2236.

Papa, A. and Pandolfi, P. P. (2016) 'Phosphatase-independent functions of the tumor suppressor PTEN', in Neel, B. G. and Tonks, N. K. (eds) *Protein Tyrosine Phosphatases in Cancer*. Springer,New York, NY, pp. 247–260. doi: 10.1007/978-1-4939-3649-6_9.

Pappas, K. *et al.* (2021) 'NOTCH and EZH2 collaborate to repress PTEN expression in breast cancer', *Communications Biology*, 4(1), p. 312. doi: 10.1038/s42003-021-01825-8.

Park, M.-J. *et al.* (2002) 'PTEN suppresses hyaluronic acid-induced matrix metalloproteinase-9 expression in U87MG glioblastoma cells through focal adhesion kinase dephosphorylation', *Cancer*

Research, 62(21), pp. 6318–6322.

Park, Y. H. *et al.* (2013) 'Statin induces inhibition of triple negative breast cancer (TNBC) cells via PI3K pathway', *Biochemical and Biophysical Research Communications*. Elsevier Inc., 439(2), pp. 275–279. doi: 10.1016/j.bbrc.2013.08.043.

Patel, L. *et al.* (2001) 'Tumor suppressor and anti-inflammatory actions of PPARγ agonists are mediated via upregulation of PTEN', *Current Biology*, 11(10), pp. 764–768. doi: 10.1016/S0960-9822(01)00225-1.

Pelengaris, S. and Khan, M. (2013) *The molecular biology of cancer: A bridge from bench to bedside*. Second edi. Edited by S. Pelengaris and M. Khan. Willey-Blackwell Publishing Ltd.

Perera, R. L. *et al.* (2013) 'Mechanism for priming DNA synthesis by yeast DNA Polymerase α', *eLife*, 2, p. e00482. doi: 10.7554/elife.00482.

Pérez-Tenorio, G. *et al.* (2007) 'PIK3CA mutations and PTEN loss correlate with similar prognostic factors and are not mutually exclusive in breast cancer', *Clinical Cancer Research*, 13(12), pp. 3577–3584. doi: 10.1158/1078-0432.CCR-06-1609.

Perren, A. *et al.* (1999) 'Immunohistochemical evidence of loss of PTEN expression in primary ductal adenocarcinomas of the breast', *American Journal of Pathology*, 155(4), pp. 1253–1260. doi: 10.1016/S0002-9440(10)65227-3.

Place, A. E., Jin Huh, S. and Polyak, K. (2011) 'The microenvironment in breast cancer progression: Biology and implications for treatment', *Breast Cancer Research*, 13(6), p. 227. doi: 10.1186/bcr2912.

Planchon, S. M., Waite, K. A. and Eng, C. (2008) 'The nuclear affairs of PTEN', *Journal of Cell Science*, 121(3), pp. 249–253. doi: 10.1242/jcs.022459.

Podsypanina, K. *et al.* (1999) 'Mutation of Pten/Mmac1 in mice causes neoplasia in multiple organ systems', *Proceedings of the National Academy of Sciences*, 96(4), pp. 1563–1568. doi: 10.1073/pnas.96.4.1563.

Poliseno, L., Salmena, L., Zhang, J., *et al.* (2010) 'A coding-independent function of gene and pseudogene mRNAs regulates tumour biology', *Nature*, 465(7301), pp. 1033–1038. doi: 10.1038/nature09144.

Poliseno, L., Salmena, L., Riccardi, L., *et al.* (2010) 'Identification of the miR-106b~25 microRNA cluster as a proto-oncogenic PTEN-targeting intron that cooperates with its host gene MCM7 in

transformation', 3(117), p. ra29. doi: 10.1126/scisignal.2000594.

Polyak, K. (2007) 'Breast cancer : Origins and evolution', *Cell*, 117(11), pp. 3155–63. doi: 10.1172/JCI33295.

Prat, A., Ellis, M. J. and Perou, C. M. (2011) 'Practical implications of gene-expression-based assays for breast oncologists', *Nature Reviews Clinical Oncology*, 9(1), pp. 48–57. doi: 10.1038/nrclinonc.2011.178.

Prendergast, G. C. (2001) 'Knockout drug screens', *Nature Biotechnology*, 19(10), pp. 919–920. doi: 10.1038/nbt1001-919.

Puc, J. *et al.* (2005) 'Lack of PTEN sequesters CHK1 and initiates genetic instability', *Cancer Cell*, 7(2), pp. 193–204. doi: 10.1016/j.ccr.2005.01.009.

Puc, J. and Parsons, R. (2005) 'PTEN loss inhibits CHK1 to cause double stranded-DNA breaks in cells', *Cell Cycle*, 4(7), pp. 927–929. doi: 10.4161/cc.4.7.1795.

Raftopoulou, M. *et al.* (2004) 'Regulation of Cell Migration by the C2 Domain of the Tumor Suppressor PTEN', *Science*, 303(5661), pp. 1179–1181. doi: 10.1126/science.1092089.

Ragab, H. M. *et al.* (2018) 'Assessment of Ki-67 as a potential biomarker in patients with breast cancer', *Journal of Genetic Engineering and Biotechnology*, 16(2), pp. 479–484. doi: 10.1016/j.jgeb.2018.03.002.

Rahmati, S. *et al.* (2020) 'An evaluation of the risk factors of breast cancer in women in Ilam Province: a case–control study based on hospital', *Breast Cancer Management*, 9(4), p. BMT49. doi: 10.2217/bmt-2020-0026.

Rakha, E. A. *et al.* (2008) 'Prognostic significance of nottingham histologic grade in invasive breast carcinoma', *Journal of Clinical Oncology*, 26(19), pp. 3153–3158. doi: 10.1200/JCO.2007.15.5986.

Rakha, E. A. *et al.* (2010) 'Breast cancer prognostic classification in the molecular era: the role of histological grade', *Breast Cancer Research*, 12(4), p. 207. doi: 10.1186/bcr2607.

Reed, D. E. and Shokat, K. M. (2017) 'INPP4B and PTEN loss leads to PI-3,4-P2 accumulation and inhibition of PI3K in TNBC', *Molecular Cancer Research*, 15(6), pp. 765–775. doi: 10.1158/1541-7786.MCR-16-0183.

Ren, W., Joshi, R. and Mathew, P. (2016) 'Synthetic lethality in PTEN-mutant prostate cancer is induced by combinatorial PI3K/Akt and BCL-XL inhibition', *Molecular Cancer Research*, 14(12), pp. 1176–1181. doi: 10.1158/1541-7786.MCR-16-0202.

Reyes, M. E. *et al.* (2017) 'Poor prognosis of patients with triple-negative breast cancer can be stratified by RANK and RANKL dual expression', *Breast Cancer Research and Treatment*. Springer US, 164(1), pp. 57–67. doi: 10.1007/s10549-017-4233-5.

Robert, N. J. (1997) 'Clinical efficacy of tamoxifen', *Oncology (Willston Park)*, 2(1), pp. 15–20.

Robson, M. *et al.* (2017) 'Olaparib for metastatic breast cancer in patients with a germline BRCA mutation', *New England Journal of Medicine*, 377(6), pp. 523–533. doi: 10.1056/NEJMoa1706450.

Roop, R. P. and Ma, C. X. (2012) 'Endocrine resistance in breast cancer: Molecular pathways and rational development of targeted therapies', *Future Oncology*, 8(3), pp. 273–292. doi: 10.2217/fon.12.8.

Rugo, H. S. *et al.* (2016) 'Endocrine therapy for hormone receptor-positive metastatic breast cancer: American society of clinical oncology guideline', *Journal of Clinical Oncology*, 34(25), pp. 3069–3103. doi: 10.1200/JCO.2016.67.1487.

Rzechorzek, N. J. *et al.* (2020) 'CryoEM structures of human CMG-ATPγS-DNA and CMG-AND-1 complexes', *Nucleic Acids Research*, 48(12), pp. 6980–6995. doi: 10.1093/nar/gkaa429.

Sahebjam, S. *et al.* (2011) 'Ki 67 is a major, but not the sole determinant of Oncotype Dx recurrence score', *British Journal of Cancer*, 105(9), pp. 1342–1345. doi: 10.1038/bjc.2011.402.

Saijo, N. (2012) 'Present status and problems on molecular targeted therapy of cancer', *Cancer Research and Treatment*, 44(1), pp. 1–10. doi: 10.4143/crt.2012.44.1.1.

Salmena, L., Carracedo, A. and Pandolfi, P. P. (2008) 'Tenets of PTEN tumor suppression', *Cell*, 133(3), pp. 403–414. doi: 10.1016/j.cell.2008.04.013.

Samuels, Y. *et al.* (2004) 'High frequency of mutations of the PIK3CA gene in human cancers', *Science*, 304(5670), p. 554. doi: 10.1126/science.1096502.

Sansal, I. and Sellers, W. R. (2004) 'The biology and clinical relevance of the PTEN tumor suppressor pathway', *Journal of Clinical Oncology*, 22(14), pp. 2954–2963. doi: 10.1200/JCO.2004.02.141.

Santi, A., Kugeratski, F. G. and Zanivan, S. (2018) 'Cancer associated fibroblasts: The architects of stroma remodeling', *Proteomics*, 18(5–6), p. 1700167. doi: 10.1002/pmic.201700167.

Sarbassov, D. D. *et al.* (2005) 'Phosphorylation and regulation of Akt/PKB by the rictor-mTOR complex', *Science*, 307(5712), pp. 1098–1101. doi: 10.1126/science.1106148.

Sato, N. *et al.* (2010) 'Activation of WD repeat and high-mobility group box DNA binding protein 1

in pulmonary and esophageal carcinogenesis', *Clinical Cancer Research*, 16(1), pp. 226–239. doi: 10.1158/1078-0432.ccr-09-1405.

Saura, C. *et al.* (2014) 'Phase lb study of buparlisib plus trastuzumab in patients with HER2-positive advanced or metastatic breast cancer that has progressed on trastuzumab-based therapy', *Clinical Cancer Research*, 20(7), pp. 1935–1945. doi: 10.1158/1078-0432.CCR-13-1070.

Scaltriti, M. *et al.* (2007) 'Expression of p95HER2, a truncated form of the HER2 receptor, and response to Anti-HER2 therapies in breast cancer', *Journal of the National Cancer Institute*, 99(8), pp. 628–638. doi: 10.1093/jnci/djk134.

Schmid, P., Cortes, J., Robson, M., *et al.* (2020) 'Abstract OT2-08-02: Capivasertib and paclitaxel in first-line treatment of patients with metastatic triple-negative breast cancer: A phase III trial (CAPItello-290)', *Cancer Research*, 80(4_Supplement). doi: 10.1158/1538-7445.SABCS19-OT2-08-02.

Schmid, P., Abraham, J., *et al.* (2020) 'Capivasertib plus paclitaxel versus placebo plus paclitaxel as first-line therapy for metastatic triple-negative breast cancer: The PAKT trial', *Journal of Clinical Oncology*, 38(5), pp. 423–433. doi: 10.1200/JCO.19.00368.

Schmid, P., Cortes, J., Pusztai, L., *et al.* (2020) 'Pembrolizumab for Early Triple-Negative Breast Cancer', *New England Journal of Medicine*, 382(9), pp. 810–821. doi: 10.1056/nejmoa1910549.

Schnitt, S. J. (2010) 'Classification and prognosis of invasive breast cancer: From morphology to molecular taxonomy', *Modern Pathology*, 23(S2), pp. 60–64. doi: 10.1038/modpathol.2010.33.

Sclafani, R. A. and Holzen, T. M. (2007) 'Cell cycle regulation of DNA replication', *Annual Review of Genetics*, 41, pp. 237–280. doi: 10.1146/annurev.genet.41.110306.130308.

Seiler, M. *et al.* (2015) 'Oral ridaforolimus plus trastuzumab for patients with HER2+ trastuzumab-refractory metastatic breast cancer', *Clinical Breast Cancer*, 15(1), pp. 60–65. doi: 10.1016/j.clbc.2014.07.008.

Sejben, A. *et al.* (2020) 'Examination of tumor regression grading systems in breast cancer patients who received neoadjuvant therapy', *Pathology and Oncology Research*, 26(4), pp. 2747–2754. doi: 10.1007/s12253-020-00867-3.

Sekulić, A. *et al.* (2000) 'A direct linkage between the phosphoinositide 3-kinase-AKT signaling pathway and the mammalian target of rapamycin in mitogen-stimulated and transformed cells', *Cancer Research*, 60(13), pp. 3504–3513.

Serra, V. *et al.* (2011) 'PI3K inhibition results in enhanced HER signaling and acquired ERK dependency in HER2-overexpressing breast cancer', *Oncogene*, 30(22), pp. 2547–2557. doi: 10.1038/onc.2010.626.

Serrano-oviedo, L. *et al.* (2020) 'Identification of a stemness-related gene panel associated with BET inhibition in triple negative breast cancer', *Cellular Oncology (Dordrecht)*, 43(3), pp. 431–444. doi: 10.1007/s13402-020-00497-6.

Shahbazian, M. D. and Grunstein, M. (2007) 'Functions of Site-Specific histone acetylation and deacetylation', *Annual Review of Biochemistry*, 76, pp. 75–100. doi: 10.1146/annurev.biochem.76.052705.162114.

Sharma, G. N. *et al.* (2010) 'Various types and management of breast cancer: An overview', *Journal of Advanced Pharmaceutical Technology and Research*, 1(2), pp. 109–126.

Shattuck, D. L. *et al.* (2008) 'Met receptor contributes to trastuzumab resistance of Her2-overexpressing breast cancer cells', *Cancer Research*, 68(5), pp. 1471–1477. doi: 10.1158/0008-5472.CAN-07-5962.

Shechter, D., Ying, C. Y. and Gautier, J. (2004) 'DNA unwinding is an MCM complex-dependent and ATP hydrolysis-dependent process', *Journal of Biological Chemistry*, 279(44), pp. 45586–45593. doi: 10.1074/jbc.M407772200.

Shen, W. *et al.* (2017) 'Expression levels of PTEN, HIF-1α, and VEGF as prognostic factors in ovarian cancer', *European Review for Medical and Pharmacological Sciences*, 21(11), pp. 2596–2603.

Shen, W. H. *et al.* (2007) 'Essential role for nuclear PTEN in maintaining chromosomal integrity', *Cell*, 128(1), pp. 157–170. doi: 10.1016/j.cell.2006.11.042.

Sheng, K. L. *et al.* (2020) 'An integrated approach to biomarker discovery reveals gene signatures highly predictive of cancer progression', *Scientific Reports*, 10(1), p. 21246. doi: 10.1038/s41598-020-78126-3.

Sheng, S., Qiao, M. and Pardee, A. B. (2009) 'Metastasis and AKT activation', *Journal of Cellular Physiology*, 218(3), pp. 451–454. doi: 10.1002/jcp.21616.

Simpson, L. and Parsons, R. (2001) 'PTEN: Life as a tumor suppressor', *Experimental Cell Research*, 264(1), pp. 29–41. doi: 10.1006/excr.2000.5130.

Singh, J. C. *et al.* (2014) 'Phase 2 trial of everolimus and carboplatin combination in patients with triple negative metastatic breast cancer', *Breast Cancer Research*, 16(2), p. R32. doi:

10.1186/bcr3634.

Singletary, S. E. (2003) 'Rating the Risk Factors for Breast Cancer', *Annals of Surgery*, 237(4), pp. 474–482. doi: 10.1097/01.SLA.0000059969.64262.87.

Skinner, H. D. *et al.* (2004) 'Vascular endothelial growth factor transcriptional activation is mediated by hypoxia-inducible factor 1alpha, HDM2, and p70S6K1 in response to phosphatidylinositol 3-kinase/AKT signaling', *The journal of Biological Chemistry*, 279(44), pp. 45643–45651. doi: 10.1074/jbc.M404097200.

Slamon, D. J. *et al.* (2001) 'Use of chemotherapy plus a monoclonal antibody against HER2 for metastatic breast cancer that overexpresses HER2', *The New England Journal of Medicine*, 344(11), pp. 783–792. doi: 10.1056/NEJM200103153441101.

Sledge, G. W. *et al.* (2017) 'MONARCH 2: Abemaciclib in combination with fulvestrant in women with HR+/HER2-advanced breast cancer who had progressed while receiving endocrine therapy', *Journal of Clinical Oncology*, 35(25), pp. 2875–2884. doi: 10.1200/JCO.2017.73.7585.

Smittenaar, C. R. *et al.* (2016) 'Cancer incidence and mortality projections in the UK until 2035', *British Journal of Cancer*, 115(9), pp. 1147–1155. doi: 10.1038/bjc.2016.304.

Song, L. B. *et al.* (2009) 'The polycomb group protein Bmi-1 represses the tumor suppressor PTEN and induces epithelial-mesenchymal transition in human nasopharyngeal epithelial cells', *The Journal of Clinical Investigation*, 119(12), pp. 3626–3636. doi: 10.1172/JCI39374.

Song, M. S. *et al.* (2011) 'Nuclear PTEN regulates the APC-CDH1 tumor suppressive complex in a phosphatase-independent manner', *Cell*, 144(2), pp. 187–199. doi: 10.1016/j.cell.2010.12.020.

Song, M. S., Salmena, L. and Pandolfi, P. P. (2012) 'The functions and regulation of the PTEN tumour suppressor', *Nature Reviews Molecular Cell Biology*, 13(5), pp. 283–296. doi: 10.1038/nrm3330.

Spurrier, B., Ramalingam, S. and Nishizuka, S. (2008) 'Reverse-phase protein lysate microarrays for cell signaling analysis', *Nature Protocols*, 3(11), pp. 1796–1808. doi: 10.1038/nprot.2008.179.

Stambolic, V. *et al.* (1998) 'Negative regulation of PKB/Akt-dependent cell survival by the tumor suppressor PTEN', *Cell*, 95(1), pp. 29–39. doi: 10.1016/S0092-8674(00)81780-8.

Stambolic, V. *et al.* (2001) 'Regulation of PTEN transcription by p53', *Molecular Cell*, 8(2), pp. 317–325. doi: 10.1016/S1097-2765(01)00323-9.

Stambolic, V., Tsao, M. and Macpherson, D. (2000) 'High Incidence of Breast and Endometrial Neoplasia Resembling Human Cowden Syndrome in pten + / − Mice', *Cancer*, 60(13), pp. 3605–

3611.

Steck, P. A. *et al.* (1997) 'Identification of a candidate tumour suppressor gene, MMAC1, at chromosome 10q23.3 that is mutated in multiple advanced cancers', *Nature Genetics*, 15(4), pp. 356–362. doi: 10.1038/ng0497-356.

Steckel, M. *et al.* (2012) 'Determination of synthetic lethal interactions in KRAS oncogene-dependent cancer cells reveals novel therapeutic targeting strategies', *Cell Research*, 22(8), pp. 1227–1245. doi: 10.1038/cr.2012.82.

Stirnimann, C. U. *et al.* (2010) 'WD40 proteins propel cellular networks', *Trends in Biochemical Sciences*, 35(10), pp. 531–538. doi: 10.1016/j.tibs.2010.04.003.

Stratikopoulos, E. E. *et al.* (2015) 'Kinase and BET inhibitors together clamp inhibition of PI3K signaling and overcome resistance to therapy', *Cancer Cell*, 27(6), pp. 837–851. doi: 10.1016/j.ccell.2015.05.006.

Subauste, M. C. *et al.* (2005) 'Vinculin controls PTEN protein level by maintaining the interaction of the adherens junction protein β-catenin with the scaffolding protein MAGI-2', *Journal of Biological Chemistry*, 280(7), pp. 5676–5681. doi: 10.1074/jbc.M405561200.

Sulis, M. L. and Parsons, R. (2003) 'PTEN : from pathology to biology', *Trends Cell Biology*, 13(9), pp. 478–483. doi: 10.1016/S0962-8924(03)00175-2.

Sumitomo, M. *et al.* (2004) 'Synergy in tumor suppression by direct interaction of Neutral Endopeptidase with PTEN', *Cancer Cell*, 5(1), pp. 67–78. doi: 10.1016/S1535-6108(03)00331-3.

Sun, H. *et al.* (1999) 'PTEN modulates cell cycle progression and cell survival by regulating phosphatidylinositol 3,4,5,-trisphosphate and Akt/protein kinase B signaling pathway', *Proceedings of the National Academy of Sciences of the United States of America*, 96(11), pp. 6199–6204. doi: 10.1073/pnas.96.11.6199.

Sun, L. *et al.* (2016) 'Novel cancer stem cell targets during epithelial to mesenchymal transition in PTEN-deficient trastuzumab-resistant breast cancer', *Oncotarget*, 7(32), pp. 51408–51422. doi: 10.18632/oncotarget.9839.

Sun, Y. S. *et al.* (2017) 'Risk factors and preventions of breast cancer', *International Journal of Biological Sciences*, 13(11), pp. 1387–1397. doi: 10.7150/ijbs.21635.

Sung, H. *et al.* (2021) 'Global cancer statistics 2020: GLOBOCAN estimates of incidence and mortality worldwide for 36 cancers in 185 countries', *CA: A Cancer Journal for Clinicians*, pp. 1–41. doi:

10.3322/caac.21660.

Surendranath, V. *et al.* (2013) 'Designing efficient and specific endoribonuclease-prepared siRNAs', *Methods Mol Biol*, 942, pp. 193–204. doi: 10.1007/978-1-62703-119-6_11.

Suzuki, A. *et al.* (1998) 'High cancer susceptibility and embryonic lethality associated with mutation of the PTEN tumor suppressor gene in mice', *Current Biology*, 8(21), pp. 1169–1178. doi: 10.1016/S0960-9822(07)00488-5.

Swain, S. M. *et al.* (2015) 'Pertuzumab, trastuzumab, and docetaxel in HER2-positive metastatic breast cancer', *New England Journal of Medicine*, 372(8), pp. 724–734. doi: 10.1056/NEJMoa1413513.

Tahmasebi, S., Amiri, M. and Sonenberg, N. (2019) 'Translational control in stem cells', *Frontiers in Genetics*, 9, p. 709. doi: 10.3389/fgene.2018.00709.

Takahashi, Y. *et al.* (2006) 'PTEN tumor suppressor associates with NHERF proteins to attenuate PDGF receptor signaling', *The EMBO Journal*, 25(4), pp. 910–920. doi: 10.1038/sj.emboj.7600979.

Takeda, D. Y. and Dutta, A. (2005) 'DNA replication and progression through S phase', *Oncogene*, 24(17), pp. 2827–2843. doi: 10.1038/sj.onc.1208616.

Tamguney, T. and Stokoe, D. (2007) 'New insights into PTEN', *Journal of Cell Science*, 120(Pt 23), pp. 4071–4079. doi: 10.1242/jcs.015230.

Tamimi, R. M. *et al.* (2008) 'Comparison of molecular phenotypes of ductal carcinoma in situ and invasive breast cancer', *Breast Cancer Research*, 10(4), p. R67. doi: 10.1186/bcr2128.

Tamura, M. *et al.* (1998) 'Inhibition of cell migration, spreading, and focal adhesions by tumor suppressor PTEN', *Science*, 280(5369), pp. 1614–1617. doi: 10.1126/science.280.5369.1614.

Tan, M. H. *et al.* (2011) 'A clinical scoring system for selection of patients for pten mutation testing is proposed on the basis of a prospective study of 3042 probands', *American Journal of Human Genetics*, 88(1), pp. 42–56. doi: 10.1016/j.ajhg.2010.11.013.

Tanaka, H. *et al.* (2009) 'Replisome progression complex links DNA replication to sister chromatid cohesion in Xenopus egg extracts', *Genes to Cells*, 14(8), pp. 949–963. doi: 10.1111/j.1365-2443.2009.01322.x.

Tang, Y. C. *et al.* (2018) 'Functional genomics identifies specific vulnerabilities in PTEN-deficient breast cancer', *Breast Cancer Research*. Breast Cancer Research, 20(1), p. 22. doi: 10.1186/s13058-018-0949-3.

Tay, Y., Song, S. J. and Pandolfi, P. P. (2013) 'The Lilliputians and the Giant: An emerging oncogenic microRNA network that suppresses the PTEN tumor suppressor in vivo', *MicroRNA*, 2(2), pp. 127–136. doi: 10.2174/22115366113029990017.

Thakur, P. *et al.* (2017) 'Breast cancer risk factor evaluation in a Western Himalayan state: A case–control study and comparison with the Western World', *South Asian Journal of cancer*, 6(3), pp. 106–109. doi: 10.4103/sajc.sajc.

Thu, Y. M. and Bielinsky, A. K. (2013) 'Enigmatic roles of Mcm10 in DNA replication', *Trends in Biochemical Sciences*, 38(4), pp. 184–194. doi: 10.1016/j.tibs.2012.12.003.

Tolaney, S. *et al.* (2015) 'Phase I/II study of pilaralisib (SAR245408) in combination with trastuzumab or trastuzumab plus paclitaxel in trastuzumab-refractory HER2-positive metastatic breast cancer', *Breast Cancer Research and Treatment*, 149(1), pp. 151–161. doi: 10.1007/s10549-014-3248-4.

Tomczak, K., Czerwińska, P. and Wiznerowicz, M. (2015) 'The Cancer Genome Atlas (TCGA): An immeasurable source of knowledge', *Contemporary Oncology*, 19(A1), pp. A68–A77. doi: 10.5114/wo.2014.47136.

Tong, C. W. S. *et al.* (2018) 'Recent advances in the treatment of breast cancer', *Frontiers in Oncology*, 8, p. 227. doi: 10.3389/fonc.2018.00227.

Topatana, W. *et al.* (2020) 'Advances in synthetic lethality for cancer therapy: Cellular mechanism and clinical translation', *Journal of Hematology and Oncology*. Journal of Hematology & Oncology, 13(1), p. 118. doi: 10.1186/s13045-020-00956-5.

Torres, J. and Pulido, R. (2001) 'The tumor suppressor PTEN is phosphorylated by the protein kinase CK2 at its C terminus. Implications for PTEN stability to proteasome-mediated degradation', *Journal of Biological Chemistry*, 276(2), pp. 993–998. doi: 10.1074/jbc.M009134200.

Travis, R. C. and Key, T. J. (2003) 'Oestrogen exposure and breast cancer risk', *Breast Cancer Research*, 5(5), pp. 239–247. doi: 10.1186/bcr628.

Trichopoulos, D., Li, F. P. and Hunter, D. J. (1996) 'What causes cancer?', *Scientific American*, 275(3), pp. 80–87. doi: 10.1038/scientificamerican0996-80.

Trimboli, A. J. *et al.* (2009) 'Pten in stromal fibroblasts suppresses mammary epithelial tumours', *Nature*, 461(7267), pp. 1084–1091. doi: 10.1038/nature08486.

Trotman, L. C. *et al.* (2007) 'Ubiquitination regulates PTEN nuclear import and tumor suppression', *Cell*, 128(1), pp. 141–156. doi: 10.1016/j.cell.2006.11.040.

Valiente, M. *et al.* (2005) 'Binding of PTEN to specific PDZ domains contributes to PTEN protein stability and phosphorylation by microtubule-associated serine/threonine kinases', *Journal of Biological Chemistry*, 280(32), pp. 28936–28943. doi: 10.1074/jbc.M504761200.

Vanhaesebroeck, B., Stephens, L. and Hawkins, P. (2012) 'PI3K signalling: The path to discovery and understanding', *Nature Reviews Molecular Cell Biology*, 13(3), pp. 195–203. doi: 10.1038/nrm3290.

Varela-Rey, M. *et al.* (2013) 'Alcohol, DNA methylation, and cancer.', *Alcohol research : current reviews*, 35(1), pp. 25–35.

Vazquez, F. *et al.* (2001) 'Phosphorylation of the PTEN tail acts as an inhibitory switch by preventing its recruitment into a protein complex', *Journal of Biological Chemistry*, 276(52), pp. 48627–48630. doi: 10.1074/jbc.C100556200.

Vellai, T. *et al.* (2006) 'Effects of sex and insulin/insulin-like growth factor-1 signaling on performance in an associative learning paradigm in Caenorhabditis elegans', *Genetics*, 174(1), pp. 309–316. doi: 10.1534/genetics.106.061499.

Velloso, F. J. *et al.* (2017) 'The crossroads of breast cancer progression: Insights into the modulation of major signaling pathways', *OncoTargets and Therapy*, 2017(10), pp. 5491–5524. doi: 10.2147/OTT.S142154.

Verkasalo, P. K. *et al.* (2001) 'Circulating levels of sex hormones and their relation to risk factors for breast cancer: a cross-sectional study in 1092 pre- and postmenopausal women (United Kingdom)', *Cancer cAuses & Control : CCC*, 12(1), pp. 47–59. doi: 10.1023/a:1008929714862.

Verma, S. *et al.* (2012) 'Trastuzumab emtansine for HER2-positive advanced breast cancer', *New England Journal of Medicine*, 367(19), pp. 1783–1791. doi: 10.1056/NEJMoa1209124.

Vidotto, T. *et al.* (2019) 'PTEN-deficient prostate cancer is associated with an immunosuppressive tumor microenvironment mediated by increased expression of IDO1 and infiltrating FoxP3+ T regulatory cells', *Prostate*, 79(9), pp. 969–979. doi: 10.1002/pros.23808.

Vogelstein, B. *et al.* (2003) 'Cancer genome landscapes', *Science*, 339(6127), pp. 1546–1558. doi: 10.1126/science.1235122.

Vu, T. and Claret, F. X. (2012) 'Trastuzumab: Updated mechanisms of action and resistance in breast cancer', *Frontiers in Oncology*, 2, p. 62. doi: 10.3389/fonc.2012.00062.

Waks, A. G. and Winer, E. P. (2019) 'Breast Cancer Treatment: A Review', *JAMA - Journal of the American Medical Association*, 321(3), pp. 288–300. doi: 10.1001/jama.2018.19323.

Walker, S. M. *et al.* (2004) 'The tumour-suppressor function of PTEN requires an N-terminal lipid-binding motif', *Biochemical Journal*, 379(2), pp. 301–307. doi: 10.1042/BJ20031839.

Wang, D. Y. *et al.* (2019) 'Molecular stratification within triple-negative breast cancer subtypes', *Scientific Reports*, 9, p. 19107. doi: 10.1038/s41598-019-55710-w.

Wang, X. *et al.* (2007) 'NEDD4-1 Is a Proto-Oncogenic Ubiquitin Ligase for PTEN', *Cell*, 128(1), pp. 129–139. doi: 10.1016/j.cell.2006.11.039.

Wang, X. and Jiang, X. (2008) 'PTEN: A default gate-keeping tumor suppressor with a versatile tail', *Cell Research*, 18(8), pp. 807–816. doi: 10.1038/cr.2008.83.

Wang, Y. *et al.* (2014) 'ASPP2 controls epithelial plasticity and inhibits metastasis through β 2-catenin-dependent regulation of ZEB1', *Nature Cell Biology*, 16(11), pp. 1092–1104. doi: 10.1038/ncb3050.

Wang, Yihua *et al.* (2019) 'Autophagy inhibition specifically promotes epithelial-mesenchymal transition and invasion in RAS-mutated cancer cells', *Autophagy*, 15(5), pp. 886–899. doi: 10.1080/15548627.2019.1569912.

Wang, Yilin *et al.* (2019) 'Human CST suppresses origin licensing and promotes AND-1/Ctf4 chromatin association', *Life Science Alliance*, 2(2), p. e201800270. doi: 10.26508/lsa.201800270.

Warburg, O. (1956) 'On respiratory impairment in cancer cells', *Science*, 124(3215), pp. 269–270.

Weigelt, B., Warne, P. H. and Downward, J. (2011) 'PIK3CA mutation, but not PTEN loss of function, determines the sensitivity of breast cancer cells to mTOR inhibitory drugs', *Oncogene*, 30(29), pp. 3222–3233. doi: 10.1038/onc.2011.42.

Wen, S. *et al.* (2001) 'PTEN controls tumor-induced angiogenesis', *Proceedings of the National Academy of Sciences of the United States of America*, 98(8), pp. 4622–4627. doi: 10.1073/pnas.081063798.

Wermke, M. *et al.* (2015) 'RNAi profiling of primary human AML cells identifies ROCK1 as a therapeutic target and nominates fasudil as an antileukemic drug', *Blood*, 125(24), pp. 3760–3768. doi: 10.1182/blood-2014-07-590646.

Whelan, J. T., Forbes, S. L. and Bertrand, F. E. (2007) 'CBF-1 (RBP-Jκ) binds to the PTEN promoter and regulates PTEN gene expression', *Cell Cycle*, 6(1), pp. 80–84. doi: 10.4161/cc.6.1.3648.

Wideman, T. H., Zautra, A. J. and Edwards, R. R. (2012) 'Intrinsic coupling of lagging-strand synthesis to chromatin assembly', *Nature*, 483(7390), pp. 434–438. doi: 10.1038/nature10895.

Williams, D. R. and Mcintosh, J. R. (2002) 'mcl1+, the Schizosaccharomyces pombe homologue of CTF4, is important for chromosome replication, cohesion, and segregation', *Eukaryotic Cell*, 1(5), pp. 758–773. doi: 10.1128/EC.1.5.758-773.2002.

Wong, J. T. *et al.* (2007) 'Pten (phosphatase and tensin homologue gene) haploinsufficiency promotes insulin hypersensitivity', *Diabetologia*, 50(2), pp. 395–403. doi: 10.1007/s00125-006-0531-x.

Wu, S. *et al.* (2018) 'Evaluating intrinsic and non-intrinsic cancer risk factors', *Nature Communications*, 9(1), p. 3490. doi: 10.1038/s41467-018-05467-z.

Wu, X. *et al.* (2000) 'Evidence for regulation of the PTEN tumor suppressor by a membrane-localized multi-PDZ domain containing scaffold protein MAGI-2', *Proceedings of the National Academy of Sciences of the United States of America*, 97(8), pp. 4233–4238. doi: 10.1073/pnas.97.8.4233.

Wu, Y. *et al.* (2000) 'Interaction of the tumor suppressor PTEN/MMAC with a PDZ domain of MAGI3, a novel membrane-associated guanylate kinase', *Journal of Biological Chemistry*, 275(28), pp. 21477–21485. doi: 10.1074/jbc.M909741199.

Xia, D. *et al.* (2007) 'Mitogen-activated protein kinase kinase-4 promotes cell survival by decreasing PTEN expression through an NFκB-dependent pathway', *Journal of Biological Chemistry*, 282(6), pp. 3507–3519. doi: 10.1074/jbc.M610141200.

Yamada, K. M. and Cukierman, E. (2007) 'Modeling tissue morphogenesis and cancer in 3D', *Cell*, 130(4), pp. 601–610. doi: 10.1016/j.cell.2007.08.006.

Yanagida, M. (2014) 'The role of model organisms in the history of mitosis research', *Cold Spring Harbor Perspectives in Biology*, 6(9), p. a015768. doi: 10.1101/cshperspect.a015768.

Yang, Y. *et al.* (2018) 'PTEN loss promotes intratumoral androgen synthesis and tumor microenvironment remodeling via aberrant activation of RUNX2 in castration-Resistant prostate cancer', *Clinical Cancer Research*, 24(4), pp. 834–846. doi: 10.1158/1078-0432.CCR-17-2006.

Yim, E. *et al.* (2009) 'Rak functions as a tumor suppressor by regulating PTEN protein stability and function', *Cancer Cell*, 15(4), pp. 304–314. doi: 10.1016/j.ccr.2009.02.012.

Yin, L. *et al.* (2020) 'Triple-negative breast cancer molecular subtyping and treatment progress', *Breast Cancer Research*. Breast Cancer Research, 22(1), p. 61. doi: 10.1186/s13058-020-01296-5.

Yin, Y. and Shen, W. H. (2008) 'PTEN: A new guardian of the genome', *Oncogene*, 27(41), pp. 5443–5453. doi: 10.1038/onc.2008.241.

Yoshizawa-Sugata, N. and Masai, H. (2009) 'Roles of human AND-1 in chromosome transactions in S phase', *Journal of Biological Chemistry*, 284(31), pp. 20718–20728. doi: 10.1074/jbc.M806711200.

Zecchin, D. *et al.* (2020) 'Combined targeting of G protein-coupled receptor and EGF receptor signaling overcomes resistance to PI 3K pathway inhibitors in PTEN -null triple negative breast cancer', *EMBO Molecular Medicine*, 12(8), p. e11987. doi: 10.15252/emmm.202011987.

Zhang, C., Xu, B. and Liu, P. (2016) 'Addition of the p110α inhibitor BYL719 overcomes targeted therapy resistance in cells from Her2-positive-PTEN-loss breast cancer', *Tumor Biology*, 37(11), pp. 14831–14839. doi: 10.1007/s13277-016-5381-7.

Zhang, H. Y. *et al.* (2013) 'PTEN mutation, methylation and expression in breast cancer patients', *Oncology Letters*, 6(1), pp. 161–168. doi: 10.3892/ol.2013.1331.

Zhang, J. guang *et al.* (2010) 'MicroRNA-21 (miR-21) represses tumor suppressor PTEN and promotes growth and invasion in non-small cell lung cancer (NSCLC)', *Clinica Chimica Acta; International Journal of Clinical Chemistry*. Elsevier B.V., 411(11–12), pp. 846–852. doi: 10.1016/j.cca.2010.02.074.

Zhang, W. *et al.* (2006) 'PPARγ activator rosiglitazone inhibits cell migration via upregulation of PTEN in human hepatocarcinoma cell line BEL-7404', *Cancer Biology and Therapy*, 5(8), pp. 1008–1014. doi: 10.4161/cbt.5.8.2887.

Zhang, Z. *et al.* (2018) 'A survey and evaluation of Web-based tools/databases for variant analysis of TCGA data', *Briefings in Bioinformatics*, 20(4), pp. 1524–1541. doi: 10.1093/bib/bby023.

Zhao, D. *et al.* (2017) 'Synthetic essentiality of chromatin remodelling factor CHD1 in PTEN-deficient cancer', *Nature*, 542(7642), pp. 484–488. doi: 10.1038/nature21357.

Zheng, G. *et al.* (2018) 'MCM2–7-dependent cohesin loading during s phase promotes sister-chromatid cohesion', *eLife*, 7, p. e33920. doi: 10.7554/eLife.33920.

Zhou, X. *et al.* (2001) 'Association of germline mutation in the PTEN tumour suppressor gene and Proteus and Proteus-like syndromes', *Lancet*, 358(9277), pp. 210–211. doi: 10.1016/s0140-6736(01)05412-5.

Zhou, Y. *et al.* (2016) 'Role of WDHD1 in Human Papillomavirus-Mediated Oncogenesis Identified by Transcriptional Profiling of E7-Expressing Cells', *Journal of Virology*, 90(13), pp. 6071–6084. doi: 10.1128/jvi.00513-16.

Zhou, Y. *et al.* (2020) 'WDHD1 facilitates G1 checkpoint abrogation in HPV E7 expressing cells by

modulating GCN5', *BMC Cancer*, 20, p. 840. doi: 10.1186/s12885-020-07287-1.

Zhou, Y. and Chen, J. J. (2021) 'STAT3 plays an important role in DNA replication by turning on WDHD1', *Cell and Bioscience*, 11(1), p. 10. doi: 10.1186/s13578-020-00524-x.

Zhu, W. *et al.* (2007) 'Mcm10 and And-1/CTF4 recruit DNA polymerase α to chromatin for initiation of DNA replication', *Genes and Development*, 21(18), pp. 2288–2299. doi: 10.1101/gad.1585607.

Ziemba, B. P. *et al.* (2013) 'The PH Domain of PDK1 Exhibits a Novel, Phospho-Regulated Monomer-Dimer Equilibrium With Important Implications for Kinase Domain Activation: Single Molecule and Ensemble Studies', *Biochemistry*, 52(28). doi: 10.1021/bi400488f.

Appendix A Materials and Methods

A.1 R scripts

All scripts were run in RStudio (version 3.4.4), Microsoft Windows (version 10).

Ensure the working directory is set.

If required, change the working directory.

A.1.1 Alignment of TNBC samples (TCGA, Provisional) with Protein (RPPA) and mRNA (IlluminaHiSeq) data from UCSC Cancer Genome Browser

Molecular subtypes of breast cancer in clinical data (TCGA, Provisional) were identified on excel in and new excel csv file for TNBC was created.

Protein and mRNA data from UCSC Cancer Genome Browser were saved as excel csv file.

Download the data on new R environment

TNBC<-read.csv("TNBC.csv", header=TRUE)

ProteinData<-read.csv("ProteinData.csv", header=TRUE)

mRNAData<-read.csv("mRNAData.csv", header=TRUE)

Put the column to row names

TNBC<- data.frame(TNBC[,-1], row.names=TNBC[,1])

ProteinData <- data.frame(ProteinData[,-1], row.names=ProteinData[,1])

mRNAData <- data.frame(mRNAData [,-1], row.names=mRNAData[,1])

Transpose protein and mRNA data to have the sample IDs on the row

tProteinData<-t(ProteinData)

tmRNAData<-t(mRNAData)

Merge TNBC with protein/mRNA data

TNBCProteinData <- merge(TNBC,tProteinData,by=c("row.names"))

```
TNBCmRNAData <- merge(TNBC,tmRNAData,by=c("row.names"))

## Write the data frame in excel as csv file

write.csv(TNBCProteinData, "TNBCProteinData.csv")

write.csv(TNBCmRNAData, "TNBCmRNAData.csv")

## Merge TNBCProteinData with TNBCmRNAData

ProteinmRNA <- merge(TNBCProteinData,TNBCmRNAData,by=c("row.names"))

## Put the column to row names

ProteinmRNA <- data.frame(ProteinmRNA[,-1], row.names=ProteinmRNA[,1])

## Write ProteinmRNA data frame as excel csv file

write.csv(ProteinmRNA, " ProteinmRNA.csv")
```

PTEN, protein and mRNA levels for TNBC samples were extracted on excel and correlation analysis was performed on GraphPad Prism8.

A.1.2 Alignment of clinical data of TNBC samples (TCGA, Provisional) with PTEN, protein (RPPA) from UCSC Cancer Genome Browser

PTEN, protein level for TNBC samples were extracted on excel as mentioned in A.1.2 and new excel csv file was created.

```
## Download the data on new R environment

Cinical<-read.csv("Clinical.csv", header=TRUE)

PTENprotein<-read.csv("PTENprotein.csv", header=TRUE)

## Put the column to row names

Clinical<- data.frame(Clinical[,-1], row.names=Clinical[,1])

PTENprotein<- data.frame(PTENprotein[,-1], row.names=PTENprotein[,1])

## Merge clinical data with PTEN protein data

ClinicalPTENprotein<- merge(Clinical,PTENprotein,by=c("row.names"))
```

Write ClinicalPTENprotein data frame as excel csv file

write.csv(ClinicalPTENprotein, " ClinicalPTENprotein.csv")

Transpose PTEN, protein data to have the protein names on the row

tPTENprotein<-t(PTENprotein)

Plotting histogram distribution graph for PTEN, protein level

quantile(as.numeric(tPTENprotein[1,]))

hist(as.numeric(tPTENprotein [1,]))

Top 40% and bottom 40% TNBC samples were chosen for high and low PTEN, protein (RPPA) expression on excel file (ClinicalPTENProtein). Then, the relationship between TNBC patients' clinical–pathological characteristics and PTEN, protein expression in TCGA data were analysed in GraphPad Prism8.

A.1.3 Identifying significantly different mRNAs between the *PTEN* high and low TNBC samples in TCGA (IlluminaHiSeq) data

Download the data on new R environment

mRNAData<-read.csv("mRNAData.csv", header=TRUE)

Put the column to row names

mRNAData <- data.frame(mRNAData [,-1], row.names=mRNAData[,1])

Plotting histogram distribution graph for PTEN, mRNA level

quantile(as.numeric(tmRNAData[2670,]))

hist(as.numeric(tmRNAData [2670,]))

Top 10% and bottom 10% TNBC samples were chosen for high and low *PTEN*, mRNA (IlluminaHiSeq) expression on excel file (mRNAData). Then, two new excel csv file for high and low *PTEN*, mRNA (IlluminaHiSeq) TNBC samples were created.

Download PTEN high and low data on the same R environment

HighPTEN=read.csv("High.csv", header=TRUE)

```
LowPTEN=read.csv("Low.csv", header=TRUE)

## Put the column to row names

HighPTEN<- data.frame(HighPTEN[,-1], row.names=HighPTEN[,1])

LowPTEN<- data.frame(LowPTEN[,-1], row.names=LowPTEN[,1])

## Transpose mRNA data to have the sample IDs on the row

tmRNAData<-t(mRNAData)

## Merge high and low PTEN data with mRNAdata

HighPTENmRNAdata<- merge(HighPTEN,mRNAdata,by=c("row.names"))

LowPTENmRNAdata<- merge(LowPTEN,mRNAdata,by=c("row.names"))

## Put the column to row names

HighPTENmRNAdata<- data.frame(HighPTENmRNAdata [,-1], row.names=HighPTENmRNAdata[,1])

LowmPTENRNAdata<- data.frame(LowPTENmRNAdata [,-1], row.names=LowPTENmRNAdata[,1])

## Transpose LowmRNAdata and HighmRNAdata to have the mRNA names on the row

HighPTENmRNAdata<-t(HighPTENmRNAdata)

LowPTENmRNAdata<-t(LowPTENmRNAdata)

## Run unpaired t-test between HighmRNAdata and LowmRNAdata

ttest=as.data.frame(t(sapply(1:nrow(HighPTENmRNAdata), function(i)
t.test(as.numeric(LowPTENmRNAdata[i,]), as.numeric(HighPTENmRNAdata[i, ])))))

## Find significantly different mRNAs between HighmRNAdata and LowmRNAdata with un-
paired t-test - P-value less than 0.05

significantgenesHighPTEN=HighPTENmRNAdata[which(ttest$"p.value"<0.05),]

significantgenesLowPTEN=LowPTENmRNAdata[which(ttest$"p.value"<0.05),]

## Combine significant mRNAs

totalsignificantPTEN<-
merge(significantgenesHighPTEN,significantgenesLowPTEN,by=c("row.names"))
```

Put the column to row names

totalsignificantPTEN <- data.frame(totalsignificantPTEN[,-1], row.names=totalsignificantPTEN[,1])

Save totalsignificantPTEN data frame as excel csv file

write.csv(totalsignificantPTEN, "totalsignificantPTEN.csv")

Plot heat-map for the significantly different mRNAs.

Install the packages to the new R environment

install.packages('massageR')

library(massageR)

library(RColorBrewer)

library(ggplot2)

library(gplots)

Download totalsignificantPTEN data frame and plot a heat-map on new R environment

data=read.csv("totalsignificantPTEN.csv", header=TRUE)

Put the column to row names

data <- data.frame(data[,-1], row.names=data[,1])

Remove NA, missing values from the data

data<- na.omit(data)

Convert the data into matrix

data<-as.matrix(data)

Create the heatmap

z <- heat.clust(data, scaledim = "row", zlim= c(-10, 10), zlim_select = c("dend", "outdata"), reorder =c("column", "row"), distfun = function(data) as.dist(1- cor(t(data))), hclustfun = function(data) hcl ust(data, method = "complete"), scalefun = scale)

heatmap.2(z$data, Rowv = z$Rowv, Colv = FALSE, trace= "none", scale = "none", symbreaks = TRU E, col=rev(colorRampPalette(brewer.pal(10, "RdBu"))(256)), margins=c(8, 12), main = "TCGA breas t invasive carcinoma (Protein, RPPA)", xlab = "High to Low BRCA", ylab = "Proteins of interest")

To extract the row names order from heat-map

```
a<-heatmap.2(z$data, Rowv = z$Rowv, Colv = FALSE, trace= "none", scale = "none", symbreaks = T
RUE, col=rev(colorRampPalette(brewer.pal(10, "RdBu"))(256)), margins=c(8, 12), main = "TCGA", x
lab = "High to Low", ylab = "Significant Genes")

sorted<-data[match(rev(labels(a$rowDendrogram)), rownames(data)),]
```

Write the extracted row names order from heat-map on excel csv file

```
write.csv(sorted, "sortedorderPTENmRNA.csv")
```

A.1.4 Identifying genes that have significant decrease in cell viability between *PTEN*-positive and *PTEN*-negative TNBC cells obtained from the whole genome siRNA screen

Download the whole genome siRNA data on new R environment

```
Greendata=read.csv("GREEN.csv", header=TRUE)

Reddata=read.csv("Red.csv", header=TRUE)
```

Put the column to row names

```
Greendata <- data.frame(Greendata[,-1], row.names=Greendata[,1])

Reddata <- data.frame(Reddata[,-1], row.names=Reddata[,1])
```

Run paired t-test between HighmRNAdata and LowmRNAdata

```
ttest=as.data.frame(t(sapply(1:nrow(Greendata), function(i) t.test(as.numeric(Greendata[i,]),
as.numeric(Reddata[i, ]), paired=TRUE))))
```

Find significantly different mRNAs between Greendata and Reddata with paired t-test - P-value less than 0.05

```
WGSsignificantGreen=Greendata[which(ttest$"p.value"<0.05),]

WGSsignificantRed=Reddata[which(ttest$"p.value"<0.05),]
```

Combine significant genes

```
totalsignificantWGS<- merge(WGSsignificantGreen,WGSsignificantRed,by=c("row.names"))
```

Put the column to row names

totalsignificantWGS<- data.frame(totalsignificant[,-1], row.names=totalsignificant[,1])

Save totalsignificantPTEN data frame as excel csv file

write.csv(totalsignificantWGS, "totalsignificantWGS.csv")

Plot the heatmap for significant genes in WGS as mentioned in A.1.3.

A.1.5 Identifying top hit candidate genes between TCGA and whole genome siRNA screen

Significantly higher mRNAs in low PTEN TNBC samples in TCGA (IlluminaHiSeq) data were extracted on excel file and new excel csv file was created.

Genes that have significant decrease in cell viability in *PTEN*-negative TNBC cells in whole genome siRNA screening data were extracted on excel file and new excel csv file was created.

Download the new created TCGA and whole genome siRNA screening data (mentioned above) on new R environment

TCGA<-read.csv("TCGA.csv", header=TRUE)

WGS<-read.csv("WGS.csv", header=TRUE)

Put the column to row names

TCGA<- data.frame(TCGA [,-1], row.names= TCGA [,1])

WGS<- data.frame(WGS [,-1], row.names= WGS [,1])

Merge TCGA data frame with WGS data frame

TopHit<- merge(TCGA,WGS,by=c("row.names"))

Save TopHit data frame as excel csv file

write.csv(TopHit, " TopHit.csv")

Extract the TCGA samples with top hit gene names form TopHit file and create a new excel csv file.

Extract the whole genome siRNA cell lines with Top hit gene names and create a new excel csv file.

Plot the heatmap for Top hit genes for TCGA and WGS as mentioned in A.1.3.

A.1.6 TCGA data mining with WDHD1

Download the data on new R environment

```
mRNAData<-read.csv("mRNAData.csv", header=TRUE)
```

Put the column to row names

```
mRNAData <- data.frame(mRNAData [,-1], row.names=mRNAData[,1])
```

Plotting histogram distribution graph for WDHD1, mRNA level

```
quantile(as.numeric(mRNAData[15653,]))

hist(as.numeric(mRNAData [15653,]))
```

Top 10% and bottom 10% TNBC samples were chosen for high and low *WDHD1*, mRNA (IlluminaHiSeq) expression on excel file (mRNAData). Then, two new excel csv file for high and low *WDHD1*, mRNA (IlluminaHiSeq) TNBC samples were created.

##The relationship between TNBC patients' clinical–pathological characteristics and WDHD1, mRNA expression in TCGA data were analysed as mentioned in A.1.3.

Significantly different mRNAs between WDHD1 high and low TNBC samples in TCGA (IlluminaHiSeq) were identified and heatmap was generated as mentioned in A.1.3.

Pearson correlation analysis for WDHD1

```
pv<-array(1,c(20530,1))   # 20530 is the number of genes in the data ## Create empty list to store p-value and correlation value

cor<-array(1,c(20530,1)) # correlation value

for (i in 1:20530)

{VL<-cor.test(as.numeric(mRNAdata[i,]),as.numeric(mRNAdata['WDHD1',]),method = "pearson")

        pv[i,1]<-VL$p.value
```

```
        cor[i,1]<-VL$estimate}

new_data<-data.frame(pv,cor,mRNAdata)

mRNAdata['WDHD1',]

cor.test(as.numeric(mRNAdata[1,]),as.numeric(mRNAdata['WDHD1',]),method = "pearson")

## Select mRNAs whose P-value less than 0.05

df_ce1<-subset(new_data,pv<=0.05)

## Rank data by their correlation value

df_ce1pos<-df_ce1[order(df_ce1$cor,decreasing = T), ]

df_ce1neg<-df_ce1[order(df_ce1$cor,decreasing = F), ]

## Select the top 50 highest and lowest correlation mRNAs

df_ce50pos<-df_ce1[order(df_ce1$cor,decreasing = T), ][1:50,]

df_ce50neg<-df_ce1[order(df_ce1$cor,decreasing = F), ][1:50,]

## Combine positive top50 genes and negative top50

po_ne_ce_all<-rbind(df_ce50pos,df_ce50neg)

## Order sample according to WDHD1

a_value<-po_ne_ce_all[order(po_ne_ce_all[1,])]

## Change data.frame into matrix

a_value1<-as.matrix(a_value[3:130])

## Remove rows with NA, missing values (no influence in here)

a1<-na.omit(a_value1)

## Create a heat-map in tiff.

library(ggplot2)

library(gplots)

library(massageR)
```

```
library(RColorBrewer)

tiff("heatmap_value_ccee.tiff", units="in", width=12, height=8, res=300)

distCor <- function(a1) as.dist(1-cor(t(a1)))

hclustAvg <- function(a1) hclust(a1, method="average")

heatmap.2(a1,trace="none", density='none',scale="row", margins = c(10,12),cexRow = 0.4, cexCol = 0.8,srtCol=45,adjCol=c(1,0),srtRow = 45,adjRow = c(0,1), Colv = T, Rowv = F, #dendrogram = 'none', distfun=distCor, hclustfun=hclustAvg, col=rev(colorRampPalette(brewer.pal(10, "RdBu"))(256)), symbreak=FALSE,key = T,keysize = 1, main = "TCGA", xlab = "Samples", ylab = "Genes of interest")
```

Overlay genes between identified top hit genes and genes that were positively correlated with WDHD1

The identified top 47 genes between TCGA and WGS (A.1.5) and positively correlated genes with WDHD1 (A.1.6) were merged as previously mentioned. The heatmaps of TCGA and WGS were plotted for the overlay genes as previously mentioned in A.1.5.

A.1.7 Proteomics analysis

Each repeat with accession number, description and peptide numbers were extracted on excel file and new excel csv files were created.

Download the data on new R environment

```
WDHD11<-read.csv("updatedWDHD1-1.csv", header=TRUE)

WDHD12<-read.csv("updatedWDHD1-2.csv", header=TRUE)

IgG1<-read.csv("updatedIgG-1.csv", header=TRUE)

IgG2<-read.csv("updatedIgG-2.csv", header=TRUE)
```

Put the column to row names

```
WDHD11 <- data.frame(WDHD11[,-1], row.names=WDHD11[,1])

WDHD12 <- data.frame(WDHD12[,-1], row.names=WDHD12[,1])

IgG1 <- data.frame(IgG1[,-1], row.names=IgG1[,1])
```

```
IgG2 <- data.frame(IgG2[,-1], row.names=IgG2[,1])

## Merging multiple data sets

library(plyr)

mylist <- list( one=df1, two=df2, three=df3, four=df4 )

join_all( mylist, type="full" )


for(i in 1:length(mylist)){

 colnames(mylist[[i]]) <- paste0( names(mylist)[i], "_", colnames(mylist[[i]]) ) ## rename column names

 mylist[[i]]$ROWNAMES <- rownames(mylist[[i]])} ## create a column according to original row names

out <- join_all( mylist, by="ROWNAMES", type="full" )

rownames(out) <- out$ROWNAMES; out$ROWNAMES <- NULL ## Delete rowname column

## Save merged data frame as excel csv file

write.csv(out, "out.csv")

## Delete rows (proteins) with NA values, missing values in more than two samples

miss2 <- c()

for(i in 1:nrow(out)) {

 if(length(which(is.na(out[i,]))) > 0.5*ncol(out)) miss2 <- append(miss2,i)

}

miss<- out[-miss2,]

## Save miss data frame as excel csv file

write.csv(miss, "miss.csv")
```

Appendix B Bioinformatic analysis to reveal the candidate gene(s) that are essential for the survival of PTEN-inactive TNBC cells

Table B.1 Identified TNBC samples in TCGA (Provisional) data from cBioPortal.

Samples	ER status	PR status	HER2 status	Subtypes
TCGA-A1-A0SK-01	Negative	Negative	Negative	TNBC
TCGA-A2-A04U-01	Negative	Negative	Negative	TNBC
TCGA-A2-A0CM-01	Negative	Negative	Negative	TNBC
TCGA-A2-A0D0-01	Negative	Negative	Negative	TNBC
TCGA-A2-A0D2-01	Negative	Negative	Negative	TNBC
TCGA-A2-A0SX-01	Negative	Negative	Negative	TNBC
TCGA-A2-A0T0-01	Negative	Negative	Negative	TNBC
TCGA-A2-A0T2-01	Negative	Negative	Negative	TNBC
TCGA-A2-A0YE-01	Negative	Negative	Negative	TNBC
TCGA-A2-A1G6-01	Negative	Negative	Negative	TNBC
TCGA-A2-A3XT-01	Negative	Negative	Negative	TNBC
TCGA-A2-A3XX-01	Negative	Negative	Negative	TNBC
TCGA-A7-A0DA-01	Negative	Negative	Negative	TNBC
TCGA-A7-A26G-01	Negative	Negative	Negative	TNBC
TCGA-A7-A6VV-01	Negative	Negative	Negative	TNBC
TCGA-A8-A07O-01	Negative	Negative	Negative	TNBC
TCGA-A8-A09X-01	Negative	Negative	Negative	TNBC
TCGA-AC-A2BK-01	Negative	Negative	Negative	TNBC
TCGA-AC-A2QJ-01	Negative	Negative	Negative	TNBC
TCGA-AC-A6IW-01	Negative	Negative	Negative	TNBC
TCGA-AN-A04D-01	Negative	Negative	Negative	TNBC
TCGA-AN-A0AL-01	Negative	Negative	Negative	TNBC
TCGA-AN-A0AR-01	Negative	Negative	Negative	TNBC

Continued on next page

Table B.1 Continued from previous page

Samples	ER status	PR status	HER2 status	Subtypes
TCGA-AN-A0AT-01	Negative	Negative	Negative	TNBC
TCGA-AN-A0G0-01	Negative	Negative	Negative	TNBC
TCGA-AN-A0XU-01	Negative	Negative	Negative	TNBC
TCGA-AO-A03U-01	Negative	Negative	Negative	TNBC
TCGA-AO-A0J6-01	Negative	Negative	Negative	TNBC
TCGA-AO-A0JL-01	Negative	Negative	Negative	TNBC
TCGA-AO-A124-01	Negative	Negative	Negative	TNBC
TCGA-AO-A128-01	Negative	Negative	Negative	TNBC
TCGA-AO-A129-01	Negative	Negative	Negative	TNBC
TCGA-AO-A12F-01	Negative	Negative	Negative	TNBC
TCGA-AO-A1KR-01	Negative	Negative	Negative	TNBC
TCGA-AR-A0TS-01	Negative	Negative	Negative	TNBC
TCGA-AR-A0TU-01	Negative	Negative	Negative	TNBC
TCGA-AR-A0U1-01	Negative	Negative	Negative	TNBC
TCGA-AR-A0U4-01	Negative	Negative	Negative	TNBC
TCGA-AR-A1AY-01	Negative	Negative	Negative	TNBC
TCGA-AR-A256-01	Negative	Negative	Negative	TNBC
TCGA-AR-A2LR-01	Negative	Negative	Negative	TNBC
TCGA-AR-A5QQ-01	Negative	Negative	Negative	TNBC
TCGA-BH-A0B3-01	Negative	Negative	Negative	TNBC
TCGA-BH-A0B9-01	Negative	Negative	Negative	TNBC
TCGA-BH-A0E0-01	Negative	Negative	Negative	TNBC
TCGA-BH-A0RX-01	Negative	Negative	Negative	TNBC
TCGA-BH-A18G-01	Negative	Negative	Negative	TNBC
TCGA-BH-A1F6-01	Negative	Negative	Negative	TNBC
TCGA-BH-A1FC-01	Negative	Negative	Negative	TNBC
TCGA-BH-A42U-01	Negative	Negative	Negative	TNBC
TCGA-C8-A12V-01	Negative	Negative	Negative	TNBC
TCGA-C8-A131-01	Negative	Negative	Negative	TNBC

Continued on next page

Table B.1 Continued from previous page

Samples	ER status	PR status	HER2 status	Subtypes
TCGA-C8-A1HJ-01	Negative	Negative	Negative	TNBC
TCGA-C8-A26X-01	Negative	Negative	Negative	TNBC
TCGA-C8-A26Y-01	Negative	Negative	Negative	TNBC
TCGA-C8-A27B-01	Negative	Negative	Negative	TNBC
TCGA-C8-A3M7-01	Negative	Negative	Negative	TNBC
TCGA-D8-A13Z-01	Negative	Negative	Negative	TNBC
TCGA-D8-A143-01	Negative	Negative	Negative	TNBC
TCGA-D8-A147-01	Negative	Negative	Negative	TNBC
TCGA-D8-A1JF-01	Negative	Negative	Negative	TNBC
TCGA-D8-A1JL-01	Negative	Negative	Negative	TNBC
TCGA-D8-A1XK-01	Negative	Negative	Negative	TNBC
TCGA-D8-A1XQ-01	Negative	Negative	Negative	TNBC
TCGA-D8-A27F-01	Negative	Negative	Negative	TNBC
TCGA-D8-A27H-01	Negative	Negative	Negative	TNBC
TCGA-D8-A27M-01	Negative	Negative	Negative	TNBC
TCGA-E2-A14N-01	Negative	Negative	Negative	TNBC
TCGA-E2-A14X-01	Negative	Negative	Negative	TNBC
TCGA-E2-A150-01	Negative	Negative	Negative	TNBC
TCGA-E2-A158-01	Negative	Negative	Negative	TNBC
TCGA-E2-A1L7-01	Negative	Negative	Negative	TNBC
TCGA-E2-A1LL-01	Negative	Negative	Negative	TNBC
TCGA-E2-A1LS-01	Negative	Negative	Negative	TNBC
TCGA-E9-A5FL-01	Negative	Negative	Negative	TNBC
TCGA-EW-A1OV-01	Negative	Negative	Negative	TNBC
TCGA-EW-A1OW-01	Negative	Negative	Negative	TNBC
TCGA-EW-A1P4-01	Negative	Negative	Negative	TNBC
TCGA-EW-A1P8-01	Negative	Negative	Negative	TNBC
TCGA-EW-A1PB-01	Negative	Negative	Negative	TNBC
TCGA-EW-A3U0-01	Negative	Negative	Negative	TNBC

Continued on next page

Table B.1 Continued from previous page

Samples	ER status	PR status	HER2 status	Subtypes
TCGA-EW-A6SB-01	Negative	Negative	Negative	TNBC
TCGA-GI-A2C9-01	Negative	Negative	Negative	TNBC
TCGA-GM-A2DB-01	Negative	Negative	Negative	TNBC
TCGA-GM-A2DF-01	Negative	Negative	Negative	TNBC
TCGA-GM-A2DH-01	Negative	Negative	Negative	TNBC
TCGA-HN-A2NL-01	Negative	Negative	Negative	TNBC
TCGA-LL-A441-01	Negative	Negative	Negative	TNBC
TCGA-LL-A5YO-01	Negative	Negative	Negative	TNBC
TCGA-OL-A6VO-01	Negative	Negative	Negative	TNBC
TCGA-S3-AA10-01	Negative	Negative	Negative	TNBC
TCGA-S3-AA15-01	Negative	Negative	Negative	TNBC

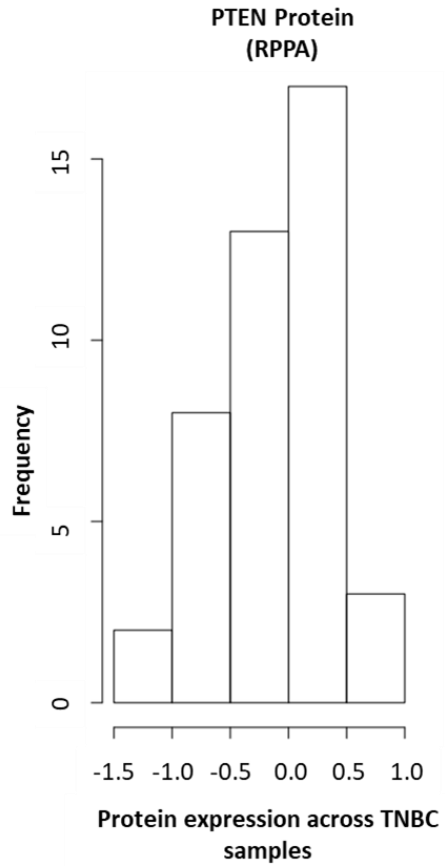

Figure B.1 Frequency distribution of PTEN, protein level across TNBC samples in TCGA breast invasive carcinoma data (RPPA).

Histograms of PTEN frequency expressed in all TNBC samples. X-axis shows PTEN, protein expression and y-axis shows the frequency of samples that have each expression level.

Table B.2 Low PTEN, protein expression (RPPA) and clinicopathological features for TNBC samples in TCGA data from UCSC Cancer browser.

Samples	Age	Location	Stage	Size	Positive LN	Metastasis
TCGA-AN-A0XU-01	54	Left Upper Outer Quadrant	Stage IIA	T2	N0	M0
TCGA-AO-A124-01	38	Left	Stage IIA	T2	N0 (i-)	M0
TCGA-AN-A0AL-01	41	Left Lower Outer Quadrant	Stage IIIB	T4	N0	M0
TCGA-AN-A0AR-01	55	Right Upper Inner Quadrant	Stage IIA	T2	N0	M0
TCGA-AR-A0U1-01	36	Left Upper Outer Quadrant	Stage IIB	T2	N1	M0
TCGA-AN-A04D-01	58	Left Upper Outer Quadrant	Stage IIB	T2	N1	M0
TCGA-AO-A12F-01	36	Right Upper Outer Quadrant|Right	Stage IIA	T2	N0 (i-)	M0
TCGA-AO-A129-01	29	Left Lower Outer Quadrant|Left	Stage IIB	T2	N1a	M0
TCGA-A2-A0T2-01	66	Right	Stage IV	T3	N3	M1
TCGA-A2-A0YE-01	48	Right Upper Outer Quadrant	Stage IIB	T2	N1a	M0
TCGA-E2-A14X-01	55	Right Upper Outer Quadrant	Stage IIIA	T2	N2	M0
TCGA-BH-A0RX-01	59	Left Upper Outer Quadrant|Left	Stage IIA	T2	N0 (i-)	M0
TCGA-AO-A0J6-01	61	Left Upper Outer Quadrant|Left	Stage IIA	T2	N0 (i-)	M0
TCGA-AN-A0AT-01	62	Right Upper Inner Quadrant	Stage IIA	T2	N0	M0
TCGA-D8-A13Z-01	51	Right Lower Outer Quadrant		T2	N2a	M0
TCGA-A2-A0T0-01	59	Right Lower Outer Quadrant	Stage IIB	T2	N1	M0

Table B.3 High PTEN, protein expression (RPPA) and clinicopathological features for TNBC samples in TCGA data from UCSC Cancer browser.

Samples	Age	Location	Stage	Size	Positive LN	Metastasis
TCGA-AO-A0JL-01	59	Left Upper Outer Quadrant|Left Lower Outer Quadrant|Left	Stage IIIA	T2	N2a	M0
TCGA-AR-A0TU-01	35	Right Lower Outer Quadrant	Stage IIA	T2	N0	M0
TCGA-AO-A03U-01	31	Left Upper Inner Quadrant|Left Upper Outer Quadrant|Left Lower Inner Quadrant|Left Lower Outer Quadrant|Left	Stage I	T1c	N0 (i-)	M0
TCGA-C8-A131-01	82	Left	Stage IIIA	T2	N2	M0
TCGA-E2-A150-01	48	Left Upper Outer Quadrant	Stage IIA	T2	N0	M0
TCGA-AO-A128-01	61	Right Lower Outer Quadrant|Right	Stage IIA	T2	N0 (i-)	M0
TCGA-A2-A0CM-01	40	Left	Stage IIA	T2	N0 (i-)	M0
TCGA-AN-A0G0-01	56	Right Upper Inner Quadrant	Stage IIA	T2	N0	M0
TCGA-A2-A0SX-01	48	Left Upper Inner Quadrant	Stage IA	T1c	N0 (i-)	M0
TCGA-D8-A147-01	45	Right Lower Outer Quadrant		T2	N0	M0
TCGA-BH-A0E0-01	38	Left Upper Outer Quadrant|Left Lower Outer Quadrant|Left	Stage IIIC	T3	N3a	M0
TCGA-D8-A143-01	51	Left Lower Inner Quadrant	Stage IIA	T2	N0	M0
TCGA-A7-A0DA-01	62	Left Lower Outer Quadrant	Stage IIA	T2	N0 (i-)	M0
TCGA-BH-A18G-01	81	Right	Stage IA	T1c	N0	M0
TCGA-BH-A0B9-01	44	Right Lower Inner Quadrant|Right Lower Outer Quadrant|Right	Stage IA	T1c	N0 (i-)	M0
TCGA-A2-A04U-01	47	Right	Stage IIA	T2	N0 (i+)	M0

Appendix C Validation of bioinformatic analysis findings with *in vitro* work and patients' samples in PTEN-inactive TNBC

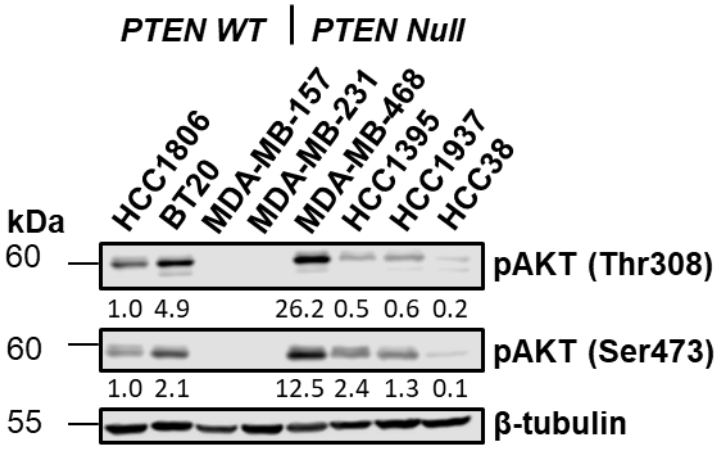

Figure C.1 Phosphorylated AKT level in TNBC cells.
PTEN WT and PTEN null type TNBC cell lines were lysed with 8 M urea buffer and 30 µg of protein was used to check protein expression of pAKT (Thr308) and pAKT (Ser473) by western blot. β-tubulin was used as a loading control.

Table C.1 Low *WDHD1*, mRNA expression (IlluminaHiSeq) and clinicopathological features for TNBC samples in TCGA data from UCSC Cancer browser.

Samples	Age	Location	Stage	Size	Positive LN	Metastasis
TCGA-BH-A42U-01	80	Right	Stage IIA	T2	N0	M0
TCGA-AC-A2QJ-01	48	Left Upper Outer Quadrant|Left Lower Outer Quadrant	Stage IIIB	T4b	N0	M0
TCGA-E2-A1LS-01	46	Right Lower Outer Quadrant	Stage IA	T1c	N0	M0
TCGA-A2-A1G6-01	50	Right	Stage IIIA	T2	N2a	M0
TCGA-AO-A03U-01	31	Left Upper Inner Quadrant|Left Upper Outer Quadrant|Left Lower Inner Quadrant|Left Lower Outer Quadrant|Left	Stage I	T1c	N0 (i-)	M0
TCGA-BH-A18G-01	81	Right	Stage IA	T1c	N0	M0
TCGA-LL-A441-01	62	Right Upper Outer Quadrant	Stage IA	T1c	N0	MX
TCGA-A2-A04U-01	47	Right	Stage IIA	T2	N0 (i+)	M0
TCGA-AO-A0JL-01	59	Left Upper Outer Quadrant|Left Lower Outer Quadrant|Left	Stage IIIA	T2	N2a	M0
TCGA-A2-A0T2-01	66	Right	Stage IV	T3	N3	M1
TCGA-D8-A27H-01	72	Right Upper Outer Quadrant	Stage IIA	T2	N0	M0

Table C.2 Low *WDHD1*, mRNA expression (IlluminaHiSeq) and clinicopathological features for TNBC samples in TCGA data from UCSC Cancer browser.

Samples	Age	Location	Stage	Size	Positive LN	Metastasis
TCGA-AR-A0TS-01	46	Right	Stage IIB	T2	N1	M0
TCGA-AO-A124-01	38	Left	Stage IIA	T2	N0 (i-)	M0
TCGA-A1-A0SK-01	54	Right Upper Outer Quadrant	Stage IIA	T2	N0 (i-)	M0
TCGA-A7-A6VV-01	51	Right	Stage IIA	T2	N0	M0
TCGA-AC-A2BK-01	78	Left Upper Outer Quadrant	Stage IIIA	T2	N2a	MX
TCGA-C8-A1HJ-01	53	Right	Stage IIA	T2	N0	M0
TCGA-AN-A0AT-01	62	Right Upper Inner Quadrant	Stage IIA	T2	N0	M0
TCGA-D8-A143-01	51	Left Lower Inner Quadrant	Stage IIA	T2	N0	M0
TCGA-AR-A0TU-01	35	Right Lower Outer Quadrant	Stage IIA	T2	N0	M0
TCGA-AN-A0XU-01	54	Left Upper Outer Quadrant	Stage IIA	T2	N0	M0
TCGA-D8-A13Z-01	51	Right Lower Outer Quadrant		T2	N2a	M0

Appendix D Functional characterisation of WDHD1 in PTEN-inactive TNBC

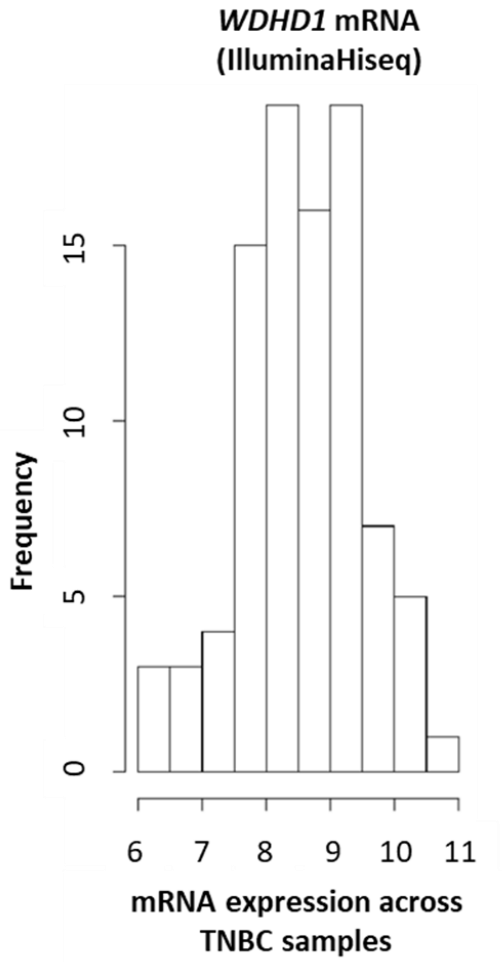

Figure D.1 Frequency distribution of *WDHD1*, mRNA level across TNBC samples in TCGA breast invasive carcinoma data (IlluminaHiSeq).

Histograms of *WDHD1* frequency expressed in all TNBC samples. X-axis shows *WDHD1*, mRNA expression and y-axis shows the frequency of samples that have each expression level. Codes are available in Appendix A.1.6.

Table D.1 Identified 64 proteins as WDHD1 binding partners in PTEN null MDA-MB-468 cells.

Description	Accession	Protein Names	#Peptides WDHD1-1	#Peptides WDHD1-2	#Peptides IgG-1	#Peptides IgG-2
WD repeat and HMG-box DNA-binding protein 1 OS=Homo sapiens OX=9606 GN=WDHD1 PE=1 SV=1	O75717	WDHD1	29	16	1	NA
C-1-tetrahydrofolate synthase, cytoplasmic OS=Homo sapiens OX=9606 GN=MTHFD1 PE=1 SV=1	F5H2F4	MTHFD1	8	NA	NA	2
HLA class I histocompatibility antigen, Cw-6 alpha chain OS=Homo sapiens OX=9606 GN=HLA-C PE=1 SV=1	A0A140T930	HLA-C	4	NA	1	NA
45 kDa calcium-binding protein OS=Homo sapiens OX=9606 GN=SDF4 PE=1 SV=1	Q9BRK5	SDF4	4	NA	1	NA
Prohibitin-2 OS=Homo sapiens OX=9606 GN=PHB2 PE=1 SV=2	Q99623	PHB2	3	3	1	1
Uncharacterized protein C7orf50 OS=Homo sapiens OX=9606 GN=C7orf50 PE=1 SV=1	Q9BRJ6	C7orf50	3	NA	1	NA
Electron transfer flavoprotein subunit beta OS=Homo sapiens OX=9606 GN=ETFB PE=1 SV=3	P38117	ETFB	3	NA	1	NA
GMP synthase [glutamine-hydrolyzing] OS=Homo sapiens OX=9606 GN=GMPS PE=1 SV=1	P49915	GMPS	3	NA	1	NA
Peroxiredoxin-6 OS=Homo sapiens OX=9606 GN=PRDX6 PE=1 SV=3	P30041	PRDX6	3	NA	1	NA
Dynamin-2 OS=Homo sapiens OX=9606 GN=DNM2 PE=1 SV=2	P50570	DNM2	3	NA	1	NA
Serum albumin OS=Homo sapiens OX=9606 GN=ALB PE=1 SV=2	P02768	ALB	3	NA	1	NA
NADPH--cytochrome P450 reductase (Fragment) OS=Homo sapiens OX=9606 GN=POR PE=1 SV=1	H0Y4R2	POR	NA	3	1	NA
Putative helicase MOV-10 OS=Homo sapiens OX=9606 GN=MOV10 PE=1 SV=2	Q9HCE1	MOV10	4	NA	2	1
Vimentin OS=Homo sapiens OX=9606 GN=VIM PE=1 SV=4	P08670	VIM	NA	21	NA	8
Coatomer subunit beta' OS=Homo sapiens OX=9606 GN=COPB2 PE=1 SV=2	P35606	COPB2	5	NA	2	NA
LanC-like protein 2 OS=Homo sapiens OX=9606 GN=LANCL2 PE=1 SV=1	Q9NS86	LANCL2	6	4	4	1

Continued on next page

Table D.1 Continued from previous page

Description	Accession	Protein Names	#Peptides WDHD1-1	#Peptides WDHD1-2	#Peptides IgG-1	#Peptides IgG-2
Perilipin-3 OS=Homo sapiens OX=9606 GN=PLIN3 PE=1 SV=3						
	O60664	PLIN3	4	NA	2	NA
Eukaryotic translation initiation factor 2 subunit 3 OS=Homo sapiens OX=9606 GN=EIF2S3 PE=1 SV=3						
	P41091	EIF2S3	4	NA	2	NA
Protein-arginine deiminase type-2 OS=Homo sapiens OX=9606 GN=PADI2 PE=1 SV=2						
	Q9Y2J8	PADI2	2	NA	1	NA
Chromobox protein homolog 3 OS=Homo sapiens OX=9606 GN=CBX3 PE=1 SV=4						
	Q13185	CBX3	3	1	1	NA
Vinculin OS=Homo sapiens OX=9606 GN=VCL PE=1 SV=4						
	P18206	VCL	4	NA	2	NA
Annexin A7 OS=Homo sapiens OX=9606 GN=ANXA7 PE=1 SV=3						
	P20073	ANXA7	3	3	2	1
Phosphatidylinositol-binding clathrin assembly protein OS=Homo sapiens OX=9606 GN=PICALM PE=1 SV=2						
	Q13492	PICALM	3	1	1	NA
Melanoma-associated antigen D2 OS=Homo sapiens OX=9606 GN=MAGED2 PE=1 SV=2						
	Q9UNF1	MAGED2	2	2	1	1
DNA replication licensing factor MCM3 OS=Homo sapiens OX=9606 GN=MCM3 PE=1 SV=2						
	J3KQ69	MCM3	2	NA	1	NA
Hypoxia up-regulated protein 1 OS=Homo sapiens OX=9606 GN=HYOU1 PE=1 SV=1						
	Q9Y4L1	HYOU1	2	NA	1	NA
Kunitz-type protease inhibitor 2 OS=Homo sapiens OX=9606 GN=SPINT2 PE=1 SV=2						
	O43291	SPINT2	2	NA	1	NA
Uncharacterized protein OS=Homo sapiens OX=9606 PE=4 SV=1						
	E7EVH7		2	NA	1	NA
Heterogeneous nuclear ribonucleoprotein R OS=Homo sapiens OX=9606 GN=HNRNPR PE=1 SV=1						
	O43390	HNRNPR	3	NA	2	1
Fatty aldehyde dehydrogenase OS=Homo sapiens OX=9606 GN=ALDH3A2 PE=1 SV=1						
	P51648	ALDH3A2	2	NA	1	NA
Acyl-coenzyme A thioesterase 2, mitochondrial OS=Homo sapiens OX=9606 GN=ACOT2 PE=1 SV=6						
	P49753	ACOT2	2	NA	1	NA
Mitochondrial proton/calcium exchanger protein OS=Homo sapiens OX=9606 GN=LETM1 PE=1 SV=1						
	O95202	LETM1	2	NA	1	NA

Continued on next page

Table D.1 Continued from previous page

Description	Accession	Protein Names	#Peptides WDHD1-1	#Peptides WDHD1-2	#Peptides IgG-1	#Peptides IgG-2
Aldehyde dehydrogenase family 1 member A3 OS=Homo sapiens OX=9606 GN=ALDH1A3 PE=1 SV=2						
	P47895	ALDH1A3	2	NA	1	NA
Guanine nucleotide-binding protein G(s) subunit alpha isoforms XLas OS=Homo sapiens OX=9606 GN=GNAS PE=1 SV=2						
	Q5JWF2	GNAS	2	NA	1	NA
Synaptic functional regulator FMR1 OS=Homo sapiens OX=9606 GN=FMR1 PE=1 SV=1						
	Q06787	FMR1	2	NA	1	NA
Cytochrome c oxidase subunit 5B, mitochondrial OS=Homo sapiens OX=9606 GN=COX5B PE=1 SV=2						
	P10606	COX5B	2	NA	1	NA
Serine/threonine-protein phosphatase 2A 55 kDa regulatory subunit B alpha isoform OS=Homo sapiens OX=9606 GN=PPP2R2A PE=1 SV=1						
	P63151	PPP2R2A	2	NA	1	NA
DNA mismatch repair protein Msh2 OS=Homo sapiens OX=9606 GN=MSH2 PE=1 SV=1						
	P43246	MSH2	3	1	1	NA
DNA replication licensing factor MCM6 OS=Homo sapiens OX=9606 GN=MCM6 PE=1 SV=1						
	Q14566	MCM6	2	NA	1	NA
Rho guanine nucleotide exchange factor 2 OS=Homo sapiens OX=9606 GN=ARHGEF2 PE=1 SV=1						
	V9GYM8	ARHGEF2	2	NA	1	NA
Cleavage and polyadenylation specificity factor subunit 7 OS=Homo sapiens OX=9606 GN=CPSF7 PE=1 SV=1						
	Q8N684	CPSF7	2	NA	1	NA
Nuclear pore complex protein Nup93 OS=Homo sapiens OX=9606 GN=NUP93 PE=1 SV=1						
	H3BVG0	NUP93	2	NA	1	NA
Heterogeneous nuclear ribonucleoprotein L OS=Homo sapiens OX=9606 GN=HNRNPL PE=1 SV=2						
	P14866	HNRNPL	2	2	1	1
40S ribosomal protein S6 OS=Homo sapiens OX=9606 GN=RPS6 PE=1 SV=1						
	P62753	RPS6	2	2	1	1
Eukaryotic translation initiation factor 3 subunit B OS=Homo sapiens OX=9606 GN=EIF3B PE=1 SV=3						
	P55884	EIF3B	2	NA	1	NA
Methionine--tRNA ligase, cytoplasmic OS=Homo sapiens OX=9606 GN=MARS PE=1 SV=2						
	P56192	MARS	2	NA	1	NA
Leukocyte surface antigen CD47 OS=Homo sapiens OX=9606 GN=CD47 PE=1 SV=1						
	Q08722	CD47	2	2	1	NA

Continued on next page

Table D.1 Continued from previous page

Description	Accession	Protein Names	#Peptides WDHD1-1	#Peptides WDHD1-2	#Peptides IgG-1	#Peptides IgG-2
CTP synthase 1 OS=Homo sapiens OX=9606 GN=CTPS1 PE=1 SV=2						
	P17812	CTPS1	2	NA	1	NA
Uncharacterized protein OS=Homo sapiens OX=9606 PE=1 SV=1						
	A0A1B0GU03		2	NA	NA	1
DnaJ homolog subfamily C member 10 OS=Homo sapiens OX=9606 GN=DNAJC10 PE=1 SV=2						
	Q8IXB1	DNAJC10	2	NA	1	NA
Methylthioribose-1-phosphate isomerase OS=Homo sapiens OX=9606 GN=MRI1 PE=1 SV=1						
	Q9BV20	MRI1	2	2	1	NA
Protein transport protein Sec61 subunit alpha isoform 1 OS=Homo sapiens OX=9606 GN=SEC61A1 PE=1 SV=1						
	B4DR61	SEC61A1	2	2	1	NA
Metalloreductase STEAP4 OS=Homo sapiens OX=9606 GN=STEAP4 PE=1 SV=1						
	Q687X5	STEAP4	2	2	1	NA
Histone H2B OS=Homo sapiens OX=9606 GN=HIST1H2BN PE=1 SV=1						
	U3KQK0	HIST1H2BN	2	4	2	1
Acetyl-CoA acetyltransferase, mitochondrial OS=Homo sapiens OX=9606 GN=ACAT1 PE=1 SV=1						
	P24752	ACAT1	2	NA	1	NA
Basic leucine zipper and W2 domain-containing protein 1 OS=Homo sapiens OX=9606 GN=BZW1 PE=1 SV=1						
	Q7L1Q6	BZW1	2	NA	1	NA
Mitotic checkpoint protein BUB3 OS=Homo sapiens OX=9606 GN=BUB3 PE=1 SV=1						
	O43684	BUB3	2	NA	1	NA
60S ribosomal protein L35a OS=Homo sapiens OX=9606 GN=RPL35A PE=1 SV=2						
	P18077	RPL35A	2	NA	1	NA
Retinoid-inducible serine carboxypeptidase OS=Homo sapiens OX=9606 GN=SCPEP1 PE=1 SV=1						
	Q9HB40	SCPEP1	2	NA	1	NA
Cytochrome c oxidase subunit 2 OS=Homo sapiens OX=9606 GN=MT-CO2 PE=1 SV=1						
	P00403	MT-CO2	2	2	1	1
Endoplasmic reticulum-Golgi intermediate compartment protein 1 OS=Homo sapiens OX=9606 GN=ERGIC1 PE=1 SV=1						
	Q969X5	ERGIC1	2	NA	1	NA
Peroxisomal multifunctional enzyme type 2 OS=Homo sapiens OX=9606 GN=HSD17B4 PE=1 SV=3						
	P51659	HSD17B4	NA	2	1	NA

Continued on next page

Table D.1 Continued from previous page

Description	Accession	Protein Names	#Peptides WDHD1-1	#Peptides WDHD1-2	#Peptides IgG-1	#Peptides IgG-2
40S ribosomal protein S16 OS=Homo sapiens OX=9606 GN=RPS16 PE=1 SV=1						
	Q6IPX4	RPS16	NA	2	NA	1
Uncharacterized protein (Fragment) OS=Homo sapiens OX=9606 PE=1 SV=1						
	H0YHG0		NA	2	1	NA

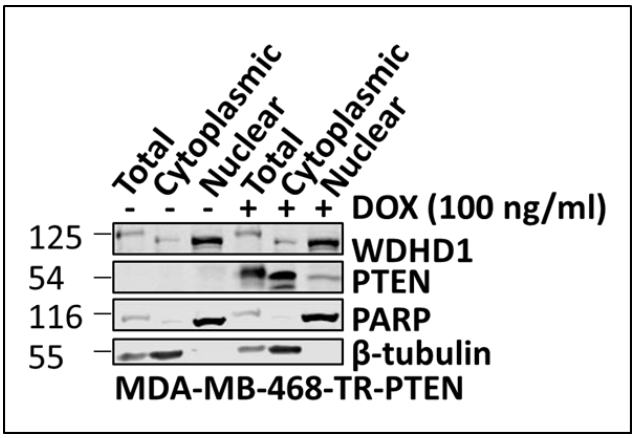

Figure D.2 WDHD1 is localised both in cytoplasm and nucleus in MDA-MB-468-TR-PTEN cell line. MDA-MB-468-TR-PTEN cell line was treated with 100 ng/ml of DOX and incubated overnight. Total labelled lanes were lysed with 8 M urea buffer and the cytoplasmic and nuclear fractions were obtained by using NE-PER Nuclear and Cytoplasmic Extraction Kit. 15 µg protein was run for western blot. Protein levels of WDHD1 and PTEN from cytoplasmic or nuclear fractions in MDA-MB-468-TR-PTEN cell line were analysed. PARP and β-tubulin were used as loading controls for the nuclear and cytoplasmic fractions, respectively.

Appendix E List of publications during the PhD

***co-first**

Yao, S.*, **Ertay, A.***, Zhou, Y.*, Yao, L., Hill, C., Chen, J., Guan, Y., Sun, H., Ewing, R., Liu, Y., Lv, X., Wang, Y. (2021) 'GRK6 depletion induces HIF activity in lung adenocarcinoma', *Frontiers in Oncology,* 11: 654812. doi: 10.3389/fonc.2021.654812.

Ertay, A., Liu, H., Liu, D., Peng, P., Hill, C., Xiong, H., Hancock, D., Yuan, X., Przewloka, M.R., Coldwell, M., Howell, M., Skipp, P., Ewing, R.M., Downward, J., Wang, Y. (2020) 'WDHD1 is essential for the survival of PTEN-inactive triple-negative breast cancer', *Cell Death and Disease,* 11(11): 1001. doi: 10.1038/s41419-020-03210-5.

Liu, D., **Ertay, A.,** Hill, C., Zhou, Y., Li, J., Zou, Y., Qiu, H., Yuan, X., Ewing, R.M., Lu, X., Xiong, H., Wang, Y. (2020) 'ASPP1 deficiency promotes epithelial-mesenchymal transition, invasion and metastasis in colorectal cancer', *Cell Death and Disease,* 11(4): 224. doi: 10.1038/s41419-020-2415-2.

Liu, H.*, **Ertay, A.*,** Peng, P., Li, J., Liu, D., Xiong, H., Zou, Y., Qiu, H., Hancock, D., Yuan, X., Huang, W.C., Ewing, R.M., Downward, J., Wang, Y. (2019) 'SGLT1 is required for the survival of triple-negative breast cancer cells via potentiation of EGFR activity', *Molecular Oncology,* 13(9): 1874-1886. doi: 10.1002/1878-0261.12530.

Wang, Y., Xiong, H., Liu, D., Hill, C., **Ertay, A.,** Li, J., Zou, Y., Miller, P., White, E., Downward, J., Goldin, R.D., Yuan, X., Lu, X. (2019) 'Autophagy inhibition specifically promotes epithelial-mesenchymal transition and invasion in RAS-mutated cancer cells', *Autophagy,* 15(5): 886-899. doi: 10.1080/15548627.2019.1569912.